

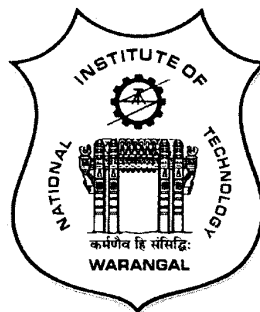
**DEVELOPMENT OF PROCESS FOR UTILIZATION OF IRON ORE SLIME OF  
BAILADILA REGION THROUGH HYBRID PELLET SINTERING**

A dissertation work  
submitted in partial fulfillment of the requirements  
for the award of the degree of  
**DOCTOR OF PHILOSOPHY**  
in  
**METALLURGICAL AND MATERIALS ENGINEERING**

by

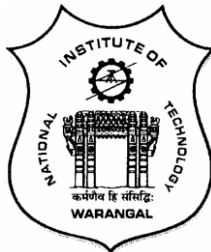
**VIBHUTI ROSHAN**  
(Roll No.701215)

Under the guidance of  
**Dr. G. V. S. Nageswara Rao**  
Professor, MMED, NIT Warangal  
&  
**Dr. Kamlesh Kumar**  
AGM (Hydro), NMDC Ltd., Hyderabad



**DEPARTMENT OF METALLURGICAL AND MATERIALS ENGINEERING  
NATIONAL INSTITUTE OF TECHNOLOGY  
WARANGAL-506 004 (TS) INDIA  
JUNE - 2019**

**DEPARTMENT OF METALLURGICAL AND MATERIALS ENGINEERING**  
**NATIONAL INSTITUTE OF TECHNOLOGY WARANGAL**  
**WARANGAL-506 004 (TS) INDIA**



**CERTIFICATE**

This is to certify that the work presented in the thesis entitled "**Development of process for utilization of iron ore slime of Bailadila region through hybrid pellet sintering**" which is being submitted by **Mr. Vibhuti Roshan (Roll No.701215)** is a bonafide work submitted to National Institute of Technology, Warangal in partial fulfillment of the requirements for the award of the degree of **Doctor of Philosophy in Metallurgical and Materials Engineering**.

To the best of our knowledge, the work incorporated in the thesis has not been submitted to any other university or institute for the award of any other degree or diploma.

**Dr. Kamlesh Kumar**  
Co-supervisor &  
AGM (Hydro)  
Research & Development Centre  
NMDC Ltd., Hyderabad

**Dr. G. V. S. Nageswara Rao**  
Thesis Supervisor & Professor  
Department of Metallurgical and Materials  
Engineering  
National Institute of Technology Warangal  
Warangal – 506 004

**Thesis Approval for Ph.D**

The thesis entitled **“Development of process for utilization of iron ore slime of Bailadila region through hybrid pellet sintering”** which is submitted by **Mr. Vibhuti Roshan (Roll No.701215)** is approved for the degree of **Doctor of Philosophy** in Metallurgical and Materials Engineering.

**Examiner**

---

**Supervisors**

---

---

**Chairman**

---

Date: \_\_\_\_\_

## ACKNOWLEDGEMENTS

I would like to express my sincere and whole hearted thanks to my supervisor **Prof. G. V. S. Nageswara Rao**, Metallurgical and Materials Engineering Department, National Institute of Technology, Warangal for his invaluable guidance and encouragement at each and every stage of this research work. His thought full guidance provided me an opportunity to improve my skills and knowledge. I will be truly indebted forever for his kind help and support throughout the research work.

I am equally grateful to my co-supervisor, Dr. Kamlesh Kumar, AGM, Research & Development Centre, National Mineral Development Corporation (NMDC) Ltd., for his invaluable advices and support in many aspects of this work.

I wish to thank sincerely Shri Rajan Kumar, Head and Shri S. K. Sharma, former Head, Research & Development Centre, NMDC Ltd., and management of NMDC Ltd. for giving me permission to carry out this research work at NMDC Ltd. and National Institute of Technology, Warangal.

I wish to express my sincere and whole hearted thanks and gratitude to Doctoral Scrutiny Committee (DSC) members Prof. M. K. Mohan, Metallurgical and Materials Engineering Department, National Institute of Technology, Warangal; Prof. A. Venugopal, Department of Mechanical Engineering, National Institute of Technology, Warangal; and Dr. G. Brahma Raju, Assistant Professor, Metallurgical and Materials Engineering Department, National Institute of Technology, Warangal for their kind encouragement and valuable suggestions in successful completion of this research work.

I wish to express my sincere and whole hearted thanks and gratitude to Dr. C. Vanitha, Head of the Department, Department of Metallurgical and Materials Engineering, National Institute of Technology, Warangal for her constant encouragement, kind help, and valuable suggestions for successful completion of this research work.

I am really grateful to Mr. Anand Chandra, Sr. Manager (Agglomeration Lab), R&D Centre., NMDC Ltd., for his helpful approach and have deep regard of his insight about the agglomeration process.

I am also thankful to Shri I. Balaji, Mechanic-cum-Operator, and Md. S. Alim, Mechanic-cum-Operator of Agglomeration and Pyrometallurgy Laboratory of R&D Centre, NMDC Ltd., for their continuous support and conducting the test works.

I wish to thank Dr. G. E. Sreedhar, DGM (Mineral Processing) and Shri Dilip Makhija for permitting me to use the beneficiation facilities available at R&D centre, NMDC Ltd. Their invaluable suggestion and guidance were very helpful during the entire study.

I also like to express my sincere thanks to Dr. Prashant Sharma and all my colleagues for extending their help and moral support during this research work.

I would like to express my deep thanks from the bottom of my heart to my parents (Dr. Vijay Kumar Singh and Smt. Shail Singh), my brother (Vinit Roshan) who are always present when I need them.

I express my sincere thanks to my wife Dr. Punam Singh for her motivation, patience, and sacrifices throughout this research work. My daughters Pranjal Singh and Priyanshi Singh, deserve special mention of appreciation for exhibiting patience during this long and arduous journey.

Finally, I thank all my friends and other well-wishers who have extended their support directly or indirectly for the successful completion of this research work.

**Vibhuti Roshan**

## **LIST OF ABBREVIATIONS AND SYMBOLS**

AES	: Atomic Emission Spectroscopy	LOI	: Loss on ignition
$\beta$	: Beta	min	: Minutes
BSE	: Back Scattered Electron	mm	: Millimetre
CO	: Carbon monoxide	$\mu\text{m}$	: Micro-meter (micron)
DDA	: Dodecylamine	N	: Nitrogen
$d_{80}$	: 80% particle passes the size	OF	: Overflow
$d_{50}$	: 50% particle passes the size	P	: Phosphorous
EDS	: Energy dispersive spectroscopy	PSO	: Pseudo ore
FCL	: Ferruginous clay	Q	: Quartz
Fe (T)	: Total iron	LDI	: Reduction Degradation Index
G	: Gauss	RINL	: Rastriya Ispat Nigam Limited
g	: Gram	RPM	: Rotation per minute
$\gamma$	: Gamma	RR	: Relative Reducibility
H	: Hematite	RUL	: Reduction Under Load
HPS	: Hybrid Pellet Sinter	SAIL	: Steel Authority of India Limited
ICP	: Inductive Coupled Plasma	S	: Sulphur
IS	: Indian Standard	SE	: Secondary Electron
ISO	: International Standard Organization	SEM	: Scanning Electron Microscope
JSW	: Jindal Steel Works	SFCA	: Silico-ferrite of calcium and alumina

TDI : Thermal Degradation Index

TGA : Thermo-gravity analyser

TI : Tumbler Index

TPH : Ton per hour

THM : Ton of hot metal

UF : Underflow

WDS : Wavelength Dispersive Spectroscope

WHIMS : Wet high intensity magnetic separator

XRD : X-ray diffraction

XRF : X-ray fluorescence

## LIST OF FIGURES

<b>Fig. No.</b>	<b>Description</b>	<b>Page</b>
2.1	Iron ore reserve / resources of India	9
2.2	Applicability of mineral Processing technique as per size of minerals	14
2.3	Schematic drawing of hydrocyclone	14
2.4	Displacement of particle in flowing film process	17
2.5	Segregation of particle in flowing film process	17
2.6	Separation of heavies in spiral concentrator	19
2.7	Magnetization curve of paramagnetic and diamagnetic minerals	22
2.8	Jones WHIMS used for beneficiation of tailing	22
2.9	Contact angle between three phases	24
2.10	Flotation Machine	26
2.11	Different steps of micro-pellet formation	29
2.12	Effect of moisture saturation on the tensile strength of the pellet	29
2.13	Effects of binder dosages on the green ball properties	32
2.14	Schematic flow diagram of industrial scale iron ore sintering plant	34
2.15	Block diagram of Intensive Mixing & Granulation System	37
2.16	Typical microstructure of sinter produced with different concentrates	40
2.17	(a) The $\text{Fe}_2\text{O}_3$ - $\text{CaO}$ - $\text{SiO}_2$ - $\text{Al}_2\text{O}_3$ quaternary system. (b) The shaded part shows the section where SFCA forms. C= $\text{CaO}$ , S= $\text{SiO}_2$ , A= $\text{Al}_2\text{O}_3$ , F= $\text{Fe}_2\text{O}_3$	42
2.18	Sequence of reaction during formation of SFCA and SFCA-I	44
2.19	Influence of Basicity on (a) cold strength and (b) degree of reduction (RI)	44
3.1	Characterization and laboratory scale beneficiation studies of Bailadila iron ore slime	48
3.2	Sampling and sample preparation by coning and quartering process	49

3.3	Gas pycnometer (AccuPyc 1340)	51
3.4	Fisher particle size analyzer	51
3.5	Wavelength Dispersive X-Ray Fluorescence equipment	53
3.6	Thermogravimetric Analyzer (LECO make; TGA 701)	53
3.7	Optical Microscope (Leica make)	56
3.8	Scanning Electron Microscope (make: TESCAN)	56
3.9	Laboratory model Wilfley table	58
3.10	<b>(a)</b> Krebs hydro-cyclone and <b>(b)</b> Slurry preparation	59
3.11(a)	Magnetisation of paramagnetic material	61
3.11(b)	Magnetisation of ferromagnetic material	61
3.12	High intensity induced magnetic separator (CARPCO make)	61
3.13	Permroll magnetic separator(STEARNS Roll)	61
3.14	Denver laboratory scale flotation cell	64
3.15	Flow sheet for pilot scale beneficiation studies	66
3.16	Flow sheet for micro-pellet making and hybrid pellet sintering in pot grate sintering furnace	68
3.17	Pot grate sintering (Hybrid pellet sintering)	69
3.18	Eirich make disc pelletizer	71
3.19	Denver make disc pelletizer	71
3.20	Pot grate furnace for sintering	77
3.21	Schematic diagram of pot grate furnace for sintering	77
3.22	Sizing and sampling of sinter prepared in pot grate furnace	79
3.23	Tumbler drum	79
3.24	Shatter Index test apparatus	79
3.25	Various metallurgical tests and their significance with respect to blast furnace operation	80
3.26	RI/RDI furnace (Lurgi)	81
3.27	RUL, R&B Automizion	81
3.28	Reduction under load tests	81
4.1	Particle size distribution of Bailadila iron ore slime	86
4.2	Distribution of Fe in different size of Bailadila iron ore slime	89

4.3	Area (%) wise distribution of minerals from Bailadila slime sample	89
4.4	Photomicrograph displaying distribution of medium to fine grains of hematite (H) and goethite (G), few pseudo ore (PSO) and irregular shaped quartz (Q). (Under transmitted light)	90
4.5	Photomicrograph showing distribution of medium to fine grain, irregular-shaped hematite (H), few coarse goethite (G) and irregular shaped highly fractured quartz (Q). (Under transmitted light)	90
4.6	Photomicrograph displaying medium to fine size highly altered hematite (H) and ferruginous clay (FCL) (Under reflected light)	91
4.7	Photomicrograph showing distribution of medium to fine size hematite (H) & few goethite (G), irregular shaped highly fractured quartz (Q) and Ferruginous clay (FCL) (Under reflected light)	91
4.8	Photomicrograph showing distribution of medium to fine grains of hematite (H) and ferruginous clay (FCL). (Under reflected light)	92
4.9	Photomicrograph depicts medium to small grains of highly altered hematite (H), goethite (G), few quartz (Q) and patches of ferruginous clay (FCL). (Under reflected light)	92
4.10	Liberated minerals present in the Bailadila slime sample	95
4.11	Stereomicroscope photomicrograph showing distribution of medium to fine grains, irregular-shaped hematite (H), few coarse goethite (G) and irregular shaped highly fractured liberated quartz (Q)	95
4.12	SEM photomicrographs showing highly altered hematite (H), few coarse goethite (G) and irregular shaped highly fractured liberated quartz (Q)	98
4.13	SEM photomicrograph of slime sample and its elemental mapping	99
4.14	XRD analysis of iron ore slime sample	101

4.15	TGA analysis of iron ore slime, coke, magnesite, dolomite and limestone samples	102
5.1	Laboratory scale beneficiation studies of iron ore slime from Bailadila mines (deposit-5)	109
5.2	Grade and recovery obtained using dry magnetic separation (CARPCO induced roll)	112
5.3	Grade and recovery as a function of pulp density in hydrocyclone at apex diameter of (a) 10 mm, (b) 12.5 mm, and (c) 15 mm	116-117
5.4(a)	SEM photomicrograph of hydro-cyclone under flow displays distribution of medium to fine grains of hematite (H) and Quartz (Q)	119
5.4(b)	EDS results displays elemental analysis of various grains of under flow from hydro-cyclone	119
5.5	Recovery and Fe(T) by using tabling and spiral studies of hydro-cyclone underflow	121
5.6	Recovery and grade as a function of magnetic field	123
5.7	Grade and recovery from Bailadila slime sample at different pH by using floatation test	127
5.8	Variation of silica and iron recovery with respect to the quantity of collector (DDA)	127
5.9	SEM photomicrograph of the concentrate obtained from pilot plant study, displays near spherical grains of concentrate	130
5.10	Pilot Scale beneficiation studies with slime from Bailadila Mines	131
5.11	Settling studies of hydro-cyclone overflow from pilot scale	135
6.1	The variation of (a) liquid saturation, (b) porosity, (c) physical strength (CCS), and (d) drop number of micro-pellets with moisture content	141
6.2	Variation of drop number and cold crushing strength with bentonite	143
6.3	Crushing strength vs. specific surface area	146

7.1	Effect of ignition time on various properties of sinter prepared from different sizes of micro-pellets. (a) Tumbler index, (b) Permeability, (c) Productivity and (d) Yield (+6.3mm)	152
7.2	Effect of moisture content on various properties of sinter prepared from different sizes of micro-pellets. (a) Tumbler index, (b) Permeability, (c) Productivity and (d) Yield (+6.3mm)	156
7.3	Effect of coke content on various properties of sinter prepared from different sizes of micro-pellets. (a) Tumbler index, (b) Permeability, (c) Productivity and (d) Yield (+6.3mm)	160
7.4	Effect of bed height on various properties of sinter prepared from different sizes of micro-pellets. (a) Tumbler index, (b) Permeability, (c) Productivity and (d) Yield (+6.3mm)	165
7.5	Hybrid pellet sinter prepared by using micro-pellets	168
7.6	Micrograph of the sinter with basicity 1.5 and its surrounding area after firing	168
7.7	XRD pattern of sinter produced with basicity 1.0	170
7.8	Photomicrographs illustrating magnetite (M) crystals forming a netlike eutectic intergrowth. Some wustite (W) also present at the ground mass. [Under reflected light]	170
7.9	Effect of basicity on quantity of various minerals in the sinter	172
8.1	Effect of basicity on yield and strength of the HPS	177
8.2	Effect of basicity on porosity and relative reducibility of HPS	178
8.3	Weight loss of HPS (with basicity 2.5) during RUL test	180
8.4	Reduction of HPS of various basicities with time	181
8.5	SEM micrograph of sinter after reduction	182
8.6	Schematic profile of cohesive zone of various dissections in blast furnaces	184
8.7	Effect of basicity of sinter on meltdown behaviour	188

## LIST OF TABLES

<b>Table No.</b>	<b>Description</b>	<b>Page</b>
2.1	Characteristics of Indian iron mineralization in zones A–E	10
2.2	Various organic and inorganic binders used for iron ore pellet making	32
3.1	Wilfley Table details	58
3.2	Details of WHIMS and process parameters	62
3.3	The composition of the sinter charge for different basicities	74
4.1	Chemical analysis of as-received slime sample	86
4.2	Physical properties of the slime	86
4.3	Particle size distribution and size wise chemical analysis	87
4.4	Detailed mineralogical observation on Bailadila slime sample	96
4.5	TGA results	103
4.6	The Proximate analysis of coke breeze	103
4.7	Chemical analysis of limestone and bentonite used in micro-pellet making	105
4.8	Size analysis of limestone, dolomite, magnesite, and coke breeze used for hybrid pellet sintering	105
4.9	Chemical analysis of fluxes used for hybrid pellet sintering	106
4.10	Chemical analysis of ash obtained from coke breeze	106
5.1	Results of straight tabling of slime sample	110
5.2	Results of dry magnetic separation of slime samples using Streans rolls	112
5.3	Results of wet magnetic separation of slime samples	114
5.4	Iron grade (Fe(T)) and recovery of the concentrate obtained from hydro-cyclone studies at various apex dia. and pulp densities	115

5.5	Chemical analysis of the underflow obtained from hydro-cyclone at 15 mm apex dia. and 1.25 in. vortex finder with pulp density 10 % solid	123
5.6	Results of first stage WHIMS test (at 2 amp)	124
5.7	Results of second stage WHIMS test (at 2 amp)	126
5.8	Overall recovery and iron grade using combination of hydro-cyclone (15 mm apex dia. and 1.25 in. vortex finder at pulp density of 10% solid) and two stage high intensity magnetic separation	126
5.9	Size analysis of the concentrate obtained from pilot plant	130
5.10	Grade, yield and recovery of pilot scale beneficiation studies	132
5.11	Settling test results of hydro-cyclone overflow	134
6.1	Details of ball mill used for grinding and Blain numbers at different durations	139
6.2	Drop number and strength of micro-pellets with varying bentonite for a specific surface area of iron ore concentrate at $1610 \text{ cm}^2/\text{g}$	143
6.3	Effect of specific surface area on drop number, crushing strength and porosity of micro-pellets with 0.50 % bentonite and 9.25 % moisture	146
7.1	Factor and their levels of variation	150
7.2	Physical characteristics of hybrid pellet sinter produced with varying ignition times (Moisture content: 6.5%, Coke breeze: 5.5% and sinter bed height: 300 mm)	151
7.3	Physical characteristics of hybrid pellet sinter produced with varying moisture contents. (Ignition time: 120 s, coke breeze: 5.5% and bed height: 300 mm)	155
7.4	Physical characteristics of hybrid pellet sinter produced with varying coke content (Ignition time: 120 s, Moisture content: 6.5% and Bed height: 300 mm)	159

7.5	Physical characteristics of hybrid pellet sinter produced with varying bed height (Ignition time: 120 s, moisture content: 6.5% and coke breeze: 5.5%)	164
8.1	Chemical compositions of the HPS with different basicities	175
8.2	Metallurgical characteristics of hybrid pellet sinter with varying basicity	177
8.3	Characteristics of iron ore lump used for softening and melting tests	186
8.4	Meltdown characteristic of HPS with different basicity	187
8.5	Comparison of HPS with blast furnace requirements	190

## Abstract

In Bailadila region of India, about 8-10% of slimes are being generated during mining and processing of iron ore. These slimes contain valuable iron source. However, these slimes are ultrafine in size and not suitable for subsequent utilization in iron making and steel making processes. Hence, these slimes are rejected and stored in tailing dams. This result in dual impact on mining operations: firstly, the loss of valuable iron value as waste and secondly, creating space constraint as huge quantities of slime are being accumulated in tailing dams. With a view to find out avenues for utilization of iron ore slimes, a systematic beneficiation studies were undertaken with slime sample from deposit-5 of Bailadila region.

In the present work, iron ore slimes from Bailadila mines located in Chhattisgarh state were selected for the study. The iron ore slimes were subjected to various standard procedures for studying their initial physical and chemical properties. The slimes were also studied microscopically by using optical and scanning electron microscopes to establish the status of liberated minerals. Based on these characterization inputs, gravity and wet magnetic techniques were used individually to beneficiate the iron ore slimes. Dry magnetic separation process was also tried considering water scarcity in future near mine site. However the process was plagued by high dust generation and relatively low recovery and productivity. As the individual techniques have yielded a limited success, combination of gravity and magnetic techniques were used to obtain beneficiated slime with maximum recovery of iron value (more than 64% Fe content). At laboratory scale, combination of hydro-cyclone followed by two stage wet high intensity magnetic separation (WHIMS) reveal that the concentrate assaying 64.74% Fe(T), 2.39 % SiO<sub>2</sub> and 1.82% Al<sub>2</sub>O<sub>3</sub> with a recovery of 85.16% Fe value could be produced. Based on the flow sheet developed at laboratory scale, a pilot plant was also designed for the beneficiation of iron ore slime on large scale. The laboratory scale results were validated by pilot scale beneficiation facility. The final flow sheet of beneficiation of slime was processed on pilot scale at 1 T/h capacity plant. The pilot scale studies reveal further improvement in the grade of the concentrate and the recovery of Fe value. Iron ore concentrate of 65.71 % Fe(T), 2.18% SiO<sub>2</sub> and 1.64% Al<sub>2</sub>O<sub>3</sub> with 87.31 % recovery is generated in pilot scale test. The concentrate thus obtained from pilot plant was used for the manufacture of micro-pellets of various sizes (between 1 and 10 mm) of sufficient strength under optimized conditions in disc pelletizer. The green properties of micro-pellets were optimized with respect to binder content,

moisture and surface area. The micro-pellets prepared from slime concentrate obtained after beneficiation of Bailadila deposit-5 slime has exhibited excellent physical properties at 0.5% bentonite content and 9.25 % moisture at surface area of 1780 cm<sup>2</sup>/gm. The micro-pellets thus obtained were used in hybrid pellet sinter making in pot grate sinter furnace. The sinter produced exclusively from micro-pellets exhibited better bed permeability and void fraction compared to conventional sinter. The results confirm that the sinter prepared from micro-pellets of size 3-6 mm can effectively replace iron ore fines in sinter making. During hybrid pellet sinter making, parameters such as moisture content, coke content in the sinter mix, bed height and ignition time for making sinter were studied and optimized. The optimized conditions for making hybrid pellet sinter are found to be: 6.5% moisture, 5.5% coke breeze, 350 mm bed height and 120 s ignition time. Six batches of sinter with basicity ranging from 0.5 to 3.0 were produced from micro-pellets of size 3-6 mm and the effect of basicity on properties of hybrid pellet sinter was also studied. The sinter thus produced from micro-pellets was subsequently evaluated for its performance under blast furnace conditions. The performance of hybrid pellet sinter under blast furnace conditions is observed to be better in comparison to conventional sinter with respect to reduction and strength at high temperature under reducing condition. The studies reveal that the metallurgical properties of the sinter (with basicity 2.5) are observed to be comparatively high with high relative reducibility of 65.7%. The higher reducibility of sinter in turn promotes higher indirect reduction and as a result significant reduction in coke rate can be obtained. On the whole, the iron ore slime from Bailabila (deposit-5) mines is convertible into useful blast furnace feed for iron making, there by alleviating the problem of space for safe disposal of slime as waste.

*Keywords: Iron ore slimes; gravity and wet magnetic separation; floatation; micro-pellet making; hybrid pellet sinter; blast furnace simulation.*

# CONTENTS

Certificate

Acknowledgements	i
List of abbreviations and symbols	iii
List of figures	v
List of tables	x
Abstract	xiii

## PART I

<b>Chapter 1: INTRODUCTION</b>	<b>1-7</b>
1.1 Introduction	1
1.2 Iron ore production in India	1
1.3 Generation of slime during iron ore processing in India	3
1.4 Generation of slime at NMDC mines	3
1.5 Problem Identification	4
1.6 Need for the study	5
1.7 Aim	6
1.8 Objectives	6
1.9 Methodology	6
1.10 Organization of the thesis	7
<b>Chapter 2: LITERATURE SURVEY</b>	<b>8- 46</b>
2.1 Introduction	8
2.2 Iron ore production in India	8
2.3 Reject generation during iron ore mining and processing in India	11

2.4	Beneficiation of iron ore slime	12
2.5	Micro pellet making and granulation	27
2.4	Iron ore sintering	33
2.5	Summary	45
<b>Chapter 3: EXPERIMENTAL PROCEDURE</b>		<b>47 - 84</b>
3.1	Introduction	47
3.2	Sampling and sample preparation	47
3.3	Characterization of slime and other raw materials	50
3.4	Laboratory scale beneficiation studies	55
3.5	Pilot scale beneficiation studies	65
3.6	Hybrid pellet sintering (HPS)	67

## **PART II : RESULTS AND DISCUSSION**

<b>Chapter 4: CHARACTERIZATION OF INITIAL RAW</b>		<b>85- 107</b>
---	--	----------------

### **MATERIALS**

4.1	Characterization of iron ore slime	85
4.2	Thermo gravimetric analysis (TGA) of iron ore slime and other raw materials	100
4.3	Characterization of other raw materials	104
4.4	Summary	107

<b>Chapter 5: BENEFICIATION STUDIES OF IRON ORE</b>		<b>108- 136</b>
---	--	-----------------

### **SLIME (Laboratory and Pilot scale studies)**

5.1	Introduction	108
5.2	Laboratory scale beneficiation studies	108
5.3	Pilot scale beneficiation studies	128

5.4	Settling studies using hydro-cyclone overflow	133
5.5	Summary	136

**Chapter 6: MICRO-PELLET MAKING AND 137- 147**

**OPTIMIZATION OF GREEN PROPERTIES**

6.1	Introduction	137
6.2	Effect of moisture content on the properties of green micro-pellets	140
6.3	Effect of bentonite on the properties of green micro-pellets	142
6.4	Effect of specific surface area on the properties of green micro-pellets	145
6.5	Optimum conditions of green micro-pellets suitable for sinter making	147

**Chapter 7: POT GRATE SINTERING STUDIES USING 148- 173**

**MICRO-PELLETS**

7.1	Introduction	148
7.2	Sintering studies in pot grate furnace	148
7.3	Optimized conditions for hybrid pellet sinter making by using micro-pellets	167
7.4	Effect of basicity on properties of hybrid pellet sinter produced from micro pellets of size 3-6 mm	167
7.5	Summary of pot grates sintering studies	171

**Chapter 8: EVALUATION OF HYBRID PELLET SINTER 174- 192**

**UNDER BLAST FURNACE CONDITIONS**

8.1	Introduction	174
8.2	Chemical composition of the hybrid pellet sinter	174

8.3	Effect of basicity on physical properties of the HPS produced from micro-pellets of 3-6 mm size	176
8.4	Effect of basicity on metallurgical properties of HPS produced from micro-pellets of 3-6 mm size	176
8.5	Effect of basicity on reduction under load (RUL) of HPS produced from micro-pellets of 3-6 mm size	179
8.6	Effect of basicity on softening and melting of HPS	183
8.7	Comparison of HPS with blast furnace feed requirement	189
8.8	Summary	191
<b>Chapter 9: CONCLUSIONS AND SCOPE FOR FUTURE WORK</b>		<b>193-199</b>
<b>REFERENCES</b>		
<b>LIST OF PUBLICATIONS</b>		205
<b>REPRINT OF PAPER PUBLISHED</b>		206

# Chapter 1

## INTRODUCTION

### 1.1 Introduction

The growth of any country can be measured by growth of its steel production. India is a developing country and has huge potential for infrastructure growth, which drive significant consumption of steel. Huge growth in infrastructure coupled with heavy industrialization has turned out to be a burden on environment as waste generation has increased many fold in the recent past. To create right balance between ecology, economy and development, it is crucial to develop technology for proper utilization of wastes. This will help in attaining sustainable growth of our country. Iron ore industries are generating primarily two types of waste, i.e. overburden and tailing. Overburden are mined and stored near the mines for future use whereas tailing (slime) is generated during iron ore processing, which is stored in tailing dam and create adverse impact on environment and sustainability of mining operation. The volume of tailing generation can be brought down by improving efficiency of existing beneficiation circuit and also by adopting improved and latest technologies, which prompt better recovery of iron value. Reduction of tailing volume will help in extending the life of tailing dam. Diverse mineralogical and chemical characteristics of iron ore in each and every deposit of iron ore makes it distinct iron ore body. So, every iron ore deposit requires an explicit beneficiation technique to get the maximum recovery with best possible quality of iron ore concentrate. Similarly, generation of tailing and its characteristics also depend upon original ore body characteristics and beneficiation technique adopted. Characteristics and quality of tailings are also distinct and need specific methods for their treatment.

### 1.2 Iron ore production in India

India is one of the leading iron ore producers of the world. In the year 2010-11, India has produced around 200 MT of iron ore (Indian Bureau of Mines, 2018). After 2010-11, the production of iron ore has come down to below 150 MT due to ban on mining in the states of Karnataka and Goa. Again, after seven years, i.e. in the year 2017-18, Indian iron ore producers have made significant contribution in iron ore production and the total production has reached

to nearly 210 MT. The increase in production of iron ore in the year 2017-18 in comparison to preceding years is made possible because of increased production in the states of Odisha and lifting of ban in Karnataka.

At present, majority of iron ore production in India comes from exploitation of hematite reserves. The production from magnetite reserve is negligible. The magnetite reserves are locked in to environmentally fragile area of Western Ghats, These magnetite minerals will remain be unexploited until a special technology has been developed, which can minimize or completely mitigate impact of mining on environment.

India has emerged as third largest steel producer in the year 2015 with production of 90 MTPA with installed capacity of 122 MTPA. India is poised to become the second largest producer of steel after China. Further, there is a considerable possibility of growth of steel industries as present per capita consumption of steel is only 61 Kg. This is very low compared to world average of 208 Kg. The per capita consumption of steel in the Indian villages is even low to a level of 10 Kg. These statistics state that there is a big opportunity for the growth of steel sector in India. Indian financial status and economy is swiftly growing with huge focus on development of infrastructure across the country. Considering all these facts, Government of India has set up a target expansion of steel capacity to 300 MTPA, with 255 MTPA crude steel productions by 2030-31(Steel, 2017). Government of India has advocated sustainable growth in the steel sector in the steel policy 2017. The focus on sustainable growth will drive industries to adopt environment friendly technology wherein waste generation will be minimal. Further, about 437 MTPA iron ore will be required for production of 255 MTPA crude steel by 2030-31 (Steel, 2017).The Indian iron ore industries need to put great efforts and gear up to achieve 437 MTPA iron ore production by 2030-31. The higher production of iron ore will also lead to generation of high amount of slime.

The total iron ore production of India in the year 2016-17 was 192.08 MT. This was about 21% higher than the previous year's (2015-16) production. The total iron ore production consists of production of lump and fines. As per Indian Bureau of Mines (IBM) list, total number of operating iron ore mines in India in the year 2016-17 was 296, as against 330 in the preceding year. 36% of India's iron ore production was contributed by Central Public Sector Enterprises (CPSEs) and rest by private sector.

### **1.3 Generation of slime during iron ore processing in India**

Huge quantities of slime are being generated during mining and washing of iron ore which amounts to about 20% of the total iron ore (lump + fines) produced per year (Indian Bureau of Mines, 2018). The slimes are very fine in size (less than 150 micron) and are discarded as waste material in tailing dams near the mine site. The presence of high amount of gangue minerals makes the slime unusable as such. The total production of iron ore in the year 2017-18 was touched to the level of 210 MT (Indian Bureau of Mines, 2018). This is the highest production achieved in last seven years. In India it is estimated that 50 % of total production of iron ore fines and lump are produced through dry processing and remaining 50 % processed through wet processing. The slime generation in dry processing is almost nil. However, during wet processing of iron ore about 20 % of iron ore slime is generated and is discarded as waste and stored in the tailing dam. So, in the year 2017-18, about 20 MT of slime was generated in India.

### **1.4 Generation of slime at NMDC mines**

National Mineral Development Corporation (NMDC) Limited is established in the year 1958 and its first mine was deposit-14 (Kirandul) of Bailadila region of Chhattisgarh. Over the period of 60 years of operation, NMDC Ltd. has grown to India's largest iron ore producer and in the year 2017-18, the total production of iron ore was 35.6 MT, which was highest ever production in a year since inception. The iron ore processing plant at NMDC Ltd. is designed to adopt wet and dry processes as per requirement. Iron ore mines situated in Bailadila region are situated in thickly dense forest and encounter heavy rain during monsoon season. Iron ore deposit in Bailadila region is relatively higher grade (>64% Fe). Hence, dry processing is sufficient to meet the requirement of customers. However, heavy rain during monsoon season increases the moisture content in iron ore and thus frequent chute and bunker jamming are faced in iron ore processing plant. This leads to loss of production and time. At Bailadila region, dry processing of iron ores is adopted for 8 months and wet processing for 4 months. The quantity of slime generation (due to wet processing) was around 12-15 % of total quantity of iron ore processed and this is rejected and stored in tailing dam. At present, all tailing dams in Bailadila region are on the verge of filling and more than 10 MT of slime of relatively higher grade is stored in tailing dam. Bailadila region falls under reserve forest area and additional land is not available for construction of new tailing dam. To alleviate this problem, various process improvements like installation of slow speed classifier followed by cyclone for recovery of iron value was

adopted in the wet processing of iron ore, and the generation of slime was successfully brought down to a level of 8-10% of total ore processed through wet circuit. As wet processing is adopted for only four months in a year, so, about 3-4 % of total iron ore processed in the year is rejected as slime. At current rate of production of 10 MTPA in the Bacheli mines of Bailadila region, about 0.3 to 0.4 MTPA slime are being generated. The total accumulated slime in Bacheli mines of Bailadila region as off now is 10 MT. This slime needs to be economically utilized to avoid impending environment hazard and also create space to dump fresh generated slimes.

## 1.5 Problem Identification

NMDC Ltd. has six fully mechanized iron ore mines in India. Of them, Bacheli complex of Chhattisgarh state has two mines, Bailadila deposit-5 and Deposit 10&11A. Both the mines are highly mechanized with wet screening plant and facilities for automatic stacking, reclaiming and loading (2500 TPH) of lump and fine ore into railway wagons. During course of crushing and wet screening of iron ore, huge amount of iron ore slime is being generated at mine site. The iron value loss in slime at mine site was substantial at the rate of 8-10 % of the total iron ore processed through wet circuit. More than half a decade of operation of iron ore processing, the plant has generated a huge quantity of iron ore slime and these slimes are stored near mine site in designated tailing dams. At present, about 20 MT slime was dumped in tailing dams at Bailadila mines and these dams are on the verge of filling. The accumulated slime is causing two problems:

- (i) **Space constraint:** The tailing dam is full with iron ore slime due to operation of mines for more than half a decade, hence additional tailing dam is required to dump/store freshly generated slime. The Bailadila mines are situated in reserved forest; hence no additional land can be made available for construction of tailing dams. To continue mining in Bailadila region additional space shall be created either by acquisition of land or evacuation of slime for storing of freshly generated slime. As the land is becoming dearer, acquisition of land would be a difficult task. Alternate routes for utilization of slime shall be sought for emptying the tailing dams for fresh storage.
- (ii) **Environment Issue:** The downstream water bodies are getting contaminated during rainy season due to over flow of water mixed with iron ore slime (red water) from tailing.

The contamination of water body has huge impact on agriculture and human being. For this reason also it is very much essential to clear the slimes by utilizing them in various ways.

## **1.6 Need for the study**

The tailing dams situated near the mine site of NMDC Ltd.(India) are on the verge of completely filled. This may be detrimental to the sustainable mining of iron ore. It is estimated that more than 20 MT of iron ore slimes are accumulated over the years with reasonably high iron content in the tailing dams. NMDC Ltd. has taken two prong strategies to deal with slimes; one is to improve the efficiency of the iron ore processing plant. As a result, the present level of slimes generation is reduced to 8-10 % as against 12-15 % a few years back. Second is to explore possible avenues for economical utilization of slime including utilization of slimes in pelletization, smelt reduction process (Hismelt & Romelt), Iron making Technology Mark 3 (ITMK3) process etc. However, after due diligence, none of these processes were found economically viable.

Sinter plant is an integral part of Integrated Steel Plant (ISP). The iron ore fines having less than 10 mm size are usually fed to the sintering process. This also includes large volume of ultra fines having less than -150 micron sizes. These ultra fines present in iron ore may choke the sinter bed and hinder the uniform air suction through the bed. As a result, sinter formation would be affected due to incomplete combustion of coke. Hence, these ultra fines are usually rejected without further use. In view of the fast depletion of iron ore deposits worldwide, it is necessary to exploit alternate routes for utilization of these iron ore ultra fines and conserve the iron ore reserves for future generations. For this reason, a new technique called hybrid pellet sintering (HPS) has been developed exclusively to utilize iron ore ultra fines (<150 microns size) in sinter making and for further charging in to blast furnace. In this new technique, iron ore ultra fines are first converted in to micro-pellets of suitable size and then these micro-pellets are in turn used in sinter making. Similarly, iron ore slime (reject) from various deposits contains high value of iron in them which can be utilized for iron making in blast furnace. However, the utilization of iron ore slime for making hybrid pellet sinter is not known / limited. Attempts are in progress to utilize 100% iron ore slime in hybrid pellet sinter making after thorough beneficiation. Since sinter is a preferred feed to the blast furnace, a successful study

will allow 100% utilization of relatively better grade slime of Bailadila mines in hybrid pellet sinter making and alleviate the environmental issues as well as space constraints.

## **1.7 Aim**

To develop a process route for 100% utilization of iron ore slimes generated at Bailadila mines (Deposite-5).

## **1.8 Objectives**

- To carry out complete characterization of iron ore slime of Bailadila mines (deposit-5)
- To carry out laboratory scale benefaction studies of iron ore slimes by adopting gravity, magnetic and physico-chemical techniques for maximum recovery of iron value and minimum loss as reject.
- To validate the laboratory scale beneficiation studies in a pilot plant of 1 TPH capacity for up gradation of slimes.
- To prepare micro-pellets of different sizes and optimization of their properties with respect to their size, moisture, binder, and surface area of slime concentrate.
- To prepare hybrid pellet sinter (HPS) using micro-pellets solely in place of iron ore fines and the impact of addition of micro-pellets in the sinter mix on permeability and void fraction of the green sinter bed.
- To study the influence of sinter basicity on physical and metallurgical properties of hybrid pellet sinter produced from micro-pellets under blast furnace conditions.

## **1.9 Methodology**

- Developing laboratory scale beneficiation process for upgradation of iron ore slime from Bailadila region with highest iron value recovery and minimum rejections.
- Validation and improvement of beneficiation process developed at laboratory scale by processing iron ore slime on pilot scale facility (1TPH).
- Utilization of iron ore concentrate obtained from pilot plant for manufacturing of micro-pellets and optimization of properties of green micro-pellets.
- Utilization of micro-pellets for blast furnace sinter making through hybrid pellet sintering.

- Evaluation of hybrid pellet sinter produced from micro-pellets under blast furnace condition.

## 1.10 Organization of the thesis

The thesis consists of nine chapters. The brief description of contents of the thesis (chapter wise) is given below.

*Chapter one* describes importance of the present study, background, objective and problem definition and approach methodology. *Chapter two* provides detailed literature survey carried out. In *chapter three*, the details of experimental work are included. The details of the characterization studies, laboratory scale and pilot scale beneficiation studies, micro-pellet making, hybrid pellet sintering and blast furnace simulation studies are discussed in various sections of this chapter. *Chapter four* deal with the characterization results of initial raw materials. *Chapter five* deal with the beneficiation studies at laboratory and pilot scale and hence development of process flow sheet for utilization of the iron ore slimes. In *chapter six*, the results of micro-pellet making, and the optimization of their green properties are explained. In *chapter seven*, the results of pot grate sintering studies using micro-pellets and the optimization of sintering parameters are explained. *Chapter eight* deal about the results obtained on evaluation of hybrid pellet sinter (HPS) under blast furnace conditions. Conclusions and future scope of the work are provided in *chapter nine*.

# Chapter 2

## LITERATURE SURVEY

### 2.1 Introduction

The most crucial raw material for iron and steel industry is iron ore and mining of iron ore is perhaps of major significance among all other mining activities carried out by any country. India is placed with very high iron ore resource of over 33.27 Billion Tonnes of magnetite ( $Fe_3O_4$ ) and hematite ( $Fe_2O_3$ ) iron ore (Fig.2.1) and also India is one of the leading iron ore producers of the world. Hematite deposits in India are from the Precambrian Iron Ore Series (Indian Bureau of Mines, 2018) and the iron ore mineral is mainly occurring as friable, laminated and massive type ore body. Hematite is also found in powder form as blue dust with very high iron content. The declared reserves of hematite type of iron ore is 22.48 Billion Tonnes (Indian Bureau of Mines, 2018) . 24% (about 5.422 Billion tonnes) of hematite are considered as reserve and rest 76% (about 17.065 Billion Tonnes) are categorized as remaining resources (Fig.2.1). State wise distribution of hematite entails that 95% of hematite reserve are placed in Odisha (34%), Jharkhand (23%), Chhattisgarh (22%), Karnataka (11%) and Goa (5%). Another type of iron ore found in India is magnetite. The total magnetite resources/reserve of India has been projected at 10.79 Billion Tonnes (Indian Bureau of Mines, 2018). Exploitation of magnetite iron ore in India is very limited and only 53 million tones categorized as reserve and rest is classified as remaining resources. Maximum magnetite reserves are located in Karnataka state (about 72%). However, exploitation is minimum as majority of magnetite reserves fall in reserve forest area. The characteristics of Indian iron mineralization in different zones of country is presented in Table 2.1.

### 2.2 Iron ore production in India

At present, majority of iron ore production in India comes from exploitation of hematite reserves. The production from magnetite reserve is negligible. The magnetite reserves are locked in to environmentally fragile area of Western Ghats, These magnetite minerals will

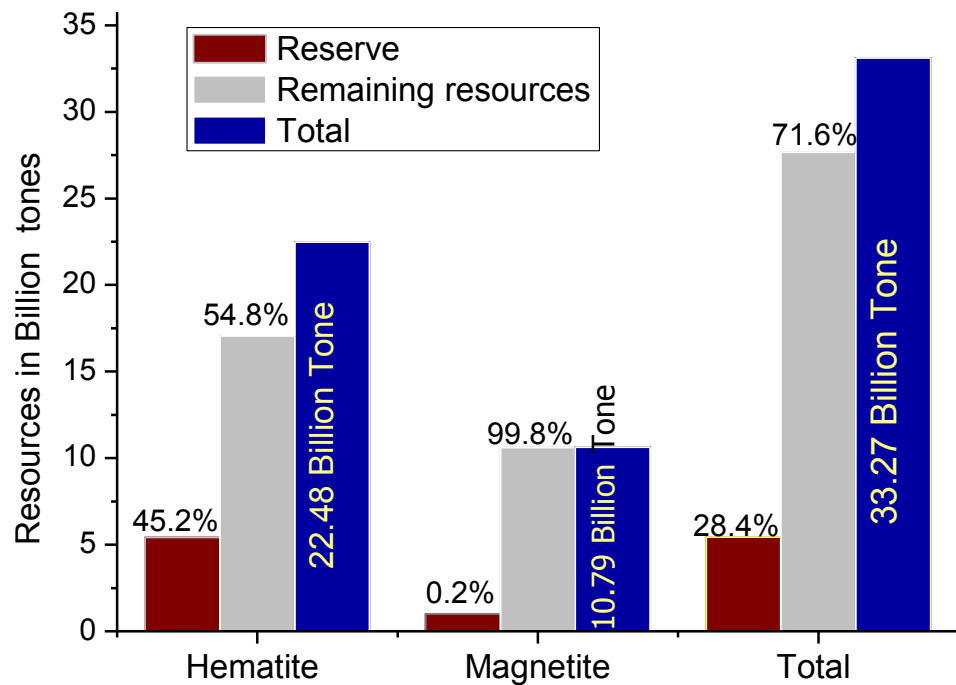


Fig.2.1 Iron ore reserves/resources of India ([Indian Bureau of Mines, 2018](#))

**Table 2.1 Characteristics of Indian iron mineralization in different zones (IBM, 2008)**

<b>Zone</b>	<b>Location</b>	<b>Mines</b>	<b>Mineralization</b>
<b>A</b>	Jharkhand & Odisha - Bonai iron ranges and attached areas in eastern India	Meghatuburu, Daitari, Chiria, Taldih, Joda, Noamundi, Kiriburu, Thakurani, Gua, Bilani, Khondbond, and Gandhamardan	Massive ore- BHQ/BHJ formations (58–66% Fe), blue dust (66–68% Fe), laminated ore, shaley ore, and lateritic ores (56–60% Fe). The hematite occurs closely attached with limonite and goethite, while the lateritic ores comprise many cavities occupied with goethite, limonite, and ochreous material
<b>B</b>	Madhya Pradesh, Chhattisgarh and east Maharashtra- linear belt trending towards North-south in central India	Rowghat, Bailadila, Aridongri, Dalli-Rajhara, Mahamaya, , , and Surajgarh	Mainly hematite ore (64–68% Fe) with high grade and massive with some pockets of laminated, associated with BHQ. Primarily hard and dense hematite with minor amounts of goethite and limonite . The main gangue minerals are clay, quartz and some amount of ferruginous shale.
<b>C</b>	Karnataka state- Region of Bellary- Hospet	Ramdurga and Donimalai	BHQ/BHJ closely associated with ferruginous shale, comprising of long, thin, and distributed patches of hematite with overriding shale bands containing 58–64% Fe. The hematite contains little quantities of goethite , magnetite, specularite, and martite, with clay and quartz as the main
<b>D</b>	West Maharashtra and Goa	North and south of Reddi and Goa	Iron ore fines (59% Fe), blue dust (63–64% Fe), and lump ore (57– 58% Fe). Limonite and goethite are principle mineral associated with gibbsite (clay) and occur with ferruginous phyllite and banded ferruginous quartzite.
<b>E</b>	Karnataka- Magnetite deposits	Baba Budan Hills, Kudremukh, and Kodachadri	BHQ/ BMQ formations (57–62% Fe), thick bands of hematite/magnetite The associated impurity is mainly quartz

remain be unexploited until a special technology has been developed, which can minimize or completely mitigate impact of mining on environment. Indian financial status and economy is swiftly growing with huge focus on development of infrastructure across the country. Government of India (GOI) has set a target capacity expansion of steel to 300 MTPA with 255 MTPA crude steel production by 2030-31 (**Steel, 2017**). The focus on sustainable growth will drive industries to adopt environment friendly technology wherein waste generation will be minimal. Further, about 437 MTPA iron ore will be required for production of 255 MTPA crude steel by 2030-31 (**Steel, 2017**). The huge demand of iron ore in coming decade will put lot of pressure on already strained iron ore mining sector.

The total iron ore production of India in the year 2017-18 was 203 MT, (**Ernst & Young, 2017**) this was about 9% higher than the last year (2016-17) production. The total iron ore production consists of production of lump and fines. As per IBM list, total number of operating iron ore mines in India in the year 2016-17 was 296, against 330 in the preceding year (**Indian Bureau of Mines, 2018**). 36% of India's iron ore production was contributed by Central Public Sector Enterprises (CPSEs) and rest by private sector.

## **2.3 Reject generation during iron ore mining and processing in India**

### **Overburden:**

The ore body is covered with unwanted rocks and soil and this unwanted material is called overburden. The first step of mining is removal of overburden to expose ore body for exploitation. Generation of overburden depends on nature of deposit. Some deposits have very high strip ratio as high as 10:1. The striping ratio is defined as volume of overburden handled for extraction of 1 ton of ore. Significant amount of overburden is being generated during iron ore mining and it is stored near mine site. Efforts are being made for development of process for utilization of overburden.

### **Slime:**

Huge quantities of slime are being generated during mining and washing of iron ore which amounts to about 20% of the total iron ore ( lump+ fines) produced per year (**Thella et al., 2012**) . The slimes are very fine in size (less than 75 micron) and are discarded as waste material

in a tailing dam near the mine site. The presence of high amount of gangue minerals makes the slime unusable as such. The total production of iron ore in the year 2017-18 was touched to the level of 210 million tones (**Reviews, 2018**). This is highest production achieved in last seven (2010-2017) years. In India it is estimated that 50% of total production of iron ore fines and lump are produced through dry processing and remaining 50% processed through wet circuit. The slime generation in dry processing is almost nil. However, during wet processing of iron ore about 20% of iron ore processed is discarded in the form of slime and is stored in the tailing dam. In the year 2017-18 about 20 million tones of slime is generated in India (**Reviews, 2018**).

## **2.4 Beneficiation of iron ore slime**

Indian iron ore industries are beleaguered due to generation and disposal of slime during processing of iron ore. The generated slime is not only creating environmental problems but also a threat for sustainability of mining operation. All most all the iron ore mines are facing space constraint for dumping of lean grade slimes. So it is very essential to develop a method(s) for utilization of slimes economically with an aim to maximum recovery of iron value. Iron ore slimes generated at various mines in India generally contains various phases of minerals like hematite, magnetite, limonite, goethite (vitreous and ochreous), quartz, kaolinite, and gibbsite (**Srivastava et al., 2001**) . The percentage of these minerals in slimes varies with locations, types of deposit, process adopted etc. in India. The composition of slime and its mineral contents purely depends upon main deposit characteristics from which it is derived. Combination minerals may present in simple and liberated form or complex and locked form. The iron ore slime of India have coarser particle of size as high as 150 micron. Majority of particle present in the slime is finer than 45 micron.

Slime characteristics depend upon main ore body from which it was generated during processing. The main iron ore body can be defined by the geological conditions it has faced during the process of mineral formation. Iron ores are mostly found in sedimentary, igneous and metamorphic hosted deposits (**Poveromo, 2000**) . Most iron ores are extracted from big open pits such as Bailadila region of Chhatisgarh, Singbhum District of Jharkhand, etc. Very few underground iron ore mines are in operation in the world such as Malmberget mine in Sweden (Kiruna).

#### **2.4.1 Characterizations of iron ore and slimes**

The characterization of iron ore slime is utmost important for developing a process for utilization of slime. The characterization of slime can be divided into three parts as physical, optical and chemical characterization. Physical characterization provides detailed information of slime, like specific gravity (true density), size wise particle distribution, mean size of particle, angle of repose etc. The optical analysis is most important characterization studies and will be the basis for selection of processing method for beneficiation of minerals and ore for up gradation. The optical microscopy is one of the oldest technique used for identification and quantification of mineral phases in rock sample. This technique is being in forefront since last 150 years for minerals characteristics. Henry Clifton Sorby has developed first petrological microscope with polarized light for characterization of rocks and minerals (**Sorby, 1858**), fundamental methods for petrological characterization was also developed by him. The chemical characterization provides information like percentage of iron content and gangue mineral.

These studies can provide information about minerals occurrence and their distribution, status about association or extent of liberation, types of minerals and structure, profile and other physical distinctiveness of every individual particles.

#### **2.4.2 Beneficiation of low grade iron ore/slimes through gravitational method**

The gravity separation method works on difference in specific gravity of valuable mineral with gangue minerals. The relative movement of mineral in air or water under gravitational force depends primarily on specific gravity of minerals and some other forces. The size of minerals to be separated play major role in selection of processes, as presented in **Fig 2.2 (Mills, 1978)**. It is apparent that the majority of mineral beneficiation techniques fail in the ultra-fine size range specially gravity concentration method. The hydro-cyclones can handle particle size up to 5 micron and rest of the wet gravitational technique including spirals can accept particle size up to 75 micron. Gravity separators are particularly susceptible to the presence of ultra-fine particles (**Wills, 1988a**). The presence of ultra fine particle (< 10 micron) increases the viscosity of the slurry and hence decrease the efficiency of separation, and also cause unclear visual cut-points. The feed to the gravity separation need to be pretreated in the most of cases to free the feed from ultra fines. Hydro-cyclone (**Fig.2.3**) is the most preferred method for removal of ultra fines (**Mohanty and Das, 2010**).

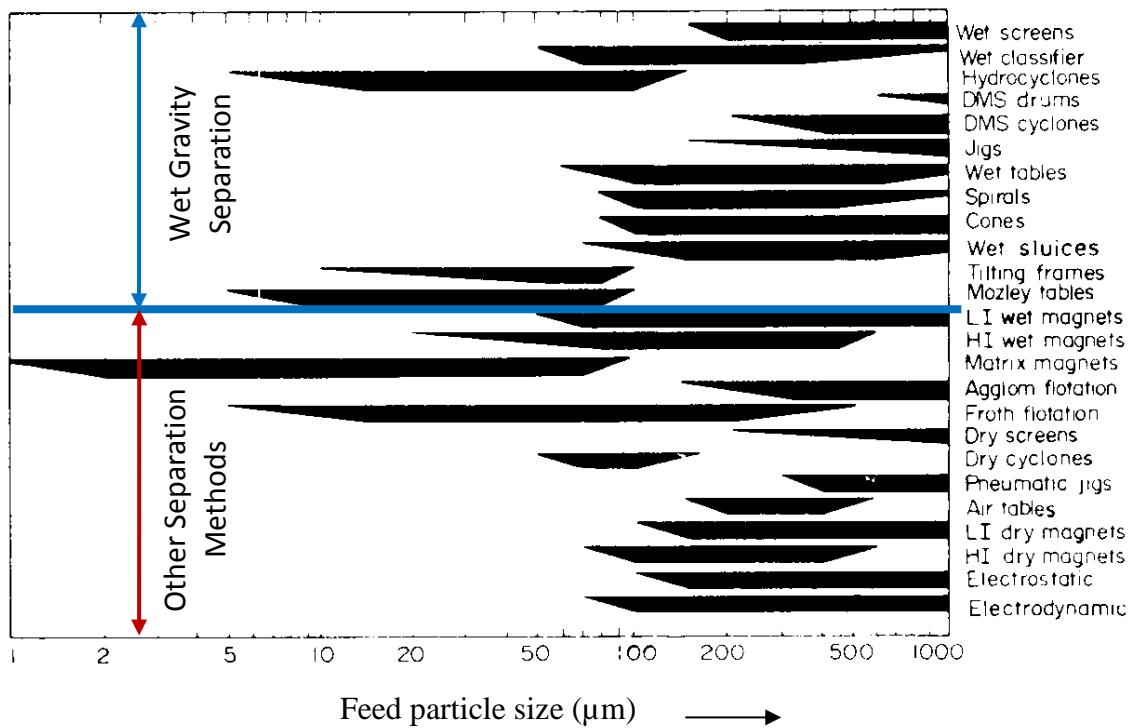


**Fig.2.2** Applicability of mineral processing technique as per size of minerals (Mills, 1978)

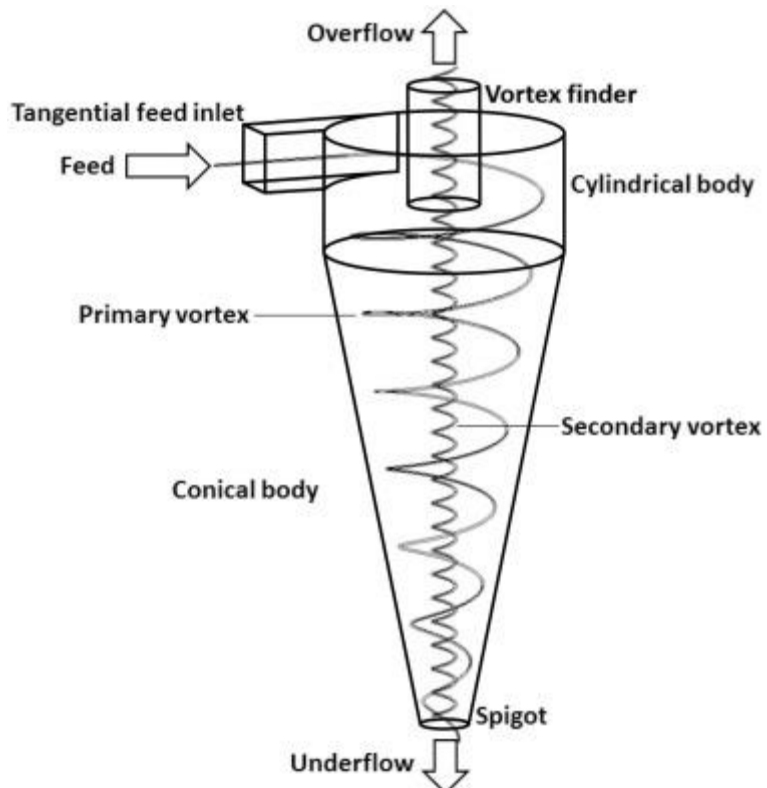


**Fig.2.3** Schematic drawing of hydro-cyclone (Vega-Garcia et al., 2018)

A schematic of hydro-cyclone is shown in **Fig.2.3** and it consists of a conically shaped section, open at its apex and other side joined to a cylindrical part. The cylindrical part is connected with inlet for tangential feed. The underflow comes out from apex. the over flow pipe is mounted above the sheet closing the cylindrical section, the vortex finder is attached with overflow pipe.

(**Mohanty and Das, 2010**) has developed mathematical model for optimization of hydro-cyclone to establish effect of vortex finder diameter, choices and quantity of dispersant, spigot diameter etc. on overall recovery and grade while treating iron ore slime. Hydro-cyclone was optimized with respect to solids consistency (%), spigot diameter (mm), dispersant (gms/kg), pressure (psi), and vortex finder diameter (mm) to obtain maximum valuable mineral (iron) from iron ore slime collected from washing plant. Separation efficiency of hydro-cyclone improves significantly by addition of dispersion agent. In this study the model has predicted that maximum iron grade 65.0% with recovery of 60% can be achieved by passing through hydro-cyclone under optimized condition of slime containing 57.84 Fe, 6.7% of  $\text{SiO}_2$  and 6.0%  $\text{Al}_2\text{O}_3$ . However this model was not validated in real use.

Literature (**Wills and Napier-Munn, 2006**) suggest that most preferred de-sliming method used in the iron ore beneficiation is hydro-cyclones. Removal of fine particles (less than 10 micron) can be achieved with minimum loss through hydro-cyclone. Hydro-cyclones are extensively employed to prepare the feed for subsequent beneficiation process. However, hydro-cyclone cannot be used for highly friable minerals due to generation of high shear forces which tend to cause size reduction of friable minerals.

Hydro-cyclone was successfully used for de-slimming by researchers (**Mukherjee et al., 2015**) for recovery of iron value from slimes. The hydro-cyclone test with three variables, namely, vortex finder diameter, spigot and inlet pressure, was carried out. The impact of these three parameters on the separation and their inter dependency on the process was established and it was found that spigot diameter has maximum influence on the efficiency of the hydro-cyclone. The vortex finder diameter has direct impact on underflow yield. Lower the vortex finder diameter, the higher the yield. The literature suggest two stage hydro-cyclone operation to obtain optimum grade of feed for subsequent process with assay of 63.34% Fe(T), and total gangue mineral around 6% ( $\text{Al}_2\text{O}_3$  and  $\text{SiO}_2$ ).

Researchers (**Seifelnassr et al., 2013**) have attempted to beneficiate the lean grade iron ore sample obtained from Wadi Halfa iron ore deposit, North of Sudan. The sample was subjected for mineralogical characterization followed by chemical analysis. Most of the iron ore present were hydrated and major gangue mineral was the quartz. The Fe(T) content in the sample was around 36% Fe and the gangue mineral ( $\text{SiO}_2$ ) content was very high at 48%. Three size fraction was chosen as -500  $\mu\text{m}$ , -350  $\mu\text{m}$ , and -150  $\mu\text{m}$  for further processing based on mineralogical and liberation studies. The first step was de-sliming through hydro-cyclone before subjecting to conventional gravity and magnetic separation method. Hydro-cyclone was effectively used for de-sliming of ground samples of iron ore.

One of the most significant process control of gravity circuit processes is to maintain right water-balance and pulp density. The percentage of solid in the feed pulp has direct impact on efficiency of the gravitational beneficiation process. Thus, monitoring and measuring of correct pulp-density is therefore crucial, and this is most significant at the feeding end of the process. Various devices are available for online monitoring of pulp density and pressure of slurry as both affect performance of the process. Shaking Table and spirals are two gravity concentration are being used for beneficiation of fine iron ore.

### **Shaking Tables**

The shaking table is a flowing film concentration method. The velocity of fluid is minimum or nil at bottom and maximum at the top of the fluid layer flowing over the table. The velocity of fluid is minimum near the surface because the fluid near the surface is experiencing backward force by the friction of the surface. The velocity rises toward the top layer. The relative motion of fluid separate the particles based upon specific gravity, size and shape of particle. The movement of particles with same specific gravity of different size is different. The smaller particle will move slower in comparison to large size particle. Similarly, particle with higher specific gravity move slower than particle with lower specific gravity. The slower moving particles will have movement that is more lateral on the shaking table. The displacement of particle in flowing film process is presented in **Fig 2.4**. Two forces are subjected on minerals on shaking table, first due to horizontal/ lateral motion of the table and second force exerted by flowing film on the minerals. The directions of both the forces are perpendicular to each other.

The resultant force move the particles diagonally based on the specific gravity and size. Collection of different particles on the table is shown in **Fig 2.5**.

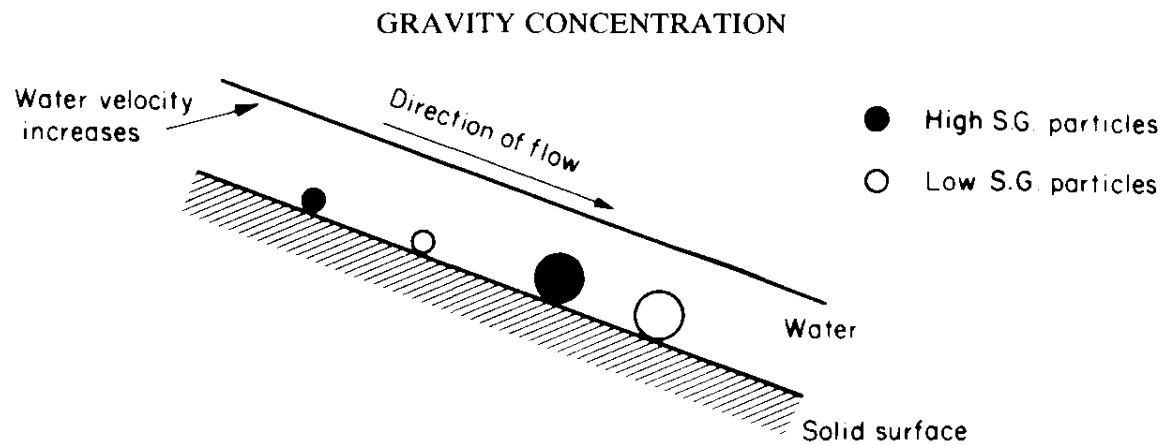


**Fig.2.4** Displacement of particle in flowing film process (Wills, 1988a)

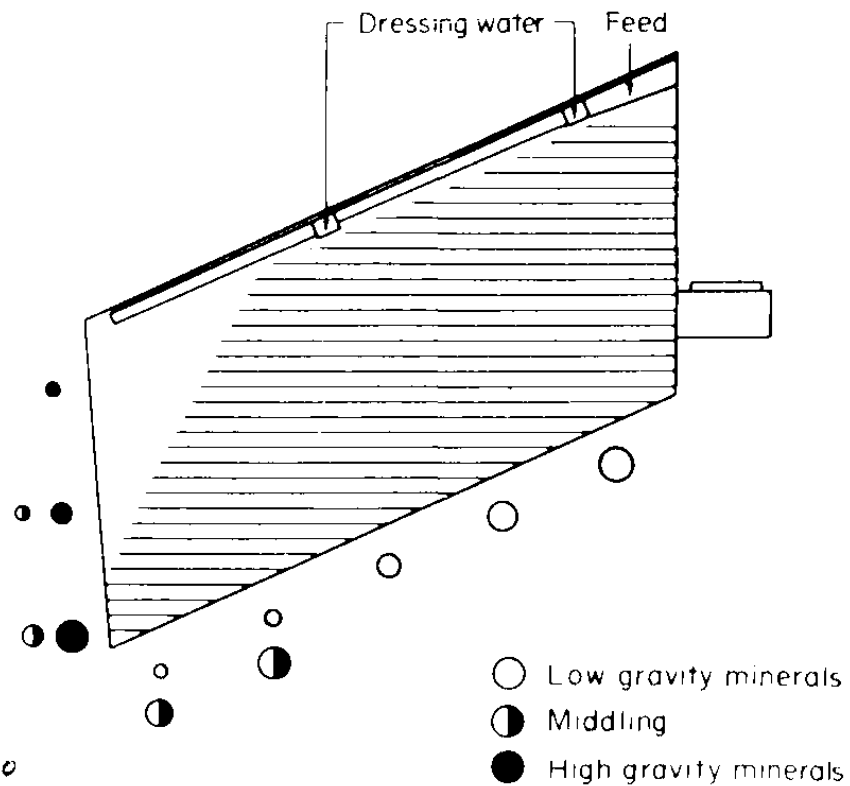


**Fig.2.5** Segregation of particle in flowing film process (Wills, 1988a)

Researchers (**Seifelnassr et al., 2013**) have attempted to use table as pre-concentrator. Tilt angle of table was tried between  $3^\circ$  and  $8^\circ$ . Best recovery and grade of concentrate was obtained at  $5^\circ$  tilt angle. At lower tilt angle ( $3^\circ$ ) huge quantity of middling are reported in the concentrate of the table. As a result, high recovery (90.1%) was recorded with inferior grade of concentrate (41.1% Fe). Huge quantity of the particles containing iron value was washed away at  $8^\circ$  tilt angle and reported in tailing part of the table product. This causes lower recovery of iron value as low as 66.0%. The highest recovery of 81.2% with grade 44.9% was achieved at tilt angle  $5^\circ$  with feed size  $-150 + 20 \mu\text{m}$ . Tabling was successfully used for first stage cleaning/beneficiation of lean grade ore.

### **Spirals**

Spiral is the most energy efficient and simple concentrator, the spiral comprises of curved canal set in the arrangement of spiral with a provision of port at inner wall of spiral for withdrawal of concentrates (**Fig.2.6**). Water is the media used in the spiral concentrator. Water flows down from top to bottom through the spiral. The feed at the top of spiral should have uniform pulp density for better separation. The heavier mineral moves towards inner edge. The velocity of water near the surface of spiral is low as lower layer of water experience frictional forces of the water absorbed at the surface of the spiral. The lower layer with least velocity carries heavy minerals and moved towards inner edge, where heavies collected through port, the adjustable splitter used for proper removal of band of concentrate. The operational cost and cost of installation of spirals are very low compared to other conventional processes. The overall maintenance cost is also very low. Very high number of spirals can be placed parallelly to achieve high throughput. The separation of heavies in spiral is shown in **Fig 2.6**.

Researchers (Srivastava et al., 2001) have explored the possibility of beneficiating iron ore fines of lower grade obtained from Kiriburu mines, Jharkhand. The attempt was made to obtain blast furnace grade concentrate for subsequent use in pellet making. The lower grade of Kiriburu mines contains up to 61% Fe(T), 3.34% SiO<sub>2</sub>, and 2.93% Al<sub>2</sub>O<sub>3</sub> and  $d_{80}$  of the sample was 110 mm. The characterization studies of the ore revealed that goethite (Fe<sub>2</sub>O<sub>3</sub>. H<sub>2</sub>O) was the major mineral in addition to the hematite. Based on the characterization data methodical simulation was carried out by using MODSIM and various flow sheets were designed. The simulation outcome indicated that the ore could be beneficiated up to 64% Fe by using a hydro-cyclone followed by spiral concentrator. Pilot plant circuit was developed

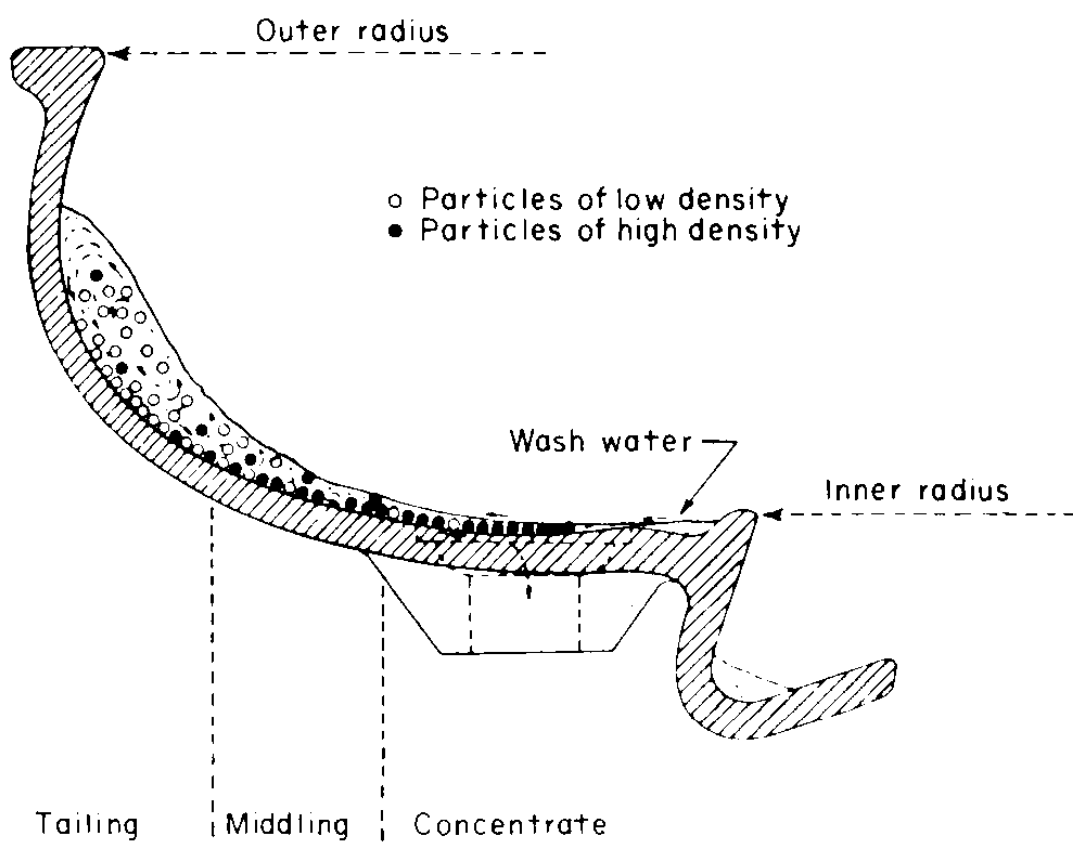


**Fig.2.6** Separation of heavies in spiral concentrator (Wills, 1988a)

using a 5 in. hydro-cyclone and spiral of capacity 2 ton/h. Pilot Plant campaign was undertaken to confirm the simulation results. It was witnessed that the iron ore could be upgraded by use of spiral to 64.17% Fe content with 53.7% recovery of iron value. The concentrate obtained was meeting feed requirement of agglomeration process.

However, spirals have limitation on particle size to be treated and specific gravity of the mineral (**Henderson and Machunter, 2000**). Spiral concentrators can beneficiate material of particle size coarser than 100  $\mu\text{m}$ . The spiral is also beneficial when used with minerals of specific gravity  $< 2.85$ . Ores with particles size less than 100  $\mu\text{m}$  have had to deal with comparatively poor separation performance, in terms of lower recoveries and grades. In recent times, new spiral has been developed (FM1 spiral) (**Millard, 2015**), which performed better with finer feed particle.

The performance of spiral separator for beneficiation of iron ore slime from Noamundi iron ore mines was studied by Dixit et al. (**Dixit et al., 2015**) using Box-Behnken with three factors three level along with response surface methodology (RSM). The slime was passed through the hydro-cyclone to pre-concentrate iron ore slime before feeding to spiral. The underflow of hydro-cyclone was used for further beneficiation. Models were developed to predict the  $\text{Al}_2\text{O}_3$  content (%) in the final concentrate and yield by changing operating conditions like splitter position, feed pulp density and feed rate. It was concluded that the concentrate with lowest  $\text{Al}_2\text{O}_3$  content of 1.63% can be produced with splitter position at 3 cm and the pulp density at 20% solid. The yield of the process was 54.54%, which is considered as good.

#### **2.4.3 Beneficiation of low-grade iron ore/slime through magnetic separation:**

Magnetic separators utilizes magnetic properties of minerals. The difference in magnetic characteristics between valuable minerals and gangue mineral are exploited to separate valuable magnetic minerals from gangue having non-magnetic characteristics or visa-a-versa. For an example, some of the tin deposits, consisting Cassiterite as ore, are associated with magnetite, which can be separated by magnetic beneficiation process (**Wills, 1988b**). Any mineral placed in the magnetic field will react in certain way depending upon its magnetic characteristics. The minerals that exhibit very little effect under magnetic field cannot be separated by magnetic forces. Minerals can be attracted or repelled under magnetic field. Therefore, the minerals can be broadly placed in two groups. (i) The minerals, which are

repelled towards lower magnetic intensity, are *Diamagnetic*. Diamagnetic minerals cannot be beneficiated magnetically. (ii) The minerals, which are attracted towards line of force of magnetic field, are called Paramagnetic minerals. The paramagnetic minerals can be separated from nonmagnetic or diamagnetic minerals by application of magnetic field. Magnetite ( $Fe_3O_4$ ), Wolframite ((Fe, Mn)W0<sub>4</sub>), Ilmenite ( $FeTiO_3$ ) etc minerals are commercially beneficiated through magnetic separators. The intensity of magnetization of paramagnetic minerals increases with increase in strength of applied magnetic field (**Fig 2.7**). The diamagnetic minerals remains unaffected by application of magnetic field.

The beneficiation iron ore tailing generated in Pilbara mines, Australia was studied by Steinberg et al. (**Steinberg et al., 2015**) by using wet high intensity magnetic separator (WHIMS). The study was also taken on de-watering of the concentrate and tailing generated after the processing. Two types of tailing samples were treated, one from tailing dam and another sample was collected from processing plant, i.e. live tailing. The size analysis of both the samples indicates that more than 58 % of the particles are below 63 micron and 100% of particles are below 250 micron. The sample were de-slimed at cut point of  $d_{50} = 10$  micron. Size wise chemical analysis of the samples reflect the presence of clay at lower size fraction of ore (-10 micron). The de-slimed tailing sample was passed through Jones WHIMS (**Fig 2.8**) for beneficiation. The Jones WHIMS (as shown in Fig 2.8) is unique in many ways. The Jones WHIMS have capability to separate feeble magnetic minerals also at very fine size. The energy required to generate high magnetic field is also very low compare to other types of WHIMS. The feed tailing with 59.7% Fe(T) was passed through Jones WHIMS at magnetic intensity 8000 to 13000 Gauss. The maximum recovery was obtained at higher gauss of 13000. The final concentrate obtained was having Fe(T) 64.9% with Fe recovery of 85.4 %. Therefore, it was a successful case of beneficiation of iron ore tailing with Jones WHIMS.

The beneficiation of -0.5 mm fines from Gua Mines, Jharkhand was studied (**Sharma et al., 2015**) by using two stage beneficiation process, i.e. multi gravity separator and wet high intensity magnetic separator (WHIMS). The as-received slime from Gua mines contains 59.03% Fe(T) with very high alumina about 6.51% and silica about 4.59%. Microscopic study revealed that most of the alumina exist in solid solution with goethite and limonite and significant part of alumina exist as clay minerals and gibbsite. The final concentrate reported

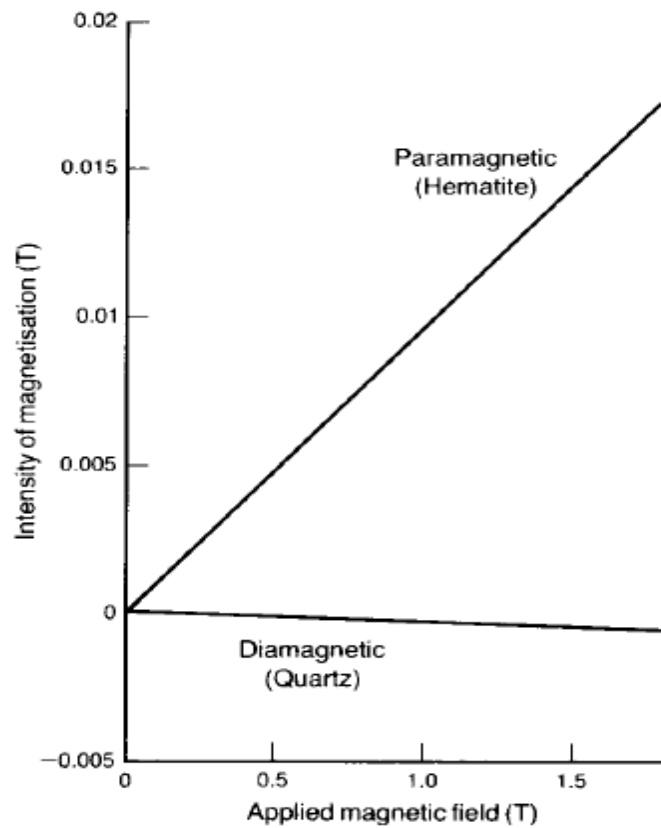


**Fig.2.7** Magnetization curve of paramagnetic and diamagnetic minerals (Wills, 1988b)

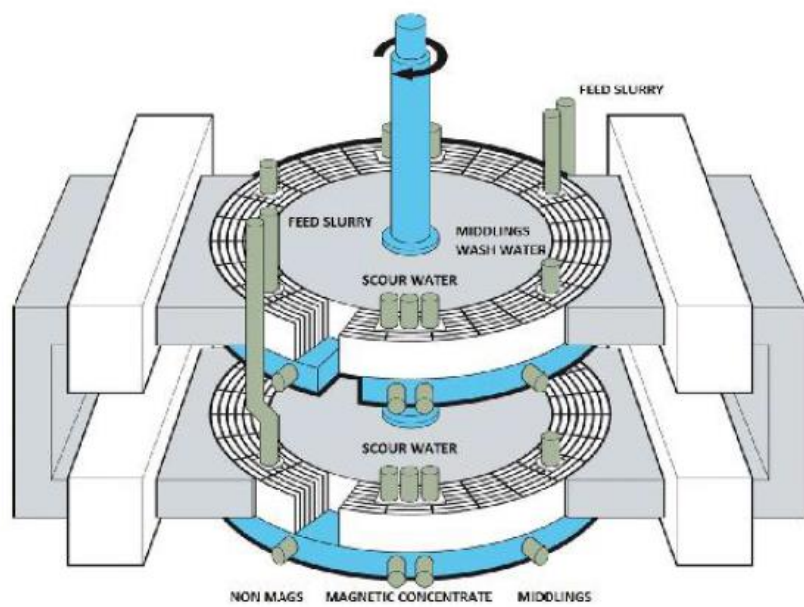


**Fig.2.8** Jones WHIMS used for beneficiation of tailing (Steinberg et al., 2015)

contains 64.68% Fe(T) was with overall recovery of 70% after two stage beneficiation. This is also an example of successful use of WHIMS for beneficiation of low grade iron ore fines.

#### **2.4.4 Beneficiation of low-grade iron ore/slime through flotation:**

The forth flotation is a physico-chemical separation method and widely used for separation of sulfide and precious minerals. The application of flotation as principle method of beneficiation in iron ore is very limited. Only one plant of Samarco in Brazil has adopted flotation technique for beneficiation of lean grade iron ore. The concentrate produced from this plant is used for pellet making. The flotation technique is suitable for the lean grade iron ore with relatively finer size (< 100 mesh). The flotation technique can also be used for the additional recovery of iron value from rejects of concentrates, presently as scavenger (recovery of iron value from tails) flotation, employed at Four-Taconite beneficiation plant in Minnesota (**Poveromo, 2000**).

Flotation technique works on difference of affinity of valuables and gangue minerals to air. In floatation, the contact angle is a very important parameter. The contact angle is represented in **Fig.2.9**. The contact angle provides an idea of in what manner the air bubble spreads or damps the solid surface. If contact angle is less than  $90^\circ$  then it is classified as low contact angle and indicates that the surface is *hydrophilic*. If contact angle is more than  $90^\circ$  then the surface of the mineral is classified as *hydrophobic*. Hydrophobic means repulsion from water so the mineral surface will contact with air than water because of lesser free energy. The mineral with hydrophobic surface will attach to air interface. Some minerals does not fall under hydrophobic can still stick to the air with the presence of a reagent.

Different types of reagents are used for selective modification of surface behavior of iron oxide and gangue minerals. In *normal flotation*, reagent is added to modify surface of iron oxide to have affinity to air. The iron oxide will be attached with bubble due to its affinity towards air and separated out. In *reverse flotation*, gangue minerals will be floated out. The reagents used to change surface property for preferential attachment with air are frequently called *promoters* or *collectors*. Frothers are added in the solution for formation of stable bubble (or formation of forth). Other constituents are supplemented to regulate pH, or to cause improved flocculation or dispersion. The substance used for control of pH is called as *modifiers*, the substances used for improvement of dispersion are known as *dispersants*.

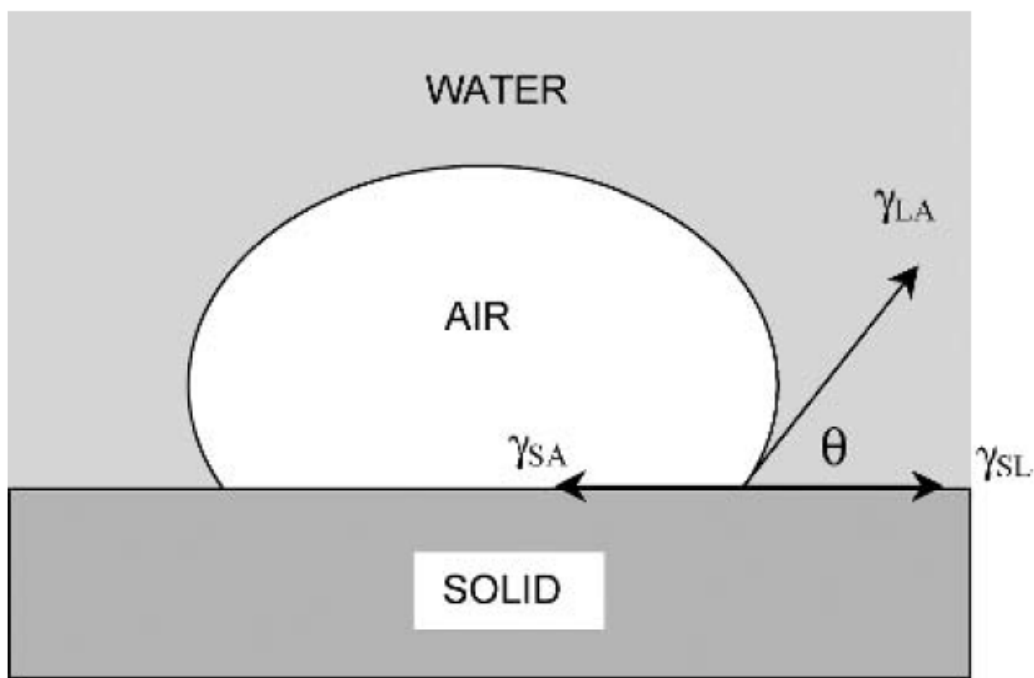


**Fig.2.9** Contact angle between three phases (air, liquid and solid)

Flotation collectors are also categorized as cationic and anionic. The fatty acid is used as collector in most of the flotation process. Petroleum sulfonate is also a common collector. Uses of fuel oil promotes better separation of iron oxide finer than 10 microns.

**Fig 2.10** represents conventional floatation cell. Pressurized air is passed along the central shaft. The central shaft is connected with stirrer and diffuser. It is an industrial model of floatation cell.

Mishra et al. (**Mishra et al., 2017**) have studied the beneficiation of iron ore tailing through floatation process. The separation of quartz from iron ore tail is more effective in basic pH through reverse floatation. The extensively used collectors for floating quartz impurity are ether amines, similarly most extensively used dispersant during floatation of iron ore is Corn starch. The performance of separation of alumina rich gangue mineral through flotation is not encouraging due to difference in surface property of alumina and silica minerals in the gangue.

The complex mineralogy, finer size and un-liberated minerals are the major challenges for up-gradation of slime as concentrate by using only froth floatation technique. The beneficiation of high alumina iron ore slime using hydro-cyclone and floatation was studied by Thella et al. (**Thella et al., 2012**). Two-stage classification by hydro-cyclone is adopted as pre-concentrator. In stage one, classification through hydro-cyclone was used. The concentrate obtained with an assay of 61.99% Fe(T), 3.22 % SiO<sub>2</sub> and 4.0% Al<sub>2</sub>O<sub>3</sub> with 54.55% recovery of iron value. After second stage classification, further improvement in grade is recorded with iron value 62.19% Fe(T) and recovery of 47.45%. The concentrate obtained after two stage of classification is beneficiated by adopting reverse cationic floatation with amines as collector and direct floatation by using fatty acid. A final concentrate with assay of 64.46% Fe(T), 2.05% SiO<sub>2</sub> and 2.66% Al<sub>2</sub>O<sub>3</sub> with 34.13% recovery of iron value. The highest yield and recovery with blast furnace grade concentrate is obtained by reverse cation floatation. Starch is used as depressant along with amine as collector.

The beneficiation of ultra-fine slimes obtained from iron ore processing plant has been addressed by Rocha et al. (**Rocha et al., 2010**) through reverse cationic floatation to obtain pellet feed concentrate. De-sliming followed by floatation with different dosage of collector and depressant were carried out with slime samples. The reverse cationic floatation technique

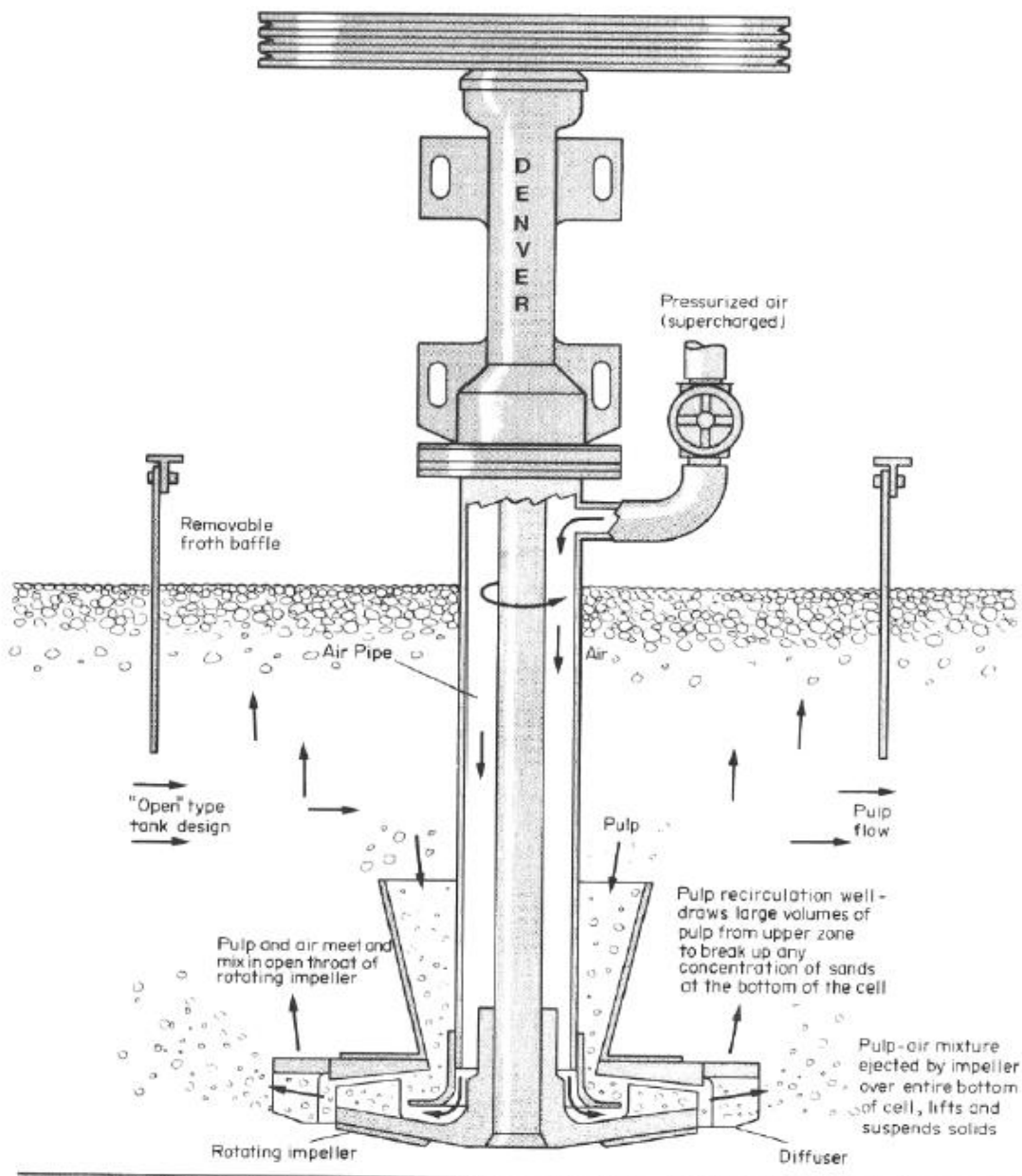


**Fig.2.10** Flotation cell (Wills and Napier-Munn, 2006)

(column flotation) was successful in obtaining concentrate with minimum impurities. The recovery of iron value is around 80 % with high grade of concentrate (less than 1%  $\text{SiO}_2$ ) and the reject of the flotation process contain only 12% Fe (T).

The influence of different minerals present in the iron ore on the flotation process was studied by Sahoo et al. (**Sahoo et al., 2016**). Synthetic blends of hematite–silica (quartz), hematite–alumina (gibbsite) and hematite–clay were prepared. These mixture of minerals were subjected to reverse and direct flotation with dodecyl amine and oleic acid as the collectors respectively. The study revealed that pure silica (quartz) response was better during flotation in comparison to gibbsite and clay minerals. The flotation of silica minerals in both direct and reverse flotation was better as compared to other minerals .Further flotation studies on naturally occurring high silica low grade ore and high alumina low grade ore were also studied and concluded that it was easier to beneficiate ore with high silica than high alumina. The iron grade and recovery obtained from high silica iron ore are 62% and 86% respectively, but in the case of high alumina iron ore the recovery was very low and up-gradation was less. This is attributed to the presence of alumina in the matrix of iron ore sample.

## **2.5 Micro-pellet making and granulation**

Iron ore lump, sinter, and pellets are the principal iron-bearing constituents of blast furnace burden. In recent times, agglomerates (sinter and pellets) are becoming preferred iron-bearing constituents for the blast furnace burden, because of limited availability of high-grade iron ore worldwide and improvement in quality of agglomerates promotes their use. During beneficiation of iron ore, very fine size concentrate is also produced, which cannot be used in blast furnace and this need to be agglomerated. Although beneficiated iron ore are normally higher in iron grade with lower gangue minerals, the finer size particles present in the concentrate restrict their usage in sintering process. Therefore, pelletizing is needed to convert fine particles of iron ore in to micro-pellets for subsequent use in sintering.

### **2.5.1 Formation of micro-pellets**

Micro-pellet formation can be achieved using either disc pelletizer or drum pelletizer. The formation of micro-pellets depends upon fineness of the iron ore and other raw materials, the moisture addition during pellet making, dosage of binder and wettability of the iron ore

particles. Iron ore fineness in pellet-making is normally expressed as specific surface area (SSA) and also called as Blaine number.

**Fig.2.11** illustrates the stages of formation of iron ore pellets. The stages A and B defines nucleation stage, stage C defines grain growth and assimilation, stage D defines densification of particles and the stages E and F illustrates growth of pellets by layering with further consolidation.

### 2.5.2 Effect of moisture on formation of micro-pellets

The pellet formation takes place due to the presence of moisture, initially the moisture covers each individual particle and attached to each other due to formation of bond at point of contact (**Fig.2.11**). The importance of capillary theory for green pellet strength is well defined in literature (**Meyer, 1980**). The highest green strength of the pellets are achieved when all pores are filled. The pores are filled with moisture and concave shape of surface formed because of capillary forces. The concave surfaces are formed with 90–95% moisture saturation, as shown in **Fig.2.12**. The strength of pellet depend upon the moisture saturation. At low moisture saturation, the pellet strength is due to liquid bridge formed between the particles. As moisture saturation increases, capillary forces, and cohesive forces also contribute to the strength of pellets.

Forsmo et al. (**Forsmo et al., 2006**) found that the plastic behavior of green pellets sets in once moisture in pellet become over saturated. The increase in moisture after over saturation causes rapid increase in plasticity of the green pellet. It is also observed that high moisture result in the generation of high porosity in the pellets, which cause very high plasticity. They defined flood point during pellet making. The moisture content in the pellets reaches to a point where pellets deform due to their own weight is defined as flooding point.

The impact of moisture content on ballability of iron ore pellet was modeled by Fan et al. (**Fan et al., 2015**). The moisture content in the green pellet defines its shape and size distribution. The moisture was categorized into molecular and capillary liquid. The final shape size and strength of the pellets was linked to the content of molecular and capillary water in the green pellets. They proposed a model for evaluation of ballability and its

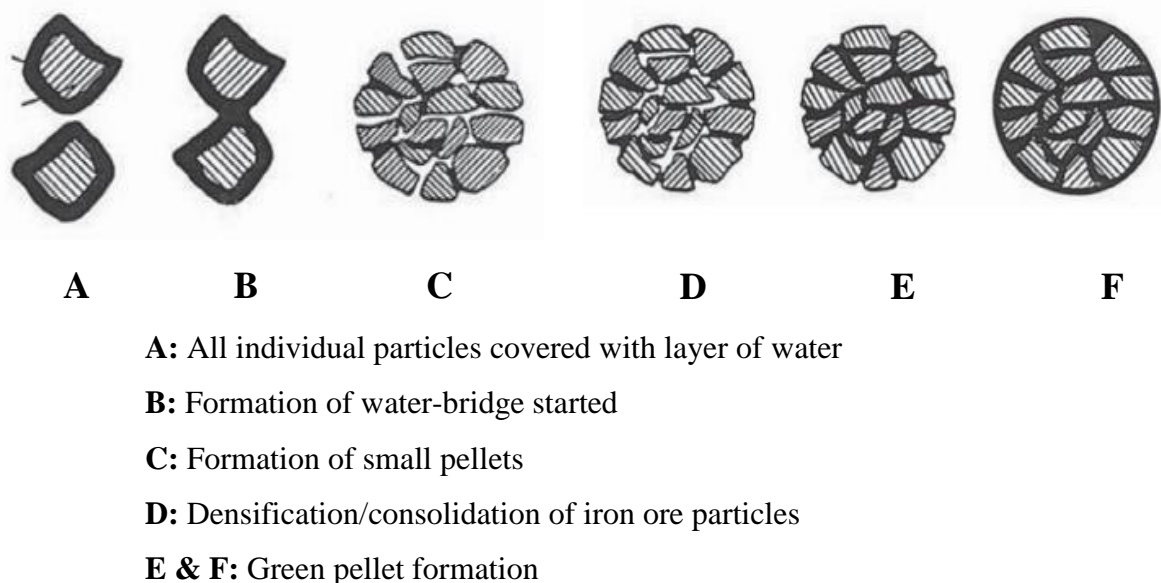


**Fig.2.11** Different steps of micro-pellet formation (Meyer, 1980)

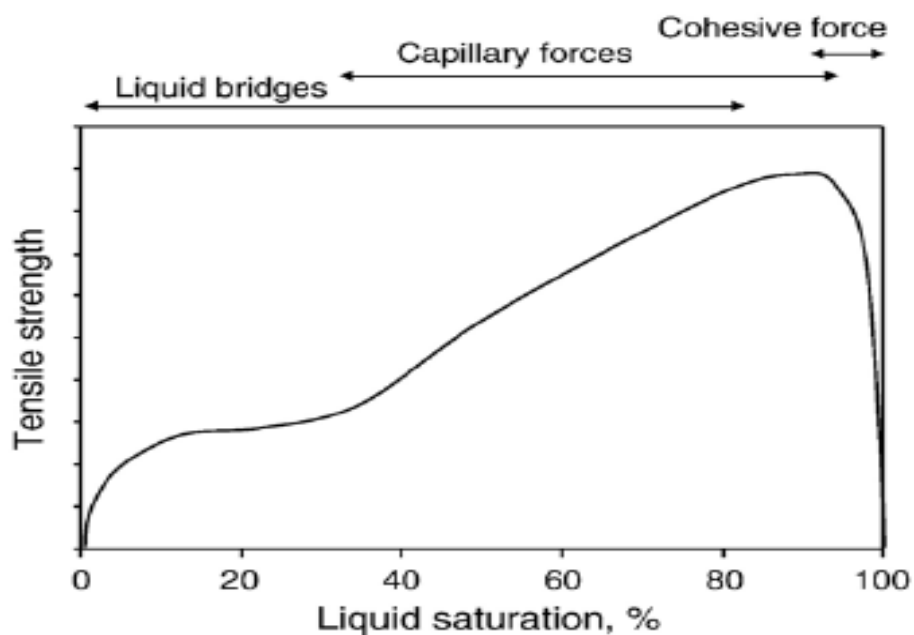


**Fig.2.12** Effect of moisture saturation on the tensile strength of the pellet (Forsmo et al., 2006)

interaction with particle size distribution and hydrophilicity of iron ore concentrate. Ten different types of concentrates were pelletized to evaluate natural ballability model. The model provides better prediction of green property of pellet in comparison to conventional ballability index (K) with only moisture (in absence of binder).

### **2.5.3 Effect of binder on formation of micro-pellets**

The binder play very important role in the formation of micro-pellet. The moisture provide spherical shapes to the iron ore micro-pellets, whereas binder provides requisite strength to the pellets so that it can be transported without disintegration from pellet making zone to firing zone. The binder has two roles in micro-pellet making: (i) The binder forms network structure and convert wet iron ore plastic, it promote nucleation of seeds that grow into well-formed pellets at very control rate and (ii) The moisture present in the pellet is removed during drying, so the binder should hold the particles together during and after drying until pellet is fired and get sufficient strength. These two criteria are used for selection of suitable binder.

Bentonite is a silicate based mineral and traditionally used as binder in pellet making. It improves the green or wet properties of micro pellets, such as wet compressive strength, drop strength, and thermal stability during firing. However, bentonite increases silica and alumina content in the fired pellet. Significant research has been occurred for reducing bentonite content in the pellet mix. Increase of surface area by high pressure gradient roll (HPGR) is one of the method used for reduction of binder (**Meer, 2015**). Research also reported the use of organic binder in place of bentonite (**Srivastava et al., 2013**). The different types of binders used by industry/researches are listed in **Table 2.2**.

The binder requirement for pellet making with hematite concentrate is less compared to magnetite concentrate to achieve minimum strength as per industry norm for drop number and green crushing strength (**Kawatra and Halt, 2011**). The pellets made with hematite concentrate without binder have 5 drops and green strength was 22 N/pellet. The similar industrial requirement of green properties of pellets made of magnetite concentrate can be achieved with bentonite content of 0.66 % (6.6 kg/ton). These studies were conducted with near particle size distribution of magnetite and hematite concentrate to eliminate effect of size distribution as a factor. The study concluded that shape and mineralogy of individual particles may be dominating factor during pelletization. The presence of residual material may also be having significant impact on green properties.

Zhu et al. (Zhu et al., 2015) have studied the effect of bentonite and hydrated lime independently during pellet making with hematite concentrate. The effect of binder dosage is presented in **Fig.2.13**. It is observed that 0.8% (8 kg/ton) bentonite as binder is sufficient to get industrially qualified green pellets (more than 5 drop from height of 0.5 m), whereas minimum 2% (20 kg/ton) hydrated lime is required to get similar strength in green pellets. The green pellets produced with hydrated lime have higher compressive strength and same drop number compared to pellets produced with bentonite. Uses of hydrated lime has additional advantages as it also act as flux and further addition of limestone is not required.

#### **2.5.4 Effect of surface area of concentrate on formation of micro-pellets**

Particle size distribution of iron ore is directly proportional to surface area. Surface area of the iron ore also depend upon porosity and shape of individual particle. Increase in surface area of iron ore concentrate results in increase in green compressive strength and drop number of the pellets. The balling efficiency increases with increase in surface area. The fired pellet also have little improvement in cold crushing strength due to increase in surface area (**Fan et al., 2012**).

Zhu et al. (**Zhu et al., 2008**) used mechanical milling on iron ore concentrate to produce high surface area and studied its impact on pelletability. The magnetite ore concentrate was passed through high pressure gradient roll (HPGR) using 120 RPM and 2.33 MPa roll pressure to improve surface area. The iron ore concentrate was passed twice through the HPGR. The bentonite dosage for pellet making has come down from 2 to 1%. Higher drop number of the pellets (3.3 times to 4.6 times) was reported. The improvement in ability to form pellet from concentrate was also noted with increase in surface area. Modification in morphology of every particle due to HPGR cause higher surface activity of the concentrate, which is attributed to mechano-chemical changes occurring during HPGR process.

**Table 2.2** Various organic and inorganic binders used for iron ore pellet making (**Srivastava et al., 2013**)

Binder	Generic Formula	Grade/Purity	Particle Size ( $\mu\text{m}$ )
Bentonite	$(\text{Na},\text{Ca})_{0.3}(\text{Al},\text{Mg})_2\text{Si}_4\text{O}_{10}(\text{OH})_2 \cdot n(\text{H}_2\text{O})$	—	14
Molasses	$\text{C}_6\text{H}_{12}\text{NNaO}_3\text{S}$	— (Liquid)	—
Wheat flour	$(\text{C}_6\text{H}_{10}\text{O}_5)_n$	100 pct Purity	176
Corn starch	$(\text{C}_6\text{H}_{10}\text{O}_5)_n$	100 pct Purity	22
Peridur	NA	NA	249 (Granular)
Sodium metasilicate	$\text{NaSiO}_3$	Reagent Grade	205 (Granular)
Calcium hydroxide	$\text{Ca}(\text{OH})_2$	Reagent Grade	44
Calcium carbonate	$\text{CaCO}_3$	Reagent Grade	44
Potato flour	$(\text{C}_6\text{H}_{10}\text{O}_5)_n$	100 pct Purity	352 (Granular)
Cellulose	$\text{C}_6\text{H}_{10}\text{O}_5$	99.9 pct Purity	20
Xylan (hemicellulose)	$\text{C}_5\text{H}_{10}\text{O}_5$	97.0 pct Purity	88
Sodium lignosulfonate	$\text{C}_{20}\text{H}_{24}\text{Na}_2\text{O}_{10}\text{S}_2$	Technical grade	80
Lactose monohydrate	$\text{C}_{12}\text{H}_{22}\text{O}_{11}\text{H}_2\text{O}$	Technical grade	76
Polyacrylamide	$(\text{C}_3\text{H}_5\text{NO})$	Technical grade	226 (Granular)
Alcotac FE8	NA	Cellulose based	80
Sodium carbonate	$(\text{NaCO}_3)$	Technical grade	42
Calcium chloride	$(\text{CaCl}_2)$	Technical grade	36
Paper sludge	NA	NA	— (Shredded)

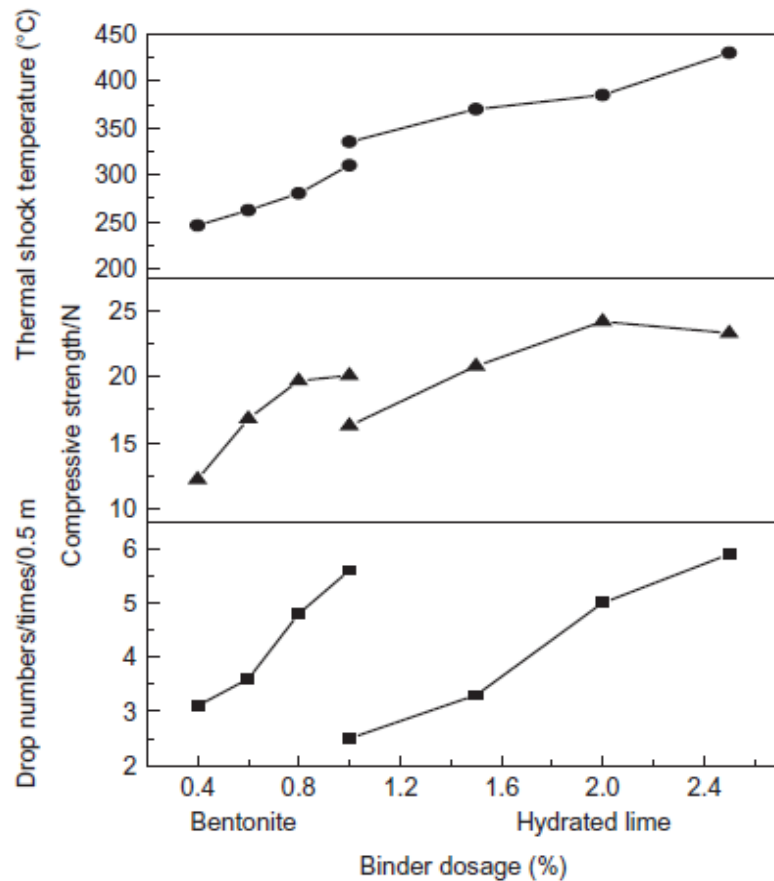


**Fig.2.13** Effect of binder dosage on the green ball properties (**Zhu et al., 2015**)

## 2.6 Iron ore sintering

Iron ore sintering process was developed in the year 1890 and process is known as Huntington Heberlein sintering method. This is a batch process. The continuous type of sintering machine was developed by Dwight and Lloyd (Maxico) in the year 1911. First sinter plant in India was installed at TATA Steel, Jamshedpur in the year 1958 under two million tons (TMT) program. The sinter plant was supplied and installed by M/s Lurgi, Germany. The oldest sinter plant has undergone various technological improvements with up-gradation of facilities. The oldest sinter plant is still able to supply desired quality of sinter and meeting stringent norm of present blast furnaces. Before installation of this sinter plant, iron ore fines were not used in the iron making processes, so the sinter helped in better utilization of mineral resources thereby reducing pressure on iron ore mining to meet the sized lump ore requirement.

The iron ore sintering is one of the oldest and widely used methods during iron making across the globe. Many western countries have discontinued the iron ore sintering due to various reasons and the main reason being worst impact on environment due to generation of high amount of greenhouse gases including SO<sub>x</sub> and NO<sub>x</sub>. Over many decades, the sintering processes have undergone various improvements. Sintering of iron ore is accomplished by converting fine particles of ore into porous and large sized lump by application of heat. The sinter formation takes place because of incipient fusion of fine ores at contact point, which bind the particles together. Another bonding mechanism contributing significant strength to the sinter is recrystallization and grain growth of hematite minerals present in the sinter mix. Formation of low melting temperature slag due to combination acidic minerals (SiO<sub>2</sub> and Al<sub>2</sub>O<sub>3</sub>) with basic minerals (CaO and MgO) also increases the strength of final sinter. Sinter is preferred iron-bearing burden for the modern blast furnace. Iron ore sintering is an art than science (**Poveromo, 2000**). The iron ore sintering process is very flexible and permits utilization of various fines generated in integrated steel plant like flue dust, sludge containing iron value etc.

The flow sheet of industrial scale iron ore sintering plant is shown schematically in **Fig.2.14**. This is a travelling grate sintering machine that carry a bed of very well mixed materials consisting of iron ore fines, coke and fluxes. Coke breeze of anthracite coal is used as fuel in iron ore sintering process. The top layer of intensely mixed ore and other raw materials

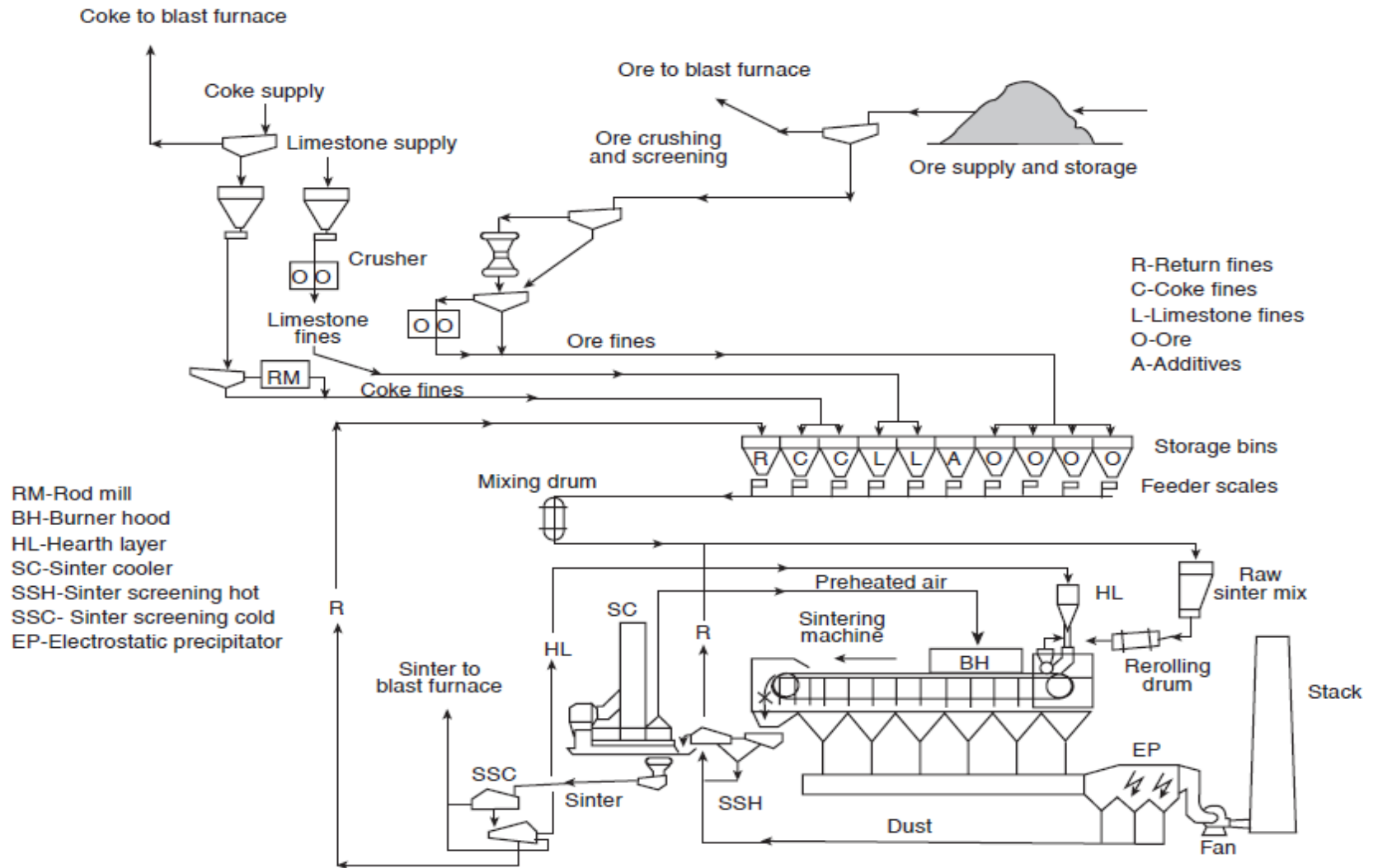


**Fig.2.14** Schematic flow diagram of industrial scale iron ore sintering plant (Poveromo, 2000).

including fuel is fired with the help of gas fired burner. The air is sucked through the bed to burn the fuel present while the mixed material moves on the travelling grate. The downdraught firing of fuel causes sufficient increase in temperature up to 1300°C to 1450°C of the mix. At high temperature, the whole mass is converted into fused lump, which again sized as per requirement of blast furnace. The sintering process will be completed once the heat front reaches to burn through point near the bottom of the mixed material just above the grate.

At initial stage of industrialization, sinter plants with smaller capacities were installed but at later stage sinter plants of larger size and higher capacity were added. At present, largest size of 496 m<sup>2</sup> sinter plants are operated by TATA Steel, Kalinganagar, Odisha and Jindal Steel Works (JSW), Tornagallu, Karnataka. The present practice is to install single sinter plant with larger capacity at most of the integrated steel plants. The total installed capacity of sinter plant in India is 80 MTPA.

### **2.6.1 Mixing and granulation in sintering process**

The high-grade iron ore resources are depleting at relatively faster pace and left over iron ore are relatively inferior in quality and have higher amount of deleterious materials. These ores need to be beneficiated before use in any agglomeration process. The beneficiation of ore may increase ultra-fines content in the iron ore fines which have detrimental impact on sintering process and quality. Similarly, higher impurities in the iron ore fines will leads to poor quality of sinter. Now-a-days, many bigger blast furnaces with useful volume more than 4000 m<sup>3</sup> are under construction in India. These bigger blast furnaces have very stringent quality requirement of sinter. The environment regulations are becoming more and more stringent with respect to emission, thereby creating addition pressure on sintering process to meet these norms. A variety of developments have been taken place in sintering technology to handle changing characteristics of raw materials and lessen emission during sinter making.

Over a period, the ultra-fines contents in iron ore fines keep on increasing. Increase in ultra-fines has adverse impact on productivity and quality of sinter. In late nineties, granulation of fines was developed in lab scale and very soon this technology of intensive mixing followed by granulation was adopted in many sinter plants (**Zhou et al., 2017**). Latest plants

are equipped with combination of high-speed three dimensional vertical mixer and a drum mixer are considered in place of conventional system (**Fig.2.15**). Further, use of vertical mixer has reduced the space requirement in sinter plant apart from other benefit of accepting iron ore fines with higher quantity of ultra-fines. This system will do away with the base blending space available at sinter plant. Many researchers have acknowledged the importance of mixing in agglomeration process (**Ennis, 1996**). The final property of the agglomerate heavily depends upon effective mixing of all raw materials.

The installation of granulation system with intensive mixer increase productivity through the improvement of permeability and also helps in lowering water consumption and generation of sinter return. Tata steel , Jamshedpur plant was the first plant in India to incorporate granulation system with intensive mixer followed by public sector steel maker, i.e SAIL, RINL. Recently JSPL has installed a sinter plant ( $490\text{ m}^2$ ) with intensive mixing granulation system (IGMS), NMDC Iron and Steel Plant, Nagarnar, Chhattisgarh is also in the process of setting up of sinter plant ( $460\text{ m}^2$ ) with IGMS.

Kasai et al. (**Kasai et al., 2008**) have used different condition of mixing for sinter feed preparation and the permeability of mix was determined before firing with the use of anemometer. The experimental small sinter pot grate system was equipped with a gas pre-heater with provision to have 29 mm high sinter bed. This system can measure pressure drop very accurately. As anticipated, the permeability of the sinter mixes before ignition was dependent on average or mean particle size of the granules and the mean granule size depend upon moisture content of the mix. It is observed that the permeability of the sinter mix (bed) remain unaffected during sintering. The sequence of raw material addition in the sinter mix is also having impact on permeability of bed. The permeability of sinter mix was improved in case of last addition of coke in the sinter mix. However, permeability achieved through sequencing raw material, during mixing, deteriorated during firing. Use of coarser size of limestone and coke caused enhancement of permeability in green condition and during firing.

Oyama et al. (**Oyama et al., 2005**) attempted to develop advanced granulation system for dealing with raw mixtures with the aim to improve productivity of commercial sinter plant along

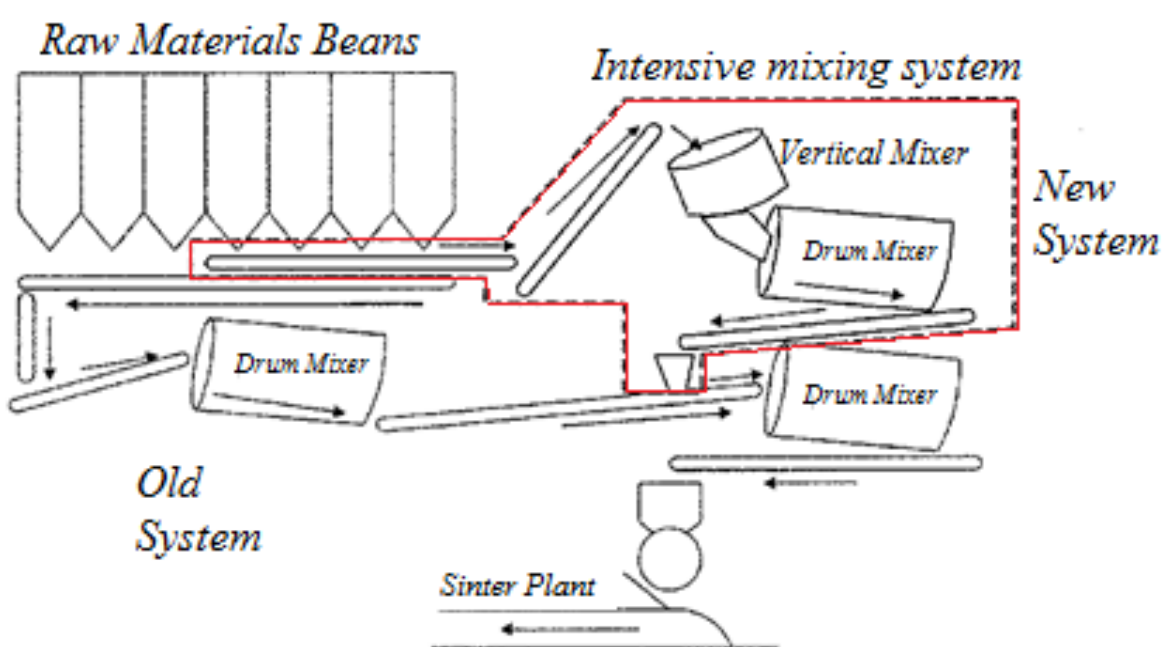


**Fig.2.15** Block diagram of intensive mixing and granulation System

with reducibility of the sinter. The coating on granules was achieved in a drum mixer. The innovative granulation system is categorized by coating very fine limestone and coke particles on the surface of quasi-particles as loosely packed layer. The quasi particles were generated at first stage mixing in horizontal drum. Specially designed mechanism was used for spraying of fine particles of limestone coke in the drum mixer. It was observed that the coating time had maximum impact on achieving desired improvement. The coating on the granules resulted in improvement in permeability. Enhanced productivity was reported due to better permeability of the bed. The innovative process extraordinarily improves both the reducibility and productivity of iron ore sinter products at commercial scale.

Zhou et al. ([Zhou et al., 2017](#)) studied the influence of addition of iron ore concentrate on granulation and packing of green bed. The green bed properties were measured at wide range of moisture and different dosages of hydrated lime. The growth of granules by layering of fine particles was observed in the presence of sufficient water and hydrated lime. However, granules form at the similar level of moisture and lime may exhibit poor permeability on addition of higher amount of iron ore concentrate. The poor permeability was attributed to breakage of weak and thick layer formed over the granules due to higher amount of concentrate. Two tests with 10% and 30% iron ore concentrate were conducted with varying hydrated lime content from 0 % to 4 % ( weight %) . The improvement in permeability of sinter bed were recorded in terms of JPU as 53.0 with 10 % concentrate and 0% lime to 65.8 with 10 % concentrate and 0.4% lime. Similarly mix prepared with 30% concentrate had improvement in permeability from 39.4 to 60.8. The higher quantity of concentrate causes higher packing with lower voids and these lower voids had adverse impact on quality and productivity of the sinter.

### **2.6.2 Effect of use of different type of iron ore in sintering process**

Chemical composition and mineralogical structure of iron ore fines have direct impact on productivity and characteristics of the iron ore sinter. The behavior of magnetite concentrate during iron ore sinter making is little known as compared to hematite type of ore. The hematite type of iron ore fines are widely used for sinter making across the world. The fuel requirement for sinter making with iron ore fine containing hematite or goethite is lower in comparison with sinter produced with iron ore fine dominated by magnetite type

of iron ore. The primary bond during sinter making is Silico Ferrite of Calcium and Aluminum (SFCA) (Webster et al., 2012). SFCA form low melting liquid and provide strength to the sinter. The SFCA is formed from hematite type iron ore and not directly from iron ore consisting of magnetite (Yang and Davis, 1999). The magnetite concentrate can be used in sinter making at low temperature (lower than 1300°C) coupled with slow cooling to get desired quality of sinter (Yang, 2006). The slow cooling of sinter will promote formation of prismatic SFCA as shown in **Fig 2.16**. The structure of sinter formed and temperature required for sinter making with concentrate of magnetite and hematite is presented in **Fig 2.16**. The iron ore fines dominated with hematite can be converted in good quality sinter at around 1250°C and above. The desired strength in the sinter was achieved due to formation of SFCA.

Hematite iron ore fines blended with different proportion of magnetite have been investigated by Clout and Manual (Clout and Manuel, 2003). The desired physical strength in sinter is produced with higher amount of magnetite, which is achieved by higher fuel dosage and firing at relatively higher temperature (1350 to 1370°C). The sintering at higher temperature causes development of magnetite–magnetite grain network formed due to diffusion bonding between magnetite at higher fuel rate. Whereas, the sinter produced with only hematite iron ore requires lower temperature to produce good quality of sinter.

Titanomagnetite material was used for preparation of sinter by Bai et al. (Bai et al., 2011). The studies revealed that titanomagnetite type of iron ore cause reduced permeability in the sinter bed before ignition and during firing. The sintering in pot grate furnace with iron ore sample containing titanomagnetite resulted in a severe non-uniform firing from top to bottom as permeability of bed constantly deteriorated in vertical direction. Iron ore sinters obtained from the top layer of sinter bed had low strength as molten particles were not enough. The time taken to melt minerals at the lower is more and time required to reach peak temperature was also high. This phenomenon had adverse effect on productivity and quality of final sinter produced.

Effect of presence of different types of gangue minerals, their amount and size distribution on the assimilation and transformation into liquid phase was studied by Matsui et al. (Matsui et al., 2004) with five iron ores samples of different gangue composition. The

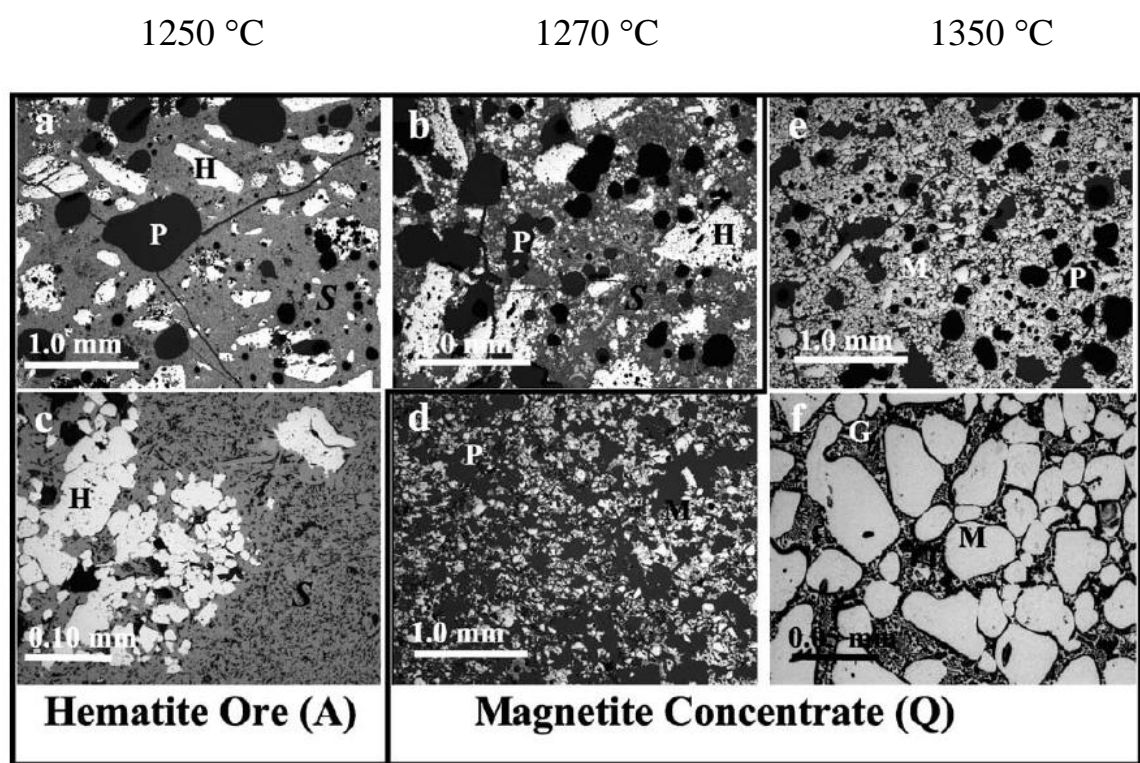


**Fig.2.16** Typical microstructure of sinter produced with different concentrates (Clout and Manuel, 2003)

lowest assimilation temperature (LAT) decreased with increase of silica ( $\text{SiO}_2$ ) in the iron ore. However, the index of fluidity of liquid phase (IFL) increased with increase of silica in iron ore. The alumina lower than 1.5% caused decrease in LAT whereas higher alumina had adverse impact on LAT. Higher quantity of quartz in the iron ore will increase number of sites for reaction with  $\text{CaO}$  thus LAT will be reduced. Further comparison between gibbsite and kaolinite minerals was carried out and found that the assimilation of gibbsite minerals was easy than kaolinite and both formed low melting liquid phase SFCA, which increases the strength of the sinter.

### 2.6.3 Formation of different phases during iron ore sintering

There are three types of minerals phases will be present in iron ore sinter (**Bhagat, 2007**) namely,

- a) Original or unaltered primary minerals,
- b) Secondary material formed from original minerals, which form primarily due to recrystallization and grain growth of hematite/magnetite in the solid state, and
- c) Constituents formed during sintering.

The most important phase in sinter making is Silico Ferrite of Calcium and Aluminum (SFCA). The physical and metallurgical characteristics of sinter depend upon distribution and morphology of SFCA in the sinter. SFCA is a quaternary system consisting of  $\text{Fe}_2\text{O}_3$ - $\text{CaO}$ - $\text{SiO}_2$ - $\text{Al}_2\text{O}_3$  and is presented in **Fig.2.17**. The SFCA is classified in to two categories on the basis of morphology, composition, and structure. The first type is called SFCA. It contains low Fe with triclinic crystal structure. It has columnar or prismatic structure under microscope. The chemical formula for SFCA is found as  $\text{M}_{14}\text{O}_{20}$  ( $\text{M} = \text{Fe, Ca, Si, Al}$ ) (**Hamilton et al., 1989**). The sinter produced in iron and steel plant is containing primary SFCA, typically contains 60-76%  $\text{Fe}_2\text{O}_3$ , 4 to 10%  $\text{Al}_2\text{O}_3$ , 3 to 10 %  $\text{SiO}_2$ , 10 to 13%  $\text{CaO}$  and about 0.75 to 2%  $\text{MgO}$  (**Patrick and Pownceby, 2002**). The second type of SFCA is named as SFCA-I and contains high-Fe and low-Si with needle like or acicular structure under microscope. Webster et al. (**Webster et al., 2014**) have established that the structure of SFCA and SFCA-I is different. The crystal structure of SFCA-I is also triclinic. For SFCA-I, silica is not essential for stabilization of its microstructure structure.

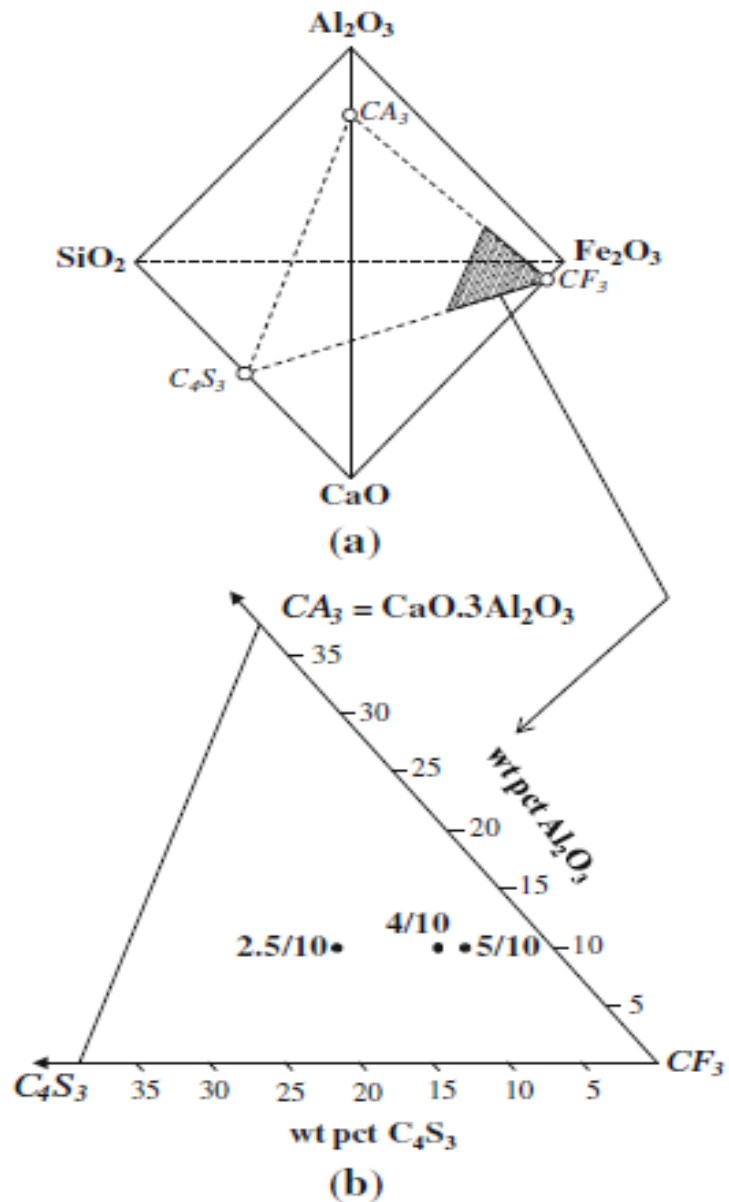


**Fig.2.17** (a) The  $\text{Fe}_2\text{O}_3$ - $\text{CaO}$ - $\text{SiO}_2$ - $\text{Al}_2\text{O}_3$  quaternary system. (b) The shaded part shows the section where SFCA forms. C=CaO, S=SiO<sub>2</sub>, A=Al<sub>2</sub>O<sub>3</sub>, F=Fe<sub>2</sub>O<sub>3</sub> (Webster et al., 2014).

The SFAC-I provide better strength and reducibility in the sinter, hence preferred structure in the fired sinter (**Scarlett et al., 2004**). The sinter containing very high amount of SFCA-I is considered as very high quality sinter. Scarlett et al. (**Scarlett et al., 2004**) have developed sequence of SFCA and SFCA-I formation. The sequence of formation is shown in **Fig.2.18**. Alumina free scenario was also studied, however the sequence of reaction presented in the **Fig. 2.18** was prepared considering alumina essentially present in the ore. Iron ore produced by Brazil, Australia and India contains alumina. Formation of  $\text{CaO-Fe}_2\text{O}_3$  system controls the creation and growth of SFCA and SFAC-I phases. The proposed sequence of reaction has not considered the energy required and changes occurs due to removal of chemically bound water and carbonates. The first reaction takes place at very lower temperature around  $740^\circ\text{C}$  to  $780^\circ\text{C}$ . At this temperature, calcium oxide combines with hematite and forms  $\text{C}_2\text{F}$  phase (calcium ferrite). Further  $\text{C}_2\text{F}$  continue to combine with hematite and ultimately converted into  $\text{CF}$  phase. The alumina formed after removal of combined water of gibbsite is very reactive and combines with  $\text{CF}$ . The silica is relatively non-reactive and start combining once temperature increases above  $1050^\circ\text{C}$ . Formation of SFCA or SFCA-I starts above  $1050^\circ\text{C}$ . The development of SFCA phase in sinter depends upon weight percent of alumina present in the iron ore.

#### **2.6.4 Relationship between sinter phases and its properties with basicity**

The ratio of basic oxides to acidic oxides in the sinter is defined as basicity. The mineralogical structure of sinter heavily dependent upon basicity of sinter (**Panychev and Nikonova, 2009**). Hematite and magnetite are the major iron bearing minerals apart from mono calcium ferrite in the sinter. SFCA and SFCA –I phases of minerals are predominant at higher basicity. At lower basicity ( $<1$ ), only hematite, magnetite and glass phase forms. However, at higher basicity (above 1-2) SFCA is predominant. At very high basicity more than 2, dicalcium silicate form, which increases the strength and reduces the reducibility of the sinter as shown in **Fig.2.19**. It is observed from **Fig.2.19** that the cold strength of the iron ore sinter increases with increase of basicity. The degree of reduction or reducibility of sinter initially increases with basicity up to 2, beyond which reducibility of the sinter decreases with increase of basicity. The slag bond form at higher basicity make a very dense mass with less porosity, which obstruct the reducing gases to penetrate the inside the sinter.

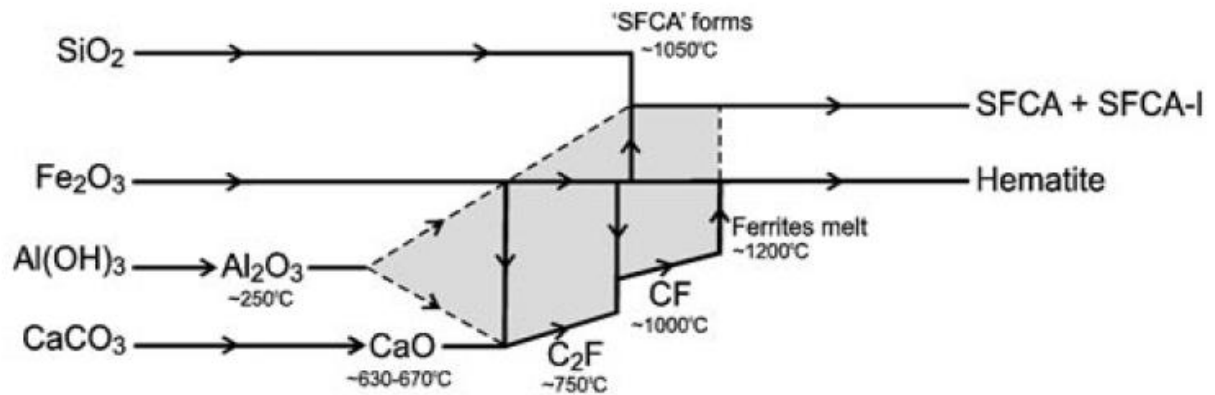


**Fig.2.18** Sequence of reaction during formation of SFCA and SFCA-I (Scarlett et al., 2004)

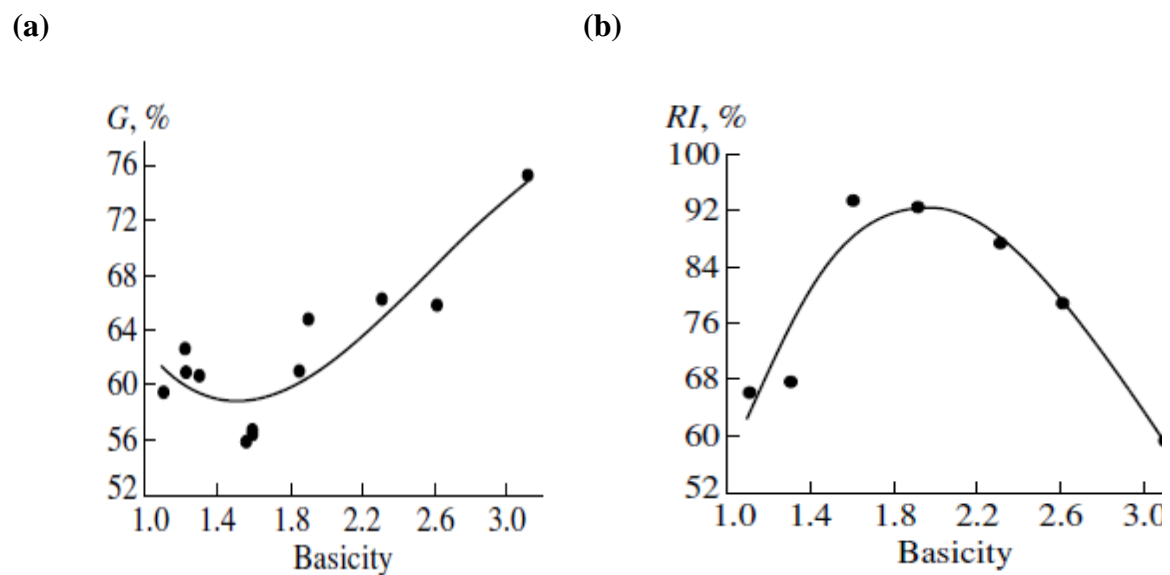


**Fig.2.19** Influence of Basicity on (a) cold strength and (b) degree of reduction (RI) (Malysheva et al., 2007)

## 2.7 Summery

### 2.6.1 Characteristics and beneficiation of iron ore slime

- The volume of tailing generation can be brought down by improving efficiency of existing beneficiation circuit and also by adopting improved and latest technologies, which prompt better recovery of iron value. Reduction of tailing volume will help in extending the life of tailing dam (**Krishna et al., 2015**).
- Diverse mineralogical and chemical characteristics of iron ore in each deposit of iron ore makes it distinct iron ore body. Generally, slimes contain various phases of minerals like hematite, magnetite, limonite, goethite (vitreous and ochreous), quartz, kaolinite, and gibbsite (**Srivastava et al., 2001**). The percentage of these minerals in slimes varies with location, types of deposit, process adopted etc in India.
- Gravity separation technique is widely used in slime processing. Gravity separators are particularly susceptible to the presence of ultra-fine particles (**Wills, 1988a**). The presence of ultra-fine particles (< 10 microns) increases the viscosity of the slurry and hence decreases the efficiency of separation and also causes unclear visual cut-points.
- Hydro-cyclone is the most preferred method for removal of ultra-fines (**Mohanty and Das, 2010**). Slime containing high silica and alumina (54.93% Fe, 7.45%  $\text{SiO}_2$  and 6.62%  $\text{Al}_2\text{O}_3$ ) from Joda East Iron Mine slime pond, India were beneficiated by using hydro-cyclone followed by floatation technique (**Manna et al., 2011**).
- The particle size of the slimes plays vital role in the selection of beneficiation technique. For coarser particles below 150 microns, physical methods like gravity separation (**Thella et al., 2012**) and magnetic separation (**Wills, 1988b**) techniques can be preferred. Similarly, for finer particles around 45 microns, floatation (**Mishra et al., 2017**) can be considered.
- Various developed technologies cannot be adopted directly for beneficiation of slime of Bailadila region due to different mineralogical and other characteristics of slime.

### 2.6.2 Sintering of iron ore slime concentrate

- Increase in ultra-fines has adverse impact on productivity and quality of sinter. Granulation of fines was developed on laboratory scale and very soon the technology of

intensive mixing followed by granulation was adopted in many sinter plants (**Kasai et al., 2008**).

- The mixing of raw material during sintering in drum is completely replaced with high-speed three dimensional vertical mixer and a drum mixer are considered in place of conventional system (**Cip et al., 2008**).
- The successful implementation of granulation system will allow certain percentage of ultra-fines (up to 40%) of iron ore in the sinter mix. Utilization of 100 % ultra-fines of iron ore in sinter making is still challenging.

# Chapter 3

## EXPERIMENTAL PROCEDURE

### 3.1 Introduction

In the present work, iron ore slimes from Bailadila mines located in Chhattisgarh state were selected for the study to meet the aim. The iron ore slimes were subjected to various standard procedures for studying their initial physical and chemical properties. The slimes were also studied microscopically by using optical and scanning electron microscopes to establish the status of liberated minerals. Based on these characterization inputs, detailed laboratory scale beneficiation studies were planned to recover iron value from the slime and is shown in **Fig.3.1**. Gravity, dry magnetic and wet magnetic techniques were used individually to beneficiate the iron ore slimes. As the individual techniques have yielded a limited success, combination of gravity and magnetic techniques were used to obtain beneficiated slime with maximum recovery of iron value. Based on the flow sheet developed at laboratory, a pilot plant was designed for the beneficiation of iron ore slime on large scale. The laboratory scale results were validated by pilot scale beneficiation facility. The concentrate thus obtained from the pilot plant was used for the manufacture of micro-pellets. The resultant micro-pellets were subjected to hybrid pellet sintering (HPS) using pot grate furnace. The sinter thus produced from micro-pellets was subsequently evaluated for its performance under simulated blast furnace conditions. The details of the characterization studies, laboratory scale and pilot scale beneficiation studies, micro-pellet making, hybrid pellet sintering and blast furnace simulation studies are discussed at various sections of this chapter.

### 3.2 Sampling and sample preparation:

#### *Iron ore slime sample from mines*

About ten tones of bulk sample of slime were received from tailing dam of Bailadila iron ore mines (deposit-5). The sample was thoroughly mixed and two representative samples weighing 500 kg and 2000 kg were drawn from it after following coning and quartering as shown in **Fig.3.2** for laboratory scale and pilot scale beneficiation studies respectively. Another 50 kg representative sample was drawn from the bulk sample for characterization purpose. The 50 kg sample was further reduced to 5 kg by using riffle

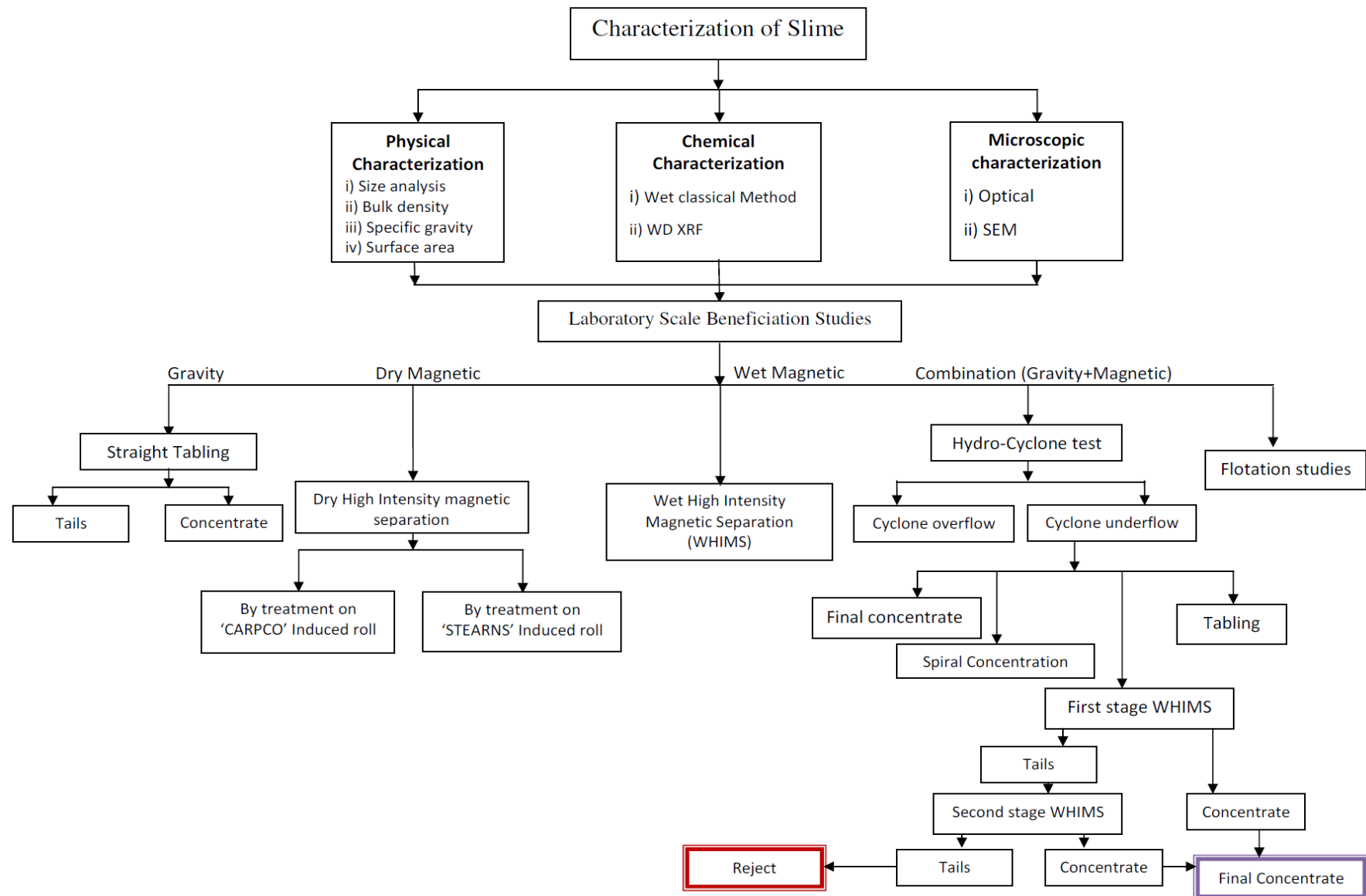


**Fig.3.1** Characterization and laboratory scale beneficiation studies of Bailadila iron ore slime



**Fig.3.2** Sampling and sample preparation by coning and quartering process

sample divider. From 5 kg sample, three samples weighing 1.25 kg each were drawn by coning and quartering technique for physical, chemical, and mineralogical analysis.

### **3.3 Characterization of slime and other raw materials:**

#### **3.3.1 Physical characterization:**

One representative slime sample of 1.25 kg was subjected to size analysis using different screen sizes [1mm,28 mesh,35 mesh, 48 mesh,65 mesh,100 mesh,150 mesh, 200 mesh, 250 mesh, 325 mesh, and 400 mesh]. The size analysis was carried out by wet screening in Ro-Tap sieve shaker. Ro-Tap sieve shaker generate two dimensional motions (horizontal and circular) of the particles with tapping from the top. The unique action of sieve shaker improves the efficiency of screen through stratification of particles. The wet screening of the sample was carried out as per IS 1607:2013 standard.

Second representative sample of 1.25 kg weight was grounded to -200 mesh in cup mill. Two samples each weighing 50 g were drawn from this by using rotary sample divider for the determination of specific gravity and chemical analysis. The specific gravity of iron ore slime was measured by using Micromeritics gas pycnometer (AccuPyc 1340) (**Fig.3.3**). The Blaine number (i.e. specific surface area) of the un-ground slime sample was measured by using Fisher sub sieve particle size analyzer (**Fig.3.4**).

The bulk density of slime was measured in accordance with IS5842:1986 standard. A metallic container of internal volume  $0.05 \text{ m}^3$  with cylindrical shape was used for measurement of bulk density. The height and internal diameter of the container are equal to 400 mm. The slime was filled in the container in three layers. After filling of each layer, the container was raised to 25 mm and dropped for better particle compactness. The weight of the container with slime and without slime was recorded. Bulk density was calculated by using the following formula:

$$\text{Bulk Density} = \frac{M_1 - M_0}{0.05} \quad (3.1)$$

where  $M_1$  = Weight of slime with container, and  $M_0$  = Weight of the empty container



**Fig.3.3** Gas pycnometer (AccuPyc 1340)



**Fig.3.4** Fisher particle size analyzer

Angle of repose of slime sample was measured by conventional method. Slime sample was filled in the same drum as used for bulk density. The filled container was covered with steel sheet and inverted on the concrete floor. The steel sheet is removed and the drum was lifted slowly in such a way that cone of slime is formed on the floor. The height and diameter of the cone was measured and the angle of repose was calculated by following formula:

$$\text{Angle of repose} = \tan^{-1}\left(\frac{H}{D/2}\right) \quad (3.2)$$

where H = height of the cone, and D = Diameter of the base of the cone

The size analysis of the iron ore slime was carried in accordance with IS 1607:2013. The sieves of size 2000, 1400, 850, 600, 425, 300, 212, 150, 105, 75, 53 and 44 micron were used during for size analysis. These sieves were meeting the specification stipulated in IS 460. After sieving, as per referred standard the test portions were dried and weight accurately. The dried sample was preserved for size wise chemical analysis in order to determine distribution of valuable mineral (iron oxide) in different size fraction of the slime.

### 3.3.2 Chemical characterization:

The chemical characterization of the slime was carried out by using Wet classical method and Instrumental method.

**Wet classical method:** It is an oldest and most accurate method for elemental analysis of ores and minerals. Only iron (Fe) content existing in the slime and other raw materials for sintering were determined by wet classical method. The Fe content was determined in accordance with IS:1493. The fine ground slime sample (-200 mesh) was dissolved in stannous chloride under boiling condition. Excess of stannous chloride was added to make sure that 100 % iron was reduced. The excess stannous chloride was cracked by the addition of mercury chloride solution. The solution obtained was containing reduced iron and the same was titrated with (0.1N) potassium dichromate solution. Sodium diphenylamine sulphonate was used as internal indicator.

**Instrumental method:** Wavelength dispersive (WD) X-ray fluorescence spectroscope (Fig.3.5) was used for chemical analysis of the slime. Wavelength dispersive (WD) X-ray fluorescence has high resolution and can detect all elements including lighter elements. For



**Fig.3.5** Wavelength Dispersive X-Ray Fluorescence equipment

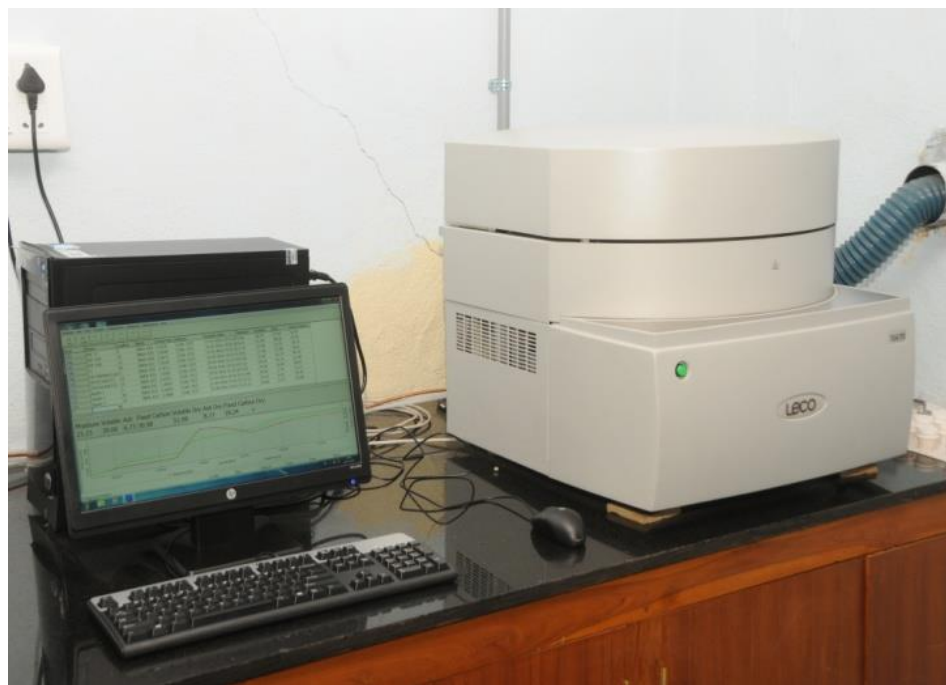


**Fig.3.6** Thermogravimetric Analyzer (LECO make; TGA 701)

this analysis, the sample is to be converted into glass beads by fusion. The sample analysis by using fusion beads eliminate error due to particle size and also minimize matrix effect on analysis results.

The test sample of slime (or iron ore or intermediate products) was mixed with sodium borate and fused in a platinum crucible. Sodium nitrate was also added in the mix to ensure complete oxidation of sulfur and iron. The molten mass was poured in a disc shaped die and disc type glass beads were obtained after cooling. The glass beads were exposed to x-ray and the fluorescence emitted from the sample was detected by WD detectors. Each individual element emits distinct radiation and the same can be recognized by the analyzing crystal based on their energy. This technique was used to measure all elements of the sample, except volatiles.

Inductively Coupled Plasma (ICP)–Atomic Emission Spectrometry (AES) technique was also used for the determination of alumina and phosphorous in the slime sample. Horiba make ICP-AES, model number JY2000 was used for the analysis. The principle of ICP-AES is measurement of energy intensity with unique wavelength emitted by electrons while moving from exited state to ground state. The wave length of energy emitted by metal and oxide are unique and intensity of energy can be converted in to concentration of that element.

The volatiles present in the slime sample and other raw materials were determined by using thermogravimetric analyzer (TGA) (LECO make; TGA 701) (**Fig.3.6**). The volatiles in the sample were represented by Loss on Ignition (LOI). The sample was heated in the absence of air up to 950°C and weight loss on heating was measured. The physical (dehydration) and chemical (dehydroxylation) bounded water in goethite mineral get removed at 100°C and 370°C respectively (**Pansu and Gautheyrou, 2006**). During LOI determination, dehydration and dehydroxylation of goethite were recorded.

### **3.3.3Microscopic analysis:**

#### **Optical microscope:**

Optical microscope was used for detailed ore mineralogical studies which include ore minerals phase analysis, ore and gangue minerals association, their mutual relationship,

mineral liberation parameters and photomicrography. The ore microscopy utilizes polarized light for identification of minerals. The sample preparation is very important and the polished surfaces of the samples were made free from scratches. The identification of minerals under microscope was made on the basis of the individual characteristics of minerals such as color, hardness, anisotropic or isotropic character, and reflectivity. Optical microscope was also used for the analysis of intermediate and final concentrates obtained after beneficiation of iron ore slime. Optical microscope was also used for quantification of phases present in the sinter. Leica make optical microscope (**Fig.3.7**) was used in the present study.

#### **Scanning Electron Microscope with EDS:**

The Scanning Electron Microscope (SEM) coupled with energy dispersive spectroscopy (EDS) provides information of an area of interest of the sample. Semi quantitative elemental analysis of any point, line or area can be obtained through EDS. SEM images show simple contrasts between different minerals and thus instantly provide a great deal of information about the area being inspected. A TESCAN make SEM (**Fig.3.8**) was used in the study.

#### **3.4 Laboratory scale beneficiation studies:**

From the ten tons of representative sample of slime received from tailing dam of Bailadila mines of deposit-5, a representative sample of 500 kg was drawn by following the standard sampling procedure for laboratory scale studies. The iron ore slime was subjected to various beneficiation techniques or combination of processes as per the schemes shown in **Fig.3.1**. All laboratory scale processes are batch type only and only one process was used at a time for studies. The concentrate obtained in every stage was chemically characterized for Fe(T), SiO<sub>2</sub> and Al<sub>2</sub>O<sub>3</sub>. Mass balance and recovery of iron value were calculated at every stage of beneficiation. The percentage recovery (%Fe) was calculated according to the formula

$$R(\%) = \frac{100Cc}{\{Cc+t(F-C)\}} \quad (3.3)$$

where,

C is the weight % of concentrate obtained in the unit process,

F is the weight % of initial feed,

c is the Fe % in the concentrate, and

t is the Fe % in the tailing.

Various laboratory scale beneficiation studies were planned based on the initial characterization results of iron ore slime from Bailadila region. The characterization results

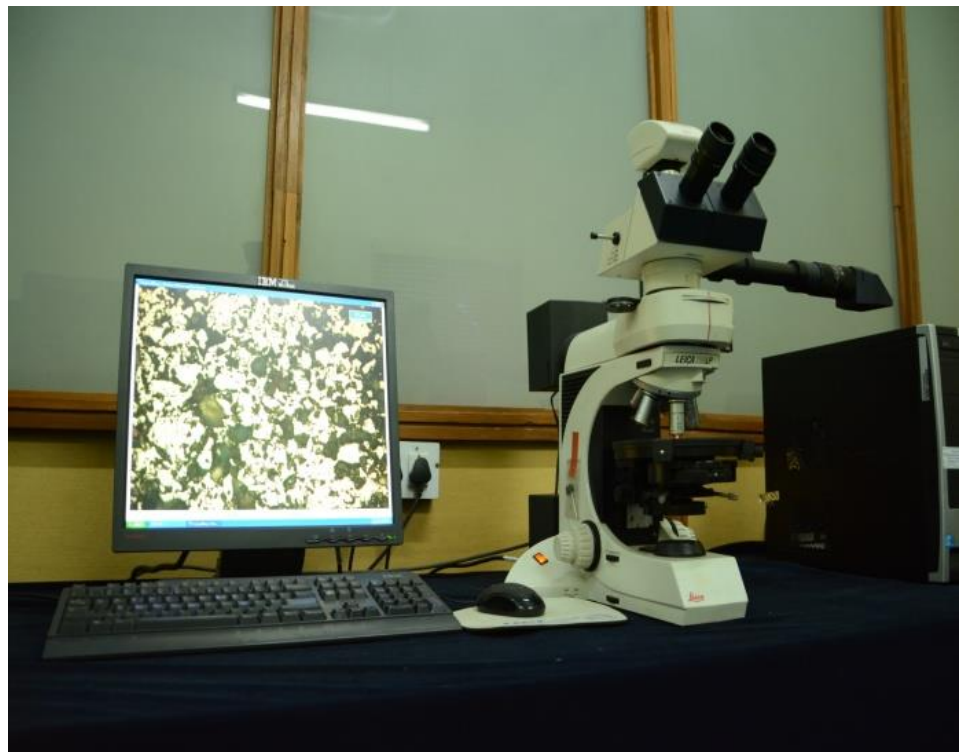


**Fig.3.7** Optical microscope (Leica make)



**Fig.3.8** Scanning electron microscope (make: TESCAN)

provide information about the presence of different types of gangue minerals. The distribution and status (liberated or locked) of gangue minerals in the slime was used for the selection of unit operation for separation of minerals. Different unit operations selected and used for laboratory scale beneficiation studies are shown in **Fig.3.1** and described in the following sections.

### **3.4.1 Gravity separation:**

In the present study, three types of gravity separation methods namely tabling, hydro-cyclone and spiral tests were used for the beneficiation studies.

#### **Tabling:**

The difference in specific gravity of iron ore and gangue minerals, like silica and alumina were utilized for processing of slime sample.

Wilfley table (**Fig.3.9**) was used for tabling studies. The details of Wilfley table and experimental parameters are shown in **Table 3.1**. The tabling test was carried with 3° to 4°inclination of the table. Feed rate was maintained at 40-50 kg/h throughout the tabling test. The sample was fed gradually to the shaking table and constant feed water was supplied at a rate of about 400 to 500 LPH. The concentrates and tailings were collected on regular time interval throughout the process. The obtained concentrates and tailings were dried and their weights were recorded. All the samples collected during tabling test were also subjected to chemical characterization through WD-XRF analysis.

#### **Hydro-cyclone Test:**

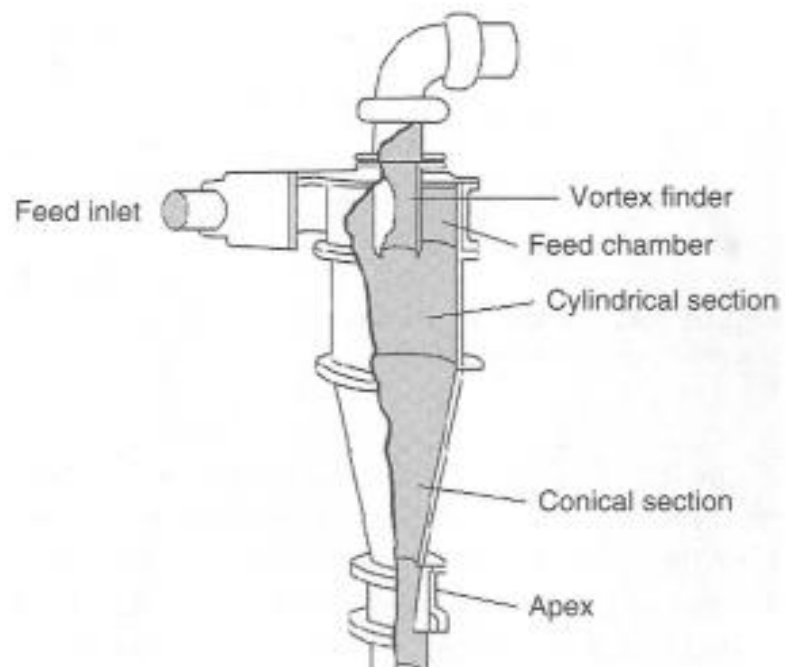
Hydro-cyclone is a classifying device that utilizes centrifugal forces to accelerate the settling rate of slurry particles and separate particles according to size, shape and specific gravity (**Jankovic, 2015**). Since iron ore slime contains lot of ultrafine particles, de-sliming with hydro-cyclone was carried out to upgrade the slime. In hydro-cyclone test, during de-sliming, grade 62%Fe(T) is considered as minimum requirement with recovery of at least 80% of iron value. The representative sample of slime was subjected to cyclone test in a 4 in. diameter Krebs hydro-cyclone (**Fig.3.10(a)** and **(b)**) using 10 mm, 12.5 mm and 15 mm apex diameters and 1.25 in. vortex finder with varying pulp densities (10%, 18% and 25%). The concentrate obtained by hydro-cyclone was analyzed for Fe(T) and recovery.



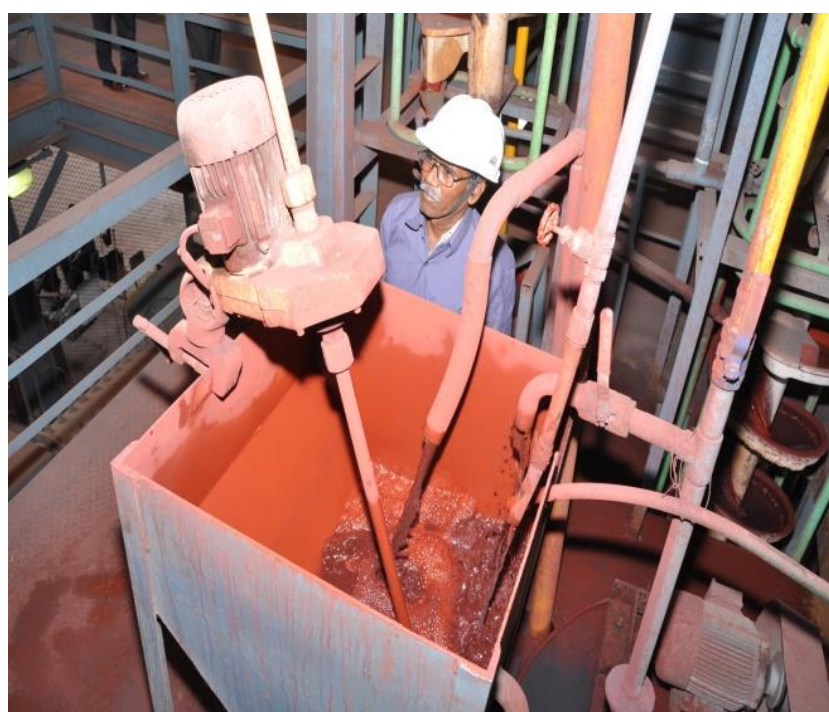
**Fig.3.9** Laboratory model Wilfley table

**Table 3.1** Wilfley Table details (**Fig.3.9**)

S.No.	Particulars	Details
1	Size	40" x 18" [L x W]
2	Make	Mine and smelter, USA
3	Motor	1/4 HP
4	Pulp Density	20% solids by weight
5	Feed Rate	40–50 kg/hr
6	Wash Water	400 to 500 LPH
7	Slope of the Deck	3° to 4°
8	Stroke Length	11 mm
9	Number of strokes/min	380



(a)



(b)

**Fig.3.10 (a)** Krebs hydro-cyclone and **(b)** Slurry preparation

### **Spiral test:**

The spiral concentrator consists of curved channel arranged in the form of a spirals having 13½ inch pitch. The spirals have provision for continuous withdrawal of concentrate near the inner part with a provision of cut point setting. The slurry along with water was fed at the top of the spiral and flows down due to gravity. The movement of slurry in spiral generates two forces on the individual particles, i.e. centrifugal force towards outside and gravitational force downwards. The lighter materials along with water occupy the outer rim and heavier ones get accumulated near the inner part of the spirals. The performance of the spiral separator depends on pulp density and particle size. The spiral tests were carried out with hydro-cyclone underflow only as spiral performance goes down with finer size of minerals. 20-30% pulp density was maintained during the entire test.

### **3.4.2 Magnetic separation:**

The magnetic properties of ore minerals and gangue minerals are different and hence the magnetic separators make use of the dissimilarity in magnetic characteristics between the gangue materials and ore minerals to separate them. In this study, the valuable mineral (iron ore) is magnetic, whereas gangue minerals (primarily silica and alumina) are non magnetic in nature. The major ore mineral in the slime was hematite ( $Fe_2O_3$ ) with small amount of goethite, which has paramagnetic characteristics. The paramagnetic and ferromagnetic materials are dealt with separate beneficiation techniques. The magnetization of paramagnetic and ferromagnetic material in magnetic field is presented in **Figs. 3.11(a) and (b)** respectively. The hematite and goethite get pulled towards the magnetic force in the direction of greater field intensity. Normally paramagnetic ore minerals can be separated out from non-magnetic gangue minerals using very high-intensity magnetic separators. In the present study, high intensity magnetic separator was used to separate iron ore from gangue minerals.

#### **3.4.2.1: Dry magnetic separation:**

The dry magnetic separation was used during laboratory scale beneficiation studies considering the dwindling water availability near the mine site for beneficiation. Prior to dry magnetic separation, the slime sample was dried for 24 h at 105°C to completely remove the moisture as even small amount of moisture in slime would severely affect performance of the magnetic separator. Hematite was the valuable mineral in the slime and requires very

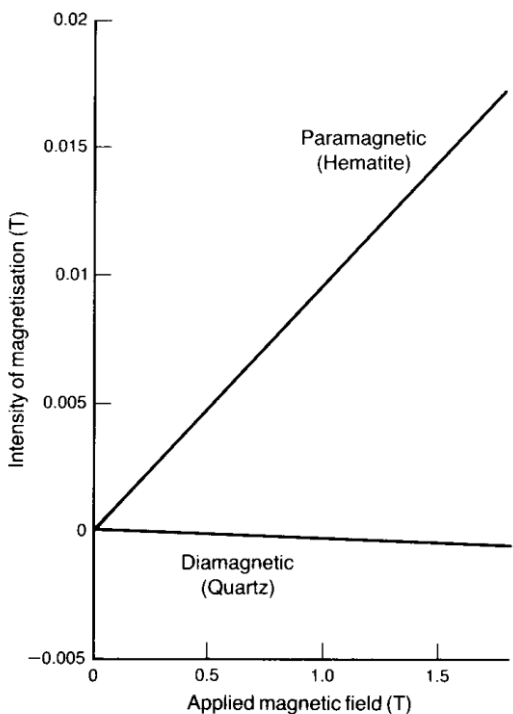


**Fig.3.11 (a)** Magnetisation of paramagnetic material (Wills, 1988)

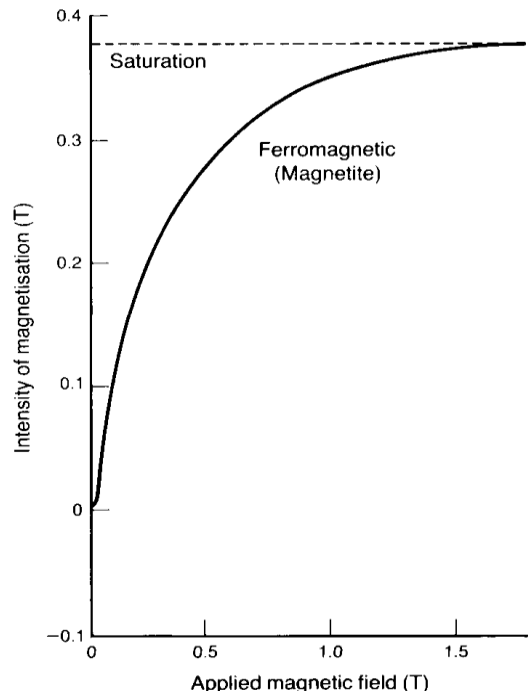


**Fig.3.11 (b)** Magnetisation of ferromagnetic material (Wills, 1988)



**Fig.3.12** High intensity induced magnetic separator (CARPCO make)



**Fig.3.13** Permroll magnetic separator (STEARNS Roll)

high magnetic intensity for separation. High intensity induced roll magnetic separator (CARPCO make) was used for this purpose (**Fig.3.12**). The beneficiation study was carried out at different intensities achieved by varying current. Permroll magnetic separator (STEARNS Roll) (**Fig.3.13**) was also used for beneficiation of slime. The permroll was equipped with permanent magnetic roll with intensity 6000 Gauss. Monolayer of slime sample was fed through the permroll. The magnetic and non-magnetic portions were collected and analyzed.

#### **3.4.2.1: Wet magnetic separation:**

Wet High Intensity Magnetic Separator [WHIMS] was used for the study of magnetic separation under wet condition. The equipment details and process parameter maintained are presented in **Table 3.2**.

**Table 3.2** Details of WHIMS and process parameters

Make	KHD Humboltz Wedag, Germany
Model	Jone's P 40
Matrix	12 R Grooved plate
Gap width	2.5 mm
Number of gaps	4
Pulp density	35% solids by weight
Power input	2 amps, 3 amps and 5 amps
Field strength	7500 Gauss, 9250 Gauss & 11000 Gauss
Feed rate	≈200 Kg/hr
Scour water	12 L/min
Pressure	3.0 Kg/cm <sup>2</sup>

#### **3.4.3 Froth flotation studies:**

Froth flotation is the most versatile mineral beneficiation technique used for the separation of selective minerals from a complex ore. The process was patented in the year 1906 and

has become popular for extraction of sulphide minerals of zinc, lead, copper etc. This technique has ability to scale to any extent at production level. The flotation process is used for relatively finer (-100 mesh) particles. The difference in physical and chemical characteristics of surface of particles of various minerals is utilized in froth flotation technique. The mineral of interest may be converted into hydrophilic or hydrophobic by the addition of a reagent.

Mineralogical studies indicated the presence of free silica in slime sample, so reverse floatation was used for beneficiation of slime in this study. Literature suggests that various type of collectors and dispersants are used for reverse floatation. Most of the reverse floatation processes have used various types of starch as depressant for hematite and other iron oxide. **(Sahoo et al., 2016)** have used dodecylamine (DDA) as collector for silica removal and soluble starch as depressant in their recent work successfully. Same collector and depressant were chosen and used in the present study also. A very commonly used frother, namely methyl isobutyl carbinol (MIBC) **(Mukherjee et al., 2015)** was used in all the experiments at the rate of 45 g /ton. It is well known that pH of the pulp play a major role in the separation of minerals in floatation process. The efficiency of the floatation process depends upon correct balance of pH and reagent concentration. The absorption of collector on the surface of target mineral largely depends upon pH of the pulp **(Wills and Napier-Munn, 2006)**. The representative portion of the slime samples were subjected to floatation at different pH values using varying quantities of the collector. The pH of the pulp was varied from 5 to 9.5 and DDA was used as collector which is varied between 20 to 160 g/ton. The floatation studies were carried out using Denver laboratory scale floatation cell **(Fig.3.14)** having an effective volume of 1.2 L. First, the slime was screened on 100 mesh size and the slime of -100 mesh size was taken for froth floatation. 500 g/ton of soluble starch was used as depressant throughout the study.



**Fig.3.14** Denver laboratory scale flotation cell

### **3.5 Pilot scale beneficiation studies:**

The pilot scale beneficiation studies of slime was carried out to validate beneficiation results obtained during laboratory scale beneficiation studies.

A pilot scale facility of 1 Ton/h capacity consisting of de-sliming by hydro-cyclone followed by two stage magnetic separation (WHIMS) was set up as shown in **Fig.3.15**. The process parameters like pulp density for de-sliming (in hydro-cyclone), magnetic field intensity, pulp density of feed to the WHIMS etc. were maintained similar to those optimized at laboratory scale tests.

- Initially two number of trial tests (Test No-1 & Test No-2) were performed to understand the feed material flow pattern and circuit operational problems.
- Two numbers of preliminary tests (Test No-3A & Test No-3B) were performed after suitable modifications for smooth operation of circuit and for optimizing parameters (Viz., wash water, splitter positions) to evaluate grade and recovery of products.
- One number of confirmatory test (Test No-4) was performed under the set parameters to obtain a target grade of  $>64\%$  Fe. At every stage, samples were collected for chemical analysis and 500 kg concentrate was produced for subsequent sintering studies. Tailings from pilot scale plant were collected for 100% utilization of slime and used as raw material for tile manufacturing.

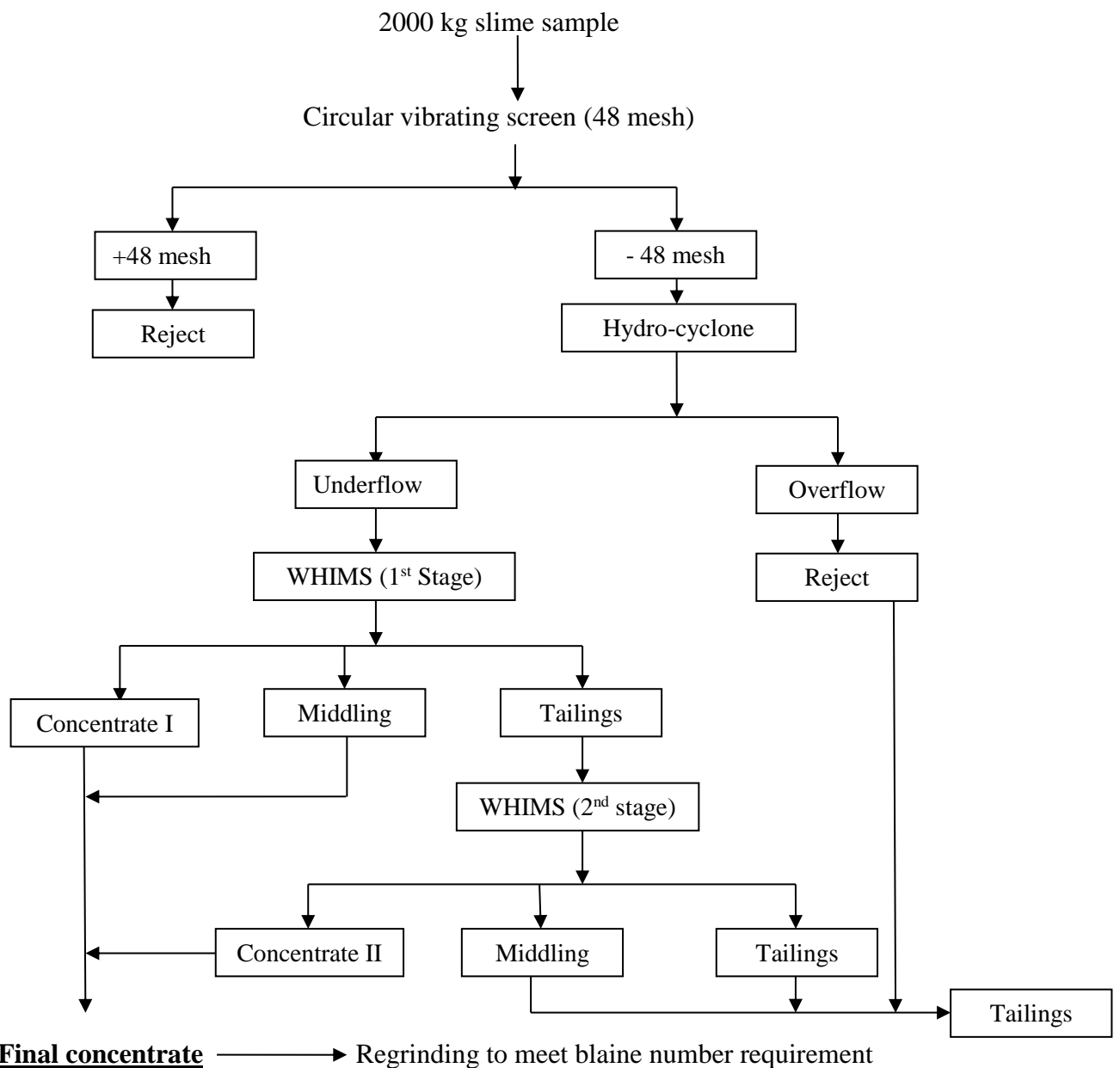


**Fig.3.15** Flow sheet for pilot scale beneficiation studies

### 3.6 Hybrid pellet sintering (HPS)

In the present study, the slime concentrate obtained from pilot scale beneficiation studies was subjected to sintering through a novel process known as hybrid pellet sintering (HPS). In this method, the slime concentrate is first converted into micro-pellets and then these micro-pellets are used for sinter making in a pot grate sintering furnace in place of iron ore fines. The flow sheet of hybrid pellet sintering process is shown in **Fig.3.16**. Different steps and the process adopted for hybrid pellet sinter preparation in the present study at laboratory are shown in **Fig.3.17**. Here, the slime concentrate was first converted into micro-pellets of suitable size and properties and then these micro-pellets were used for sinter making in pot grate furnace.

#### 3.6.1 Preparation of micro-pellets and their evaluation:

The slime concentrate obtained from pilot scale beneficiation studies was used as a principal iron bearing mineral for micro-pellet making. In pelletizing phase, the preparation and characterization of green micro-pellets was carried out. About 500 kg of slime concentrate was drawn by adopting the standard sampling procedure (i.e. coning and quartering) from the concentrate obtained from pilot scale beneficiation studies. The slime concentrate was thoroughly mixed and the representative samples were taken to determine its chemistry, size analysis, and specific surface area. The need for any additional grinding becomes apparent from this information and the required additives and/or binder can be initially selected. This may require modification during later testing to correct or improve properties of pellets produced. The Fisher's particle size analyzer was used for measurement of the surface area of the slime concentrate. The surface area of the slime concentrate obtained was observed to be low and does not meet the requirement of micro-pellet making. Therefore, further grinding of the slime concentrate was carried out to meet the feed requirement for micro-pellet making in terms of surface area. To meet this, the slime concentrate was subjected to dry grinding in a ball mill. The details of the ball mill are as follow:

- Length: 45 in.
- Diameter: 30 in.
- Speed of rotation: 12 rpm
- Ball size: 20 mm
- Ball weight: 100 kg {Number of balls: 2300(20mm) + 6100 (10mm)}.

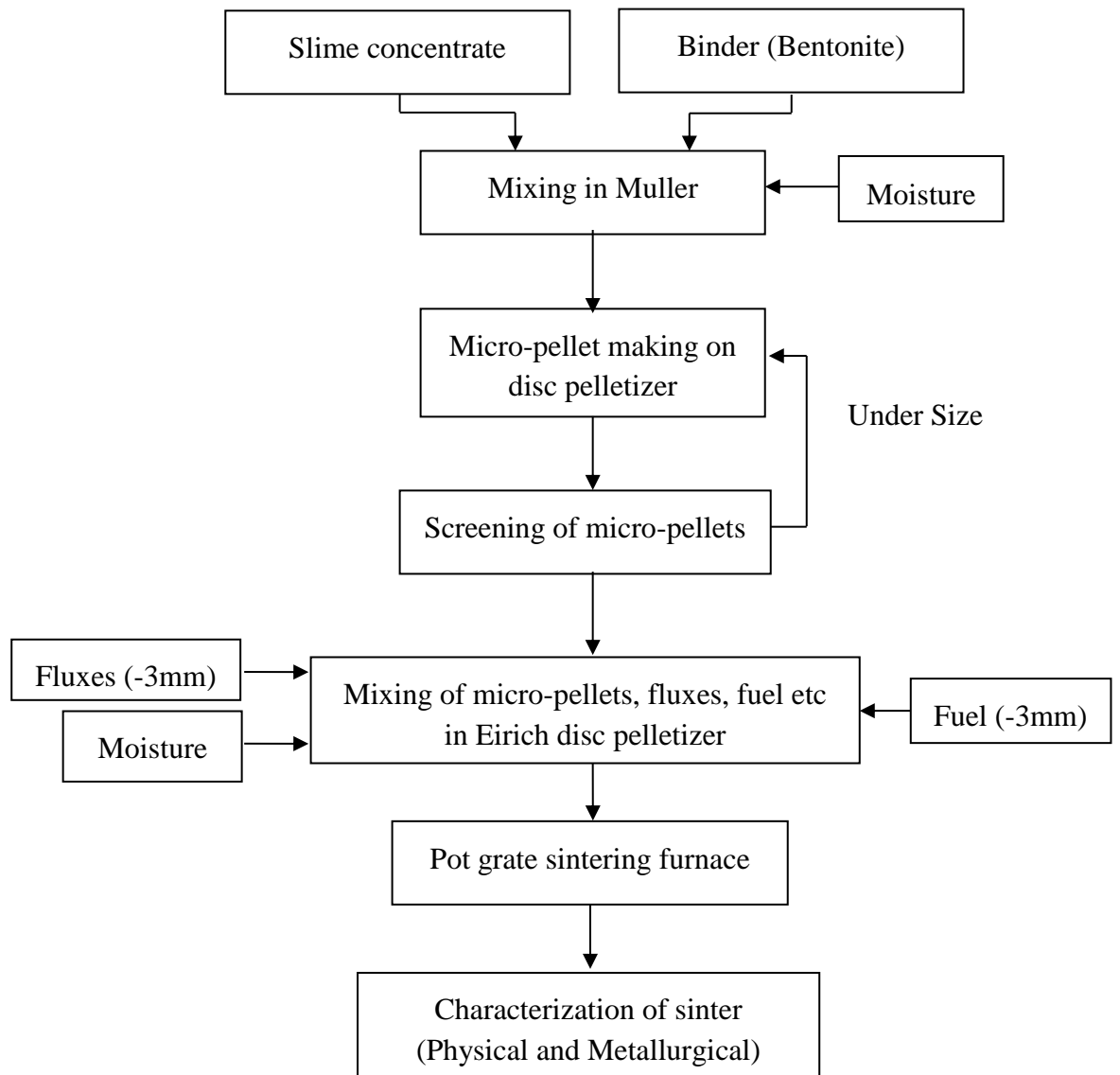


**Fig.3.16** Flow sheet for micro-pellet making and hybrid pellet sintering in pot grate sintering furnace

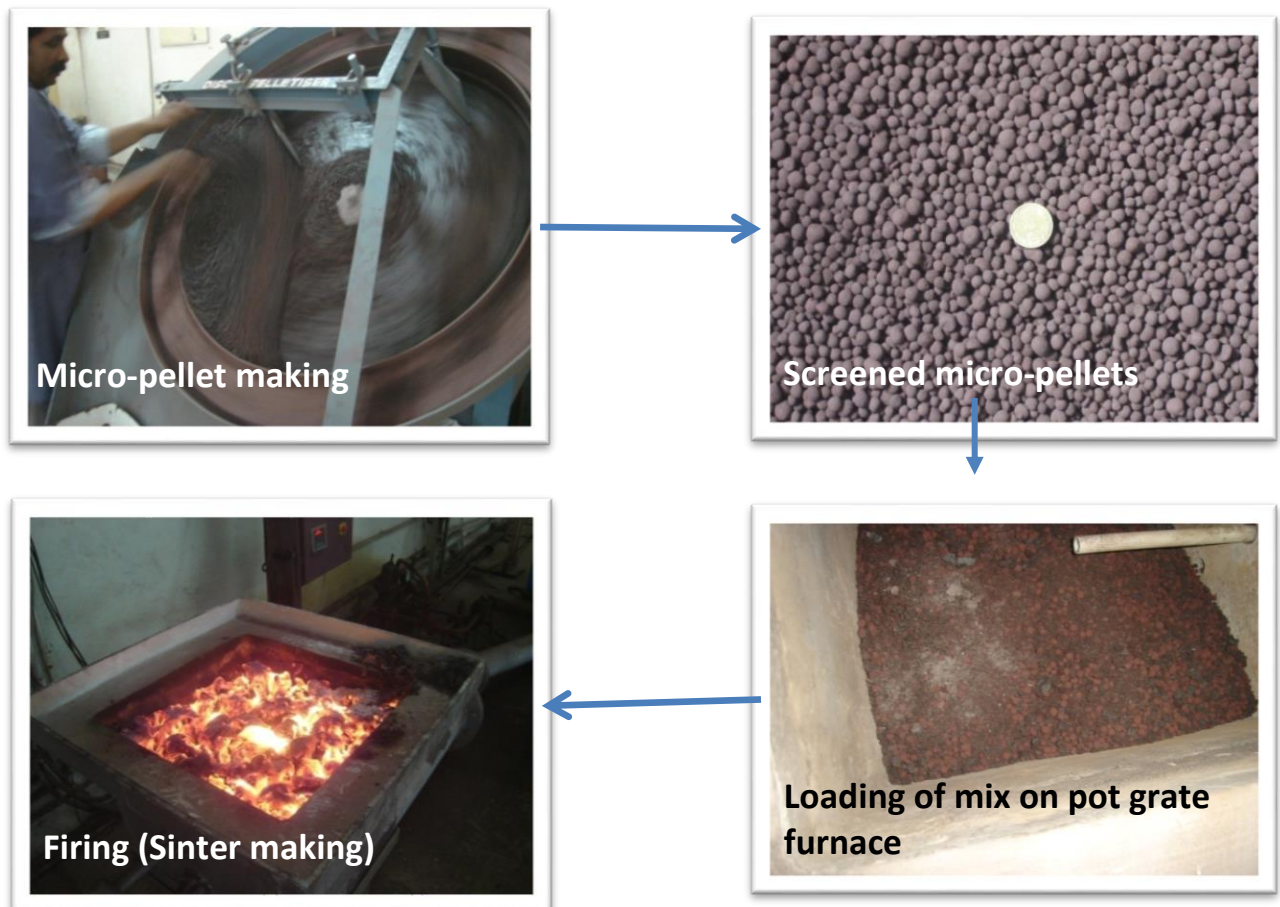


**Fig.3.17** Pot grate sintering (Hybrid pellet sintering)

To study the effect of specific surface area on properties of the micro-pellets, the slime concentrate was subjected to grinding in a ball mill for different durations (viz. 45 min and 60 min) to obtain slime concentrate with different specific surface area / Blain numbers.

Finely ground bentonite (-75 microns) containing 54.0%  $\text{SiO}_2$  and 13.0%  $\text{Al}_2\text{O}_3$  was used as binder for micro-pellet making. The binder was initially dried in an air oven for overnight at 105°C before using in micro pelletizing. Prior to use in micro-pellet making, the suitability of the binder was tested by soaking in distilled water for 4 h. The volume increase of the binder is found to be 819 %, which is more than as required, i.e. 800 % for pellet making (**Gupta, 2015**).

The required quantities of additives (viz. bentonite and little lime) were initially selected based on the past experience. The slime concentrate, moisture, and additives were mixed in different proportions in Eirich mixer (**Fig.3.18**) before feeding to a 100 cm (1 m) diameter disc pelletizer (**Fig.3.19**). Each batch of 20 kg of the particular composition of slime concentrate and bentonite required were mixed in Muller mixer with desired level of water for balling process. The mix was fed from a vibratory feeder or manually to a 1 m diameter disc where balling was accomplished. The green micro balls were produced under carefully controlled conditions. During micro-pellet making in disc pelletizer the parameters such as disc inclination, disc rotational speed and feed rate are maintained as 45°, 15 rpm and 200 kg/h respectively. The green micro-pellets were manually screened to get a product in the size range of 1 mm to 10 mm.

### **3.6.2 Optimization of properties of green micro-pellets**

The prime objective in optimization of properties of green micro-pellets is to produce desired quality of micro-pellets with minimum binder (bentonite) content and low blain number. The green micro-pellet properties have direct relation with the blain number and binder dosages. The higher the blain number, the better the green properties. However, it increases the grinding cost. Similarly, higher binder (bentonite) dosages improve overall properties of the green micro-pellets. But higher amounts of bentonite increases silica and alumina (gangue materials) content in the micro-pellets. In order to achieve the correct composition of micro-pellets with desired properties, the optimization of green properties of micro-pellets was carried out with respect to moisture content, binder content and specific



**Fig.3.18** Eirich make disc mixer

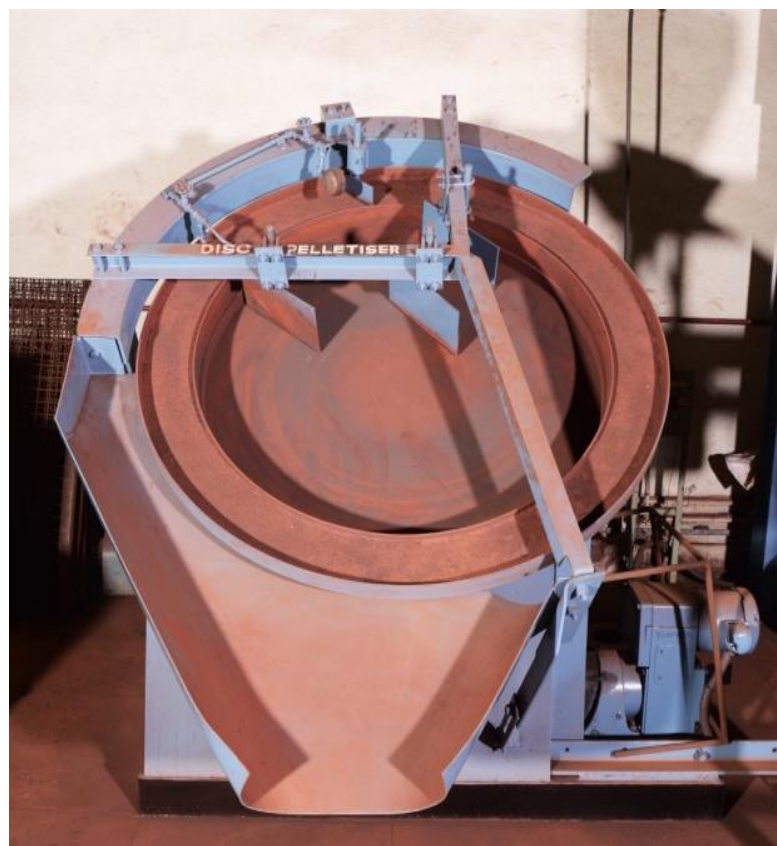


**Fig.3.19** Denver make disc pelletizer

surface area of the slime concentrate. This was done with the aim of using a minimum amount of bentonite for obtaining desired properties of green pellets at low specific surface area. For this purpose, green micro-pellets with varying amounts of moisture, binder and specific surface area were produced. The effects of moisture content, binder content and specific surface area of slime concentrate on properties of green micro-pellets were studied. For studying the effect of moisture content, the amount of binder and specific surface area of slime concentrate were fixed while varying the moisture content; for studying the effect of binder content, the specific surface area of the slime concentrate was fixed while varying the binder content; and for studying the effect of specific surface area, the binder and moisture contents were maintained constant while varying the specific surface area of the slime concentrate.

### **Characterization of green micro-pellets**

The micro-pellets obtained were analyzed to determine various properties such as green compression strength, impact strength, porosity, moisture content, absolute density and envelop volume. The compression strength of green micro-pellet was measured by cold crushing strength (CCS) equipment of capacity 50 kg (500 N) with least count 10g (0.01 N) (**Srb and Ruzickova, 1988**). During measurement of CCS, the pressure drop of 10 % after reaching maximum load is taken as breakage point. The impact strength of the green pellet was measured by drop number. The amount of moisture in the green pellet was determined by drying in an air oven at 105 °C, and weight loss was recorded at an interval of 30 min. The moisture determination was concluded when the difference between two successive weight measurements is less than 0.02 g. The porosity of micro-pellets was measured by using GeoPyc 1360 instrument after drying the pellets. Gas displacement pycnometer (AccuPyc 1330) was used to measure absolute density. The envelope volume of the green pellet was measured by using GeoPyc instrument by using dry flow material.

#### **3.6.3. Hybrid pellet sintering (HPS) studies using micro-pellets**

##### **Preparation of sinter charge**

The sinter charge is to be prepared on the basis of basicity arrived at. The basicity of the sinter is given by the ratio of (CaO+MgO) and (SiO<sub>2</sub>+Al<sub>2</sub>O<sub>3</sub>). The sintering studies were carried out with different basicities ranging from 0.5 to 3.0 in increments of 0.5. Charge composition for each basicity was calculated with different amounts of fluxes keeping lime,

coke, return sinter and moisture at constant. Based on this, the charge composition i.e. the amount of micro-pellets, limestone, dolomite and coke breeze were drawn from the respective bulk samples to prepare a sinter charge of 120kg for each heat. The composition of the charge for each basicity is presented in **Table 3.3**.

The amount of return sinter required in the sinter charge was collected from the sinter fines generated from the previous heat. All the materials other than return sinter and coke breeze were drawn as per the charge composition and mixed manually followed by mixing in a disc pelletizer. The mixing in disc pelletizer was carried out in two stages. During first stage, the micro-pellets and the additives were mixed for a period of 3 min with 70% of moisture. During second stage of mixing, the return sinter fines and coke breeze were added and mixed with limestone and dolomite for a further period of 3 min with the balance 30% of water.

The

total moisture maintained during mixing was 7% (optimized value) of the total charge. On completion of the mixing, the charge was unloaded from the mixer and transferred to sinter pot that was kept ready with the hearth layer.

### **Preparation of sinter bed and evaluation of sinter bed properties**

Preparation of sinter bed and evaluation of sinter bed properties such as bed permeability, void fraction and mean granule size of green sinter bed were carried out in a small grate pot unit. The sinter mix consisting of micro-pellets, fluxes, coke breeze, and return sinter was used for these studies.

For each test, all raw materials including moisture were mixed in drum mixer and the mixed charge was transferred into a pot grate (tube) up to a bed height of 500 mm. 1 mm grate spacing was maintained in the pot to retain finer particles without hearth layer. A venturi equipped with a differential pressure gauge was placed at the top of the pot and sealed properly. Air was passed through the packed bed to measure the bed permeability. The air flow through the packed bed was manually adjusted with the help of knob to maintain a pressure drop of 1000 mm of water level through the green bed. The air flow was measured by venturi. The pressure drop across the bed was measured. The permeability of the packed bed was determined by using the following formula and reported as Japanese Permeability Unit (JPU).

$$JPU = \frac{Q}{A} \times \left( \frac{h}{\Delta P} \right) \left( \frac{h}{\Delta P} \right)^{0.6} \quad (3.4)$$

**Table3.3** The composition of the sinter charge for different basicities

S.No	Charge particulars	Basicity					
		0.5	1.0	1.5	2.0	2.5	3.0
1	Micro-Pellets (kg)	74.5	64.3	59.5	54.7	50.2	45.7
2	Lime stone (-3mm) (kg)	0	2.4	6.0	9.0	12	14.4
3	Dolomite (-3mm) (kg)	0	1.8	3.0	4.8	6.4	8.4
4	Lime (kg)	0.5	0.5	0.5	0.5	0.5	0.5
5	Coke (kg)	6.6	6.6	6.6	6.6	6.6	6.6
6	Return sinter (kg)	30	36	36	36	36	36
7	Moisture (kg)	8.4	8.4	8.4	8.4	8.4	8.4
	Total charge (kg)	120	120	120	120	120	120

where  $Q$  is the air flow rate ( $\text{m}^3/\text{min}$ ),  $A$  is the cross sectional area of the bed ( $\text{m}^2$ ),  $h$  is the bed height (mm) and  $\Delta P$  is the pressure drop across the bed (mm of water).

The void fraction ( $\varepsilon$ ) in the green bed was estimated from the following formula developed by Hinkley (**Hinkley et al., 1994**).

$$\varepsilon = 1 - \frac{\rho_b}{\rho_a} \quad (3.5)$$

where  $\rho_b$  is the bulk density and  $\rho_a$  is the apparent density.

The bulk density of sinter mix was measured by comparing the masses of full and empty 1 litre flask and the apparent density was determined by kerosene displacement method (**Hinkley et al., 1994**). The apparent density is calculated by the equation:

$$\rho_a = \frac{M_{tot} - M_{ker}}{500ml - V_m} \quad (3.6)$$

where  $M_{tot}$  is the total mass of the flask,  $M_{ker}$  is the mass of the flask filled with 500 ml of kerosene before pouring granules into the flask and  $V_m$  is the volume of kerosene required to fill the flask up to the 1 liter mark.

The mean granule size, also known as Sauter mean diameter (**Sinnot, 2005**) of the granules was determined from the size distribution of the sinter mix using the equation:

$$d_p = \frac{100}{\sum_i \frac{X_i}{d_{pi}}} \quad (3.7)$$

where  $d_p$  is the Sauter mean diameter,  $X_i$  is the mass percent (wet basis) of granules size fraction, and  $d_{pi}$  is the mean granule diameter for size fraction  $i$ .

The effect of moisture on sinter bed permeability, void fraction and mean granule size of the bed was evaluated by varying moisture content between 5.5 and 7.5% for different sizes of micro-pellets, viz. 1-3 mm (i.e. +1,-3 mm), 3-6 mm (i.e. +3, -6 mm) and 6-10 mm (i.e. +6, -10 mm).

### **3.6.4.Hybrid pellet sintering (HPS) process:**

Sintering studies were carried out in a batch type square shaped sintering unit (also known as sinter pot or pot grate furnace) having  $40 \times 40 \text{ cm}^2$  cross sectional area and 350 mm height box with removable grate at the bottom. The pot grate furnace used for sintering and its schematic diagram are shown in **Figs.3.20** and **3.21** respectively. Initially, the inner side of the sinter pot and the grate were given a thin coating of lime to prevent sticking of the sinter and to facilitate free unloading. Sinter from previous batch (return sinter) of size -25mm, +15mm was used as the material for forming hearth layer. An amount of 14kg of sinter was used to form the hearth layer of 40mm height. The prepared sinter charge mix was loaded into the sinter pot over the hearth layer. The height of the bed excluding the hearth layer was maintained at 350 mm. The sinter charge was ignited using a layer of coke breeze and saw dust spread uniformly over the bed. The ignition was maintained for a period of 120 s to ensure the uniform firing on the top portion of the bed. Suction was employed by using the double stage blower. During ignition, suction at 800mm WG was maintained and after the completion of ignition period the same was raised to 1100mm WG and maintained throughout the sintering period. The temperature of the exhaust gas was noted continually using a thermometer in the suction line placed at 500mm above the grate. Sintering was assumed to be completed in one minute after the exhaust gas temperature reaches the maximum. The sinter was allowed to cool under suction till the temperature of exhaust gas reaches 100°C. The sinter cake was then dislodged and subjected to further analysis.

### **3.6.5. Analysis of the sinter:**

The cooled sinter was given four drops on the shatter apparatus for breaking down to -50mm size and was screened at 10mm. The -50mm, +10mm fraction was weighed to arrive at the quantity of useful sinter produced, which is equal to the weight of the -50mm, +10mm fraction minus the weight of the hearth layer. The yield of sintering was calculated from the ratio of useful sinter to the total sinter produced and is expressed in percentage. The productivity was calculated as the tonnage of useful sinter produced per square meter of the grate area per hour from the weight of the useful sinter produced and the sintering time. The 10mm fines were used as return sinter for subsequent sintering. The -50mm, +40mm fraction was manually crushed to -40mm size and size analyzed. The feed samples of -40mm, +10mm size for tumbler test and shatter test were drawn from the different size fraction according to their respective proportions. **Fig.3.22** shows the sizing and sampling of sinter prepared in pot grate furnace.



**Fig.3.20** Pot grate furnace for sintering

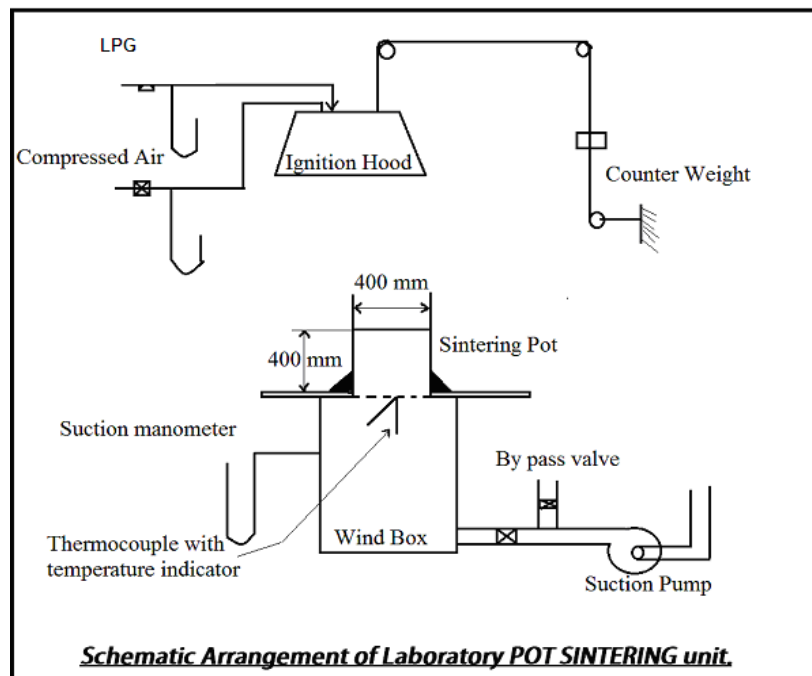


**Fig.3.21** Schematic diagram of pot grate furnace for sintering

### **3.6.6 Physical characterization of sinter:**

**Tumbler test:** The tumbler test (as shown in [Fig.3.23](#)) was carried out on the sinter product as per the ISO 3271 standard. 15 kg of sinter sample was taken in the size range of -40mm, +10 mm from the sinter produced. The sinter sample was subjected to 200 revolutions in the tumbler drum of size 1m diameter and 500 mm width. The drum was rotated at a speed of 25 rpm. The weight percent of the +6.3mm size in the material obtained after 200 revolutions was taken as the tumbler index.

**Shatter Index:** Shatter index test (as shown in [Fig.3.24](#)) was carried out in accordance with IS 9963:1981 standard. A 20kg sample of -40mm, +10mm size was dropped from a height of 2000mm for four times on a 4 mm thick sheet of steel. The weight percent of the -10 mm fraction obtained after four drops is taken as the shatter index.

### **3.6.7 Metallurgical characterization of sinter:**

The sinter produced from the slime concentrate after beneficiation of slime from Bailadila region was subjected to various metallurgical tests such as reduction degradation index (RDI), relative reducibility (RD) and reduction under load (RUL) to evaluate its performance under blast furnace conditions. The various metallurgical tests and their significance with respect to blast furnace operation are shown in [Fig.3.25](#). The metallurgical characterization of sinter was carried out in accordance with respective international standards.

#### **3.6.7.1 Reduction Degradation Index (RDI) and Relative Reducibility (RR):**

RDI and RR tests using sinter were carried out in accordance of ISO 4696-2 and ISO 7215 methods respectively as shown in [Fig. 3.26](#). Approximately 500g of sinter sample of size - 20mm, +15mm was drawn from the sinter produced for the determination of RDI and RR. The RDI and RR tests involve heating of the test sample to a temperature of 550°C and 900°C respectively in an inert atmosphere of nitrogen. During heating, the nitrogen gas at a flow rate of 5 L/min was maintained. After stabilizing the sample temperature at 550°C and 900°C, the reduction was carried out with a mixture of carbon monoxide and nitrogen gases in the ratio of 30:70 at a flow rate of 15 L/min. The reduction was carried out isothermally for a period of 30 min and 3 h for RDI and RR tests respectively during which the loss in weight



**Fig.3.22** Sizing and sampling of sinter prepared in pot grate furnace



**Fig.3.23** Tumbler drum



**Fig.3.24** Shatter Index test apparatus

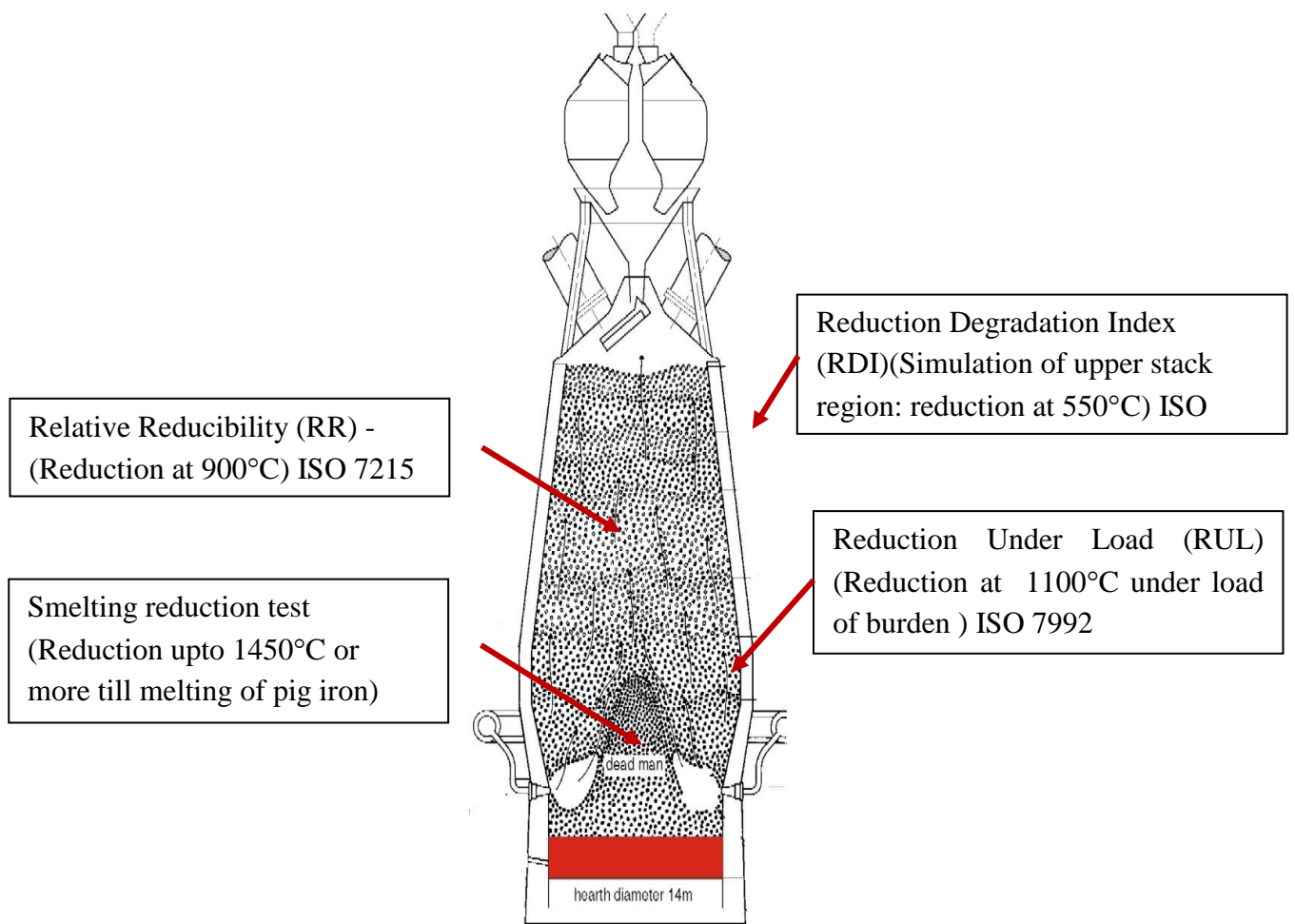


**Fig.3.25** Various metallurgical tests and their significance with respect to blast furnace operation



**Fig.3.26** RI/RDI furnace  
(Lurgi) Italy make



**Fig.3.27** RUL, R&B Automizion

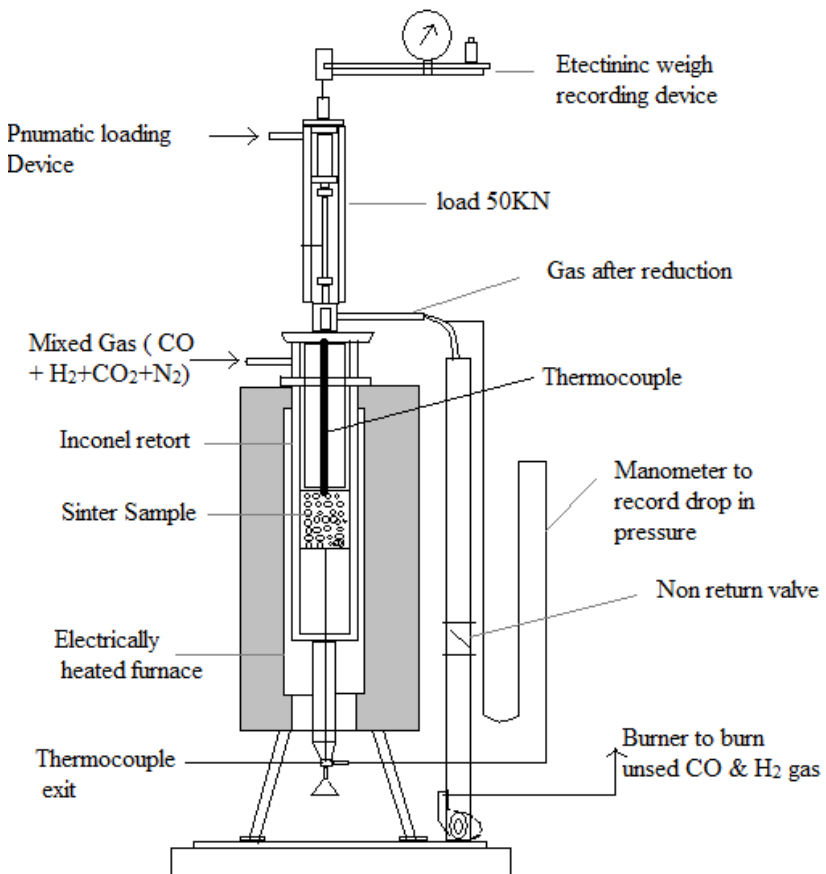


**Fig.3.28** Reduction under load tests

of the sample was recorded continually. After completion of reduction, the sample was cooled to room temperature in an atmosphere of nitrogen. In RDI test, the reduced mass was given 900 revolutions and screened on 2.9 mm circular screen. The amount of sample that passes through the 2.9 mm screen was recorded as RDI. In RR test, the weight loss during 3 h reduction was recorded and the percentage loss of oxygen from the sample during reduction at 900°C was recorded as RR.

### **3.6.7.2 Reduction under load test:**

The reduction under load (RUL) test simulates the condition of bosh region of the blast furnace. The RUL test was carried out as per ISO 7992 standard. R&B Automizion, Italy make RUL equipment (**Figs.3.27** and **3.28**) was used during this study. About 6 Kg of sinter sample was drawn by following standard (coning and quartering) sampling procedure from the bulk sample for RUL test. The obtained sample was air dried in an oven for 24 h at 105°C. Each test requires about 1200 g of sample and the same was drawn from 6 Kg sample with the help of reffiler. The sample was loaded in a reduction tube. The reduction tube is made of Inconel 601 alloy which can withstand very high temperature without deforming under mild load. Concentric tube was used in RUL for reduction having inner tube diameter of 125 mm  $\pm$  1 mm. The inner tube has provision for holding the sample on circular perforated disc of diameter slightly less than 125 mm. The perforated base holds one layer of ceramic balls, which do not participate in any reaction but preheat the reducing gas before reaching the sample.

The reduction study was carried out at 1050°C until 80% of oxygen present in the sample was removed. The composition of the reduction gas (volume fraction) used is as below:

CO - 40 %  $\pm$  0.5 %

H<sub>2</sub> - 2 %  $\pm$  0.5 %

N<sub>2</sub> - 58 %  $\pm$  0.5 %

During initial heating and cooling, N<sub>2</sub> gas was passed through the sample. The N<sub>2</sub> gas of high purity 99.9% was used to avoid any re-oxidation during cooling. The flow rate of N<sub>2</sub> gas was kept at 50 L/min until the temperature of the test sample reached to 1050°C. Before introducing the reducing gas, the flow rate of nitrogen was increased to 83 L/min to stabilize the sample temperature at high flow of gas. The reduction gas was introduced in to the

furnace at a flow rate of 83 L/min once the temperature was stabilized. The reduction was stopped after reaching 80% reduction of the sample. After reduction (during cooling), the flow of nitrogen was maintained at 5 L/min until sample temperature reached to 100°C. A pressure of 50 kPa  $\pm$  2 kPa was applied on the top of the sample bed after placing the sample in reducing chamber. The load was maintained during initial heating and also during reduction process. Rate of reduction with time was recorded.

### **3.6.7.3 Smelting and melting study with sinter sample:**

The sinter undergoes various thermo-chemical transformations once charged in to the blast furnace. In the stack region it faces thermal shock. Similarly, softening and melting of sinter start in the cohesive zone. The cohesive zone has alternate layer of coke and iron bearing material (sinter) and its shape and size has direct impact on performance of the blast furnace. The softening and melting test is designed to simulate cohesive zone condition in the laboratory and behavior of sinter in blast furnace can be predicted for better control of blast furnace. The softening and melting test was carried out in accordance with IS 9660:2001 standard. A sinter sample of 225 g was placed between two layers of coke in a graphite crucible. The crucible was heated from room temperature to 1600°C. The following sequence of heating rate was maintained during entire test:

- (i) 0 to 900°C - 10°C /min
- (ii) 900to 1200°C - 3°C/min
- (iii) 1200to 1600°C - 5°C/min

Reducing gas consisting of 70%CO and 30% N<sub>2</sub> was introduced in to the furnace at a temperature of 200°C and at a flow rate of 15 L/min. The flow of reducing gas was maintained until sample reached 1600°C. Softening start temperature, temperature at melting finishes and its range of temperature were recorded.

### **3.6.8 Effect of basicity on the sinter quality:**

To study the effect of basicity on physical and metallurgical properties of sinter, the hybrid pellet sinter with varying basicity were prepared from slime concentrate in pot grate furnace. The basicity during study was maintained in terms CaO/SiO<sub>2</sub> ratio. Six batches of

sinter were produced with basicity 0.5, 1.0, 1.5, 2.0, 2.5 and 3.0. Limestone and dolomite were varied for achieving the desired basicity in the sinter. The ratio of MgO and CaO was maintained at 0.2 during the entire study. The sinter obtained after pot grate firing was subjected to physical, chemical and metallurgical characterization. The sinter samples were also subjected to optical micrography and mineral estimation. XRD analysis of sinter was also carried out to confirm the results of phase distribution obtained by optical image analysis.

## Chapter-4

# CHARACTERIZATION OF INITIAL RAW MATERIALS

### 4.1 Characterization of iron ore slime:

About 10 tons of representative sample of slime was received from tailing dam of Bailadila deposit-5. A 50 kg representative sample was drawn from this bulk sample for chemical, physical, and mineralogical characterization studies.

#### 4.1.1 Chemical analysis of iron ore slime:

The chemical analysis of the iron ore slime sample as determined by wet chemical method (for Fe(T)), WD-XRF (for SiO<sub>2</sub>, MnO, FeO and S), ICP-AES (for alumina and phosphorous) and TGA (for LOI) is presented in **Table 4.1**.

The silica (SiO<sub>2</sub>) and alumina (Al<sub>2</sub>O<sub>3</sub>) contents in the iron ore slime were 7.76% and 3.10% respectively. The blast furnace iron bearing material should have silica and alumina put together less than 5%. However, the total gangue mineral (i.e. SiO<sub>2</sub>+Al<sub>2</sub>O<sub>3</sub>) in the slime is 10.86%, which is on higher side to charge in to blast furnace. Hence, the slime as such cannot be used in any of the iron making processes. Higher gangue minerals in the charge materials would lead to increased coke rate in the blast furnace and also increased slag volume significantly. Thus, the slime need to be beneficiated and gangue minerals should be reduced to minimum level with higher recovery of iron value.

#### 4.1.2 Physical properties of slime:

The physical properties such as specific gravity, bulk density and angle of repose of the slime sample measured by using standard procedures are presented in **Table 4.2**. The particle size distribution of the slime sample is presented in **Fig.4.1** and the size wise chemical analysis results are presented in **Table 4.3**.

**Table 4.1** Chemical analysis of as-received slime sample

Constituents	Fe[T]	SiO <sub>2</sub>	Al <sub>2</sub> O <sub>3</sub>	P	S	MnO	FeO	LOI
Assay, %	60.64	7.76	3.10	0.058	0.02	0.003	0.92	1.98

**Table 4.2** Physical properties of the slime

S. No	Property	Value	Method/Standard used
1	Specific gravity (relative to the water)	3.66	AccuPyc 1340 automatic Gas pycnometer
2	Bulk density (t/m <sup>3</sup> ) (kg/m <sup>3</sup> )	1.78 (1780)	ISO-3852
3	Angle of repose	48°	ASTM-C1444

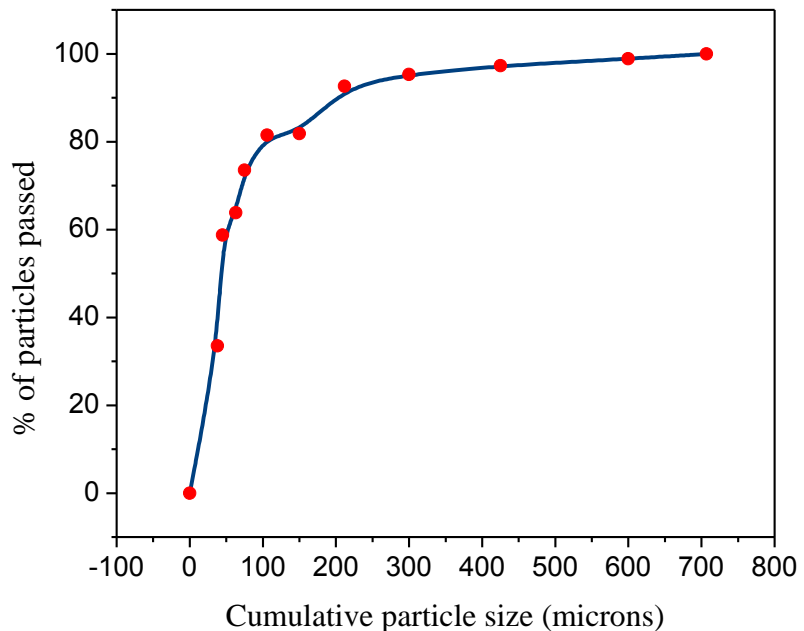


**Fig.4.1** Particle size distribution of Bailadila iron ore slime

**Table 4.3** Particle size distribution and size wise chemical analysis

Size		Wt. %	Assay, %			Distribution, % Fe
Mesh size (Tyler)	Micron		Fe(T)	SiO <sub>2</sub>	Al <sub>2</sub> O <sub>3</sub>	
+10	+2000	2.1	56.83	5.98	6.50	2.0
-10,+14	+1400	2.1	55.29	6.28	6.25	1.9
-14, +20	+850	2.1	53.62	9.80	7.75	1.9
-20, +28	+600	2.1	52.27	12.96	7.00	1.8
-28, +35	+425	2.5	50.91	17.62	4.90	2.1
-35, +48	+300	3.1	48.78	22.44	3.75	2.5
-48, +65	+212	4.1	49.36	24.16	2.80	3.3
-65, +100	+150	5.1	53.26	20.20	2.10	4.5
-100, +150	+105	6.2	59.59	12.34	1.45	6.1
-150,+200	+75	14.7	63.95	6.66	1.20	15.5
-200, +270	+53	8.5	65.74	4.14	1.10	9.2
-270, +325	+44	10.7	66.52	3.14	1.10	11.7
-325	-44	36.7	61.97	4.10	4.50	37.5
Head (Calculated)		100.0	60.65	7.82	3.16	100.0
Head (Actual)			60.64	7.76	3.10	

More than 80 % of particles in the slime are below 100 mesh (200 micron). The distribution of valuable minerals (Fe) in the slime is presented in the **Fig.4.2**. Majority of valuable minerals were present in finer size portions.

#### **4.1.3. Mineralogy and liberation studies of iron ore slime:**

The slime sample was observed under the polarized light microscope to unravel the phases of minerals and extent of liberation or association of minerals in the slime sample. **Fig.4.3** shows the area wise distribution of ore minerals and gangue minerals present in the Bailadila slimes. On the whole, the slime of Bailadila mines shows the presence of moderate to high amount of ore minerals and low amount of gangue minerals. Hematite (H) is the principle ore mineral and Goethite (G) present as secondary ore mineral. The gangue minerals present in the slime are quartz (Q), pseudo ore (PSO) and ferruginous clay (FCL). The detailed ore mineralogical studies suggest that the slime sample consist of approximately 78% of ore minerals and 22% of gangue minerals by area of their distribution.

##### **4.1.3.1 Ore mineralogy**

###### **Hematite:**

Hematite (H) is the principle ore mineral present in the slime sample. It covers around 55% area by area distribution (**Fig.4.3**). Coarsest liberated hematite up to size of 1 mm was present in the slime and the same was separated out before mineralogical studies. The remaining slime sample has 70 micron size coarsest mineral (hematite). Hematite grains were present in various shapes and sizes and texturally they are categorized into two groups as medium and small grains. While the medium grains are coarser than 30 microns, the smaller grains are less than 30 microns in size. Of the 55% total area of hematite, 45% area consists of medium sized hematite grains, of which around 20% grains were in fully liberated state and the remaining 80% grains were un-liberated and are associated with gangue minerals of below 40 microns size. Remaining 55% area of total hematite (55%) was covered by fine grains, mainly less than 30 microns. Among these, around 40% grains were in fully liberated state; whereas remaining 60% grains were very fine and associated with gangue minerals of size less than 20 microns (**Figs.4.4 to 4.9**).

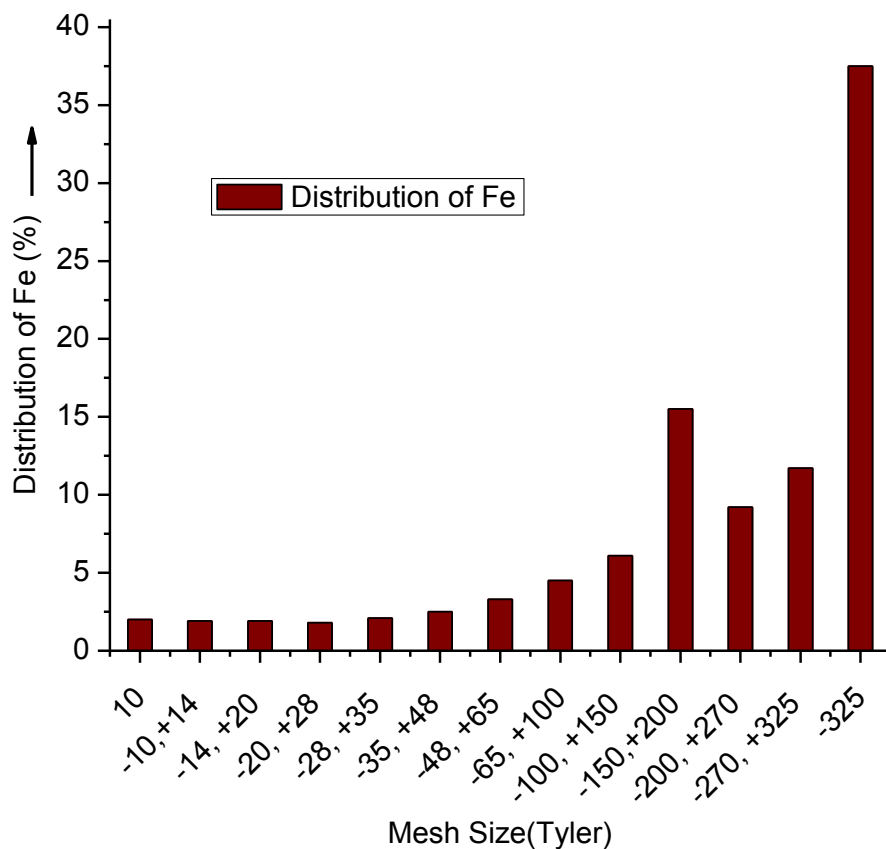


**Fig.4.2** Distribution of Fe in different size of Bailadila iron ore slime

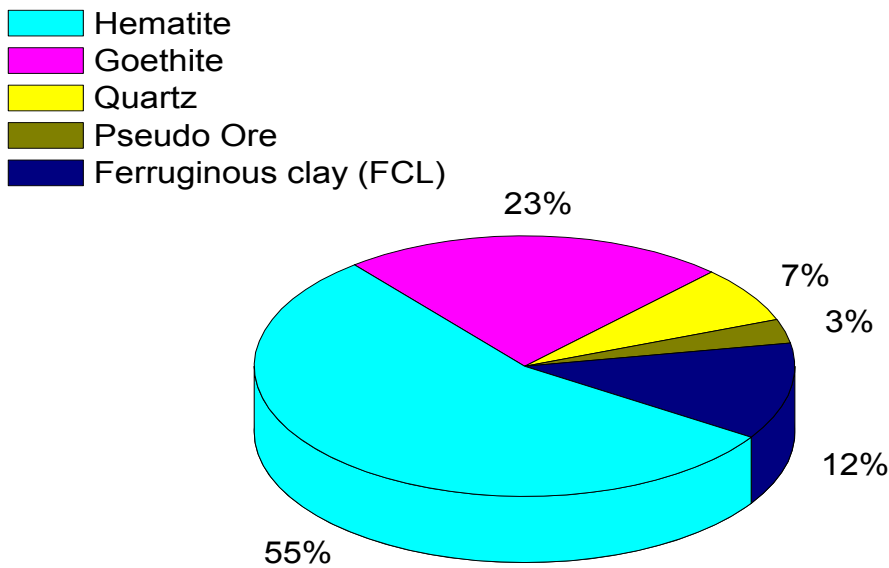


**Fig.4.3** Area (%) wise distribution of minerals from Bailadila slime sample.

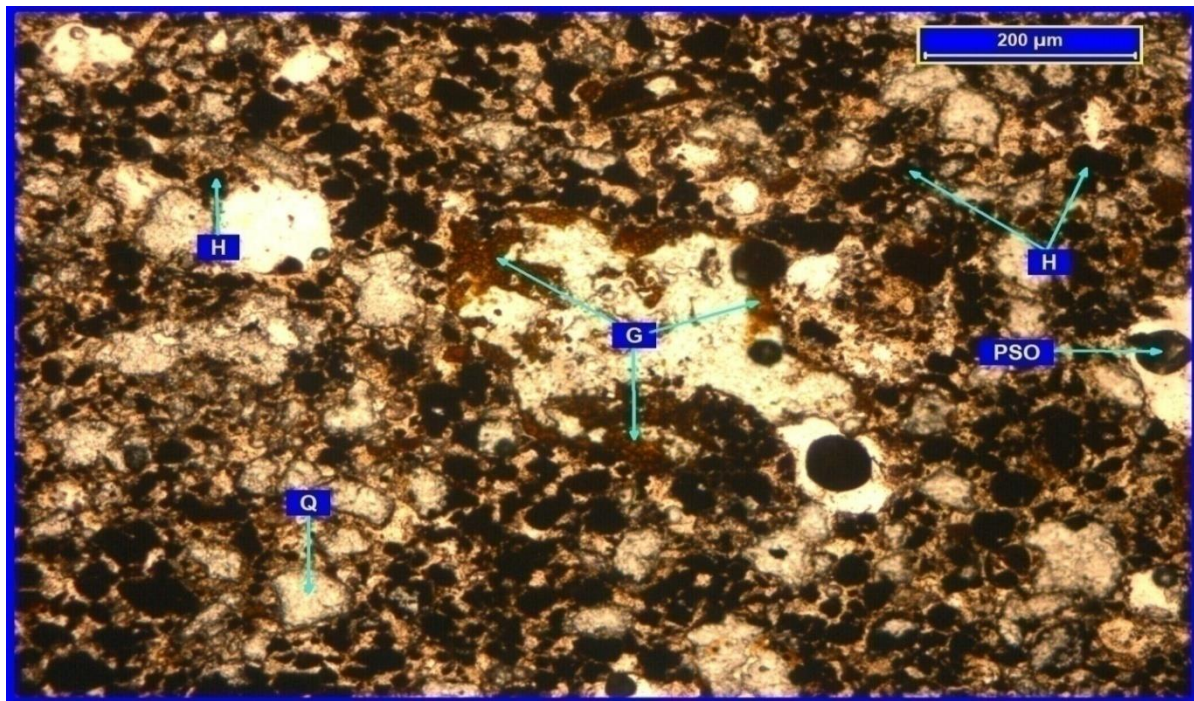


**Fig.4.4** Photomicrograph displaying distribution of medium to fine grains of hematite (H) and goethite (G), few pseudo ore (PSO) and irregular shaped quartz (Q). (Under Transmitted Light).

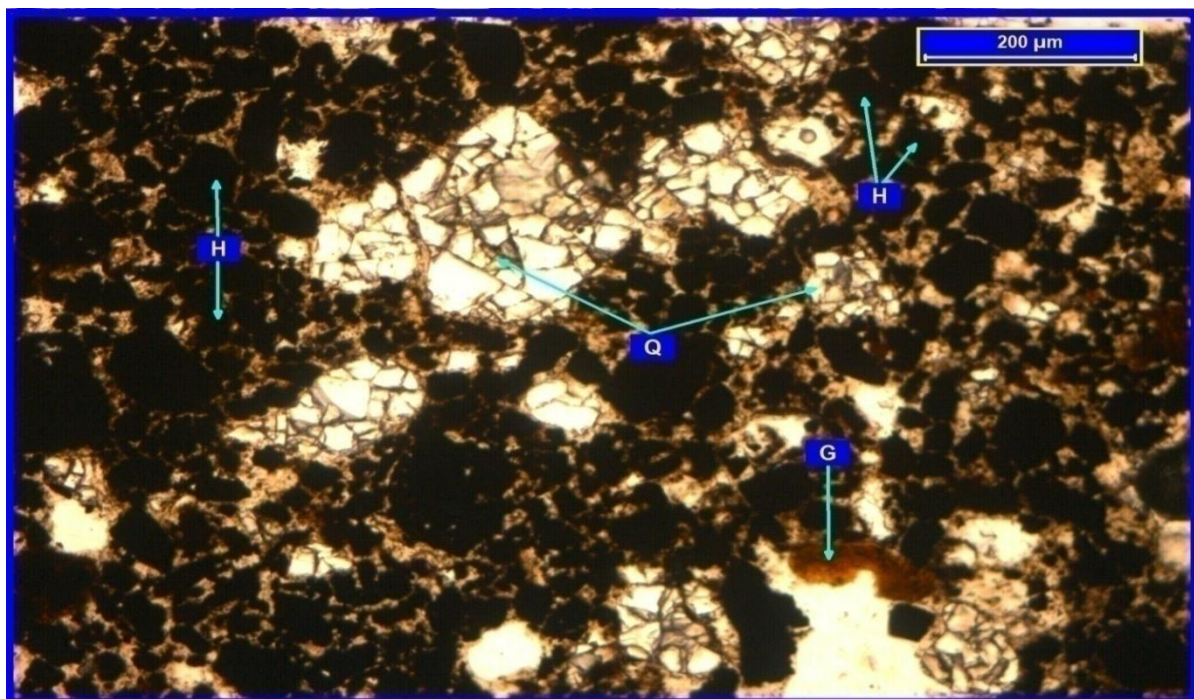


**Fig.4.5** Photomicrograph showing distribution of medium to fine grain, irregular-shaped hematite (H), few coarse goethite (G) and irregular shaped highly fractured quartz (Q). (Under transmitted light).

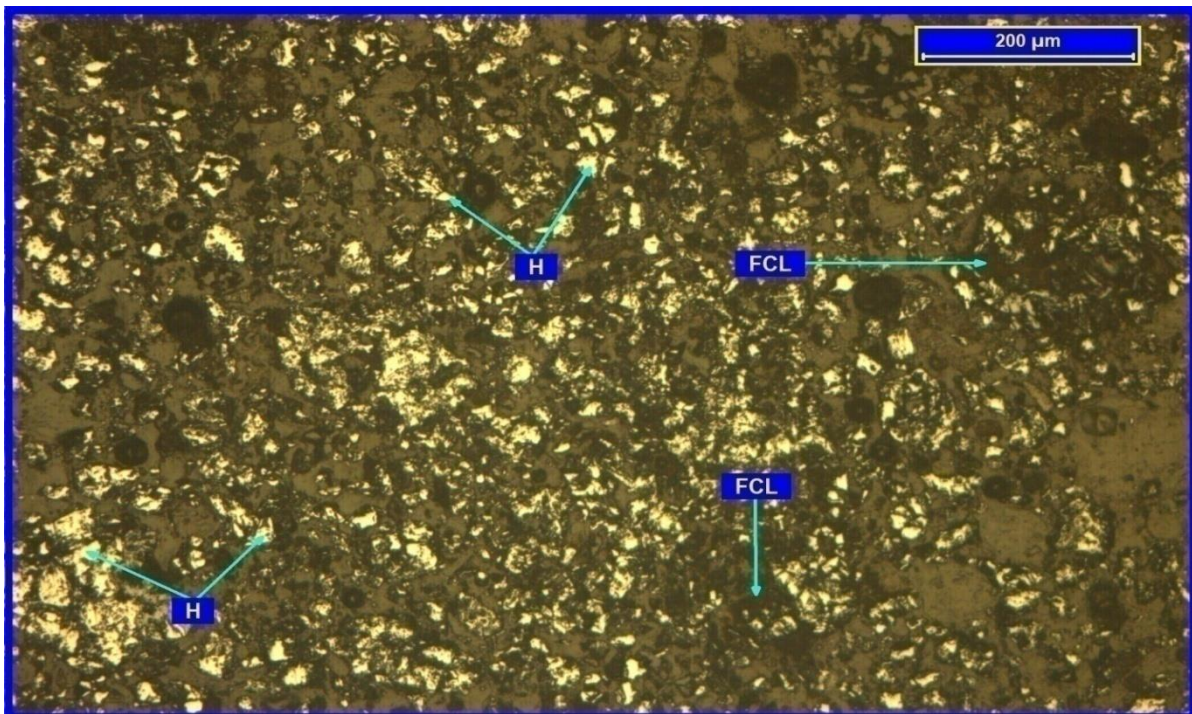


**Fig.4.6** Photomicrograph displaying medium to fine size highly altered hematite (H) and ferruginous clay (FCL) (Under Reflected Light).

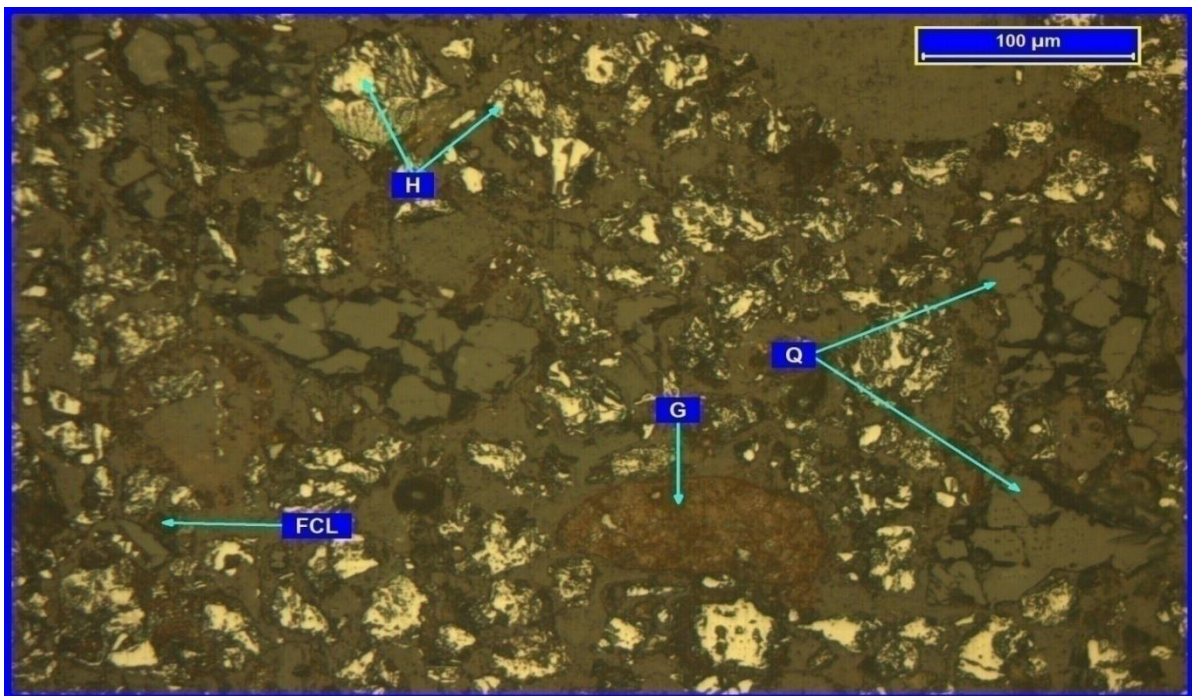


**Fig.4.7** Photomicrograph showing distribution of medium to fine size hematite (H) & few goethite (G), irregular shaped highly fractured quartz (Q) and Ferruginous clay (FCL) (Under Reflected Light).

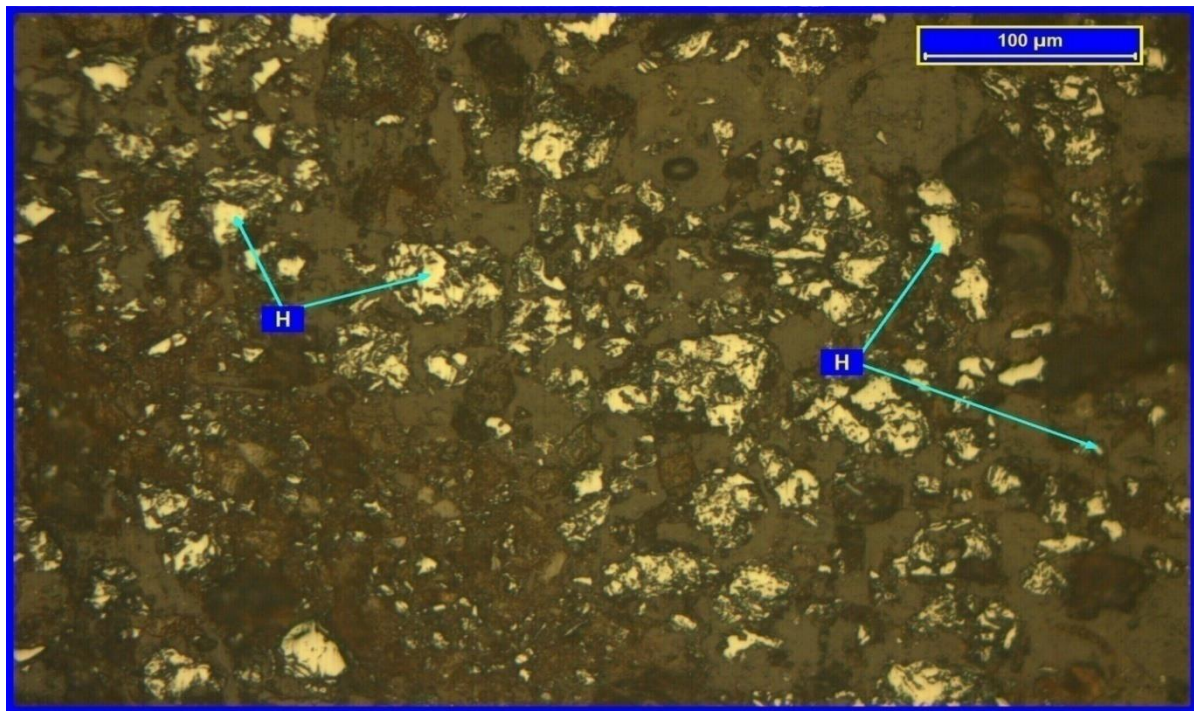


**Fig.4.8** Photomicrograph showing distribution of medium to fine grains of hematite (H) and ferruginous clay (FCL). (Under Reflected Light).

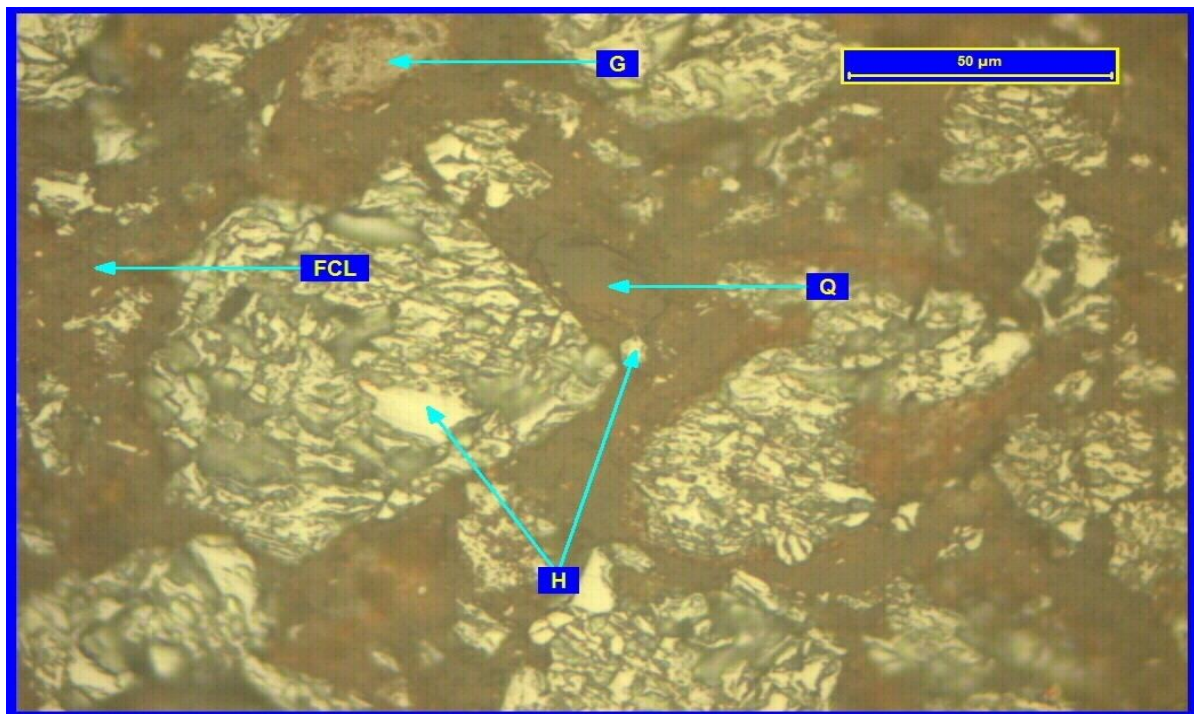


**Fig.4.9** Photomicrograph depicts medium to small grains of highly altered hematite (H), goethite (G), few quartz (Q) and patches of ferruginous clay (FCL). (Under Reflected Light).

### **Goethite:**

Goethite (G) is present as secondary ore mineral that covers around 23% area as a whole next to hematite in the slime sample. All goethite grains were categorized into three classes based on their size as: coarse, medium and small. Coarse grains are in the size range of 120 to 100 microns, medium grains in the size range of 100 to 30 microns and small grains are less than 30 microns. Coarse grains cover around 3% area, medium grains cover around 35% area whereas small grains cover around 62% area of the total goethite distribution (23%). Among the coarse grains (3%), around 5% grains were in fully liberated state and remaining 95% grains were in locked state with other minerals. All un-liberated grains were exhibited in close association with other ore and gangue minerals at less than 90 micron size. Among the medium grains of goethite (35%), around 30% grains were in fully liberated state and remaining 70% grains were in un-liberated state. All un-liberated grains show close association with other ore and gangue minerals at less than 50 micron size. Among the small grains (62%), around 55% grains were in free-state and remaining 45% grains were in un-liberated state and are associated with other ore and gangue minerals at less than 20 micron size (**Figs.4.4, 4.5, 4.6 & 4.9**).

#### **4.1.3.2 Gangue mineralogy:**

The gangue minerals present in the slime sample are quartz (Q), pseudo ore (PSO) and ferruginous clay (FCL).

### **Quartz:**

Quartz (Q) is covering around 7% area as a whole by its area wise distribution. Quartz minerals were present in various shapes and sizes and texturally they are categorized into three groups as coarse, medium and small grains. Coarse grains are in the size range of 200 to 100 microns, medium grains are in the size range of 100 to 30 microns, whereas small grains are less than 30 microns in size. Around 10% area is covered by coarse grains, 42% area is covered by medium grains, and remaining 48% is covered by smaller grains. Among the coarse grains, around 38% grains exist in fully liberated state and free from other minerals association and remaining 62% grains are in un-liberated state and shows close association with other grains at less than 70 micron size. Among the medium grains, around

75% grains are in fully liberated state and the remaining 25% grains exist un-liberated state and are associated with less than 45 micron sized gangue minerals. Among smaller grains, around 85% grains are in fully liberated state, whereas remaining 15% grains are un-liberated state and shows association with other minerals at very fine size, mainly less than 20 micron sized grains (**Figs.4.4, 4.5, 4.8 & 4.9**).

#### **Pseudo ore:**

Pseudo ore (PSO) is another type of gangue mineral present in the slime. Pseudo ore is classified as the mineral that exhibit some properties (for example, optical properties) of the ore mineral but differs in other properties (for example, physical properties) and hence was termed as pseudo ore. This mineral covers around 3% area as a whole. All pseudo ore minerals are less than 40 microns in size. None of the pseudo ore exist in free-state (**Fig.4.4**).

#### **Ferruginous clay:**

Ferruginous clay (FCL) is another type of gangue mineral present in the slime. FCL is grains of minerals that are very finer in size, mainly less than 5 microns to sub-microscopic, and appears as patches of variable sizes and shapes. It covers around 12% area as a whole (**Fig.4.3**). The maximum size of the FCL patches is around 70 microns. All patches are in close association with other mineral grains by their margins. None of the patches of this gangue mineral exist in the free-state (**Figs.4.6, 4.7 & 4.9**).

#### **4.1.3.3 Mineral inter-locking and liberation of gangue:**

The percent amount of librated minerals present in the slime is presented in **Fig.4.10**. The microphotograph obtained with stereomicroscope is shown in **Fig.4.11**, which also indicates the presence of liberated silica and hematite minerals. Around 17% grains of hematite are in free-state whereas remaining 38% grains are in un-liberated state. About 10% goethite grains are in free-state and remaining 13% grains are in un-liberated state. Most of the quartz mineral is observed in librated state. Other gangue mineral present in the slime sample is ferruginous clay (FCL), as shown in **Figs.4.6, 4.7 & 4.9**, which covers around 12% area as a whole and occurs below 70 micron size patches. None of the FCL is observed in free-state. Therefore, the major impurity present in the Bailadila slime is quartz and exists mostly in

the free-state. The detailed mineralogical observations on Bailadila slime sample is presented in **Table 4.4**.

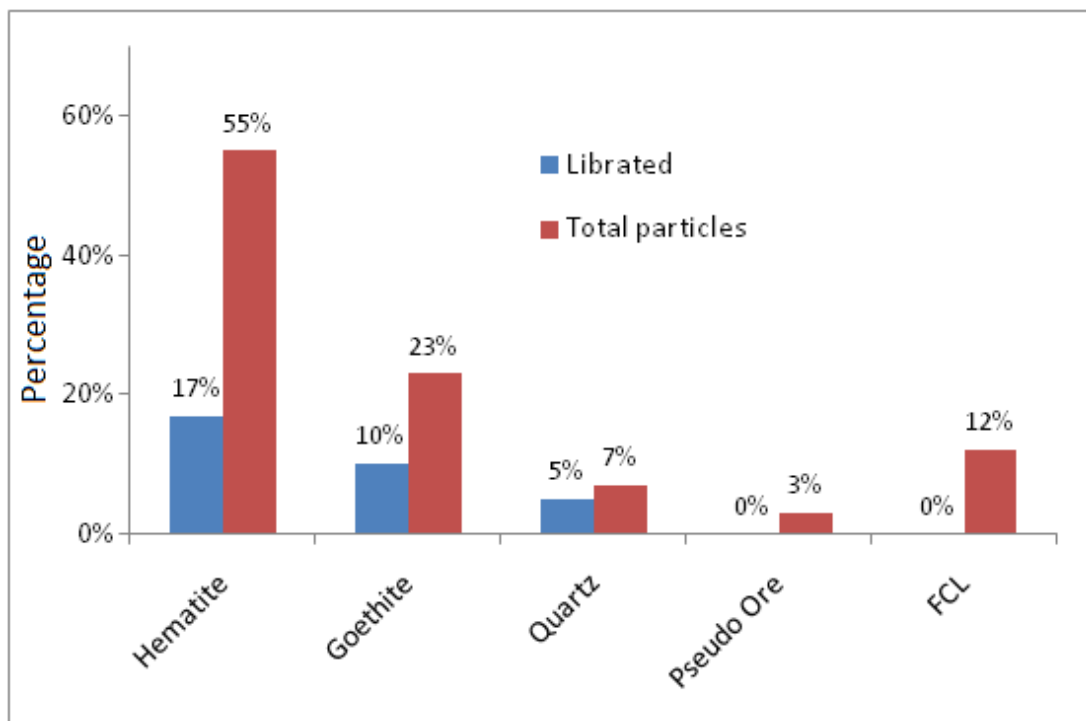


**Fig.4.10** Liberated minerals present in the Bailadila slime sample

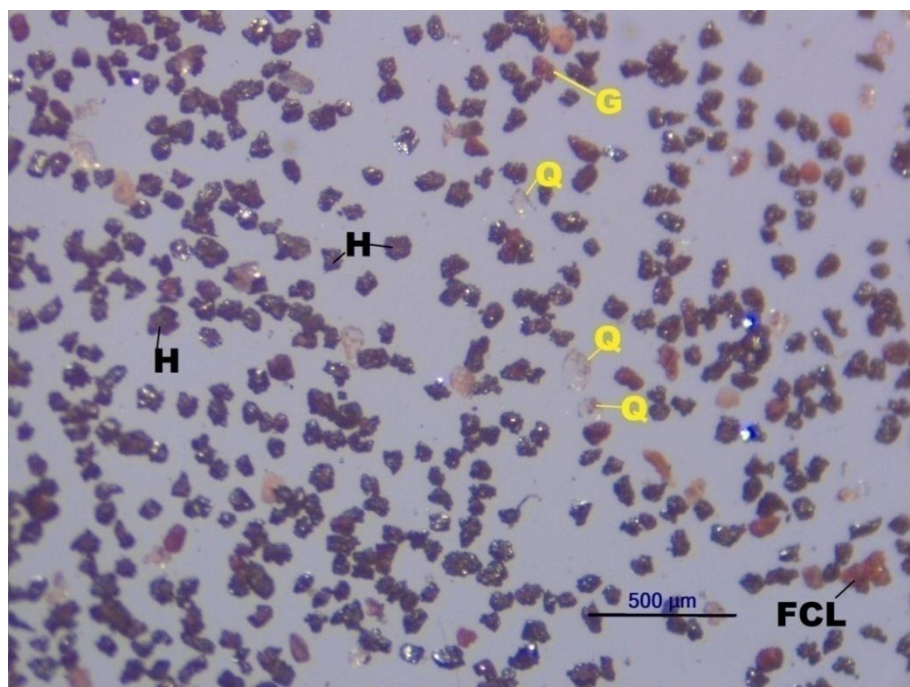


**Fig.4.11** Stereomicroscope photomicrograph showing distribution of medium to fine grains, irregular-shaped hematite (H), few coarse goethite (G) and irregular shaped highly fractured liberated quartz (Q).

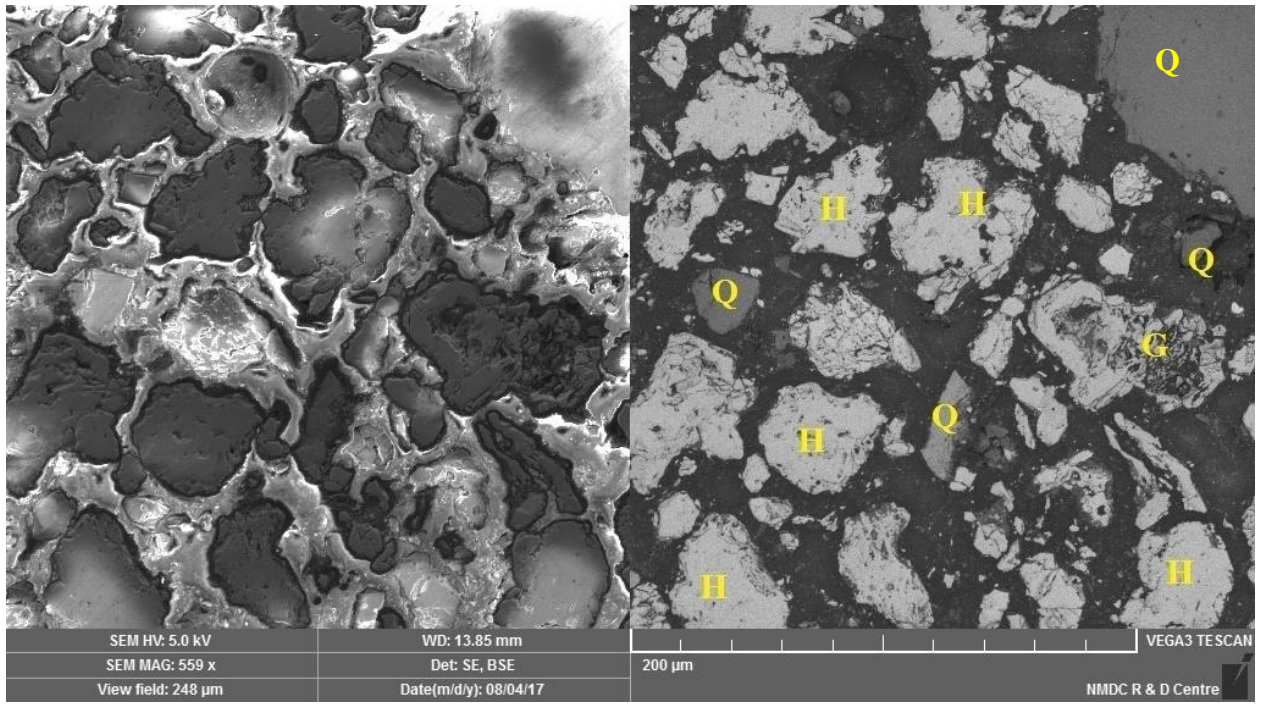
**Table 4.4** Detailed mineralogical observation on Bailadila slime sample.

Ore/Gangue Mineral	Overall Distribution Area wise (%)	Grain Size (microns)		Area (%)	Distribution (w. r. t OM)	Fully liberated Grains (%)		Liberated grains (%)	Unliberated grains (%)	Distribution Unlib. Grains (%)	Unliberated Gangue size (micron)
Hematite (H)	55	Medium	70-30	45	24.75	70-30 $\mu\text{m}$	20	5.0	80	19.8	< 40
		Small	< 30	55	30.25	< 30 $\mu\text{m}$	40	12.1	60	18.2	< 20
								17			38
Goethite (G)	23	Coarse	120-100	3	0.69	120-100 $\mu\text{m}$	5	0.0	95	0.7	< 90
		Medium	100-30	35	8.05	100-30 $\mu\text{m}$	30	2.42	70	5.6	< 50
		Small	< 30	62	14.26	< 30 $\mu\text{m}$	55	7.84	45	6.4	< 20
								10			13
Quartz (Q)	7	Coarse	200-100	10	0.70	200-100 $\mu\text{m}$	38	0.3	62	0.4	< 70
		Medium	100-30	42	2.94	100-30 $\mu\text{m}$	75	2.21	25	0.7	< 45
		Small	< 30	48	3.36	< 30 $\mu\text{m}$	85	2.86	15	0.5	< 20
								5			2
Pseudo ore (PSO)	3	Small	< 40	100	3.00	< 40 $\mu\text{m}$	Nil	0.0	Nil	Nil	< 30
								0.0			0.0
Ferruginous Clay (FCL)	12	Small	< 70	100	12.00	< 70 $\mu\text{m}$	Nil	Nil	Occurs as patches of variable shapes and sizes in close association with other minerals.		

#### 4.1.4 Characterization of iron ore slime by SEM-EDS

Characterization of the slime sample received from mines was carried out using SEM-EDS to understand the distribution of iron ore and gangue minerals in the sample. As per mineralogical analysis, mineral phases present in the sample are hematite and goethite as iron ore minerals and ferruginous clay, alumina and quartz as gangue minerals. Hematite and goethite are present in the proportion of 55% and 23% respectively. Distribution of alumina was not clear under optical microscope. Hence, SEM-EDS was used for better understanding of slime sample. The SEM micrograph is presented in **Fig.4.12**. The minerals cannot be distinguished in micrograph obtained by secondary electron (SE) detector. However, minerals can be identified based on difference in shade (atomic number contrast) in micrograph obtained by back-scattered electron (BSE) detector.

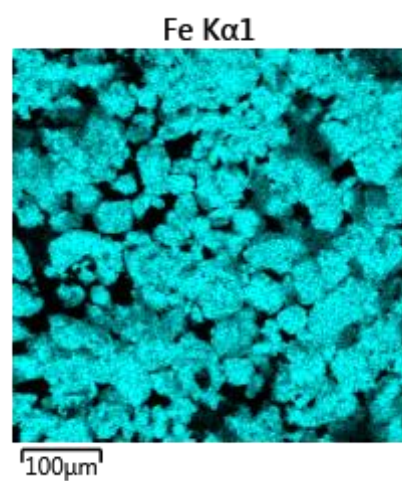
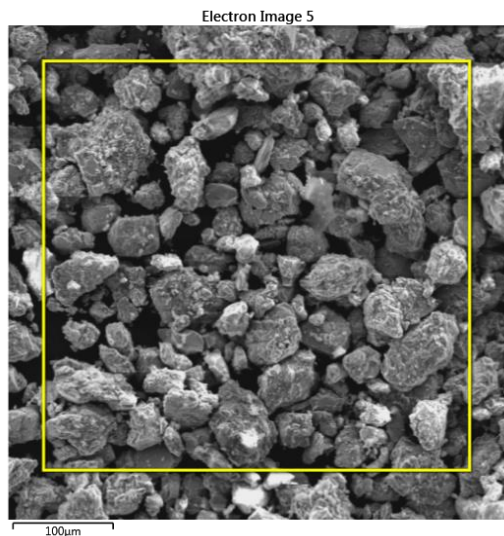
The hematite appears in very weathered condition with no sharp edges. Most of the hematite is rounded off at the outer surface with some extent of conversion to goethite. It indicates prolonged weathering of slime in tailing dam at mine site. EDS was used to determine elemental distribution in the slime sample and the same is presented in **Fig.4.13**. **Figs. 4.13(a) and (d)** represents distribution of Fe and oxygen in the slime sample. It was observed that all minerals were present in oxide form only and Fe is associated with majority of mineral particles in the slime. **Fig. 4.13(b)** indicates distribution of silica and is observed that majority of silica particles were in libratory state, whereas alumina is distributed uniformly throughout the sample except few libratory minerals as shown in **Fig.4.13(c)**.



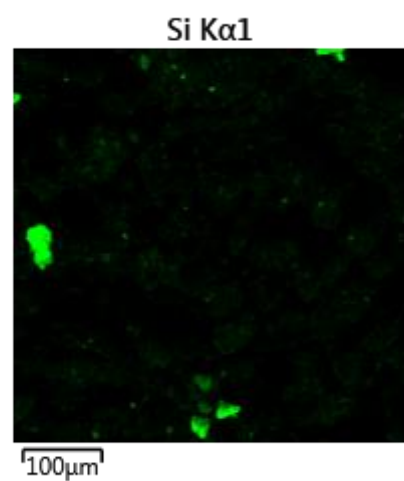
Secondary electron image

Backscattered electron image

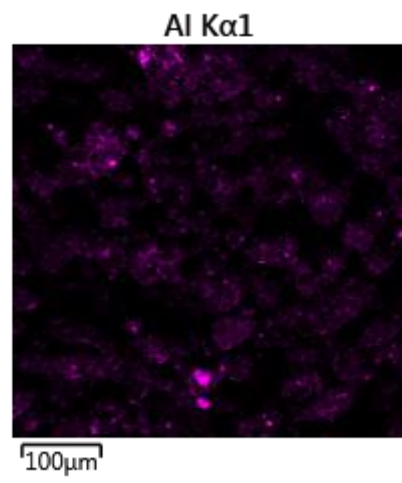
**Fig.4.12** SEM photomicrographs showing highly altered hematite (H), few coarse goethite (G) and irregular shaped highly fractured liberated quartz (Q).



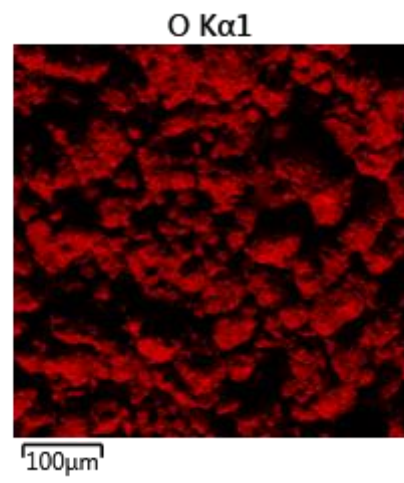
(a) Distribution of Fe



(b) Distribution of Si



(c) Distribution of Al



(d) Distribution of Oxygen

**Fig.4.13** SEM photomicrograph of slime sample and its elemental mapping.

#### 4.1.5 XRD analysis of iron ore slimes

The XRD analysis of iron ore slime received from Bailadila mines is shown in **Fig 4.14**. From this analysis, the presence of hematite and quartz can be identified. The hematite content in the slime is found to be 71.2% and the rest is quartz and other gangue materials. These results are not in agreement with phases measured through optical microscope. Literature (**Mos et al., 2018**) suggest that analysis of iron containing ore sample using copper radiation produce a large background noise owing to high fluorescence and hence, the analysis results close to optical/SEM may not be reflected. This could be the probable reason for incorrect estimation of phases in the iron bearing minerals (iron ore slime) by XRD using copper tube. It may necessitates cobalt tube for obtaining proper analysis.

## 4.2 Thermo gravimetric analysis (TGA) of iron ore slime and other raw materials

In the present study, bentonite is used as binder in micro-pellet making, whereas limestone, dolomite and magnesite were used as fluxes in sinter making to achieve the desired basicity level. Coke breeze is also used in sinter making as fuel. The iron ore slime and other raw materials were used in micro-pellet making and sinter preparation. The results of the analysis of these raw materials by using TGA are presented in **Fig.4.15**. From these results, it is evident that the decomposition of magnesite started at a lower temperature of around 450°C and completed at 520°C followed by the decomposition of dolomite (around 560°C) and limestone (around 600°C). The dissociation of limestone is completed at 950°C. Loss on ignition (LOI) test is carried out under inert atmosphere (N<sub>2</sub>). After LOI test, the temperature of furnace is brought down to 580°C and the atmosphere was changed to oxidizing for the determination of fixed carbon in the coke sample. **Table 4.5** shows the TGA analysis of limestone, magnesite, dolomite and iron ore slime. While the volatile material (expressed as LOI) present in the slime is found to be 0.93% only, the volatile material in the limestone, magnesite and dolomite is found to be more than 40%. The proximate analysis of coke breeze studied by TGA is presented in **Table 4.6**. The fixed carbon in the coke is 73.33% and ash content is 23.837%. The coke is having higher ash content than the desired level (less than 20%).

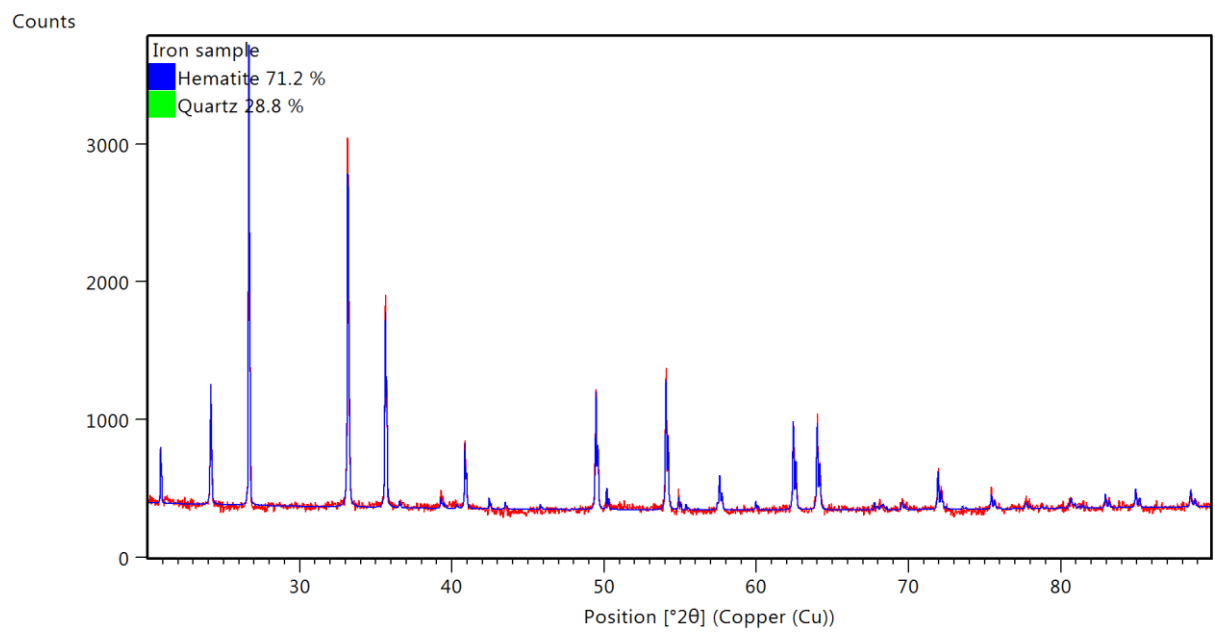


**Fig 4.14** XRD analysis of iron ore slime sample

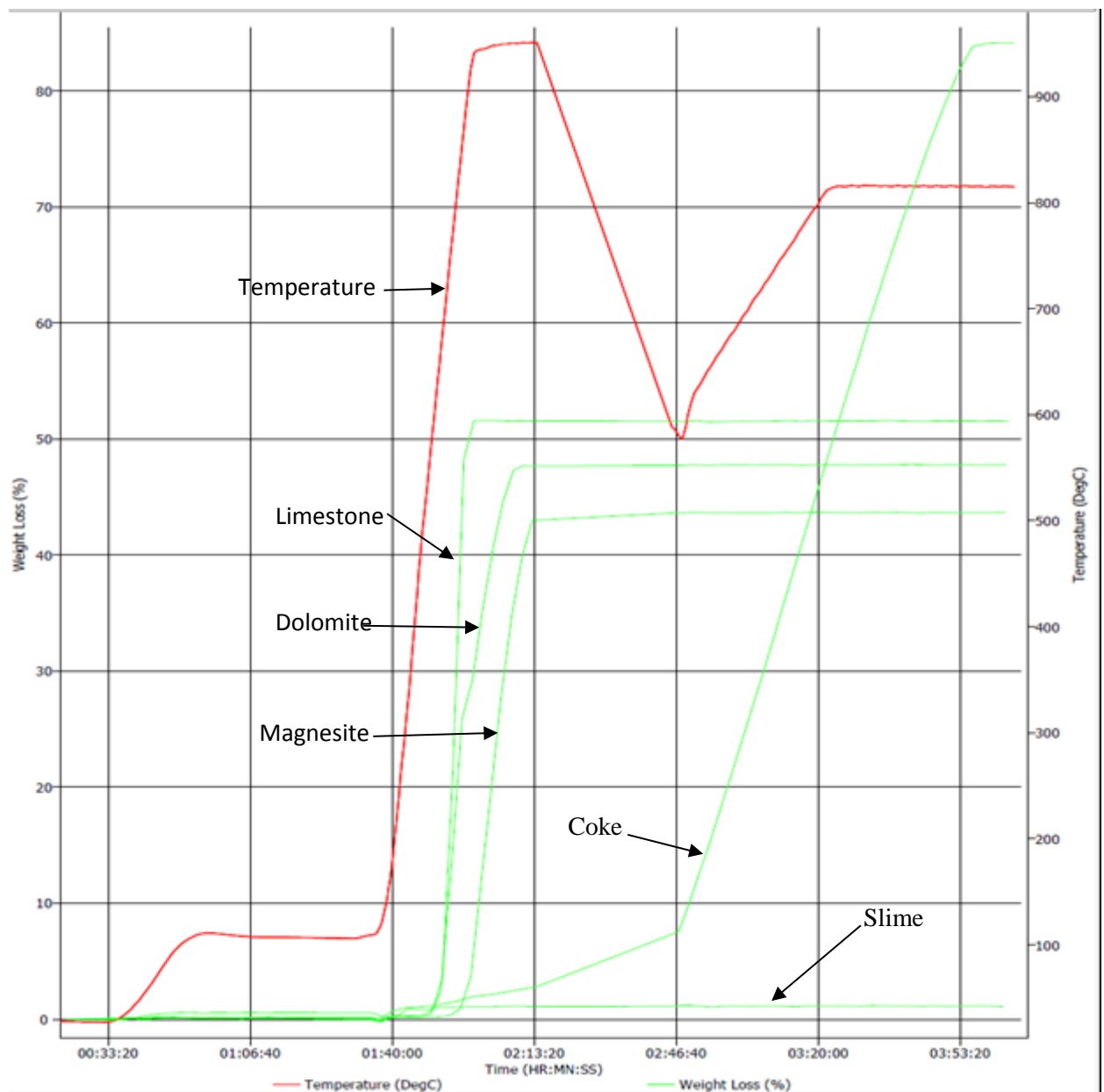


**Fig.4.15** TGA analysis of iron ore slime, coke, magnesite, dolomite and limestone samples.

**Table 4.5** TGA results

S. No.	Raw material	Moisture (%)	Loss on Ignition (%)	Mass after removal of LOI and moisture (%)
1	Limestone	0.08	42.89	57.03
2	Magnesite	0.11	51.44	48.50
3	Dolomite	0.05	47.58	52.36
4	Slime (Bailadila)	0.14	0.93	98.93

**Table 4.6** The proximate analysis of coke breeze

Raw material	Fixed carbon (%)	Volatile (%)	Moisture (%)	Ash (%)
Coke breeze	73.33	2.683	0.147	23.837

### 4.3 Characterization of other raw materials

#### **Binder and flux for micro-pellet making:**

The limestone and bentonite were used as additive and binder in the preparation of micro-pellets in association with the concentrate obtained from beneficiation studies of the Bailadila slime sample. These materials were received from various mines and plants. Limestone was received in the form of lumps of size ranging from 50 to 150 mm, whereas the bentonite was received with the size below 75 microns. The limestone was crushed and ground to below 75 micron size for subsequent pelletization studies. The chemical analysis of limestone and bentonite is presented in **Table 4.7**. It can be observed that the amount of gangue minerals in limestone is very less. However, bentonite possess high amount of silica and alumina. Therefore, the amount of bentonite as binder should be optimized.

#### **Fluxes and fuel for hybrid pellet sintering:**

The limestone, dolomite and magnesite were used as fluxes and coke breeze was used as fuel during hybrid pellet sintering. The limestone, dolomite and magnesite were received from various mines of NMDC Ltd. in lump form. Hence, they were stage crushed to -3mm size prior to their use in sintering. Limestone and dolomite were crushed to -3 mm size by using jaw and roll crusher. The coke breeze was received from RINL, Visakhapatnam. The size analyses of the fluxes and coke breeze are presented in **Table 4.8**. All the flux materials used in hybrid pellet sintering were chemically analyzed by WD-XRF spectroscope and the results are shown in **Table 4.9**. The silica and alumina content in the limestone and magnesite were found to be very low. The coke breeze (fuel) was burnt in the ashing furnace at 900°C and the ash obtained was analyzed by XRF for its chemical composition. The constituents of the coke breeze ash are given in **Table 4.10**. It can be observed that the  $\text{SiO}_2$  and  $\text{Al}_2\text{O}_3$  contents of the ash are high and require extra fluxes in the sinter to form slag. The S and P contents are also present in high amount in the ash.

**Table 4.7** Chemical analysis of limestone and bentonite used in micro-pellet making

Raw material	Constituents, assay %						
	Fe[T]	SiO <sub>2</sub>	Al <sub>2</sub> O <sub>3</sub>	LOI	CaO	MgO	P
<b>Limestone</b>	0.78	0.71	0.09	42.89	51.10	4.20	0.03
<b>Bentonite</b>	9.2	54.0	13.0	7.76	2.8	6.2	0.068

**Table 4.8** Size analysis of limestone, dolomite, magnesite, and coke breeze used for hybrid pellet sintering

Size in Tyler mesh	Raw material			
	Limestone Wt. %	Dolomite Wt. %	Magnesite Wt. %	Coke breeze Wt. %
+6	-	-	17.4	-
- 6 + 10	44.0	24.3	21.0	39.7
- 10 + 20	27.4	26.4	18.2	24.8
- 20 + 35	11.4	13.3	15.8	13.4
- 35 + 48	3.9	6.1	9.0	5.4
- 48 + 65	1.7	4.9	6.5	4.0
- 65 + 100	1.9	4.8	5.0	3.1
- 100 + 150	1.7	4.5	3.3	2.5
- 150 + 200	1.3	3.5	1.7	1.7
- 200 + 270	1.7	3.1	1.0	1.3
- 270 + 325	2.1	2.0	0.2	0.8
- 325	2.9	7.1	0.9	3.3
<b>Total</b>	100.0	100.0	100.0	100.0

**Table 4.9** Chemical analysis of fluxes used for hybrid pellet sintering

Flux	Constituents, assay %							
	Fe	FeO	SiO <sub>2</sub>	Al <sub>2</sub> O <sub>3</sub>	CaO	MgO	Mn	LOI
<b>Limestone</b>	0.78	ND	0.71	0.09	51.10	4.20	ND	42.89
<b>Dolomite</b>	0.49	ND	2.24	0.30	30.25	18.50	ND	47.58
<b>Magnesite</b>	1.03	ND	0.56	0.28	2.01	45.12	ND	51.40

ND - Not detected

**Table 4.10** Chemical analysis of ash obtained from coke breeze

	Constituents, assay %						
	Fe	SiO <sub>2</sub>	Al <sub>2</sub> O <sub>3</sub>	CaO	MgO	P	S
<b>Coke breeze ash</b>	18.80	39.83	23.00	1.19	0.70	0.25	0.38

#### **4.4 Summery:**

The silica ( $\text{SiO}_2$ ) and alumina ( $\text{Al}_2\text{O}_3$ ) contents in the iron ore slime were 7.76% and 3.10% respectively. The blast furnace iron bearing material should have silica and alumina put together less than 5%. However, the total gangue mineral (i.e.  $\text{SiO}_2+\text{Al}_2\text{O}_3$ ) in the slime is 10.86%, which is on higher side to charge in to blast furnace. Hence, the slime as such cannot be used in any of the iron making processes. Higher gangue minerals in the charge materials would lead to increased coke rate in the blast furnace and also increased slag volume significantly. Thus, the slime need to be beneficiated and gangue minerals should be reduced to minimum level with higher recovery of iron value.

# Chapter-5

## BENEFICIATION STUDIES OF IRON ORE SLIME

### (Laboratory and Pilot scale studies)

#### 5.1 Introduction:

The testing program for laboratory scale beneficiation was designed based on the literature survey and past experience. The beneficiation studies were taken up on batch scale facilities with an aim for development of optimum flow sheet for processing of slime to obtain concentrate containing more than 64% Fe(T) and SiO<sub>2</sub> and Al<sub>2</sub>O<sub>3</sub> each  $\leq 2.0\%$  with highest possible recovery of more than 80%. At laboratory scale, all possible gravity, magnetic and flotation separation techniques and combination thereof were considered to meet this requirement as shown in **Fig.5.1**. Considering the scarcity of water in future at mine site, a few dry beneficiation studies were also attempted.

#### 5.2 Laboratory scale beneficiation studies:

##### 5.2.1 Scheme – I (Gravity separation technique)

In scheme-I, the representative sample of iron ore slime was subjected to straight tabling (Wilfley table) independently and the results of tabling studies are presented in **Table 5.1**. These results indicate that the desired grade of concentrate (i.e., with more than 64% Fe) could be produced from the slime. However, the recovery of iron value is very low, i.e., 15.4%. Hence, tabling concentrate cannot be considered for commercial exploitation. The combination of tabling concentrate and middling had a recovery of 74.15% with a Fe value of 61.24%. This indicate that even the combination of tabling concentrate with middling does not yielding the requirement of  $>64\%$  Fe(T) and recovery of  $>80\%$ . Hence, the addition of middling to the concentrate does not possess any beneficial effect commercially. On the whole, scheme-I is not an encouraging route for the beneficiation of Bailadila iron ore slime.

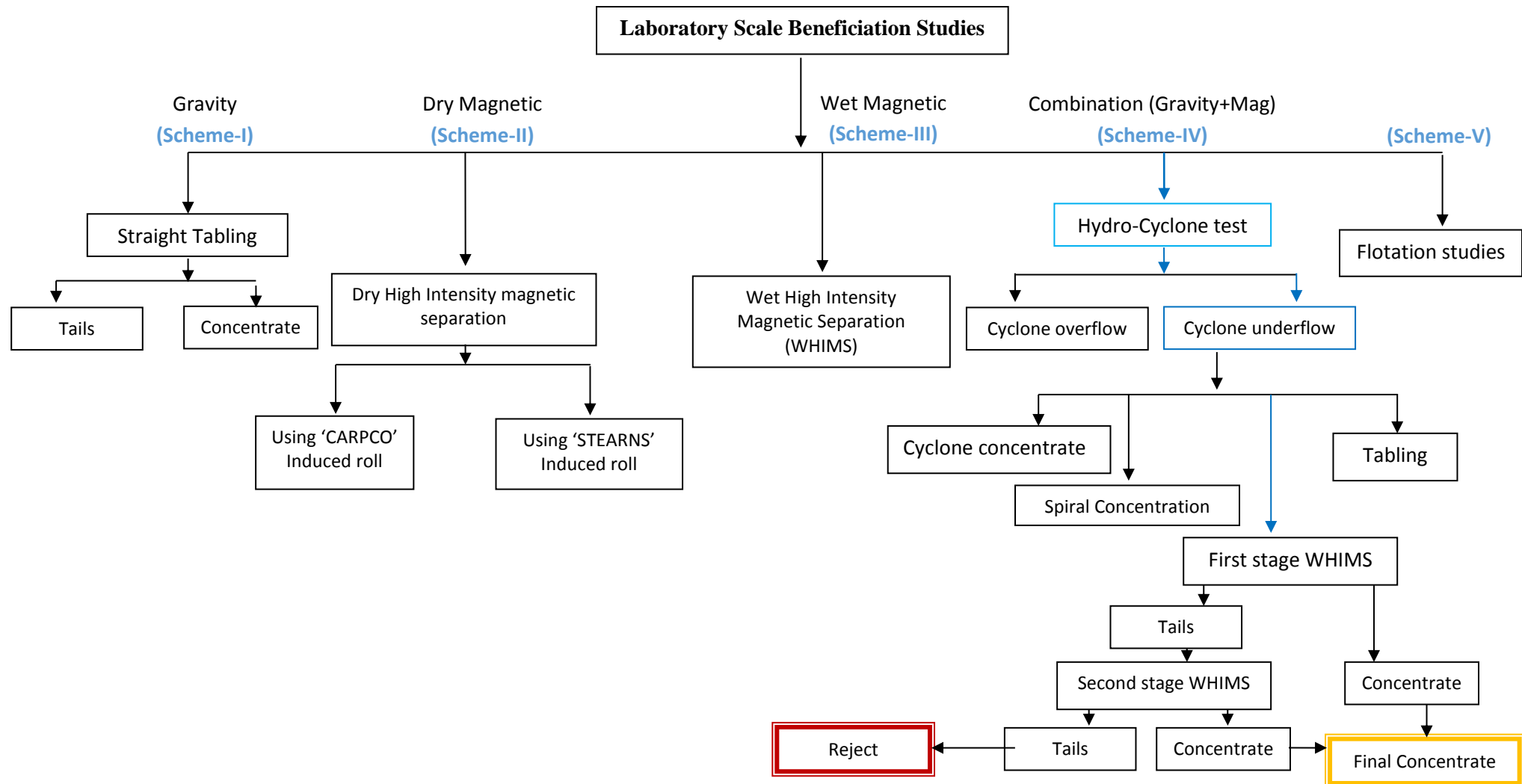


**Fig.5.1** Laboratory scale beneficiation studies of iron ore slime from Bailadila mines (deposit-5)

**Table 5.1** Results of straight tabling of slime sample

S. No.	Products	Weight %	Assay, % Fe	Recovery, % Fe
1.	Table concentrate	14.3	65.55	15.4
2.	Table middling	59.4	60.20	58.75
3.	Table tailing	7.50	58.40	7.20
4.	Table slime	18.8	60.40	18.6
Calculated head		100.0	60.87	100.0

*Model calculations:*

$$\% \text{ Fe value in combination of table concentrate and middling} = \frac{(14.3 \times 65.55 + 59.4 \times 60.20)}{(14.3 + 59.4)} = 61.24$$

$$\text{Total assay, \%Fe} = \frac{(14.3 \times 65.55 + 59.4 \times 60.20 + 7.50 \times 58.40 + 18.8 \times 60.40)}{100} = 60.87$$

### **5.2.2 Scheme – II (Dry magnetic separation technique)**

In scheme-II, the high intensity dry magnetic separation was carried out by using (a) CARPCO induced roll and (b) STEARNS induced roll.

#### **a) High intensity dry magnetic separation using ‘CARPCO’ induced roll**

The representative slime samples from Bailadila mines were directly treated on CARPCO high intensity dry magnetic separator at three different currents, viz. 0.25, 0.5 and 0.75 amperes, which corresponds to magnetic intensities of 3000, 5500 and 8000 Gauss respectively. The dry magnetic separation test was carried out using bone dry (without any traces of moisture) slime samples. The presence of even small amount of moisture is detrimental on efficiency of separation in dry magnetic process. Hence, the moisture in the sample was completely removed by heating the sample at 105 °C in an oven for overnight prior to dry magnetic separation. The sample was carefully fed to the magnetic separator as mono layer since maximum efficiency of separation is achieved with mono layer feeding. The overall iron grade of the concentrate and percent recovery after passing through CARPCO magnetic separator is presented in **Fig 5.2**. The concentrate from CARPCO magnetic separator was analysed and found to meet the grade requirement of 64% Fe(T) at all currents used, but failed to meet recovery requirement of more than 80% at all current levels. In addition, the process is prone to generate immense quantity of dust and possess low productivity due to mono layer feeding of the slime. In view of these drawbacks, the high intensity dry magnetic separation using 'CARPCO' roll is found to be not a viable route for the beneficiation of Bailadila iron ore slime.

#### **b) High intensity dry magnetic separation using “STEARNS” roll**

The representative fractions of the slime samples were subjected to high intensity dry magnetic separation using Stearns roll magnetic separator operating at a constant intensity of 6000 Gauss and the results are presented in **Table 5.2**. Although the desired grade of concentrate (64.32% Fe(T)) could be produced with STEARNS roll, the recovery of iron value is observed to be very low at 31%. Thus, the process cannot be considered for commercial production due to very low recovery of iron value.

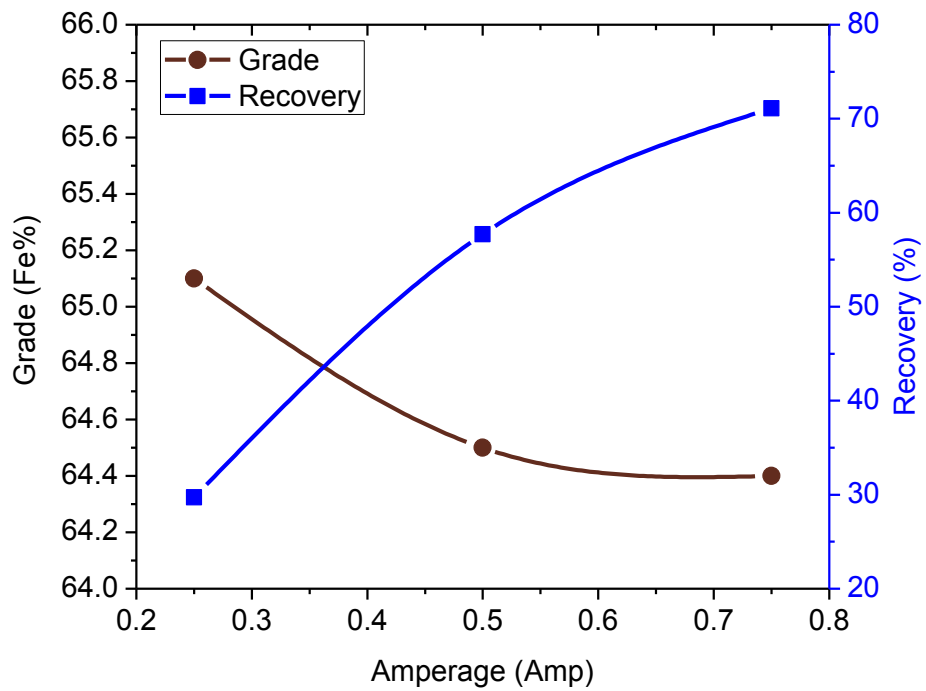


**Fig.5.2.** Grade and recovery obtained using dry magnetic separation (CARPCO induced roll)

**Table 5.2** Results of dry magnetic separation of slime samples using Streans rolls

S. No.	Product	Weight %	Assay, % Fe	Recovery, % Fe
1	Mag. concentrate -I	29.4	64.32	31.0
2	Mag. concentrate -II	35.9	63.09	37.6
3	Mag. concentrate -III	17.6	62.02	18.2
4	Non-mag. tails	17.1	47.04	13.2
	Head (Calculated)	100.0	60.67	100.0

### **5.2.3 Scheme – III (Wet magnetic separation technique)**

In scheme-III, wet high intensity magnetic separation (WHIMS) was used to generate beneficiated slime. The slime sample was treated at three different currents, viz. 2.5, 5.0, and 7.5 amperes. The results of WHIMS process are shown in **Table 5.3**. Although the iron grade appears to meet the requirement of  $>64\%$  Fe(T) at 2.5 and 5 amperes, the observed recovery is very low. However, the concentrate obtained at 7.5 amperes shows Fe value of 64.85% with 76% recovery of valuable minerals. These results suggest that the desired grade of iron ore concentrate with high recovery of iron value can be obtained at amperage of 7.5 amperes. As the recovery observed is close to the required level (80%), the WHIMS process could be a better option for the beneficiation of Bailadila iron ore slime.

### **5.2.4 Scheme – IV (Combination of gravity and magnetic separation)**

The microscopic studies revealed the presence of hematite and goethite as ore minerals. Siliceous and lateritic materials including ferruginous clay formed the gangue. Mostly siliceous materials were observed in free-state, which suggests the use of either gravity separation or magnetic separation independently or in combination. In the present scheme, combination of gravity separation using hydro-cyclone and WHIMS was chosen to obtain the desired concentrate. Prior to the combination with WHIMS process, the concentrate (underflow) direct from hydro-cyclone was analyzed for its suitability with respect to iron grade and recovery. The underflow from hydro-cyclone was also subjected to spiral concentration and tabling separately with a view to improve the quality of the concentrate.

#### **5.2.4.1 Beneficiation of slime sample using hydro-cyclone:**

The results of hydro-cyclone test conducted at 10 mm, 12.5 mm, and 15 mm apex dia. using various pulp densities are presented in **Table 5.4** and in **Figs. 5.3a to c**, which shows that the grade and recovery are inversely proportional. As grade increases, the recovery drops. From **Fig. 5.3a** it can be observed that both iron grade and recovery are not meeting the minimum requirements. Although the iron grade obtained at 10 mm apex dia. and pulp densities of 18%

**Table 5.3** Results of wet magnetic separation of slime samples

**(a) Amperage: 2.5 Amp**

S. No.	Product	Weight %	Assay % Fe	Recovery, % Fe
1	Mag. concentrate	54.4	65.07	58.7
2	Middling	21.0	62.40	21.7
3	Tails	24.6	48.18	19.6
	Head (Calculated)	100.0	60.35	100.0

**(b) Amperage: 5.0 Amp**

S. No.	Product	Weight %	Assay % Fe	Recovery, % Fe
1	Mag. concentrate	65.3	64.95	70.8
2	Middling	16.2	61.60	16.7
3	Tails	18.5	41.30	12.5
	Head (Calculated)	100.0	60.03	100.0

**(c) Amperage: 7.5 Amp**

S. No.	Product	Weight %	Assay % Fe	Recovery, % Fe
1	Mag. concentrate	70.6	64.85	76.0
2	Middling	14.7	59.08	14.5
3	Tails	14.7	38.41	9.5
	Head (Calculated)	100.0	60.12	100.0

**Table 5.4** Iron grade (Fe(T)) and recovery of the concentrate obtained from hydro-cyclone studies at various apex dia. and pulp densities.

			Pulp density								
			10%			18%			25%		
Operational condition of cyclone		Product	Wt %	Fe(T)	Recovery (% Fe)	Wt %	Fe(T)	Recovery (% Fe)	Wt %	Fe(T)	Recovery (% Fe)
Apex Dia.	Vortex (Inch)										
10 mm	1.25	Underflow	78.6	61.62	80.0	74.7	62.20	76.6	66.6	62.87	69.3
		Overflow	21.4	56.40	20.0	25.3	55.50	23.4	33.4	55.60	30.7
		Head (cal)	100.0	60.50	100.0	100.0	60.50	100.0	100.0	60.44	100.0
12.5mm	1.25	Underflow	88.2	61.34	89.9	79.5	62.34	81.9	73.8	62.53	76.2
		Overflow	11.8	51.60	10.1	20.5	53.38	18.1	26.2	54.80	23.8
		Head (cal)	100.0	60.19	100.0	100.0	60.50	100.0	100.0	60.50	100.0
15mm	1.25	Underflow	93.0	61.24	94.1	84.6	61.69	86.2	82.7	62.00	84.8
		Overflow	7.0	50.50	5.9	15.4	52.90	13.8	17.3	52.96	15.2
		Head (cal)	100.0	60.50	100.0	100.0	60.34	100.0	100.0	60.50	100.0

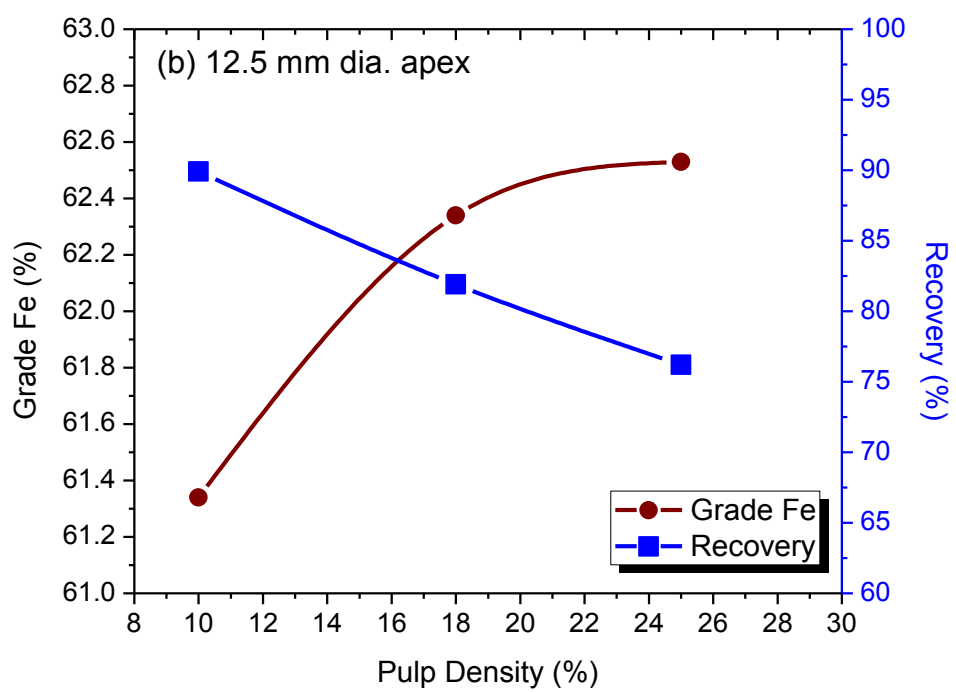
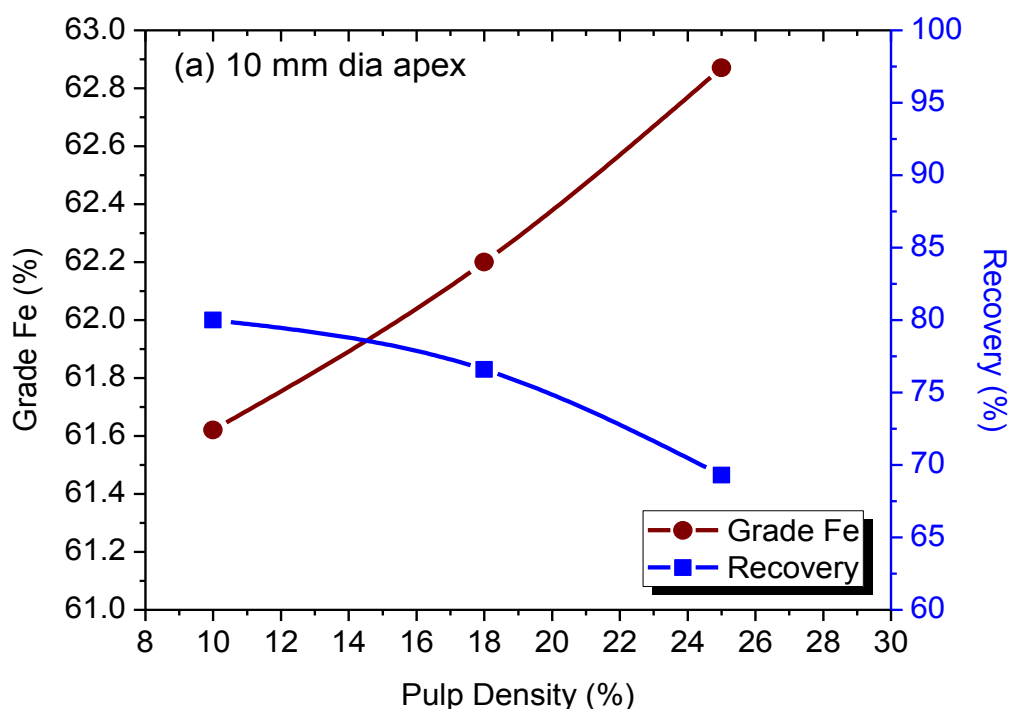


**Fig.5.3.** Continued in next page

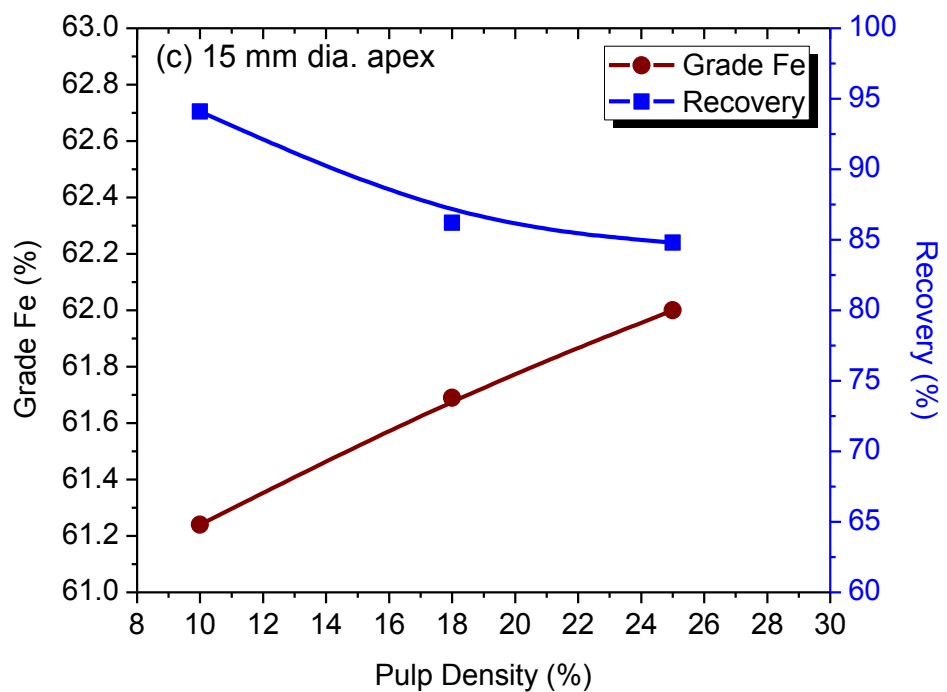


**Fig. 5.3** Grade and recovery as a function of pulp density in hydrocyclone at apex diameter of (a) 10 mm, (b) 12.5 mm, and (c) 15 mm

and 25% meeting the minimum requirement of 62% Fe(T), the recovery is observed to be low. Hence, hydro-cyclone with 10 mm apex dia. using pulp densities of 10%, 18% and 25% is not suitable to be used as a pre-concentrator. Similarly, in hydro-cyclone with 15 mm apex dia. using all three pulp densities, the concentrate obtained does not contain the minimum requirements of Fe(T) (**Fig. 5.3c**) even though meeting the minimum required recovery value of 80% (min). Maximum recovery of 94.1% with 61.24% Fe grade was achieved with 15 mm apex dia. and 10% pulp density. Maximum recovery is achieved due to controlled removal of ultra-fines from slime sample. Thus, hydro-cyclone with 15 mm apex dia. and 10% pulp density can be considered as de-sliming unit. In case of hydro-cyclone test with 12.5 mm apex dia. and 18% pulp density, the concentrate obtained was analysed and found to contain 62.34 % Fe with recovery of more than 80 % (**Fig. 5.3b**). Hence, hydro-cyclone with 12.5 mm apex dia. and pulp density of 18% can be used as pre-concentrator for spiral and tabling process. The sample of underflow of hydro-cyclone with 12.5 mm apex dia. and 18% pulp density was collected and subjected for SEM-EDS analysis. The SEM-EDS images are shown in **Figs.5.4a** and **b**. The SEM micrograph reveals that the underflow of hydro-cyclone contains medium to fine grains of hematite and is free from fine clay particles, which will be helpful for subsequent concentration. Some quartz particles are also seen in free-state. The EDS analysis confirms the presence of Fe and O as major elements in hematite and Si and O as major elements in quartz.

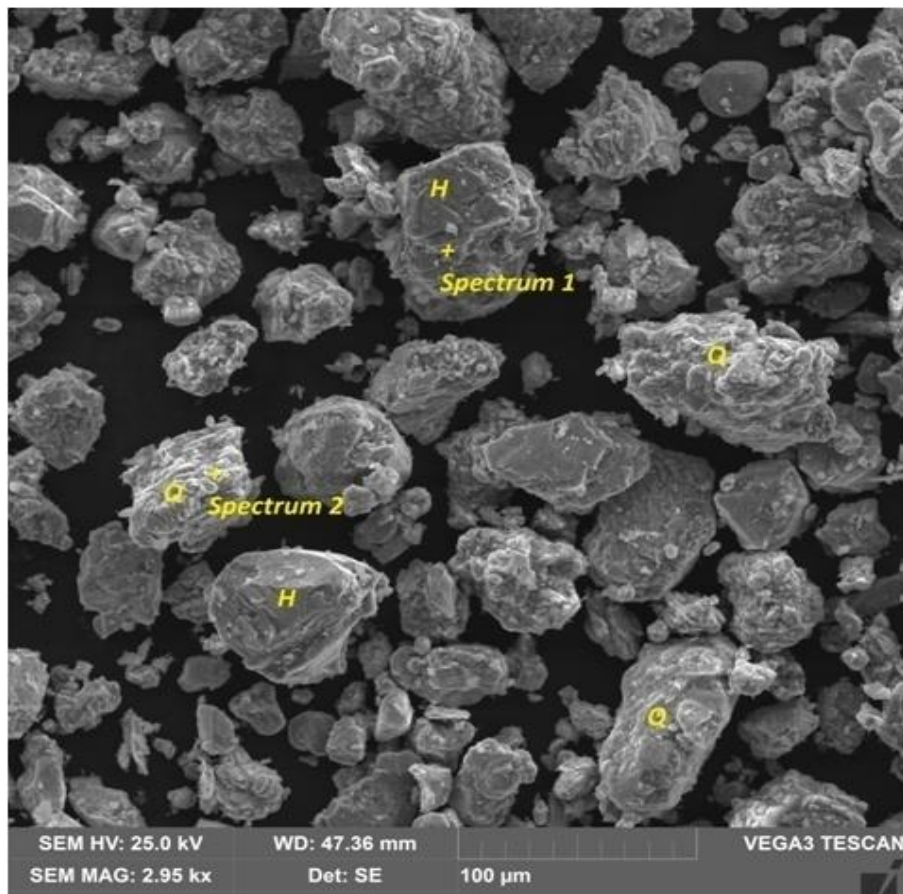


**Fig. 5.4 (a)** SEM photomicrograph of hydro-cyclone underflow, displays distribution of medium to fine grains of hematite (H) and Quartz (Q).

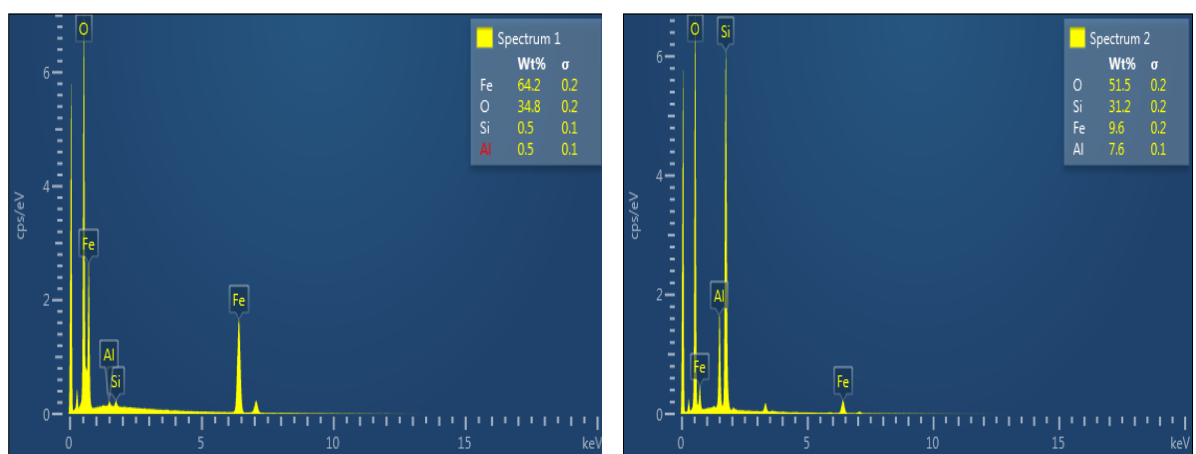


**Fig. 5.4(b)** EDS results displays elemental analysis of various grains of underflow from hydro-cyclone.

#### 5.2.4.2 Hydro-cyclone followed by spiral and tabling:

Gravity separation technique is used in the cases where a significant density difference exists between the ore minerals and the gangue materials. The effectiveness of the separation depends upon concentration criterion (**Wills and Napier-Munn, 2006**), which is defined by

$$\text{Concentration criterion} = \frac{D_h - D_f}{D_l - D_f} \quad (5.1)$$

where  $D_h$ ,  $D_f$ , and  $D_l$  are specific gravities of heavy mineral, fluid medium and light mineral respectively. Higher the concentration criterion, better the separation; and concentration criterion should be more than 2.5 (**Wills, 1988**).

As per mineralogy study explained in section 4.1.3.2, majority of the silica particles present in the slime are in liberated state with hematite as primary ore mineral. Considering water as liquid medium of separation, concentration criterion was calculated according to eq. 5.1 and it was found to be 2.6. Hence the slime is amenable for gravity separation by spiral and tabling.

The underflow obtained from the hydro-cyclone at 12.5 mm apex dia. and 1.25 in. vortex finder with 18 % pulp density was analysed and found to contain 62.34 %Fe with more than 80 % recovery of iron value. However, the iron grade is not sufficient for the blast furnace feed stock requirement (64% Fe). Hence, this underflow was further treated for second stage gravity separation using spiral and tabling (using 12.5 mm stroke) separately with a view to improve the iron grade of the concentrate. The results of spiral and tabling experiments are shown in **Fig 5.5**. It can be observed that, the concentrate with high Fe(T) content (68.17%) was obtained after tabling studies of hydro-cyclone underflow. However, the recovery of iron value was very low at 37.5%. Similarly, it can be observed from the results of spiral test (in **Fig. 5.5**) that the concentrate of maximum 65.6% Fe(T) with 56% recovery was obtained under optimized condition. Both the gravity separation methods were failed to achieve desired level of recovery (min. 80%) even though they result in acceptable iron values Fe(T).

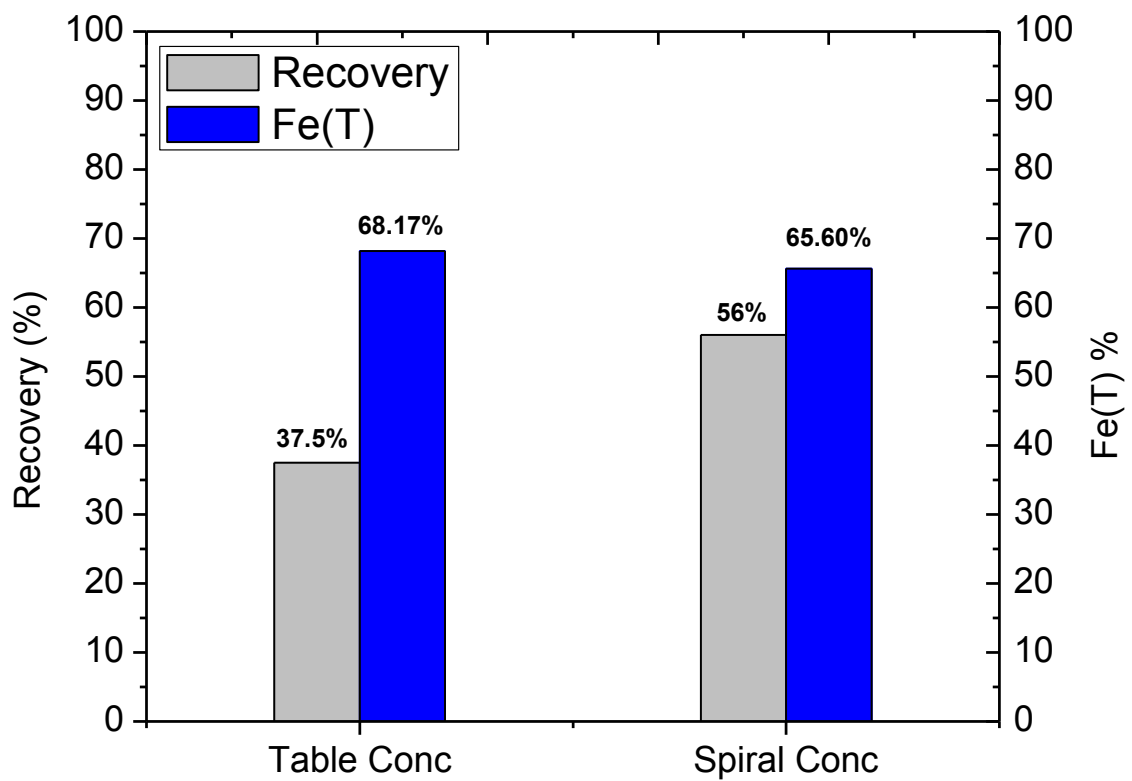


**Fig.5.5.** Recovery and Fe(T) by using tabling and spiral studies of hydro-cyclone underflow.

### 5.2.4.3 Hydro-cyclone followed by two stage magnetic separation:

As claimed from microscopic studies (in section 4.1.3.1), the main ore minerals of slime are hematite and goethite. Majority of ore minerals are present in free state, which indicate that further grinding of sample is not required for liberation of minerals and can be subjected to two stage high intensity magnetic separation for obtaining maximum recovery (**Das et al., 2010**). The presence of ultra-fine particles in the sample may increase viscosity of the slurry. The increase in viscosity of the slurry may affect efficiency of the magnetic separation. Hence, removal of ultra-fines (de-sliming) by hydro-cyclone is essential before using high intensity magnetic separation. The underflow from hydro-cyclone tests was analyzed for its chemical analysis and recovery. The chemical analysis of the underflow from hydro-cyclone with 15 mm apex dia. and 1.25 in. vortex finder with pulp density of 10% solid is shown in **Table 5.5**. Higher recovery with optimum removal of ultra-fines can be observed. Hence, the underflow of hydro-cyclone (15 mm apex dia. and 1.25 in. vortex finder with pulp density of 10 % solid) was selected for wet high intensity magnetic separation (WHIMS).

The underflow from the hydro-cyclone was passed through a batch type WHIMS at four magnetic field intensities, viz. 13250, 14500, 15500 and 16255 G in order to optimize the intensity that results in higher recovery of iron grade suitable for blast furnace feed. The results of WHIMS test are presented in **Fig. 5.6**. It can be noticed that a good recovery of 67.8% with 64.81% Fe(T) grade was obtained at 14500 G (2 amp) intensity. Hence, a magnetic field intensity of 14500 G (2 amp) was used for two stage magnetic separation. Jone's P40 model of WHIMS was used for these studies. The results of first stage WHIMS test are presented in **Table 5.6** and they indicate that it is possible to produce a concentrate assaying 65.01% Fe(T), 1.83 % SiO<sub>2</sub> and 1.68% Al<sub>2</sub>O<sub>3</sub> with an yield of 58.68% with respect to original. The middling assaying about 62.40% Fe(T), 6.12 % SiO<sub>2</sub> and 2.96% Al<sub>2</sub>O<sub>3</sub> could also be blended with the concentrate to get a combined concentrate assaying 64.81% Fe(T), 2.16 % SiO<sub>2</sub> and 1.78% Al<sub>2</sub>O<sub>3</sub>. The combined yield of concentrate and middling was observed to be 63.52% and the equivalent recovery of iron is found to be 67.86 %.

**Table 5.5** Chemical analysis of the underflow obtained from hydro-cyclone at 15 mm apex dia. and 1.25 in. vortex finder with pulp density 10 % solid.

S. No.	Product	Weight %	Fe(T)	SiO <sub>2</sub>	Al <sub>2</sub> O <sub>3</sub>	Recovery (% Fe)
1.	Underflow	93.0	61.24	7.11	2.6	94.1
2.	Overflow	7.0	50.50	17.5	10.5	5.9
Calculated head		100.0	60.5	7.84	3.15	100.0

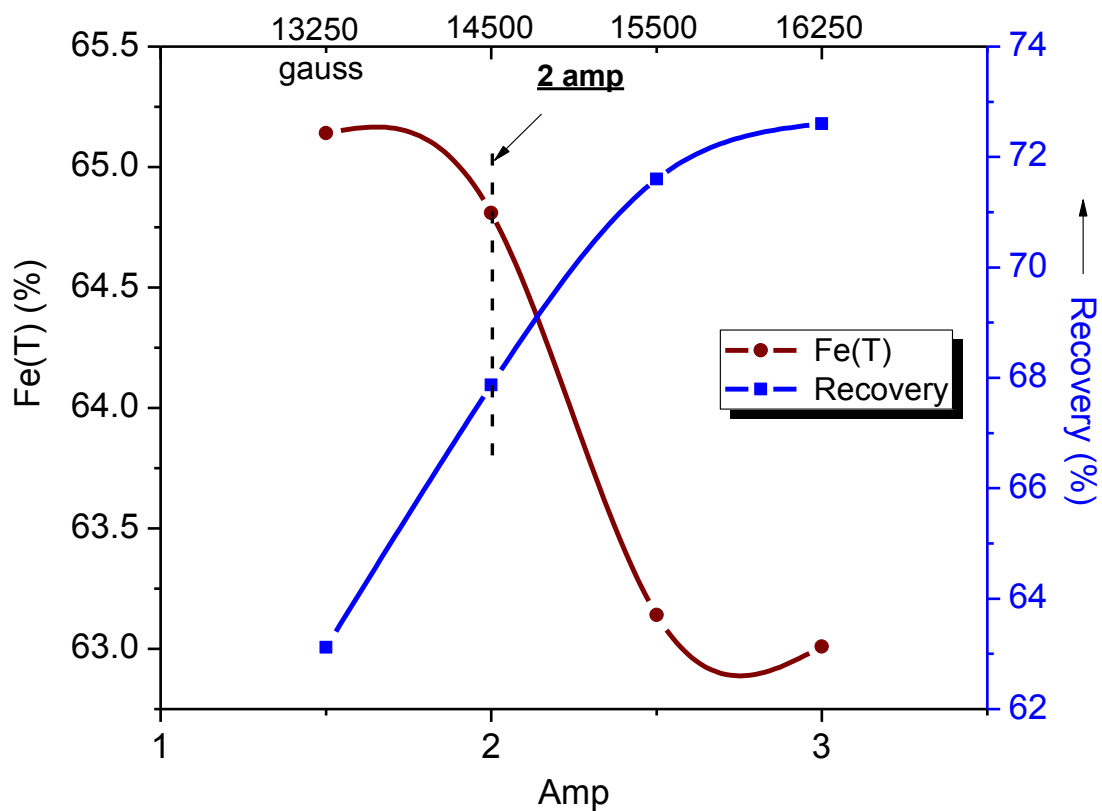


**Fig.5.6.** Recovery and grade as a function of magnetic field

**Table 5.6** Results of first stage WHIMS test (at 2 amp)

Products	Wt.%	Yield		Assay %					Recovery %
		Wt.% w.r.t original		Fe(T)		SiO <sub>2</sub>		Al <sub>2</sub> O <sub>3</sub>	
Concentrate	63.10	<b>58.68</b>	63.52	<b>65.01</b>	64.81	<b>1.83</b>	2.16	<b>1.68</b>	62.89
Middling	5.20	4.84		62.40		6.12		2.96	4.97
Tail	31.70	29.48		53.51		18.21		4.41	26.01
Head (actual)	100.00	93.00		61.23		7.25		2.61	93.87

In order to obtain further recovery of iron values from the tailings of first stage WHIMS test, a second stage WHIMS operation was adopted. The results of second stage WHIMS test are presented in **Table 5.7** and are observed to be quite encouraging. The concentrate assaying 64.82% Fe(T), 2.93 % SiO<sub>2</sub> and 1.87% Al<sub>2</sub>O<sub>3</sub> with an yield of 14.77% with respect to original. The middling assaying about 61.09% Fe(T), 7.18 % SiO<sub>2</sub> and 3.06 % Al<sub>2</sub>O<sub>3</sub> could also be blended with the concentrate to get a combined concentrate assaying 64.48% Fe(T), 3.32 % SiO<sub>2</sub> and 1.98% Al<sub>2</sub>O<sub>3</sub>. The combined yield of concentrate and middling is observed to be 16.27 % and the equivalent recovery of iron is found to be 17.29 %.

The overall yield, iron grade, and recovery obtained after blending the concentrate from first stage and second stage WHIMS operations is presented in **Table 5.8**. The final yield obtained is about 79.79% with an equivalent iron recovery of 85.16%. The final concentrate assaying 64.74% Fe(T), 2.39 % SiO<sub>2</sub> and 1.82% Al<sub>2</sub>O<sub>3</sub> meets the desired blast furnace feed concentrate specifications. However, the concentrate obtained is found to have a top size of 48 mesh. Hence, the same was further grinded to –200 mesh to meet the size and Blaine number specifications of hybrid pellet sinter feed concentrate. Hence, the process of desliming in hydro-cyclone followed by two stage wet high intensity magnetic separation (WHIMS) is meeting the objective of desired highest recovery of 85.16% with an iron grade of 64.74 %.

### 5.2.5 Scheme - V (Floation)

A series of systematic floatation tests were conducted for obtaining best possible grade and recovery. In the present study, reverse floatation was used for beneficiation of slime. The grade and recovery obtained from slime samples of Bailadila mines using floatation cell as a function of pH are presented in **Fig. 5.7**. The analysis of the floatation test results indicate that the desired grade concentrate (> 64% Fe(T)) with highest recovery (around 74%) could be obtained at an optimum pH value of 7.5. The variation of silica and iron recovery with respect to the quantity of collector (DDA) used is shown in **Fig. 5.8**. The optimum quantity of collector is identified to be 60 g/ton to obtain concentrate with lowest silica content at 3.51%. It can also observed that 64.1% of the total iron present in the slime sample could be recovered under optimized condition (pH: 7.5 and collector dosage: 60 g/ton), which is

not meeting our objective of the present study. Hence, this technique cannot be used for commercial exploitation.

**Table 5.7** Results of second stage WHIMS test (at 2 amp.)

Products	Wt.%	Yield Wt.% w.r.t original	Assay %				Recovery %
			Fe(T)	SiO <sub>2</sub>	Al <sub>2</sub> O <sub>3</sub>		
Concentrate	50.10	14.77	64.82 61.09	2.93	1.87	15.78	1.51
Middling	5.10	1.50		7.18	3.06	1.98	
Tail	44.80	13.21	40.12	36.51	7.39	8.74	
Head (actual)	100.00	29.48	53.56	18.19	4.40	26.03	

**Table 5.8** Overall recovery and iron grade using combination of hydro-cyclone (15 mm apex dia. and 1.25 in. vortex finder at pulp density of 10% solid) and two stage high intensity magnetic separation.

Product	Yield	Fe(T), %	SiO <sub>2</sub>	Al <sub>2</sub> O <sub>3</sub>	% Fe recovery
Concentrate	79.79 %	64.74	2.39	1.82	85.16

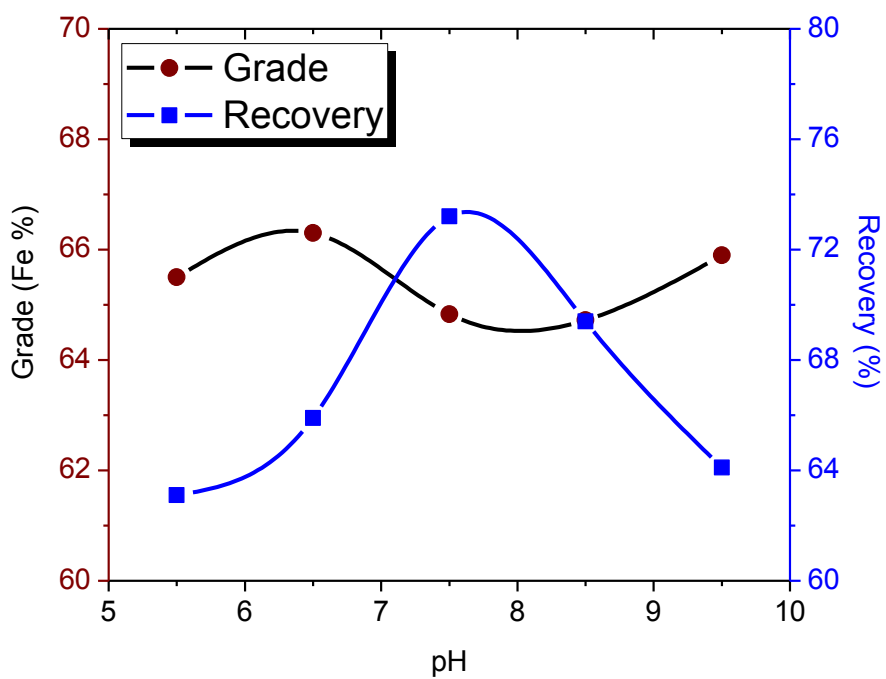


**Fig.5.7** Grade and recovery from Bailadila slime sample at different pH by using floatation test.

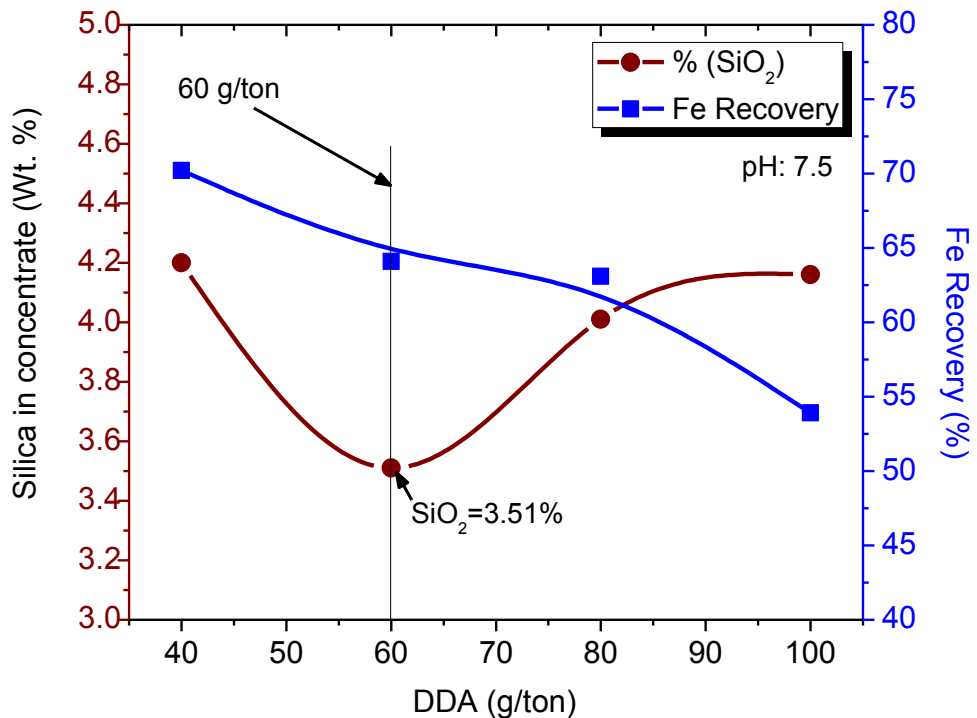


**Fig.5.8** Variation of silica and iron recovery with respect to the quantity of collector (DDA).

In summary, the laboratory scale beneficiation studies reveal that the concentrate assaying 64.74% Fe(T) with a recovery of 85.16% Fe value could be produced by following de-sliming using hydro-cyclone followed by two stage wet high intensity magnetic separation (WHIMS). The highest recovery of 85.16 % iron value has become possible by introducing second stage wet high intensity magnetic separator in the circuit. The addition of second stage wet high intensity magnetic separator in the beneficiation circuit may cause increase in capital investment. However, it helps in achieving the objective of high iron value coupled with highest recovery suitable to convert in to blast furnace feed. Therefore, the results of laboratory scale studies indicate that the iron ore slime from Bailadila is amenable for beneficiation with only loss of 14.84% Fe value in the reject.

### **5.3 Pilot scale beneficiation studies:**

#### **5.3.1 Validation of flow sheet at pilot scale facility (1 Ton/hr) and production of concentrate:**

In order to obtain the concentrate in bulk production, to meet the requirements of micro-pellet making and hybrid pellet sintering, a pilot scale facility of capacity 1 Ton/h involving de-sliming through hydro-cyclone followed by two stage wet high intensity magnetic separation (WHIMS) was set up for validation of the flow sheet developed in laboratory scale beneficiation. The process parameters like pulp density for de-sliming (hydro-cyclone), magnetic field intensity of WHIMS, pulp density of feed to the WHIMS etc. were maintained similar to those optimized at laboratory scale tests.

The raw data along with characterization test results obtained during the batch scale tests was used for setting up of pilot scale beneficiation circuit. 24" circular Vibro Screen was also placed with sizing screen cloth of 16 mesh after slurry preparation tank. The pulp density around 20% was maintained at slurry preparation tank. The overflow of the circular vibro screen is rejected and underflow is subjected to hydro-cyclone for de-sliming of ultra fines present in the slime sample. The overflow of the hydro-cyclone is collected for settling test. The settling test was conducted to generate data for designing a thickener. The underflow obtained was subjected for first stage (rougher) magnetic separator. The intensity of magnetic field was maintained at 14500 G as observed in laboratory scale. The concentrate and the middling of the rougher magnetic separator are taken as final

concentrate and the tailing was further processed for better recovery of iron value. The tailing of first stage magnetic separator was processed through second stage magnetic separator. The intensity of magnetic field of second stage magnetic separator was also maintained at 14500 G. Initially, the pilot scale test was started with the feed rate of 500 kg/h. The pilot plant was stabilized after operating at 500 kg/h feed rate for about 1 h. During stabilization of pilot plant, flow rate of water was adjusted to get desired pulp density and sampling devices are placed at various locations for collection of the sample. Test products (concentrate and rejects) were collected when the circuit was stabilized and the products were individually characterized for chemical assay and particle size distribution. Further, the pilot plant was operated for three hours for generation of concentrate for subsequent sintering studies.

The size analysis of the final concentrate produced at pilot plant is presented in Table 5.9. The concentrate contain only 48.47% of the particles below 325 mesh (45 micron). The surface area of the concentrate is found to be  $821\text{cm}^2/\text{g}$ , which is low. The SEM micrograph of the concentrate (Fig.5.9) shows near spherical particles due to prolonged weathering, which might be the reason for its low surface area (Blain number). However, the literature indicate that the surface area of the concentrate should be more than  $1500\text{ cm}^2/\text{g}$  (Zhu et al., 2008) for making of micro-pellets with sufficient strength. Hence, the concentrate is not suitable for micro-pellet making. Therefore, the concentrate needs to be grinded to meet surface area and size distribution requirement (normally 80% particles should be below 325 mesh) for micro-pellet making. Hence, the concentrate obtained is further subjected to ball mill grinding to achieve higher surface area. The surface area of the concentrate obtained after grinding is  $1610\text{ cm}^2/\text{g}$ .

The results of pilot scale beneficiation studies at various stages are presented in Fig.5.10. The data on iron grade, yield and recovery of the concentrate obtained from pilot scale beneficiation of slime is presented in Table 5.10. This study reveals an improvement in grade of the concentrate and the recovery of Fe value. Iron ore concentrate of 65.71 % Fe(T) with 87.31 % recovery was generated in pilot scale. About 1500 kg of concentrate was produced for subsequent utilization for micro-pellet making and hybrid pellet sintering.

**Table 5.9:** Size analysis of the concentrate obtained from pilot plant

S. No.	Size (Mesh)	Slime concentrate
		Weight %
1.	+100 #	15.36
2.	+150 #	7.16
3.	+200 #	12.25
4.	+270 #	8.09
5.	+325 #	8.67
6.	-325 #	48.47
	<b>Total</b>	<b>100.0</b>

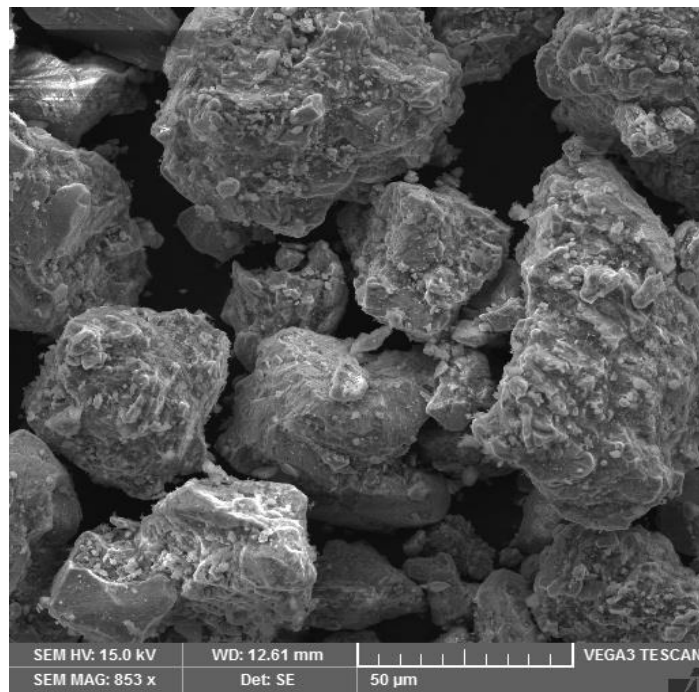


**Fig.5.9.** SEM photomicrograph of the concentrate obtained from pilot plant study, displays near spherical grains of concentrate.

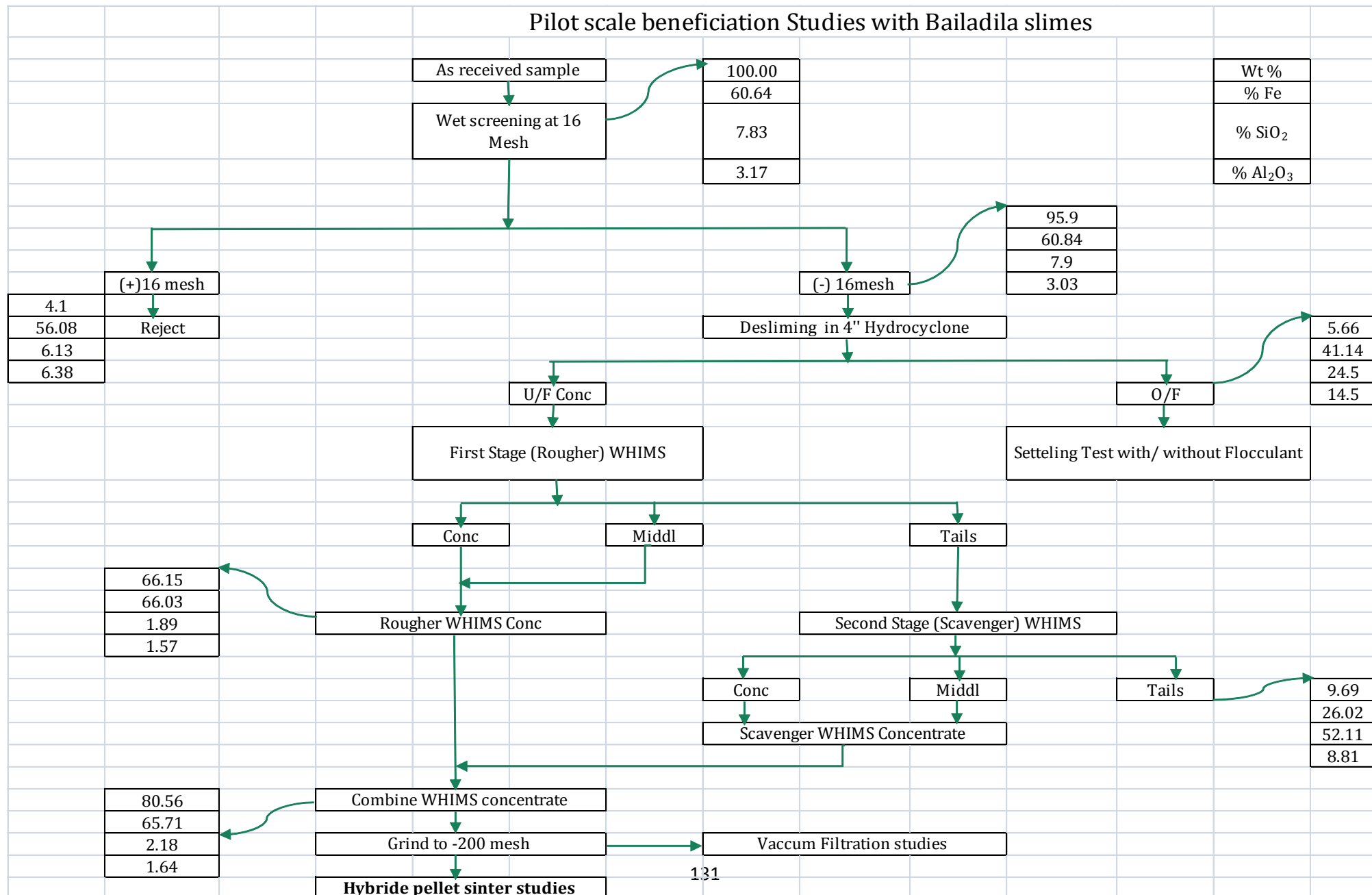


**Fig.5.10** Pilot Scale beneficiation studies with slime from Bailadila mines

**Table 5.10:** Grade, yield and recovery of pilot scale beneficiation studies

S. No.	Product	Yield, %	Fe(T), %	SiO <sub>2</sub> , %	Al <sub>2</sub> O <sub>3</sub> , %	Fe recovery, %
1	Concentrate	80.56	65.71	2.18	1.64	87.31

#### 5.4 Settling studies using hydro-cyclone overflow:

Settling tests were conducted using hydro-cyclone overflow in a 1000 ml jar with and without the addition of flocculant. The flocculant used was ULTRAFLOC 2222 (from M/s. Amog chemicals). About 0.05% flocculant solution was prepared by using water. All the settling tests were conducted at 10% solids by weight. The rate of fall of interface with respect to time was noted down to calculate the settling rates. The clarity of supernatant liquor is hazy in case of natural settling (without flocculant), whereas the same is found to be clear in the presence of flocculant. The suspended solids present in the overflow are not determined. However, they could be in the range of 80 to 150 ppm. The results of settling tests are presented in **Table 5.11** and **Fig.5.11**. The settling rate is increased with increasing the amount of flocculant. The settling test results indicate the requirement of flocculant for enhancing the settling rate and higher settling rate will result in minimum thickener area required for maximum recovery of water. The natural rate of settling of the sample (without flocculant) is observed to be extremely poor and is about 0.24 m/h, while the settling rate is increased about five folds with the addition of 13.78 g/ton, ten folds with the addition of 22.97 g/ton and fifteen folds with the addition of 32.15 g/ton of flocculent with respect to natural settling. Therefore, the addition of 32.15 g/ton of flocculant is recommended as thickener area is 0.64 sq. m/ton. Such a low thickener area will contribute in the reduction of capital cost.

**Table 5.11** Settling test results of hydro-cyclone overflow

S. No.	Volume of Cylinder, in ml	Height of cylinder, in cm	Dosage of 0.05% Flocculant solution, ml			
			0.0	3.0	5.0	7.0
			Number of inversions: 3			
			Time, in seconds			
1.	1000	28.7	0	0	0	0
2.	950	27.26	154	33	12	8
3.	900	25.83	345	70	27	18
4.	850	24.39	529	109	43	28
5.	800	22.96	734	136	60	39
6.	750	21.52	947	196	78	50
7.	700	20.09	1129	241	97	61
8.	650	18.65	1321	285	116	72
9.	600	17.22	1662	339	136	84
10.	550	14.78	1971	394	157	96
11.	500	14.35	2113	445	181	112
12.	450	12.91	2410	512	218	136
13.	400	11.48	3195	683	259	176
14.	380	10.90	3407	764	313	199
15.	360	10.33	3644	863	356	224
16.	340	9.75	3903	983	407	259
17.	320	9.18	4305	1144	474	303
18.	300	8.61	4752	1361	561	359
19.	280	8.03	--	--	691	446
20.	260	7.46	--	--	898	581
	Settling rate in m/h		0.24	1.11	2.44	3.94
	Underflow pulp density (UPD) (% Solid)		38	43	48	52
	Thickener area required (Sq. m/ton)		9.59	2.16	1.10	0.64
	Consumption of flocculant in g/ton		0.00	13.78	22.97	32.15

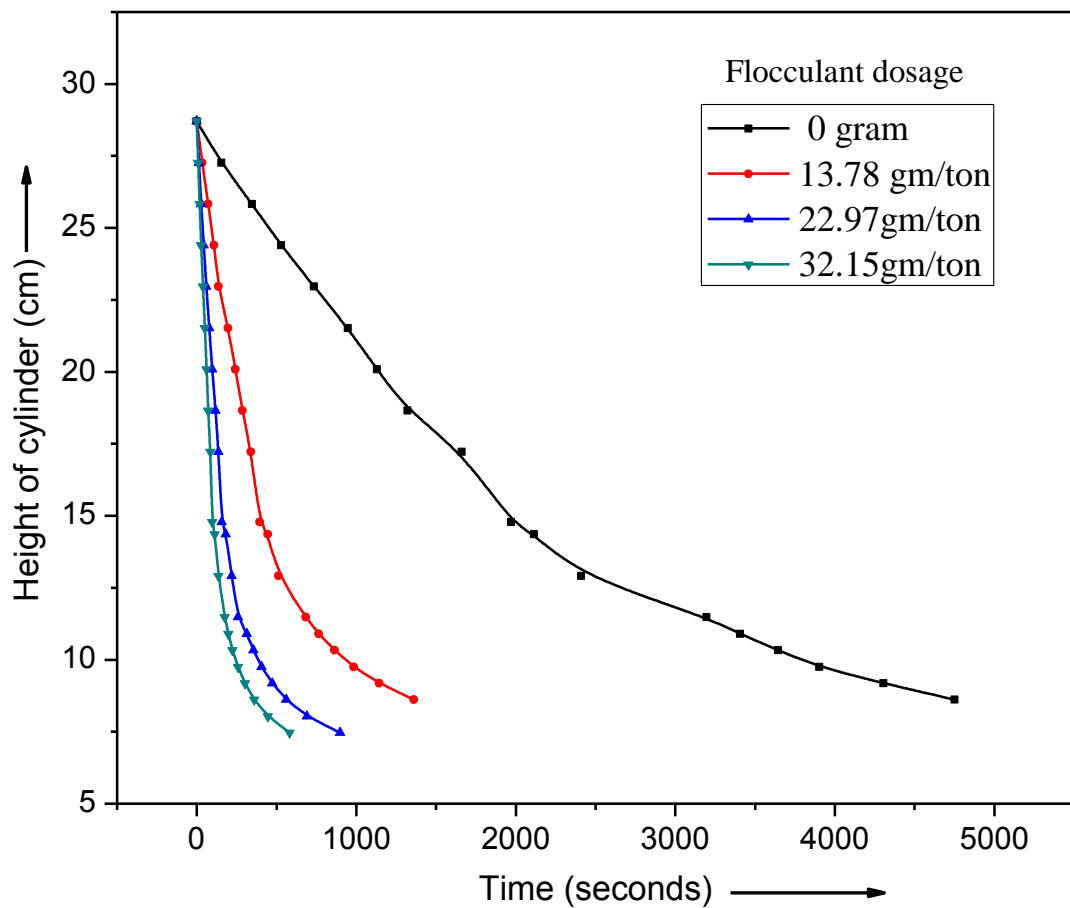


**Fig.5.11** Settling studies of hydro-cyclone overflow from pilot scale

## **5.5 Summary:**

At laboratory scale, all possible gravity, magnetic and flotation separation techniques and combination thereof are considered to obtain slime concentrate meeting the requirement of blast furnace feed with maximum possible recovery. The hydro-cyclone followed by two-stage magnetic separation is found to be encouraging. The yield obtained after blending the concentrate from first stage and second stage wet high intensity magnetic separation (WHIMS) operations is about 79.79% with an equivalent iron recovery of 85.16%. The final concentrate assaying 64.74% Fe(T), 2.39 % SiO<sub>2</sub> and 1.82% Al<sub>2</sub>O<sub>3</sub> meets the desired blast furnace feed concentrate specifications. Hence, the process of de-sliming in hydro-cyclone followed by two stage WHIMS is meeting the objective. The laboratory scale findings have been validated using pilot scale facility with capacity 1TPH. The pilot scale studies reveal further improvement in the grade of the concentrate and the recovery of Fe value. Iron ore concentrate of 65.71 % Fe(T) with 87.31 % recovery is generated in pilot scale test.

## Chapter 6

# MICRO-PELLET MAKING AND OPTIMIZATION OF GREEN PROPERTIES

### 6.1 Introduction:

The pilot plant concentrate obtained after beneficiation of slimes from Bailadila sector does not have a favorable particle size for making sinter that is suitable for blast furnace charging. The acceptable size of iron ore fines for sinter making is -10 mm, +100 mesh. However, the slime concentrate obtained is having particle size lower than 100 mesh. Hence, hybrid pellet sinter method was explored for production of sinter from slime concentrate. In hybrid pellet sintering, iron ore concentrate of relatively finer size is first converted into micro-pellets and these micro-pellets are used in place of iron ore fines for sinter making. The prerequisite for micro-pellets to be used in hybrid sintering is to have sufficient green strength so that they do not get disintegrated during mixing with other raw materials and during charging on to the sinter machine. The preparation of micro-pellets with sufficient strength containing iron ore fines and coal bearing material for use in iron making was reported in the literature (Pal et al., 2015). The primary factors influencing the formation of green micro balls and their properties are enumerated as electrostatic forces, Van der Waals forces, surface properties, magnetic forces and individual material characteristics (Forsmo et al., 2008; Rumpf, 1962; Sastry and Fuerstenau, 1972). During addition of water for micro-pellet making, the capillary forces also play a significant role in the formation of micro-pellets and thus providing strength to the green micro-pellets (Srivastava et al., 2013). The surface properties of slime concentrate in general can be represented by particle shape, particle size distribution and crystalline structure. Similarly, individual material characteristics can be represented by wettability, liquid absorptive capacity due to porous structure, etc.(Tigerschiöld and Ilmoni, 1950) .

During sintering, the intimately mixed iron bearing material with other raw materials is fed to the grate and the top layer of the bed is ignited by gas burner. The heat transfer through the

sinter bed depends upon the air resistance offered by the bed or ability to permeate air through the bed (**Poveromo, 2000**). The improvement in permeability and sinter quality was reported through addition of micro-pellets in the iron ore fines (**Panigrahy et al., 1984**). Thus, the permeability of the sinter bed is a very important parameter. A good permeability of the sinter bed is desirable to transfer heat from the top layer to the bottom layer in shorter time and to obtain better productivity of the sinter plant (**Poveromo, 2000**). The air flow through the packed sinter bed is also dependent on void fraction and mean particle diameter (**Gupta, 2015; Poveromo, 2000**).

In the present study, the slime concentrate was used for making micro-pellets of sufficient size and strength by using disc pelletizer. The requirement of surface area for producing an optimum quality of green micro-pellets with respect to size and strength is established. The effect of moisture content, binder content and specific surface area of slime concentrate on properties of green micro-pellets was studied. These micro-pellets were used as feed stock for preparation of sinter bed in a pot grate furnace. The effect of moisture content and size of micro-pellets on permeability of sinter bed were also studied. The impact of the addition of micro-pellets on mean granules size of sinter mix was also studied.

The pilot plant slime concentrate was subjected to screening using 45 and 90 micron size sieves. While 67.6% concentrate was passed through 45 microns size sieve, 96.8% concentrate was passed through 90 microns size sieve. A cyclosizer was used for analysis of fines (-45 microns). The results indicate that 18.5% of slime concentrates lies below 9.4 micron size. The specific surface area and specific gravity of the slime concentrate obtained from pilot scale studies were found to be  $1610 \text{ cm}^2/\text{g}$  and  $5.21 \text{ g/cm}^3$  respectively. Further grinding of the slime concentrate resulted in specific surface area (Blain Number) of the slime concentrate as  $1780 \text{ cm}^2/\text{g}$  and  $1930 \text{ cm}^2/\text{g}$  after dry grinding for 45 min and 60 min respectively. The ball mill details and the Blain numbers obtained at different durations of grinding operation are presented in **Table 6.1**.

**Table 6.1** Details of ball mill used for grinding and Blain numbers at different durations

Details of ball mill	Condition	Specific surface area/ Blain Number (cm <sup>2</sup> /g)
Length: 45 in. Diameter: 30 in. Speed of rotation: 12 rpm Ball size: 20 mm Ball weight: 100 kg	Initial slime concentrate	1610
	After dry grinding for 45 min	1780
	After dry grinding for 60 min	1930

## 6.2 Effect of moisture content on the properties of green micro-pellets

For studying the effect of moisture content on the properties of green pellets, the amount of binder was kept constant at 0.5% and the specific area of slime concentrate was fixed at 1610 cm<sup>2</sup>/g and moisture content was varied between 8.0 % and 9.5 %. The percentage of the pore volume that is occupied with the moisture (liquid) is termed as liquid saturation (S) and is expressed by

$$S = \frac{100F}{100 - F} \cdot \frac{1 - \varepsilon}{\varepsilon} \cdot \frac{\rho_p}{\rho_L} \quad (6.1)$$

where S = liquid saturation;  $\varepsilon$  = fractional porosity; F = moisture content determined through air oven drying;  $\rho_L, \rho_p$  = true density for water and particles.

The wet strength of the green micro-pellet will be maximum when the pores are entirely occupied with moisture. The capillary forces acts upon filled pores, which causes concave shaped exterior surfaces in the pore openings and responsible for binding of the particles. According to the capillary theory, at S (Liquid saturation) =100%, i.e. in the case of 100 % water saturation, the situation is called flooding. In this case, the micro-pellets deform either due to its own weight or weight of the load lying over it in the sinter pot. During further processing, the micro-pellet needs to be dried and while drying the primary binding force changes from capillary forces to the liquid bridge. Literature (**Sastray and Fuerstenau, 1972**) suggests that after a point of S = 30%, the liquid bridge become predominant than capillary forces. After that, the strength of the pellets is provided by liquid bridges. 35 % of the total strength of micro-pellets is contributed by fully developed liquid bridges (S = 30%).

In the present study, Equation (6.1) was used to calculate liquid saturation (S). The variation of liquid saturation with moisture content is shown in **Fig.6.1a**. Liquid saturation is increased with increasing moisture content. 100 % liquid saturation is achieved at around 8.75 % moisture content. It implies that the green micro-pellets can be obtained with 8.75% moisture content in 1 m diameter disc pelletizer. It is observed that once the moisture content crosses 8.75%, the pellet growth can be achieved by spraying additional water. The effect of moisture on green porosity of the micro-pellets is shown in **Fig.6.1b**. The porosity increases with moisture content. The variation of physical strength (i.e. cold crushing strength, CCS) with moisture content is shown

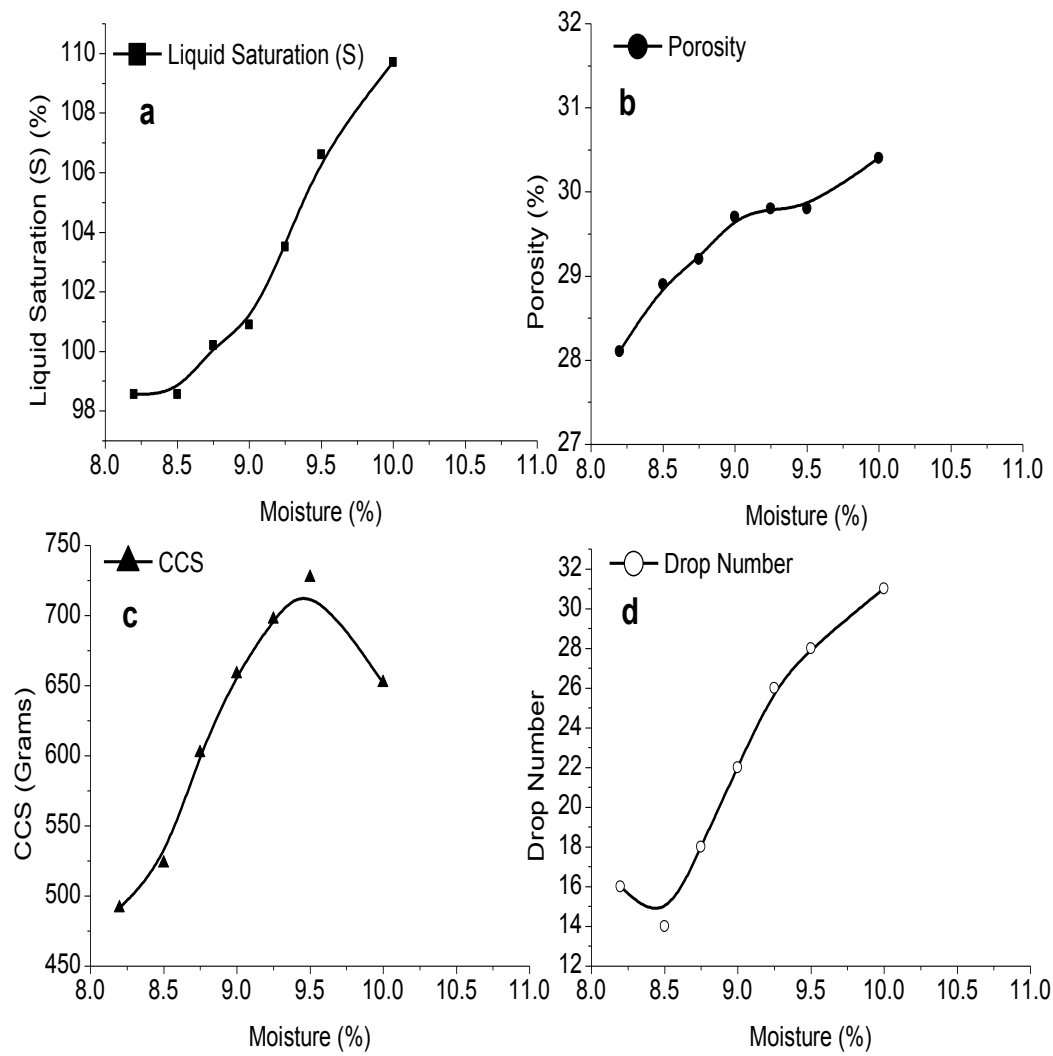


**Fig.6.1.** The variation of (a) liquid saturation, (b) porosity, (c) physical strength (CCS), and (d) drop number of micro-pellets with moisture content.

in **Fig.6.1c**. The CCS increases with increasing moisture content up to 9.5 % and thereafter decreased. The micro-pellets produced with moisture content below 8.75% are under-saturated and have lower physical strength (**Fig.6.1c**) with relatively good porosity values (**Fig.6.1b**). During green balling it was observed that once 100 % liquid saturation point is crossed, further balling process became self-controlled in such a way that the liquid saturation remains constant. Further addition of moisture has the direct impact on the porosity and physical strength . As explained before, the porosity and physical strength of pellet increase with moisture content till 9.5% and deteriorates thereafter. The variation of drop number with moisture content is shown in **Fig.6.1d**. The effect of moisture content in the micro-pellet can be seen as an increase in drop number. The drop number increases almost linearly with moisture content (8.5% to 9.5%) and the results were in line with earlier findings (**Pietsch, 1997**). With increase in moisture content in micro-pellet, the plasticity behavior sets and thus the drop number increases.

### 6.3. Effect of bentonite on the properties of green micro-pellets

In order to study the effect of bentonite on green properties of micro-pellets, the bentonite content in the feed mixture was varied between 0 % and 1.25% keeping specific surface area of the slime concentrate constant as  $1610 \text{ cm}^2/\text{g}$ . As the bentonite requires higher moisture, it is difficult to maintain constant moisture with the relatively wider range of bentonite. Keeping this in mind, studies on extra moisture requirement at higher bentonite content were carried out through some additional tests separately. Bentonite addition and its corresponding moisture requirement were determined in the pellet feed. Considering the moisture requirement of the binder (bentonite), initial moisture content was maintained at 9% in the green micro-pellet with 0 % bentonite and gradually increased to 9.5 % at 1.25 % bentonite. It is evident from the results that during balling extra water spraying was required, though pellet feed is containing higher moisture (up to 9.5%). In some cases, it is apparent that the moisture content as high as 9.8% is observed in the green micro-pellets. Each test with varying bentonite content was carried out at least twice and replicate batches of green micro-pellets were produced at each amount of binder. The average value of the properties of the green pellets of duplicate tests is reported in **Table 6.2** and shown pictorially in **Fig.6.2**. The mean value represent the repeatability and the level of confidence. From this data, it can be observed that both the drop number and cold crushing

**Table 6.2:** Drop number and strength of micro-pellets with varying bentonite for a specific surface area of iron ore concentrate at  $1610 \text{ cm}^2/\text{g}$ .

Particulars	Test 1	Test 2	Test 3	Test 4	Test 5	Test 6
Moisture content [%]	9.0	9.0	9.25	9.25	9.50	9.50
Bentonite content [%]	0	0.25	0.50	0.75	1.0	1.25
Drop Number [45 cm]	1.7	2.1	3.5	8.0	14.6	17.4
Crushing strength [Kg]	0.365	0.471	0.684	1.042	1.264	1.430

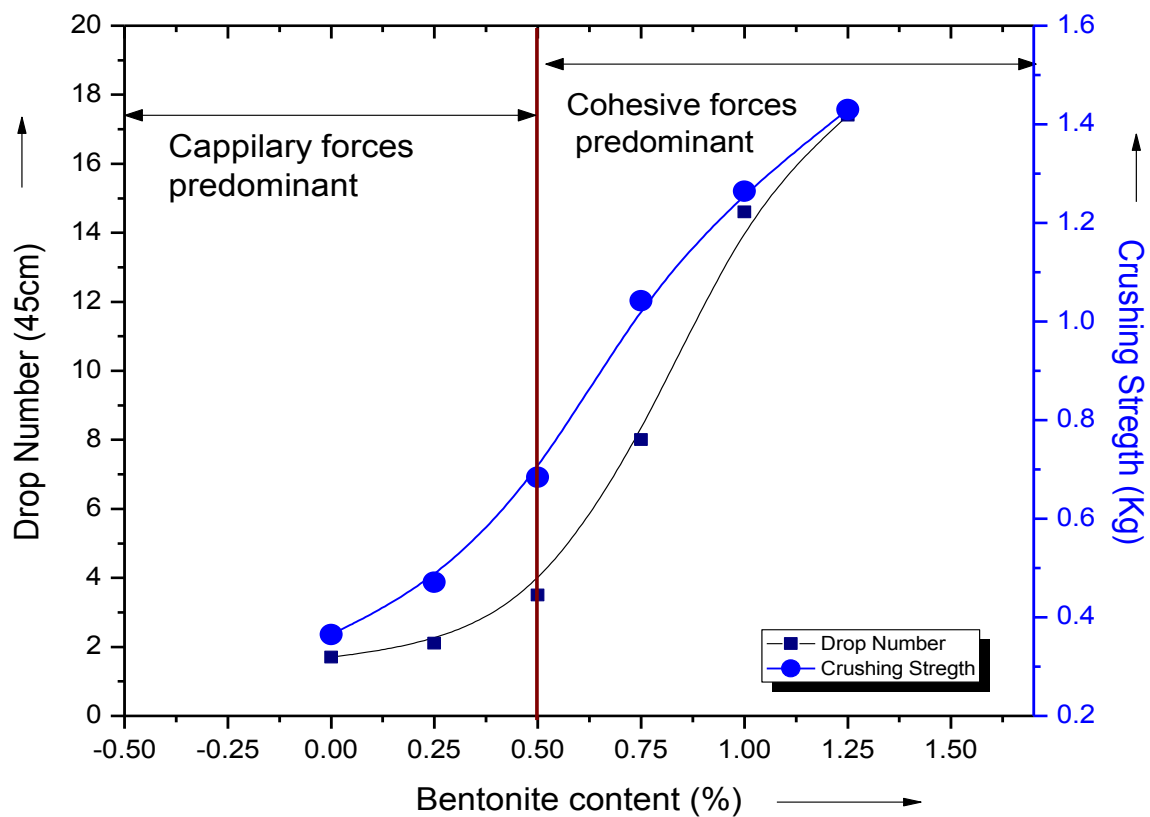


**Fig.6.2.** Variation of drop number and cold crushing strength with bentonite

strength (CCS) of micro-pellets is increasing with increasing bentonite content. The bentonite addition has positive impact on elastic deformation as shown in **Fig.6.2**. Green micro-pellets absorb kinetic energy due to formation of high viscous liquid phase at high shear rates. The elastic deformation of micro-pellet up to a certain extent is desirable to survive during mixing for hybrid sinter production in mixing drum. The CCS of micro-pellet can be demonstrated through drop number and minimum acceptable drop number (45 cm) is around 5 [**H. Rumpf (1962)**]. The drop number provide immediate indication of quality of micro-pellets produced hence drop number is used for controlling the parameter to get optimum quality of micro-pellets. Drop number is mainly dependent on quantity of bentonite and moisture added during pellet making. It is claimed that drop number is more important parameter than CCS due to its practical uses during micro-pellet making (**Hinkley et al., 1994**).

CCS largely depends upon binder (Bentonite) addition. However, moisture content also has impact on CCS (**Fig.6.1c**). The literature suggests that CCS increases with increase in binder (bentonite) addition (**Meyer, 1980**). The effect of binder (bentonite) addition on CCS can be classified into two segments. The cohesive force (viscous binder) and the capillary force (freely movable liquid) combination act as a main binding force. It is suggested in the literature that individual force contribution depends upon quantity of bentonite addition. At lower quantity of bentonite, the capillary forces are predominantly providing strength to the green micro-pellets. However, with increasing the quantity of bentonite the cohesive force (or viscous binder) becomes main binding force. From **Fig.6.2** and **Table 6.2**, it is evident that changeover from capillary forces to cohesive force takes place at around 0.5% bentonite. Further addition of binder has significant improvement in the drop number of the green pellets, which indicates the increase of elasticity of the green pellets. Therefore, at higher amount of bentonite the cohesive force (viscosity) become major binding forces and also set in high viscous behavior of the green pellets. The increase in adhesion of the particles also increases the CCS. The specific surface area, binder, and moisture requirement were interdependent. For higher binder content, moisture requirement is higher for green micro-pellet making.

## 6.4. Effect of specific surface area on the properties of green micro-pellets

In order to study the effect of specific surface area on the properties of green micro-pellets, the micro-pellets were prepared by using slime concentrate with three specific surface areas viz. 1610 cm<sup>2</sup>/g, 1780 cm<sup>2</sup>/g and 1930 cm<sup>2</sup>/g keeping constant bentonite (0.5 %) and moisture content (9.25 %). The properties of green micro-pellets have direct relation with specific surface area (Blain Number) and binder content. It is known that higher blain number will impart better green properties and higher bentonite (binder) content will improve overall properties of the green pellets (Pietsch, 1997). However, higher blain number leads to increased cost of grinding. Hence, it is important to use slime concentrate with optimum blain number for making green micro-pellets. The properties, such as drop number, crushing strength and porosity of the green micro-pellets obtained with concentrate of different blain numbers are listed in **Table 6.3** and also shown in **Fig.6.3**. The micro-pellets obtained with a blain number of 1610 cm<sup>2</sup>/g possess low drop number and crushing strength, thus they are not suitable. Whereas, although the micro-pellets obtained with a blain number of 1930 cm<sup>2</sup>/g possesses higher drop number and crushing strength, their porosity is low. Further, it also increases the grinding cost. The micro-pellets obtained with a blain number of 1780 cm<sup>2</sup>/g possess optimum values of drop number, crushing strength and porosity. Hence, from these results, it is evident that the micro-pellets with optimum properties can be produced with slime concentrate having a blain number of 1780 cm<sup>2</sup>/g at 0.50 % bentonite and 9.25 % moisture contents.

During the study, it is established that increasing the specific surface area resulted in better packing of particles which results in higher consolidation of the micro-pellet. In micro-pellet experiments, the time of formation of agglomerate was kept constant. The porosity of micro-pellets was highly influenced by specific surface area of slime concentrate and its pattern of consolidation although the binder was maintained constant. The specific surface area of the feed material and quantity of moisture added in micro-pellets were controlling factors of porosity of micro-pellets. The porosity of pellet was reduced from 30.3% to 25.8% with increase of specific surface area. This was indication of better consolidation of the particle at higher specific surface area. The improvement of drop number and CCS with increase of specific surface area is also an indication of better consolidation of particles during micro-balling. Porosity is considered as very important parameter and should be more than 28%.

**Table 6.3** Effect of specific surface area on drop number, crushing strength and porosity of micro-pellets with 0.50 % bentonite and 9.25 % moisture.

Property	Surface area or Blain number [cm <sup>2</sup> /g]		
	1610	1780	1930
Drop number [45 cm]	3.5	8.2	11.4
Crushing strength [kg]	0.684	1.164	1.367
Porosity (%)	30.3	28.6	25.8

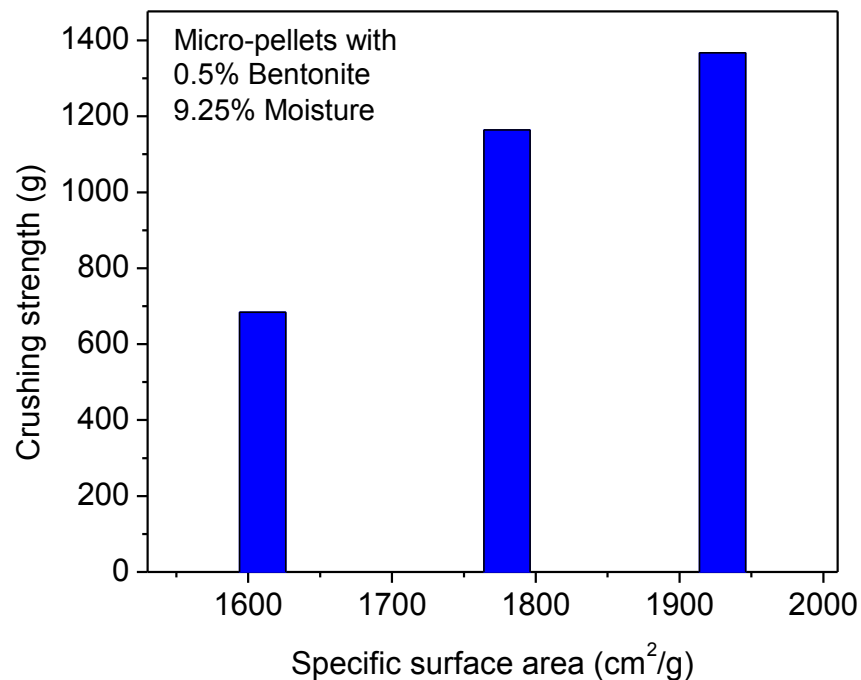


**Fig.6.3.** Crushing strength vs. specific surface area

The increase in specific surface area has direct impact on elastic strength of micro-pellets. Higher the drop number, higher the elastic strength. The drop number is increased significantly with surface area (**Table 6.3**). The elastic strength is utmost important for micro-pellets to withstand strain and stress during mixing in drum before hybrid pellet sintering. Higher crushing strength at higher specific surface area may be attributed to better consolidation during green balling stage.

## **6.5 Optimum conditions of green micro-pellets suitable for sinter making:**

The micro-pellets with higher specific surface area have exhibited better consolidation and as a result higher drop number and higher green crushing strength were achieved. The drop number has a direct correlation with elastic strength and should be sufficiently high to avoid fines generation during mixing of all raw materials for hybrid pellet sinter making. Similarly effect of addition of bentonite as binder on micro-pellets was established. It is evident from the results that the green properties of micro-pellets improve with addition of bentonite. However, micro-pellets with sufficient strength were produced at 0.5% bentonite content. The micro-pellets prepared from slime concentrate obtained after beneficiation of Bailadila (deposit-5) slimes has exhibited excellent physical properties at 0.5% bentonite content and 9.25 % moisture and surface area of  $1780 \text{ cm}^2/\text{gm}$ . Hence, this condition is considered optimum for micro-pellet production for hybrid pellet sinter making.

## **Chapter -7**

# **POT GRATE SINTERING STUDIES USING MICRO-PELLETS**

### **7.1 Introduction:**

Blast furnace cannot accept iron ore fines (slime concentrate) as feedstock. These fines need to be converted into lumps of +10mm size for charging into blast furnace. Sintering is a technique to convert ore fines into lumps by using heat. The sinter produced should be porous lump with sufficient strength to withstand transportation and handling stresses. Iron ore sinter is formed by incipient fusion of heat which binds iron ore fines together. Formation of slag bond and diffusion bond contribute strength to the sinter. All these bonds exist in sinter due to heat generated by combustion of coke particles. Sintering process is usually accomplished at 1300°C to 1400°C. In modern iron making sinter is preferred feed to the blast furnace. Almost all integrated steel plants in India has sinter plants. In this work, attempts were made to produce sinter from micro-pellets using hybrid pellet sintering in pot grate sintering furnace. Thus the developed process of sinter making from slimes will alleviate slime problems at mines site.

### **7.2 Sintering studies in pot grate furnace:**

In Chapter 6, it was concluded that the micro-pellets with optimum properties can be obtained with a blain number of 1780 cm<sup>2</sup>/g with 0.50% bentonite and 9.25% moisture content. Accordingly, micro-pellets of different sizes of 1-3 mm, 3-6 mm and 6-10 mm were produced and used as charge material for sintering studies. Hybrid pellet sinters with varying amounts of ignition time, moisture, coke breeze and bed height were prepared using all sizes of micro-pellets as charge materials. The effect of ignition time, moisture, coke breeze and bed height on sinter properties (tumbler index and bulk density), sinter bed properties (permeability and vertical sintering speed) and on coke rate, yield and productivity of the sintering process were studied for all sinters prepared from micro-pellets of different sizes.

The hybrid pellet sintering experiments were designed with the help of statistical technique called fractional factorial design of experiments. In this technique, four parameters (B, C, D, &

E) were varied with respect to micro-pellet size (A) at four predetermined levels and the total number of experiments conducted was 48. The variation of levels of different factors is shown in **Table 7.1**. Some experiments were repeated in order to confirm reliability and repeatability of results. The basicity of the sinter and suction pressure were fixed initially at 1.6 and 1100 mm of water level respectively throughout the study. 0.5 % lime was mixed uniformly to all the batches of sinter.

### **7.2.1 Effect of micro-pellet size and ignition time on various properties:**

Hybrid pellet sinters were produced by using all three sizes of micro-pellets with varying ignition times. During sinter making, the moisture content, amount of coke breeze and sinter bed height were fixed at 6.5%, 5.5% and 300 mm respectively whereas ignition time varied as 60, 90, 120 and 150 s. The top layer of sinter was fired uniformly to get good quality of sinter (**Loo et al., 2012**). The ignition time for firing of top layer of sinter mix has significant impact on sinter properties, sinter bed properties, yield and productivity. The physical properties, yield and productivity of the hybrid pellet sinter with respect to micro-pellet size and ignition time are presented in **Table 7.2**. The variation of tumbler index, permeability, yield and productivity with respect to ignition time for different micro-pellet sizes is presented in **Figs.7.1a-d**.

For all the sinters produced from different sizes of micro-pellets, the tumbler index of the sinter (**Fig.7.1a**), permeability of the sinter bed (**Fig.7.1b**), productivity (**Fig.7.1c**) and yield of +6.3 mm sinter (**Fig.7.1d**) increases with increasing the ignition time, reaches maximum at about 120 s, beyond which they decreases. As evidenced from **Fig.7.1a**, the tumbler index of the sinter increases with increasing ignition time. This signifies uniform combustion of coke breeze at the top layer. The highest tumbler index of 68.92% is obtained at 120 s ignition time with micro-pellets of size 3-6mm. Similar trend can also be seen in respect of sinter bed permeability (**Fig.7.1b**) and the highest sinter bed permeability of 23.07 JPU is observed at 120 s ignition time with micro-pellets of size 3-6mm. Flame front movement (as indicated by vertical sintering speed, VSS) during sintering is also recorded and presented in **Table 7.2**. The high value of VSS (18.11 mm/min) at 120 s ignition time signifies fast ignition rate, thus resulting in high permeability of the sinter bed.

**Table 7.1:** Factor and their levels of variation

S. No.	Micro- pellet size (mm)	L E V E L	Factors			
			Ignition time (s)	Moisture (%)	Coke breeze (%)	Bed height (mm) (excluding hearth layer)
A	B	C	D	E		
1	1-3, 3-6, 6-10	1	Varied (60, 90, 120, 150)	6.5	5.5	300
		2	120	Varied (5.5, 6.0, 6.5, 7.0)	5.5	300
		3	120	6.5	Varied (4.5, 5.0, 5.5, 6.0)	300
		4	120	6.5	5.5	Varied (300, 350, 400, 450)

**Table 7.2: Physical characteristics of hybrid pellet sinter produced with varying ignition times**

(Moisture content: 6.5%, Coke breeze: 5.5% and sinter bed height: 300 mm)

S. No.	Micro-pellet size (mm)	Ignition Time (s)	Sinter Properties		Sinter bed properties		Sintering process properties			
			Tumbler Index (%)	Bulk Density (t/m <sup>3</sup> )	Green permeability (JPU)	V.S.S (mm/min)	Coke rate (kg/T)	Productivity (+6.3mm) (t/m <sup>2</sup> /h)	Yield of +6.3mm (%)	Return Sinter (%)
1	1-3	60	64.09	1.879	19.81	15.17	77.2	1.1091	71.22	28.78
		90	66.12	2.038	19.98	16.03	76.1	1.1780	72.31	27.69
		120	67.05	2.100	20.52	16.11	75.7	1.2101	72.60	27.40
		150	66.82	1.994	19.56	16.12	75.8	1.2009	72.52	27.48
2	3-6	60	66.95	1.992	22.79	17.92	80.4	1.2309	68.42	31.58
		90	67.99	1.968	22.87	18.03	78.7	1.2533	69.91	30.09
		120	68.92	2.001	23.09	18.11	77.8	1.2927	70.73	29.27
		150	67.82	1.902	23.01	17.64	78.4	1.2701	70.10	29.90
3	6-10	60	65.11	2.091	21.78	16.76	78.4	1.1899	70.16	29.84
		90	66.73	1.966	22.07	17.62	77.5	1.1908	70.87	29.13
		120	66.92	1.983	22.35	17.66	77.6	1.1969	70.99	29.01
		150	65.85	2.084	22.09	17.29	78.2	1.1991	70.32	29.68

V.S.S: Vertical sintering speed

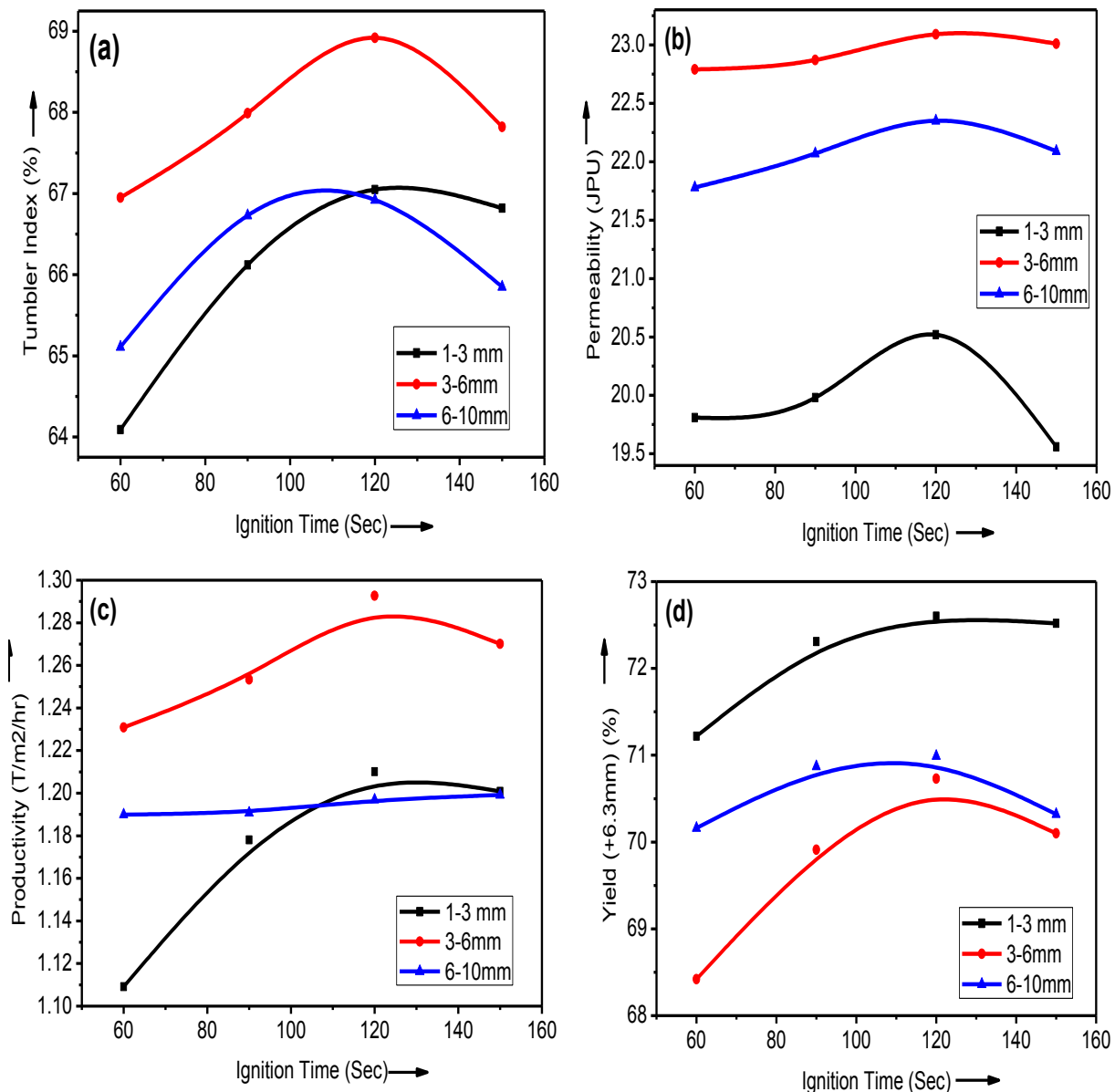


**Fig.7.1:** Effect of ignition time on various properties of sinter prepared from different sizes of micro-pellets. (a) Tumbler index, (b) Permeability, (c) Productivity and (d) Yield (+6.3mm).

The highest productivity of 1.2927 t/m<sup>2</sup>/h is achieved with micro-pellets of size 3-6mm at ignition time of 120 s as shown in **Fig.7.1c**. The yield of +6.3 mm follows inverse trend with respect to productivity, i.e. higher the productivity the lower the yield. However, the yield of +6.3mm sinter should be > 70% for acceptance. The coke rate should be minimum for the success of sintering process. The coke rate decreases with increasing ignition time as shown in **Table 7.2** and reaches minimum at 120 s of ignition time. The percent return sinter decreases with increase in ignition time for all the sizes of micro pellets, and reaches minimum at 120 s. Beyond 120 s, there is marginal increase in percent return sinter. As per industrial accepted norms (**Lu, 2015**), the return sinter should be less than 30%. About 29.27 % return sinter is generated in case of the sinter produced from micro-pellets of size 3-6mm and keeping ignition time 120 s. Hence, 120 s ignition time with micro-pellets of size 3-6mm can be considered optimum with respect to return sinter generation. Based on the above results obtained on the effect of ignition time, it can be concluded that the combination of high tumbler index, high bulk density, high permeability together with low coke rate, low return sinter and high productivity is observed in the sinter prepared from the micro pellets of 3-6mm size with 120 s ignition time. These conditions (*3-6 mm size micro-pellets and 120 s ignition time*) results in the optimum sinter properties, sinter bed properties and sintering process properties.

### **7.2.2 Effect of micro-pellet size and moisture on various properties:**

Moisture in the sinter mix is very important parameter and has significant impact on the permeability of the sinter bed. Optimum moisture content needs to be maintained, as higher moisture may cause flooding and filling of the pores apart from requirement of higher energy for its removal. Similarly, low moisture may cause lower permeability of sinter bed and thus promote non-uniform suction of air through the bed leaving behind some pockets of unfired sinter. Hybrid pellet sinters were produced by using all three sizes of micro-pellets with varying moisture content. During sinter making, the ignition time, coke breeze and bed height were fixed at 120 s, 5.5% and 300 mm respectively whereas moisture content was varied as 5.5%, 6.0%, 6.5% and 7.0%. A suction pressure 1100 mm of water level was also maintained throughout the study. The physical properties of the sinter, the productivity, and the yield of the hybrid pellet sinter process with respect to micro-pellet size and moisture content are presented

in **Table 7.3**. The variation of tumbler index, permeability, productivity and yield with respect to moisture content for different micro-pellet sizes is presented in **Figs.7.2a-d**.

**Figure 7.2a** shows the variation of tumbler index with moisture content (**Fig.7.2a**) for the sinters prepared from different sizes of micro-pellets. At low moisture levels, the tumbler index is increasing with increasing the size of micro-pellets. This is because of increased permeability in the sinter bed (**Fig.7.2c**), which causes an effective firing of the bed and result in high tumbler index. However, while the tumbler index of the sinter is improved with increase in moisture content for hybrid pellet sinters produced from micro-pellets of sizes 1-3mm and 3-6mm; it is gradually declined with moisture content for the sinter prepared from micro-pellets of size 6-10mm. As per the literature (**Nyembwe et al., 2017**), the finer micro-pellet provides higher surface area and thus result in higher grain growth during sinter preparation (firing) in conjunction with higher moisture level, thereby leading to higher tumbler index. The highest tumbler index of 69.37% is obtained for the sinter prepared from micro-pellets of size 3-6mm with 6.5% moisture content. Higher bulk density of  $2.106 \text{ t/m}^3$  is observed at 6.5% moisture for the sinter prepared from micro-pellets of size 3-6mm (**Table 7.3**).

**Figure 7.2b** shows the influence of moisture content on permeability of the sinter bed. The trend of permeability curves with respect to moisture content is similar to that of tumbler index observed in **Fig.7.2a**. While the permeability of the sinter bed increases with increase in moisture content up to 6.5% for the sinter prepared from micro-pellets of sizes 1-3mm and 3-6mm, it shows gradual decrease for the sinter produced from micro-pellets of size 6-10mm. Although the sinter prepared from micro-pellets of 6-10mm exhibit higher permeability at low moisture levels (5.5% & 6.0%), further increase in moisture causes filling of the void spaces with moisture and resulted in lower permeability beyond 6.0% moisture. Alternately, the bigger voids in the sinter mix prepared from micro-pellets of size 6-10mm may have been filled by fine particles of fluxes and coke as well as moisture thus resulting in decrease in permeability. The low permeability resulted in low productivity (**Fig 7.2c**). The highest permeability of 23.09 JPU is observed in the sinter bed prepared from micro-pellets of 3-6mm at 6.5% moisture. Beyond 6.5% moisture, the permeability of the bed decreases due to

**Table 7.3: Physical characteristics of hybrid pellet sinter produced with varying moisture contents.**

(Ignition time: 120 s, coke breeze: 5.5% and bed height: 300 mm)

S. No.	Micro-pellet size (mm)	Moisture in the sinter mix (%)	Sinter Properties		Sinter bed properties		Sintering process properties			
			Tumbler Index (%)	Bulk Density (t/m <sup>3</sup> )	Green permeability (JPU)	V.S.S (mm/min)	Coke rate (kg/T)	Productivity (+6.3mm) (t/m <sup>2</sup> /h)	Yield of +6.3mm (%)	Return Sinter (%)
1	1-3	5.5	63.97	2.080	17.11	15.26	78.4	1.0997	70.18	29.82
		6.0	65.12	2.073	17.94	15.61	76.6	1.1623	71.83	28.17
		6.5	66.82	2.100	19.98	16.11	75.7	1.2001	72.60	27.40
		7.0	66.43	1.994	19.47	16.32	75.1	1.1949	73.19	26.81
2	3-6	5.5	66.89	1.952	20.94	16.93	79.3	1.2311	69.32	30.68
		6.0	67.71	1.902	21.86	17.67	78.4	1.2618	70.59	29.41
		6.5	69.37	2.106	23.09	18.11	77.8	1.2927	70.73	29.27
		7.0	68.92	1.994	22.76	18.03	79.4	1.2891	69.29	30.71
3	6-10	5.5	68.70	2.070	22.08	18.24	77.2	1.2406	71.60	28.79
		6.0	68.01	2.019	22.47	18.08	76.8	1.2319	71.21	28.40
		6.5	66.92	1.983	22.35	17.66	77.6	1.1969	70.91	29.13
		7.0	66.32	1.904	21.62	17.12	77.6	1.1962	70.87	29.09

V.S.S – Vertical sintering speed

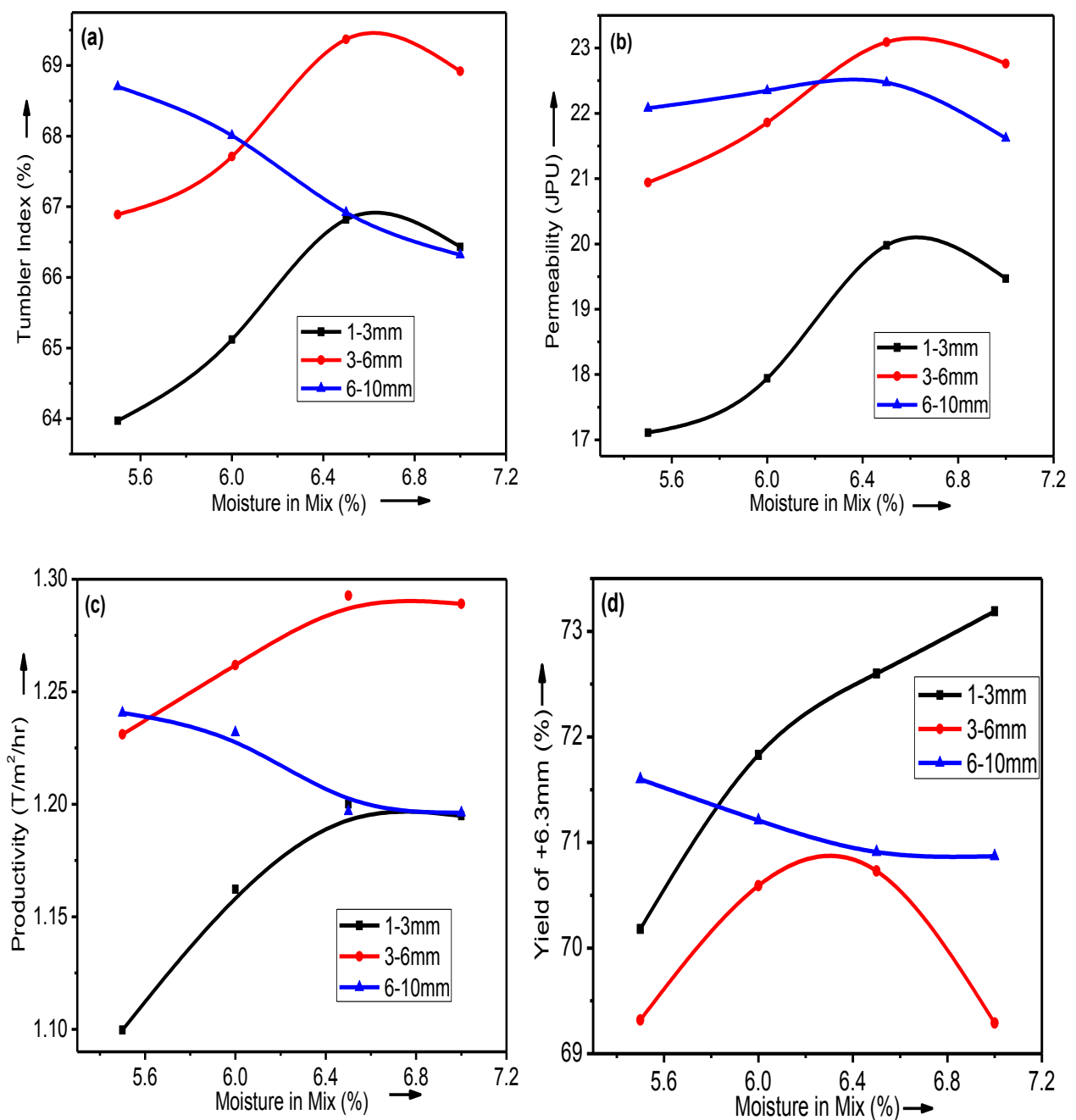


**Fig.7.2** Effect of moisture content on various properties of sinter prepared from different sizes of micro-pellets. (a) Tumbler index, (b) Permeability, (c) Productivity and (d) Yield (+6.3mm).

flooding of the pores with moisture. Flame front movement (as indicated by vertical sintering speed, VSS) during sintering is also recorded and presented in **Table 7.3**. The high value of VSS (18.11 mm/min) at 6.5% moisture content signifies fast ignition rate, thus resulting in high permeability of the sinter bed.

While the productivity of the sinter increases with increase in moisture content for micro-pellets of sizes 1-3mm and 3-6mm, it decreases for the sinter produced from micro-pellets of size 6-10mm (**Fig 7.2c**). The bigger void sizes in the sinter mix prepared from micro-pellets of size 6-10mm may have been filled by fine particles of fluxes and coke, thus resulting in decrease of productivity. Besides, the high moisture in the sinter mix prepared from micro-pellets of size 6-10mm may add in consolidation of finer particles in the voids. As a result, lower productivity is observed. The highest productivity of  $1.2927 \text{ t/m}^2/\text{h}$  is observed with micro-pellets of size 3-6mm at a moisture level of 6.5%. Beyond 6.5% moisture, the productivity decreases. This is because of the lower permeability and lower vertical sintering speed.

The variation in the yield of the sinter obtained (represented by percent +6.3 mm size sinter) as a function of moisture content is presented in **Fig.7.2d**. The yield of +6.3 mm follows inverse trend with respect to productivity, i.e. higher the productivity the lower the yield. However, the yield of +6.3mm sinter should be  $> 70\%$  for acceptance. In case of the sinter produced from micro-pellets of size 1-3mm, the yield is observed to be increased with increasing the moisture content. Higher amount of fusion bond in the hybrid sinter made of micro-pellets of size 1-3mm may contribute to acceptable physical properties (tumbler index) and as a result higher yield of sinter of size +6.3 mm is observed (**Table 7.3**). However, it results in lower permeability and productivity. In case of sinter prepared from micro-pellets of size 6-10 mm, the yield is decreasing with increasing moisture content. In this case, though the yield is higher than 70%, the other properties are comparatively lower than the sinter produced from 3-6mm size micro-pellets. In case of sinter produced from micro-pellets of size 3-6mm, the yield increases with increasing the moisture content, reaches maximum ( $>70\%$ ) at 6.5% moisture and drops with further moisture content. At 6.5% moisture content, the other properties such as tumbler index, permeability and productivity are higher for the sinter produced from 3-6mm micro-pellets.

The coke rate should be minimum for the success of sintering process. The coke rate more or less decreases or remains constant with increasing moisture content as shown in **Table 7.3**. The percent return sinter decreases with increase in moisture content for all the sizes of micro pellets, with few exceptions. As per industrial accepted norms (**Lu, 2015**), the return sinter should be less than 30%. In the present study, almost in all cases the return sinter generated is less than 30%. About 29.27 % return sinter is generated in case of the sinter produced from micro-pellets of size 3-6mm by keeping moisture level at 6.5%.

### **7.2.3 Effect of micro-pellet size and coke content on various properties:**

The coke content in the sinter mix has direct impact on sinter properties, sinter bed properties, yield and productivity and on overall economy of production of iron. Optimization of coke content is essential to get desired quality of sinter with minimum dosages of coke. In the present study, hybrid pellet sinters were produced by using all three sizes of micro-pellets with varying coke contents. During sinter making, the ignition time, moisture content and bed height are fixed as constant at 120 s, 6.5% and 300 mm respectively and coke content is varied as 4.5%, 5.0%, 5.5% and 6.0%. A suction pressure 1100 mm of water level was also maintained throughout the study. The physical properties, yield and productivity of the hybrid pellet sinter with respect to micro-pellet size and coke content are presented in **Table 7.4**. The variation of tumbler index, permeability, yield and productivity with respect to coke content for different micro-pellet sizes is presented in **Figs.7.3a-d**.

For all the sinters produced from different sizes of micro-pellets with varying coke content, the tumbler index of the sinter (**Fig.7.3a**), permeability of the sinter bed (**Fig.7.3b**), productivity (**Fig.7.3c**) and yield of +6.3 mm sinter (**Fig.7.3d**) increases with increasing the coke content. As

**Table 7.4: Physical characteristics of hybrid pellet sinter produced with varying coke content**  
 (Ignition time: 120 s, Moisture content: 6.5% and Bed height: 300 mm)

S. No.	Micro-pellet size (mm)	Coke in sinter mix (%)	Sinter properties		Sinter bed properties		Sintering process properties			
			Tumbler Index (%)	Bulk Density (t/m <sup>3</sup> )	Green permeability (JPU)	V.S.S (mm/min)	Coke rate (kg/T)	Productivity (+6.3mm) (t/m <sup>2</sup> /h)	Yield of +6.3mm (%)	Return Sinter (%)
1	1-3	4.5	55.69	1.893	17.02	16.32	77.0	1.0572	58.42	41.58
		5.0	62.37	2.079	17.61	16.03	77.4	1.1499	64.61	35.39
		5.5	66.82	2.100	19.98	16.11	75.7	1.2001	72.60	27.40
		6.0	69.89	2.143	20.41	17.26	86.3	1.2190	75.32	24.68
2	3-6	4.5	58.81	1.997	21.03	17.04	72.4	1.1425	62.11	37.89
		5.0	64.33	1.809	22.63	17.91	76.5	1.1922	65.32	34.68
		5.5	69.92	1.902	23.09	18.11	77.8	1.2927	70.73	29.27
		6.0	73.18	2.109	24.12	18.82	87.9	1.3182	73.96	26.04
3	6-10	4.5	54.78	1.911	21.09	17.81	75.2	0.8902	59.84	40.16
		5.0	62.31	2.173	21.31	17.06	77.9	1.1421	64.21	35.79
		5.5	66.92	1.983	22.35	17.66	77.6	1.1969	70.87	29.13
		6.0	71.77	2.101	22.73	17.93	85.7	1.2511	75.83	24.17

V.S.S – Vertical sintering speed

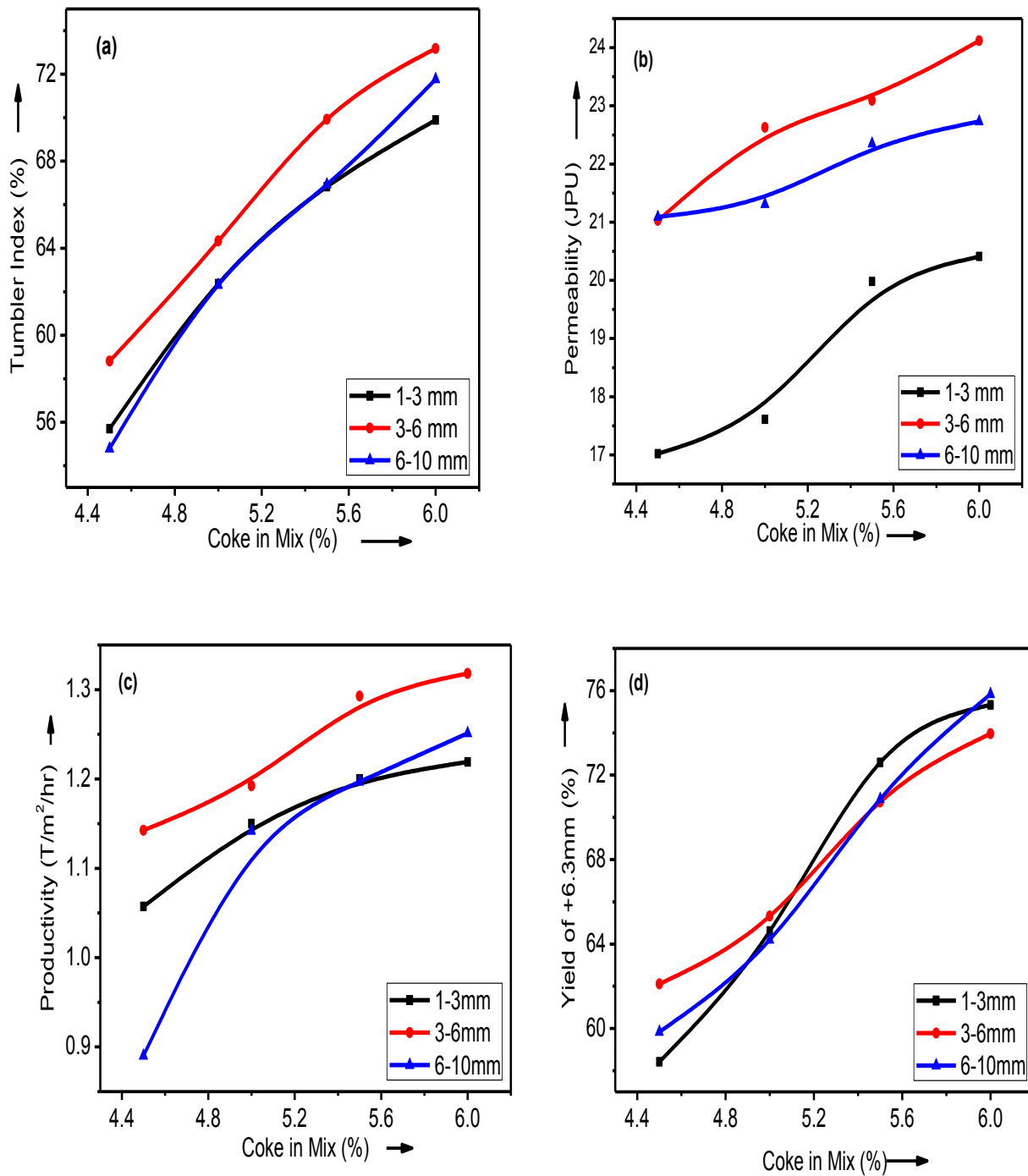


**Fig.7.3:** Effect of coke content on various properties of sinter prepared from different sizes of micro-pellets. (a) Tumbler index, (b) Permeability, (c) Productivity and (d) Yield (+6.3mm).

evidenced from **Fig.7.3a**, the tumbler index of the sinter increases with increasing coke content for all three sizes of micro pellets. However, the sinter prepared from micro-pellets of size 3-6 mm recorded higher tumbler index than that prepared from micro-pellets of sizes 1-3 mm and 6-10 mm. Higher content of coke increases the incipient fusion of fine particles and as a result higher tumbler index is recorded. Highest tumbler index of 73.18% is obtained at 6% coke with micro-pellets of size 3-6mm. However, as per industrial accepted norms (**Lu, 2015**)  $\approx 70\%$  tumbler index would be sufficient for blast furnace feedstock and which is achievable at 5.5% coke with micro-pellets of size 3-6mm with acceptably reasonable low coke rate (77.8 kg/T) and good bulk density (1.902 t/m<sup>3</sup>) (**Table 7.4**). Whereas, for the sinter produced from micro-pellets of sizes 1-3mm and 6-10 mm, minimum 6% coke is required to get  $\approx 70\%$  (or more) tumbler index, which result in high coke rate (87.9 kg/T), almost 10kg/T, which is substantially huge amount.

The sinter bed permeability (**Fig.7.3b**) increases with increasing the micro-pellets size from 1-3mm to 3-6mm and decreased with micro-pellets of size 6-10. Also, the permeability of the bed is increasing with increasing coke content for all sizes of micro-pellets. However, the bed prepared from 6-10mm micro-pellets resulted in lower permeability compared with that prepared from 3-6mm micro-pellets. The decrease in permeability of the bed containing 6-10mm micro-pellets can be attributed to filling of voids by finer size of coke (-3 mm). It should be noted that higher the permeability, the lower the coke rate. Under the present experimental conditions, a higher bed permeability of 24.12 JPU is observed with 6% coke in the bed prepared from micro-pellets of size 3-6mm. This yields a coke rate of 87.9 kg/T, which is higher by 10 kg/T that is achievable with 5.5% coke in the bed prepared from same size of micro-pellets with next highest permeability of 23.09 JPU. Therefore, keeping all the above points in mind, it can be concluded that optimum bed permeability can be obtained with micro-pellets of size 3-6 mm with 5.5% coke.

The productivity of the hybrid pellet sinter increases with increase in coke addition for all the sizes of micro-pellets (**Fig.7.3c**). However, the highest productivity is observed with the sinter prepared from micro-pellets of size 3-6mm for all coke additions. The flame front movement

(indicated by vertical sintering speed, VSS, see **Table 7.4**) is highest with a value of 18.82 mm/min for the sinter prepared from micro-pellets of size 3-6mm at 6% coke addition and the corresponding productivity is found to be 1.3182 T/m<sup>2</sup>/h (**Table 7.4**). The sintering process is completed in short duration owing to higher vertical sintering speed (VSS) for the hybrid pellet sinter produced from micro-pellets of size 3-6mm. The high VSS translate in higher productivity and hence better yield of +6.3mm (**Table 7.4**). However, once again, if we look at the coke rate, it is very high (87.9 kg/T) compared with the sinter produced from micro-pellets of same size 3-6 mm with 5.5% coke. In addition, the sinter with 5.5% coke prepared from micro-pellets of size 3-6 mm satisfies the minimum requirement of 70% yield with a productivity of 1.2927 t/m<sup>2</sup>/h. Therefore, keeping all the above points in mind, it can be concluded that optimum productivity and yield can be obtained with micro-pellets of size 3-6 mm with 5.5% coke.

As per industrial accepted norms (**Lu, 2015**), the return sinter should be less than 30%. About 29.27% and 26.04% return sinter is generated in case of the sinter produced from micro-pellets of size 3-6mm with 5.5% and 6.0% coke content respectively. Minimum coke requirement for producing sinter with sufficient strength (tumbler index) and recovery is considered as optimum. Hence, coke content of 5.5% and 6.0% for all three sizes of micro-pellets can be considered optimum with respect to return sinter generation. However, addition of 6.0% coke leading to higher coke rate. Based on the above results obtained on the effect of coke rate, it can be concluded that the combination of high tumbler index, high bulk density, high permeability together with low coke rate, low return sinter and high productivity is observed in the sinter prepared from the micro pellets of 3-6mm size with 5.5% coke content. These conditions (*3-6 mm size micro-pellets and 5.5% coke content*) results in the optimum sinter properties, sinter bed properties and sintering process properties.

#### **7.2.4 Effect of micro-pellet size and bed height on various properties:**

Higher bed height results in higher productivity but with lower physical and metallurgical properties of the sinter. Hence, optimum bed height of sinter mix over hearth layer should be maintained to get higher productivity and quality of sinter. Hybrid pellet sinters were produced

by using all three sizes of micro-pellets with varying sinter bed height. During sinter making, ignition time, moisture content, and the amount of coke were fixed as 120 s, 6.5% and 5.5% respectively, whereas sinter bed height varied as 300, 350, 400 and 450mm. A suction pressure 1100 mm of water level was also maintained throughout the study. Bed height in conjunction with suction pressure helps to achieve higher productivity in commercial sinter plant. The physical properties, yield and productivity of the hybrid pellet sinter with respect to micro-pellet size and sinter bed height are presented in **Table 7.5**. The variation of tumbler index, permeability, yield and productivity with respect to sinter bed height for different micro-pellet sizes is presented in **Figs.7.4a-d**.

The bed height of the sinter is found to have significant effect on physical properties (tumbler index and bulk density) of the sinters prepared from micro-pellets of all sizes (**Fig.7.4a**). There is an initial increase in tumbler index of the sinter followed by gradual drop with increasing bed height for sinters produced from all three different sizes of micro-pellets as shown in **Fig.7.4a**. However, the sinter produced from micro-pellets of size 1-3 mm has an adverse impact on tumbler index may be due to non-uniform firing and low permeability as shown in **Fig 7.4b**.

The sinter bed permeability is affected by sinter bed height and it slightly increases with increase of bed height, attaining maximum at 350 mm as shown in **Fig.7.4b** and thereafter drops. The drop in sinter bed permeability with increase in bed height can be attributed to the insufficient suction pressure at higher bed heights. The bed prepared from 6-10mm micro-pellets resulted in lower permeability compared with that prepared from 3-6mm micro-pellets. The decrease in permeability of the bed containing 6-10mm micro-pellets can be attributed to filling of voids by finer size of coke and other raw materials. It is well known that better permeability of the sinter bed is desirable for uniform firing of sinter. Highest sinter bed permeability of 23.18 JPU is observed at a bed height of 350mm with bed prepared from micro-pellets of size 3-6mm. Flame front movement (as indicated by vertical sintering speed, VSS) during sintering is also recorded and presented in **Table 7.5**. The high value of VSS (18.52 mm/min) at bed height of 350mm signifies fast ignition rate, thus resulting in high permeability of the sinter bed.

The productivity of the sinter bed increased with micro-pellets of size from 1-3 mm to 3-6 mm but decreased to lowest for 6-10 mm micro-pellets which is due to low VSS and yield.

**Table 7.5: Physical characteristics of hybrid pellet sinter produced with varying bed height**

(Ignition time: 120 s, moisture content: 6.5% and coke breeze: 5.5%)

S. No.	Micro-pellet size (mm)	Bed Height (mm)	Sinter Properties		Sinter bed properties		Sintering process properties			
			Tumbler Index (%)	Bulk Density (t/m <sup>3</sup> )	Green permeability (JPU)	V.S.S (mm/min)	Coke rate (kg/T)	Productivity (+6.3mm) (t/m <sup>2</sup> /h)	Yield of +6.3mm (%)	Return Sinter (%)
1	1-3	300	66.82	2.100	19.98	16.11	75.7	1.2001	72.60	27.40
		350	67.92	1.981	20.11	17.02	75.2	1.2399	73.11	26.89
		400	64.21	2.089	19.72	16.72	77.9	1.3121	70.63	29.37
		450	58.33	2.002	19.09	16.32	84.2	1.3043	65.32	34.68
2	3-6	300	68.92	1.902	23.09	18.11	77.8	1.2927	70.73	29.27
		350	70.02	1.983	23.18	18.52	76.8	1.3224	71.62	28.38
		400	69.11	2.162	22.73	17.83	80.8	1.3491	69.06	30.94
		450	67.39	2.199	21.10	17.00	82.0	1.3393	67.04	32.96
3	6-10	300	66.84	1.983	21.99	17.66	77.6	1.1969	70.87	29.13
		350	66.92	1.970	22.35	17.01	77.1	1.2219	71.29	28.71
		400	65.31	2.096	20.73	16.20	80.8	1.2808	68.11	31.89
		450	63.94	1.997	19.06	15.67	84.1	1.2749	65.36	34.64

V.S.S – Vertical sintering speed

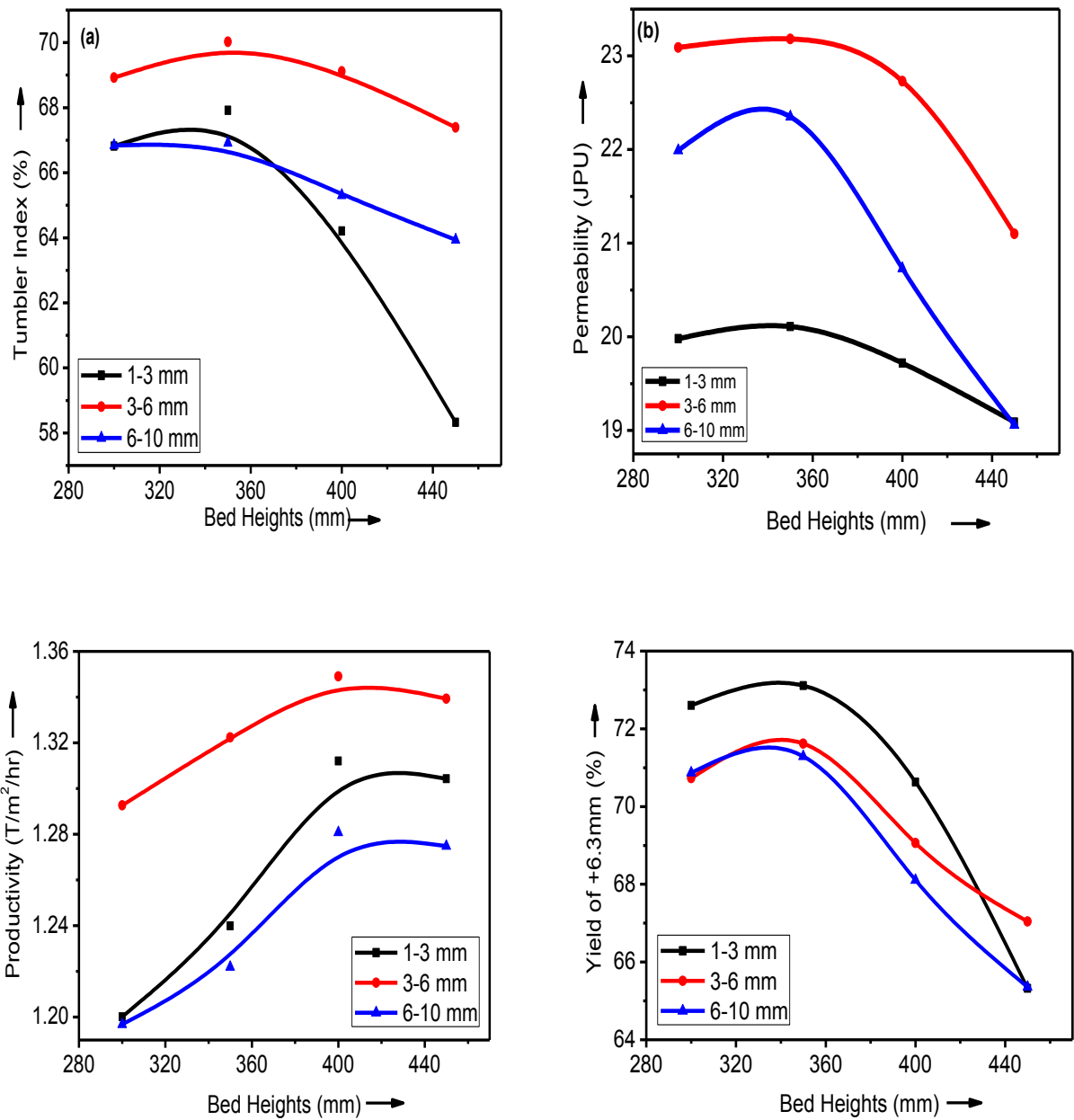


**Fig.7.4:** Effect of bed height on various properties of sinter prepared from different sizes of micro-pellets. (a) Tumbler index, (b) Permeability, (c) Productivity and (d) Yield (+6.3mm).

Further, the productivity of the hybrid pellet sinter increases with increase in sinter bed height for all the sizes of micro-pellets (**Fig.7.3c**) up to 400 mm and afterwards decreased. The highest productivity of  $1.3491 \text{ t/m}^2/\text{h}$  is observed with the sinter bed prepared from micro-pellets of size 3-6mm for a bed height of 400 mm. However, with a bed height of 400 mm, the coke rate is increased and yield is decreased. From **Table 7.5**, it can be observed that a bed height of 350 mm resulted in low coke rate and acceptable level of yield ( $> 70\%$ ). Thus, a sinter bed of 350 mm prepared from micro-pellets of 3-6 mm size result in optimum properties.

The yield of +6.3mm sinter is also depends upon physical properties of sinter and should be  $> 70\%$  for acceptance. The yield of +6.3 mm sinter is found to be higher for the sinter prepared from 1-3mm micro-pellets. However, this sinter does not possess better properties compared to the sinter produced from 3-6mm and 6-10 mm micro-pellets. The yield of +6.3 mm sinter prepared from 6-10 mm size micro-pellets is very low and also possess low properties. The yield of +6.3 mm sinter prepared from micro-pellets of size 3-6 mm is observed to meet the industrial acceptance and possess good characteristics compared to the remaining two sinters. Further, the yield is initially increased with increasing bed height up to 350 mm and then decreased with increasing the bed height due to non-uniform firing of the sinter. Therefore, it can be concluded that a bed height of 350 mm with micro-pellets of 3-6 mm provide optimum properties of the sinter.

About 28.38% return sinter is generated with high physical properties, high productivity and low coke rate in case of the sinter produced from micro-pellets of size 3-6mm and keeping sinter bed height at 350mm. Hence, a sinter bed height 350mm with micro-pellets of size 3-6mm can be considered optimum with respect to return sinter generation.

Based on the above results on the effect of bed height, it can be concluded that the combination of good physical strength (tumbler index) with high productivity, is observed in the sinter prepared from the micro pellets of 3-6mm size at sinter bed height 350mm. These conditions (3-6 mm size micro-pellets and 350mm sinter bed height) results in the optimum sinter properties, sinter bed properties and sintering process properties.

### **7.3 Optimized conditions for hybrid pellet sinter making by using micro-pellets:**

Based on the above studies, it can be summarized that desirable sinter having properties suitable for blast furnace feed can be produced by using micro-pellets of sufficient strength of size 3-6 mm. The optimized conditions for hybrid pellet sinter making in pot grate furnace with micro-pellets of 3-6mm size are as below:

- (i) Moisture: 6.5%,
- (ii) Coke breeze : 5.5%
- (iii) Bed height: 350 mm
- (iv) Ignition time: 120 s

### **7.4 Effect of basicity on properties of hybrid pellet sinter produced from micro pellets of size 3-6 mm:**

In present practice of iron making through blast furnace, super-fluxed sinter is preferred as feedstock. The super-fluxed sinter contain total flux requirement of iron making in it. The major acid contents in the blast furnace burden are contributed by ore and coke ash. The fluxes are incorporated in the sinter by considering all acid inputs in the feed of blast furnace. So it is essential to understand effect of basicity on the quality of hybrid pellet sinter. This study will compliment to produce super-fluxed sinter of desired quality with pre-decided basicity. Six batches of hybrid pellet sinters were produced by using micro-pellets of sizes 3-6 mm with varying values of basicity under optimized conditions listed in section 7.2 to study the impact of basicity of on sinter quality. The basicity in the sinter was varied between 0.5 and 3.0 with an increment of 0.5. Microstructural and XRD analysis were carried out to assess the quality of the sinter.

#### **7.4.1 Microstructural studies of hybrid pellet sinter produced with varying basicity (fluxes)**

Six batches of hybrid pellet sinters, consisting of charge compositions as presented in [Table 3.3](#), were prepared in pot grate furnace. [Figure 7.5](#) shows the photograph of the hybrid pellet

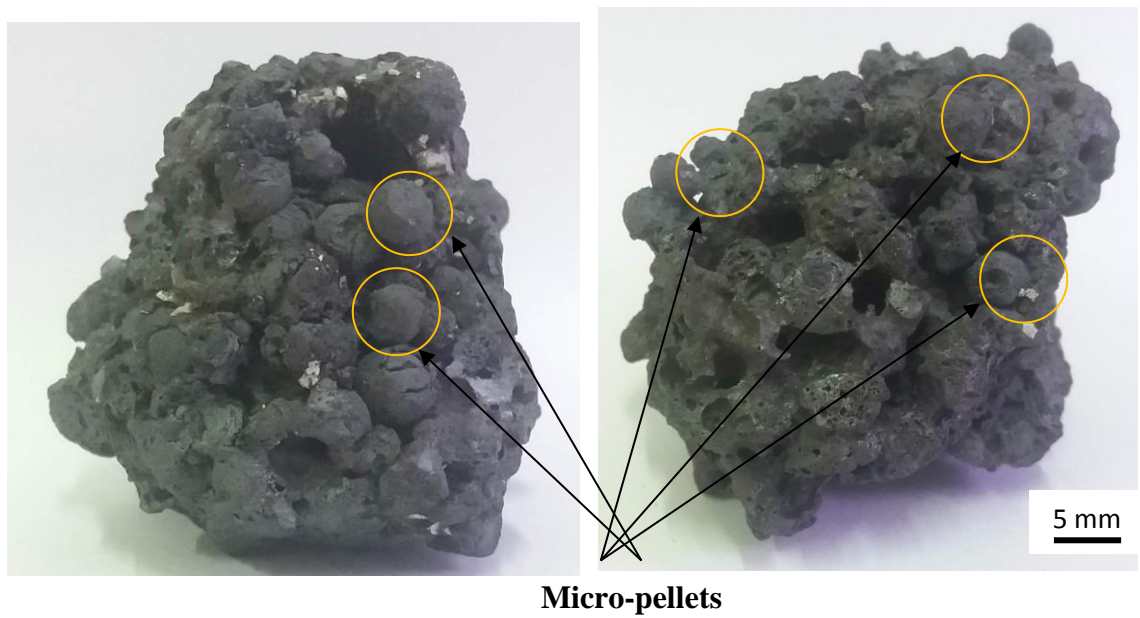


**Fig.7.5** Hybrid pellet sinter prepared by using micro-pellets

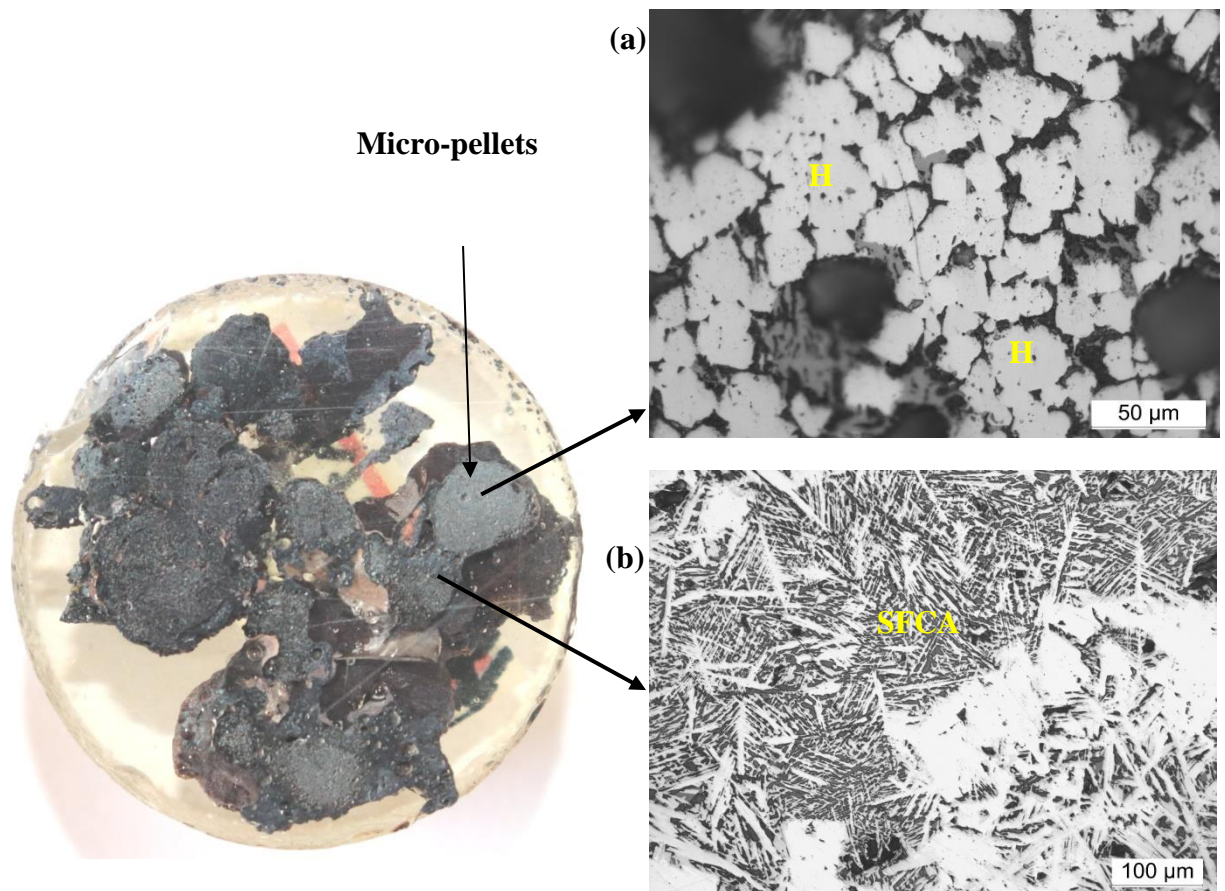


**Fig.7.6** Micrograph of the sinter with basicity 1.5 and its surrounding area after firing

sinter. It can be clearly observed that the micro-pellets retain their shape and size during sinter making and bonded to the mass of the sinter by incipient fusion of fine particles at the contact points. In fluxed hybrid pellet sinter, bonding is derived either by incipient fusion or diffusion. Formation of silico-ferrite of calcium and alumina (SFCA) improves strength of the sinter. (Scarlett et al., 2004) suggest that at lower temperature (750-780 °C) calcium ferrite is formed by solid state reaction. Beyond 1050 °C calcium ferrite is converted in to SFCA in the

presence of silica and alumina. **Fig.7.6** shows the micrograph of the sinter with basicity 1.5. It can be observed that the micro-pellets retains their shape and strengthen during sinter making. The interior of the micro-pellets are well connected through large hematite grains formed due to recrystallization and grain growth. The micro-pellets are surrounded by needle shaped SFCA. The amount of silica and alumina in the slime concentrate and addition of fluxes (CaO & MgO) influence the amount and chemistry of SFCA in the sinter.

#### **7.4.2 XRD studies of hybrid pellet sinter produced with varying basicity (fluxes)**

Characterization of hybrid pellet sinter was also carried out for estimation of phases formed during sinter making at different basicities. The sinter produced with basicity 1.0 was subjected to XRD analysis and the results are shown in **Fig.7.7**. It can be noted that the magnetite content in the sinter observed by XRD analysis is in agreement with measured by optical microscope. However, the other phases present in the sinter could not be quantified through XRD due to limitation in the instrument. Literature (Mos et al., 2018) suggest that the use of cobalt tube is required for XRD analysis of sample containing iron oxide. However, the availability of cobalt tube (in India) is limited and hence further characterization of the sinter by XRD was not taken up.

Although a great variety of textural relationships have been noticed during optical microscope studies, it must be emphasized that a large amount of magnetite has precipitated from the melt at lower basicity of 0.5 and majority of the hematite and wustite also formed in this manner. The micrograph of hybrid pellet sinter with basicity 0.5 is shown in **Fig.7.8.**

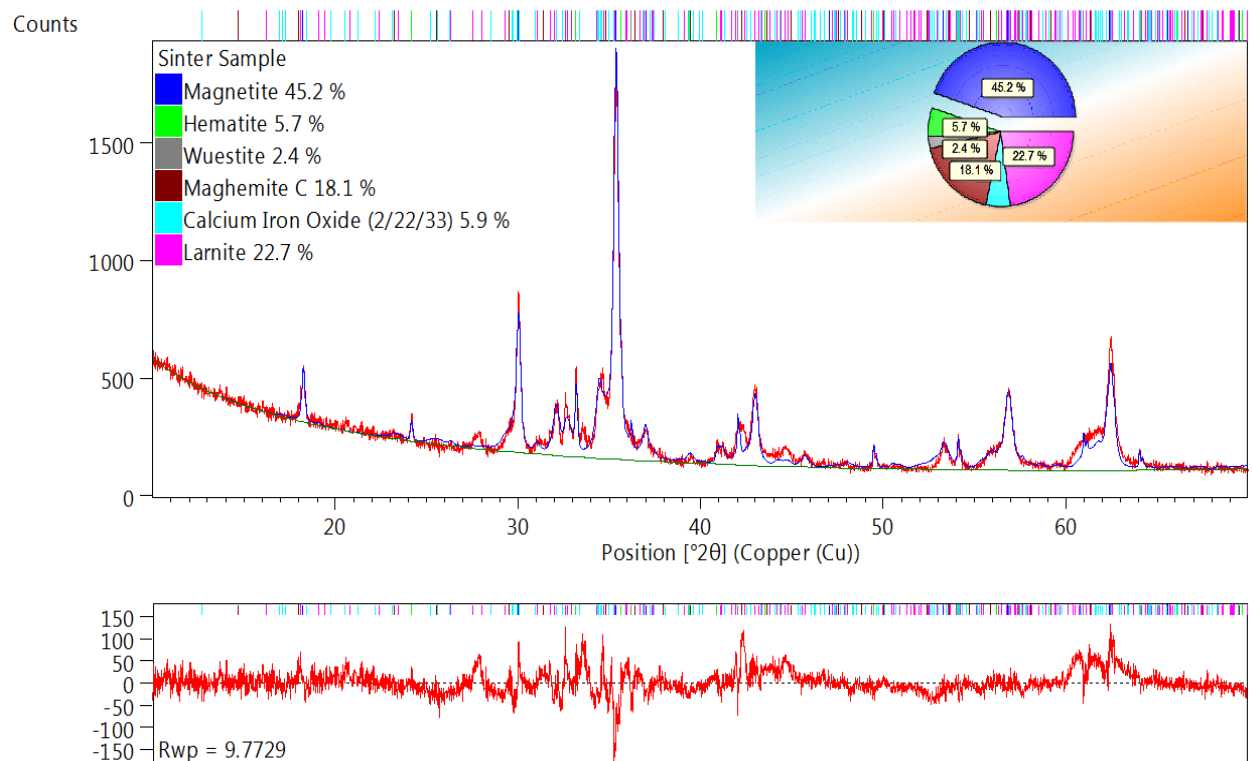


**Fig.7.7** XRD pattern of sinter produced with basicity 1.0

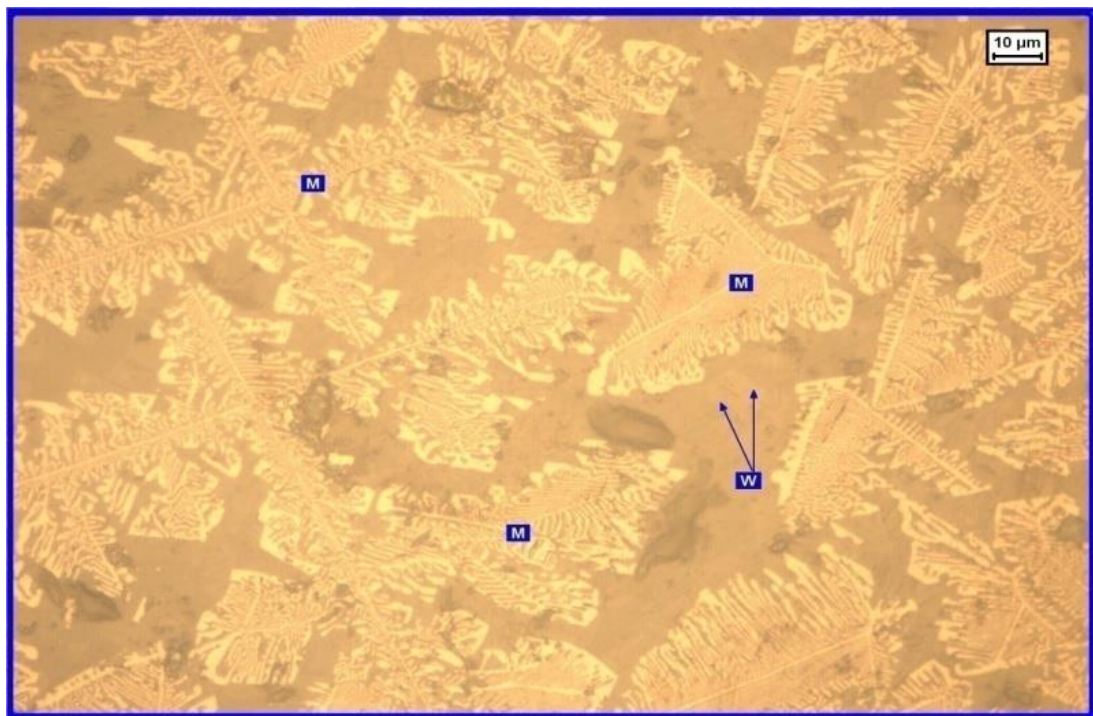


**Fig.7.8** Photo-micrographs illustrating magnetite (M) crystals forming a netlike eutectic intergrowth. Some wustite (W) also present [Under reflected light]

The phase distribution in hybrid pellet sinter was measured for all six batches of sinter produced with basicity 0.5, 1.0, 1.5, 2.0, 2.5 and 3.0 by using optical microscope. **Fig.7.9**

depicts the mineral phase distribution in the sinters. Some amount of calcium ferrites (SFCA) begins to appear at basicity around 1.0 and at 1.5 to 2.0, at initial stage (at Basicity 1.0) the crystallization of dicalcium silicate ( $\beta$ -2CaO.SiO<sub>2</sub>) begins and later converted to SFCA at higher basicity. Magnetite is major phase in the hybrid pellet sinter in the range of 0.5 to 1.5 basicity. In this basicity range the sinter strength will be minimum because volume of glass phase is maximum (Scarlett et al., 2004) . Sinter particle in the basicity range of 1.0 to 2.0 exhibited micro cracks that may be formed due to expansion in volume while phase transformation of  $\beta$  to  $\gamma$ - dicalcium silicate during cooling of hybrid pellet sinter (Webster et al., 2012) . The increase in volume during cooling generates cracks and point of weakness in the sinter. At higher basicity ( $> 2.0$ ), the major phase present is SFCA. The hybrid pellet sinter exhibit strong bonding created by SFCA, thereby improves the tumbler index of the sinter with minimum quantity of magnetite. Lower magnetite content at higher basicity also improves reducibility of the hybrid pellet sinter.

## 7.5 Summary of pot grates sintering studies:

The effect of micro-pellet size on the physical and metallurgical characteristics of the sinter is significant. The sinter produced with 3-6 mm size of micro-pellets resulted in high productivity and tumbler index and thus meeting the requirements of blast furnace feedstock. The results confirm that the micro-pellets of size 3-6 mm can effectively replace iron ore fines in sinter making. Various parameters, like ignition time, moisture and coke content in the sinter mix, and bed height for making sinter were optimized. The optimized conditions are:

- (i) Moisture: 6.5%,
- (ii) Coke breeze : 5.5%
- (iii) Bed height: 350 mm
- (iv) Ignition time: 120 s

Six batches of sinter with basicity ranging from 0.5 to 3.0 were produced under optimized condition and sinters were subjected to optical microscopy and XRD analysis. A wide variety of minerals were observed in the final hybrid pellet sinter. The percentage of various minerals

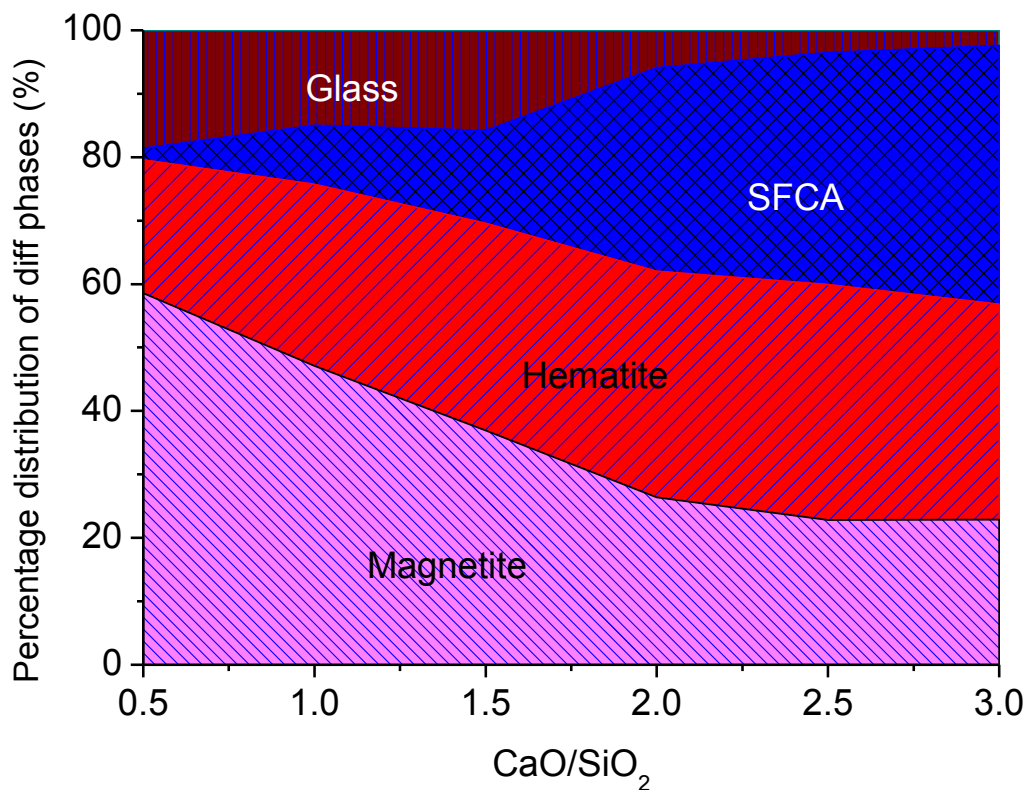


**Fig.7.9** Effect of basicity on quantity of various minerals in the sinter

and their structures varies with basicity of the sinter. Degree of oxidation improves with increasing basicity and accordingly magnetite content decreases with basicity. Formation of SFCA phases starts at basicity above 1. At higher basicity glassy phases are replaced by calcium silicate and ferrite phases and later phase become predominant at high basicity. The various types of ferrites form during cooling at different stages (**Malysheva et al., 2015**). Needle like ferrite (SFCA) forms in the matrix which hold the micro-pellets together. The micro-pellets retain their shape during sintering and converted into single crystal through recrystallization and grain growth. The micro-pellets are imbedded in the ferrite structure. Therefore, the micro-pellets size has direct impact on the physical properties and mineral presence in the sinter (**Malysheva et al., 2007**).

## Chapter -8

# EVALUATION OF HYBRID PELLET SINTER UNDER BLAST FURNACE CONDITIONS

### 8.1 Introduction:

The use of strong, porous, highly reducible sinter in the blast furnace is essential for high productivity with minimum energy consumption. The medium to large capacity blast furnaces are designed to accept 70 % sinter as feedstock for iron making. So physical, chemical and metallurgical quality of sinter dictate overall economy of the blast furnace. In the present work, hybrid pellet sinter with varying basicity from 0.5 to 3.0 with an increment of 0.5 was prepared from micro-pellets of 3-6 mm size with an aim of replacing it in blast furnace in place of regular sinter. The hybrid pellet sinter thus obtained was tested for its overall performance under simulated blast furnace conditions.

### 8.2 Chemical composition of the hybrid pellet sinter

The chemical composition of the hybrid pellet sinter is very important for iron making because the sinter with higher iron content is required in the blast furnace. The chemical compositions of the hybrid pellet sinters (HPS) produced from micro-pellets of 3-6 mm size with different basicities were analyzed and are presented in **Table 8.1**. The iron content in the sinter with basicity 0.5 is observed to be 63.41%. It signifies that for the production of 1 ton of liquid pig iron, about  $\left(\frac{100}{63.41} \times 1000\right)$ , i.e. **1.58** tons of sinter need to be charged in the blast furnace. Similarly, the iron content in the sinter with basicity 3.0 is found to be 54.07% implying that  $\approx 1.85$  tons of sinter is required for production of 1 ton of liquid pig iron in the blast furnace. Therefore, the basicity of the sinter produced will be decided by the blast furnace operator by considering the chemistry of the coke and other iron bearing materials (viz. sinter/iron ore/pellets). Now-a-days, total flux requirement for iron making is substituted in the sinter only. Hence sinter properties need to be evaluated at all basicity levels.

**Table 8.1:** Chemical compositions of the HPS with different basicities

Constituents of the HPS	Sinter Basicity					
	0.5	1.0	1.5	2.0	2.5	3.0
Fe(T)*	63.41	61.50	59.68	57.80	55.94	54.07
SiO <sub>2</sub>	3.30	3.43	3.45	3.48	3.51	3.61
Al <sub>2</sub> O <sub>3</sub>	1.99	1.97	1.94	1.98	1.88	1.91
LOI	0.03	0.10	0.07	0.04	0.09	0.08
CaO	2.38	4.51	6.76	8.99	11.22	13.37
MgO	0.44	0.94	1.33	1.81	2.27	2.82

\* In the form of Fe<sub>2</sub>O<sub>3</sub>

### **8.3 Effect of basicity on physical properties of the HPS produced from micro-pellets of 3-6 mm size:**

**Figure 8.1** portrays the effect of basicity on yield and tumbler index (physical strength) of the HPS. **Figure 8.1** also illustrates the metallurgical strength of the sinter, expressed in %, as a function of basicity under mild reducing atmosphere (30% CO and 70% N<sub>2</sub>) at 550 °C (under simulated blast furnace condition). At lower basicity of 0.5, the tumbler index and yield of the sinter are higher with values of 71.3% and 74.7% respectively. Higher tumbler index and yield of the hybrid pellet sinter at lower basicity are ascribed to the formation of fayalite phase with low melting point in the presence of Fe<sub>3</sub>O<sub>4</sub>, SiO<sub>2</sub> and FeO. At low basicity, large amount of liquid phase forms and makes the hybrid pellet sinter stronger with low degree of oxidation. Some calcium ferrites (silico-ferrite of calcium and alumina, SFCA) begins to appear at basicity around 1.0 and at 1.5 to 2.0 the crystallization of dicalcium silicate ( $\beta$ -2CaO.SiO<sub>2</sub>) takes place. In this basicity range, the metallurgical strength of the sinter decreases to its lowest value (**Fig 8.1**) due to increase in volume of the sinter (due to increase in the liquid phase) while phase transformation of  $\beta$  to  $\gamma$ -dicalcium silicate ( $\gamma$ -2CaO.SiO<sub>2</sub>) occurs during cooling of hybrid pellet sinter (**Webster et al., 2012**). The increase in volume during cooling generates crack and point of weakness in the sinter. At higher basicity (above 2.0), the strong bonds created by ferrite, improves the tumbler index of the sinter with minimum quantity of magnetite. The sinter with basicity of 1.5 exhibited lowest metallurgical strength under mild reducing condition. The poor metallurgical strength can be attributed to the generation of higher amount of fines at upper stack region of the blast furnace. This high amount of fines generation is detrimental to the permeability of the burden inside the blast furnace. The hybrid pellet sinters at basicities below 1 and above 2 have exhibited good metallurgical strength under mild reducing condition.

### **8.4 Effect of basicity on metallurgical properties of HPS produced from micro-pellets of 3-6 mm size:**

The metallurgical characteristics of the HPS with varying basicity are furnished in **Table 8.2**. The porosity of the hybrid pellet sinter is 14.6% at basicity of 0.5 and is decreased to 12.1% at basicity of 1.0 and found to increase with further increase in the basicity beyond

1.0 (**Table 8.2 & Fig.8.2**). The higher porosity at basicity of 0.5 may be due to the formation of higher amount

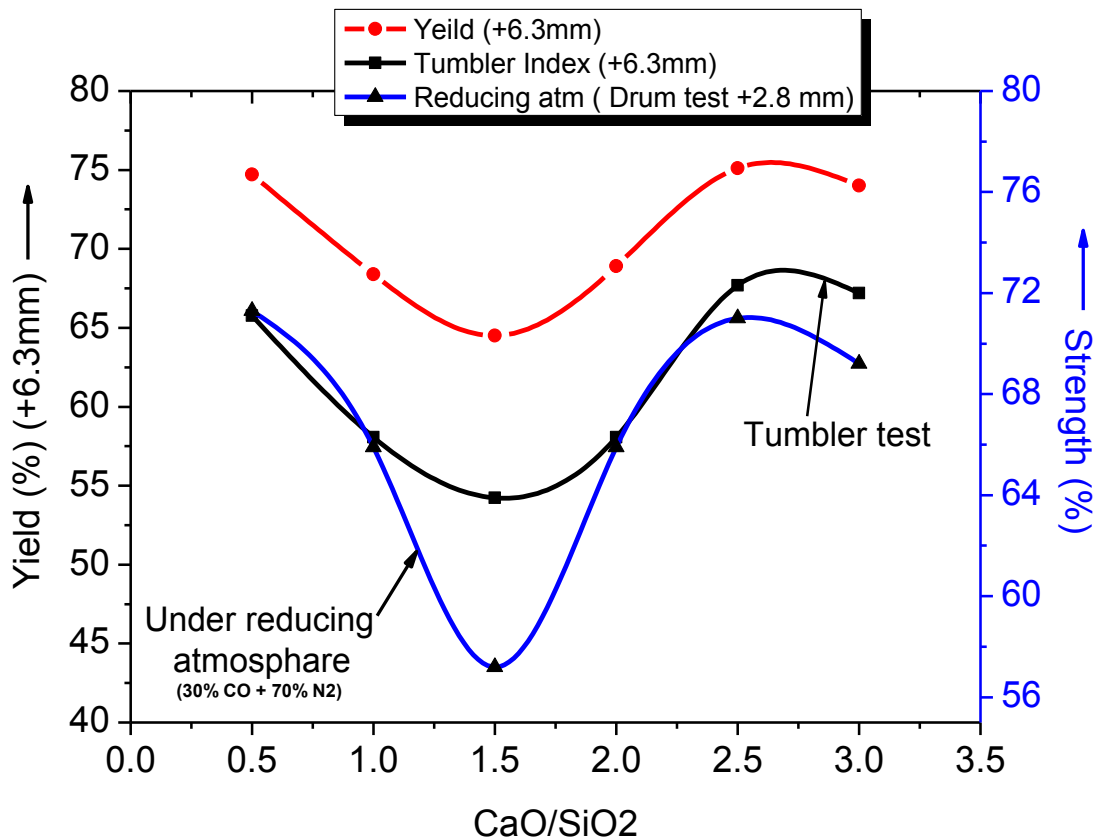


**Fig.8.1** Effect of basicity on yield and strength of the HPS

**Table 8.2** Metallurgical characteristics of hybrid pellet sinter with varying basicity

Metallurgical Characteristic	Basicity					
	0.5	1.0	1.5	2.0	2.5	3.0
Porosity (%)	14.6	12.1	13.9	15.4	17.2	19.1
Relative reducibility (ISO 7215)	48.7%	51.7%	53.4%	62.7%	65.7%	72.1%
Productivity (t/m <sup>3</sup> /day)	1.1978	1.2191	1.2211	1.2765	1.3009	1.2871

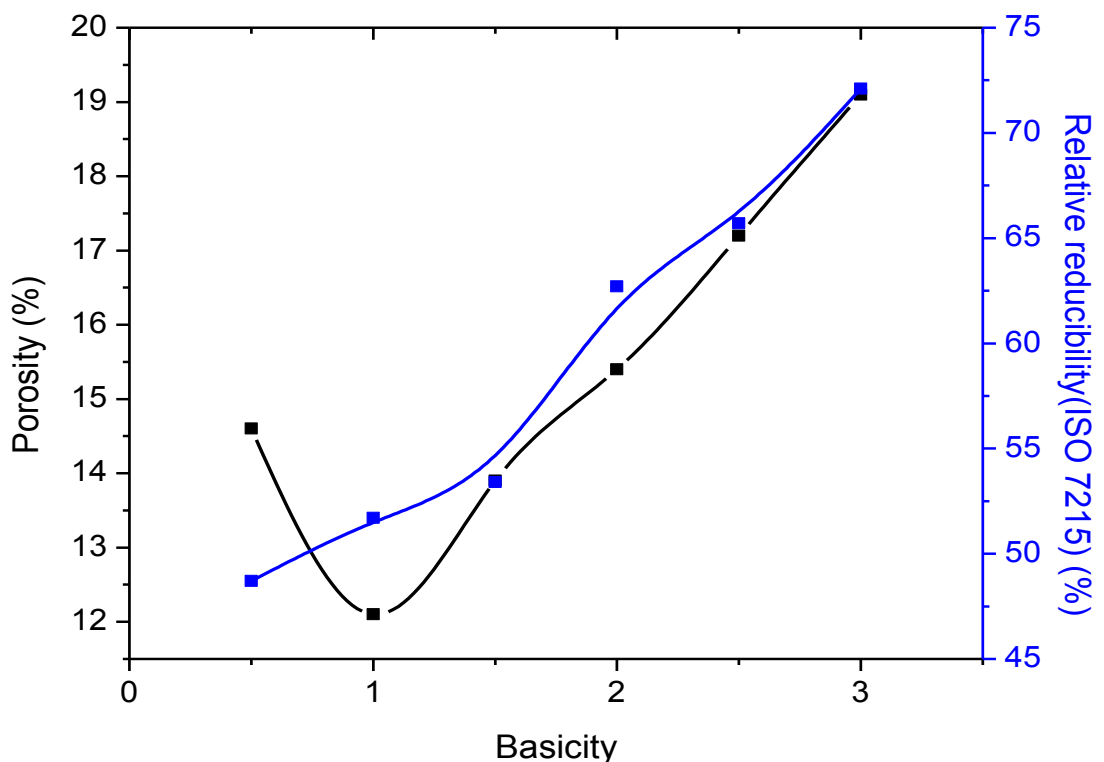


**Fig.8.2** Effect of basicity on porosity and relative reducibility of HPS

of liquid slag in comparison to sinter with basicity 1.0. The maximum porosity of 19.1% is observed at highest basicity of 3.0. The calcination of flux during sintering may contribute to enhancing the porosity apart from higher amount of slag formation at higher basicity.

The reducibility of hybrid pellet sinter is proportional to the porosity. Higher the porosity, higher is the reduction. At basicity of 0.5, the porosity in the sinter is higher than that with basicity of 1.0. However, reducibility is lower. The formation of fayalite phase with low melting point at lower basicity may be the cause for low reducibility or reduction. The reduction of sinter for 3 h under static reducing condition at a temperature of 900 °C is represented as relative reducibility. The relative reducibility of HPS increases with increasing basicity as shown in **Fig 8.2** and reaches 72.1% at basicity of 3.0. The presence of higher CaO at higher basicity may improve the rate of reduction.

The productivity of the sinter increases with basicity and reach maximum at 2.5 and afterwards decreased. The productivity is calculated from sinter yield (**Yu et al., 2015**). Sinter strength improves with basicity, higher strength of sinter will result in higher yield so higher productivity.

## **8.5 Effect of basicity on reduction under load (RUL) of HPS produced from micro-pellets of 3-6 mm size:**

Modern blast furnace with large capacity that operate at high efficiency requires highly improved burden. The reduction under load of 50 KN/cm<sup>2</sup> is used to understand the successive changes in the burden while it is descending in the blast furnace. The test condition is designed to simulate load of burden above it under high temperature (1050 °C) and reducing condition. Once the sample temperature reaches 1050 °C, reducing gas is introduced in to the furnace. The weight loss with time during reduction under load is shown in **Fig.8.3**. Rapid weight loss of the sample is noticed for sinters of all basicities. **Figure 8.4** delineates the reduction under load of hybrid pellet sinter for different basicities with time. As it can be seen from **Fig.8.4**, the basicity has direct impact on reduction behavior of HPS. The rate of reduction increases with increasing basicity. The reduction under load test was terminated after 80% of reduction for sinters of all basicities, whereas the test was terminated after 70 % of reduction for the sinter with basicity 3.0.

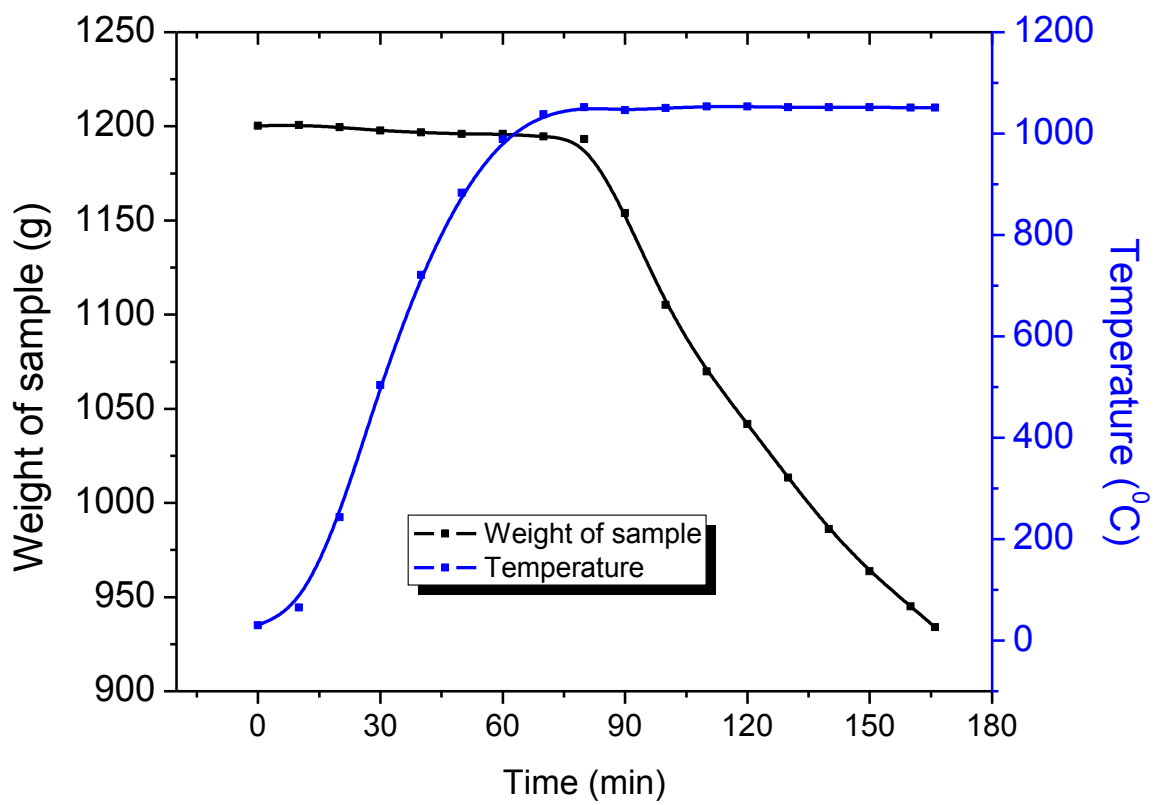


**Fig.8.3** Weight loss of HPS (with basicity 2.5) during RUL test

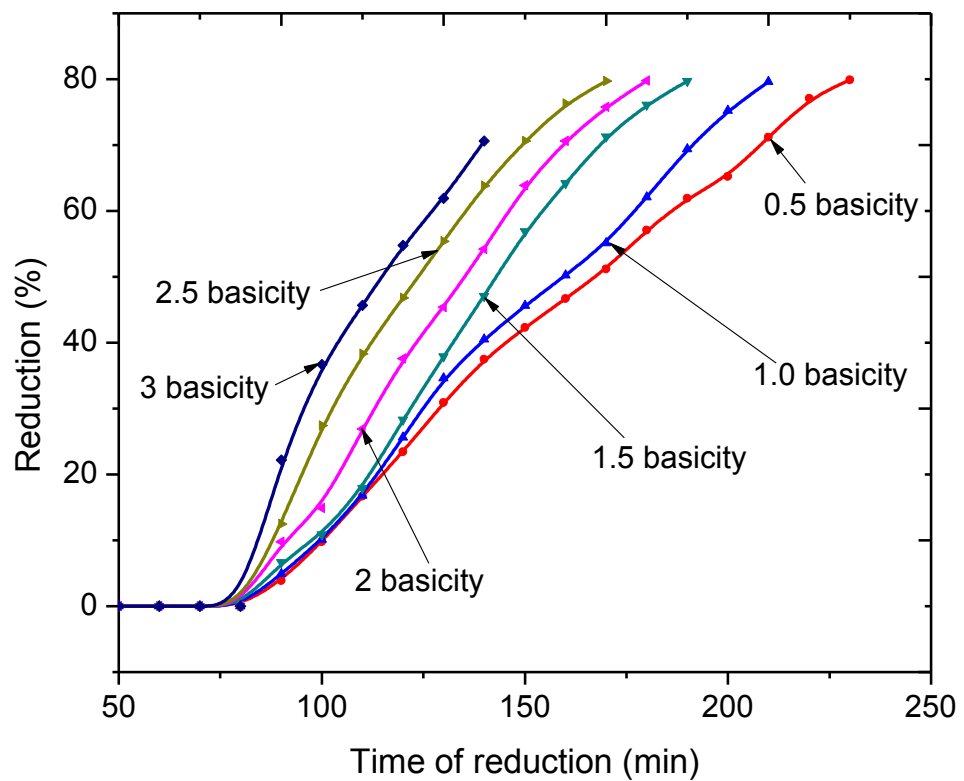


**Fig.8.4** Reduction of HPS of various basicities with time

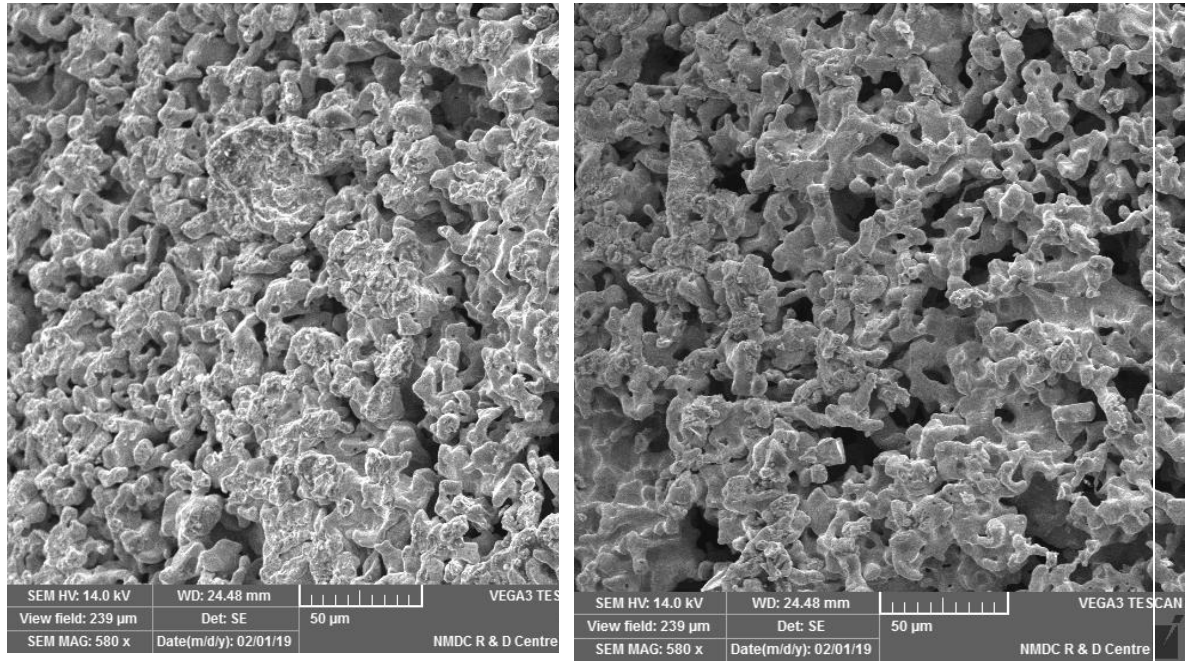


**Fig.8.5** SEM micrograph of sinter after reduction

The reducing gases passing through the sinter sample at high temperature (1050 °C) causes reduction of the sinter and hence result in weight loss as shown in **Fig.8.3**. In case of HPS with basicity 3.0, the sample bed inside the furnace become impervious after 70% reduction under constant pressure. Thus, the reducing gas could not pass through the sinter sample, hence the test was terminated. It implies that only a maximum of 70% indirect reduction (reduction by gases) can be achieved inside the blast furnace if hybrid pellet sinter with basicity 3.0 is used. Remaining reduction will be completed by direct reduction in the presence of coke inside the blast furnace, which increases the consumption of coke.

The SEM micrographs of the reduced hybrid pellet sinter of basicity 3.0 and 2.5 are shown in **Fig.8.5**. A very dense and reduced mass can be seen in the sinter of basicity 3.0 (**Fig 8.5a**). High rate of reduction and pressure acting upon the sample causes formation of impervious/fused bed and hence decreases the reducibility in case of sinter with basicity 3.0. The reduced mass of hybrid pellet sinter with basicity 2.5 exhibited net like structure with visible pores (**Fig.8.5b**) and make the sinter available for further reduction.

It can be summarized from the RUL studies that the reduction rate of HPS increases with increase in basicity. More than 80% indirect reduction can be achieved in the blast furnace with HPS for all basicities except at higher basicity of 3.0. Higher degree of indirect reduction (through gases) is desirable and helps in the reduction of coke rate for iron making.

## **8.6 Effect of basicity on softening and melting of HPS:**

Cohesive zone in the blast furnace consists of alternate layers of iron bearing feed material and coke. Iron bearing material get reduced and forms impervious layer as it descends in the blast furnace and thus the gases passes through the coke layer only. The shape and size of cohesive zone is very important with respect to productivity of blast furnace. The dissection studies of blast furnace provide information about existence of cohesive zone inside the blast furnace (**Omori and Takahashi, 1977**). The different shapes, sizes and profiles of cohesive zones were observed during dissection studies of various modern blast furnace and the same is illustrated in **Fig 8.6 (Omori and Takahashi, 1977)**

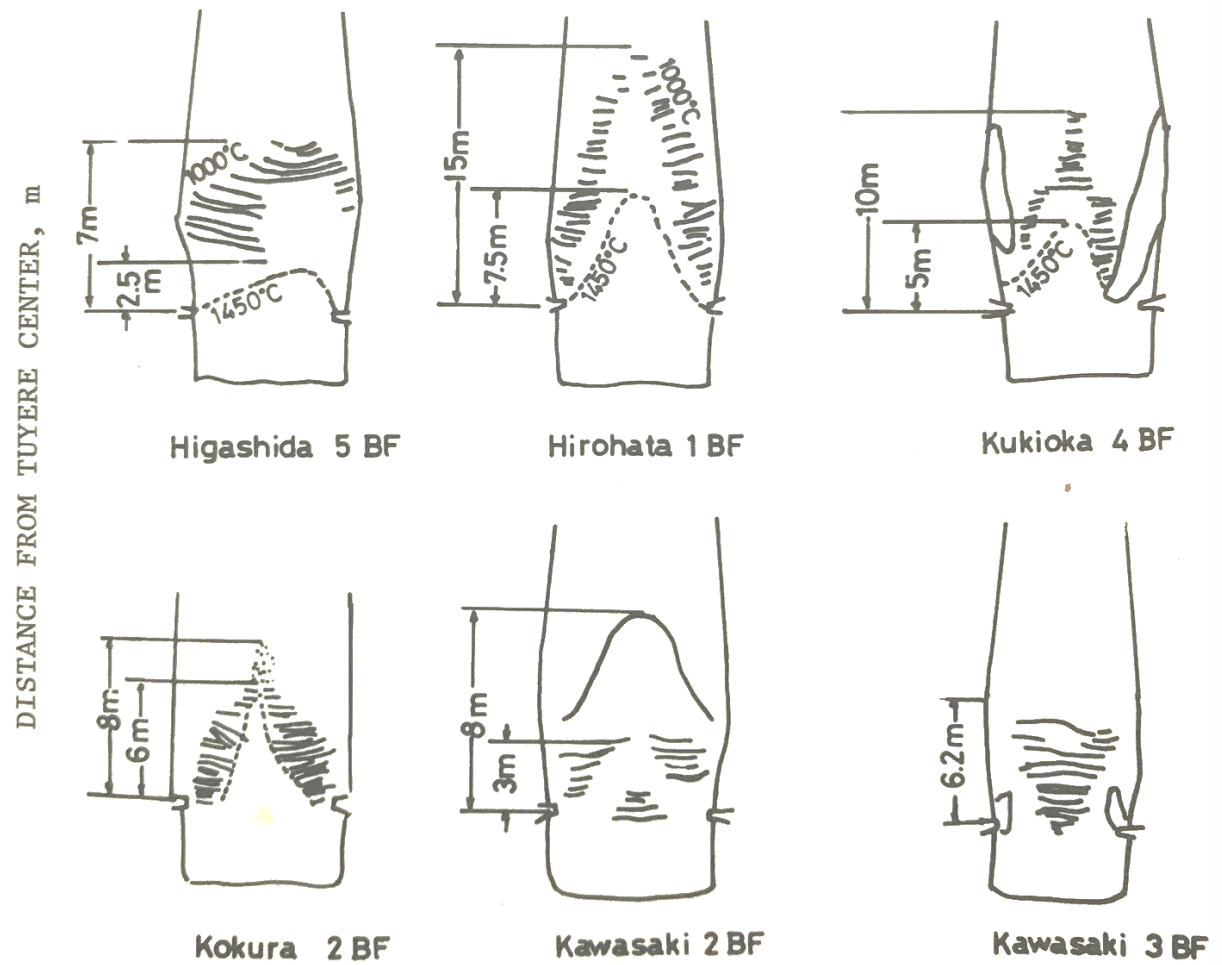


**Fig.8.6** Schematic profile of cohesive zone of various dissections in blast furnaces (Omori and Takahashi, 1977)

Cohesive zone also known as softening and melting zone exist at lower portion of the blast furnace and offer maximum resistance to the gas flow. Stability of this region under high temperature (higher than 1100 °C) and intensive reducing conditions depends on the characteristics of iron bearing burden. Evaluation of hybrid pellet sinter under softening and melting condition was carried out to establish its uses in blast furnace as feedstock.

In the present study, the softening and melting tests were carried out using a burden consisting of 70% hybrid pellet sinter and 30% sized iron ore lump (-20,+10mm) received from Bailadila deposit-5. The characteristics of sized iron ore lump from Bailadila deposit-5 are presented in **Table 8.3**. The iron content of the ore sample is 68.54 % and the gangue ( $\text{SiO}_2 + \text{Al}_2\text{O}_3$ ) content is 1.17 % which are meeting the blast furnace feed requirements. The tumbler index and abrasion index of the sample are 88.30% and 8.7% respectively. The thermal degradation index (TDI), reduction degradation index (RDI) and relative reducibility (RR) of iron ore sample are 6.21 %, 23.78 % and 53.94%, respectively. All the physical, chemical and metallurgical characteristics of iron ore lump (-20, +10mm) are meeting the requirement of feed of iron production in blast furnace.

Meltdown characteristic of HPS with various basicity are summarized in **Table 8.4**. Slag content and its basicity in the final meltdown material increases with increase in basicity of sinter primarily due to the higher amount of flux. If sinter with basicity of 3.0 is used in iron making process, about 43.53 g of slag is obtained, which corresponds to a slag rate of  $\approx 288$  kg/THM (see at the end of the chapter for model calculation) with a slag basicity of 2.69 without considering contribution of slag by coke ash (No coke is added in these experiments). However, the basicity of the slag should be around 1.0 to 1.1 with coke addition. In the present study, a slag of basicity 1.37 could be achieved using sinter with basicity 1.5 without addition of coke.

The effect of basicity of the HPS on its meltdown behavior is elucidated in **Fig.8.7**. The temperature of beginning of softening of HPS is observed to be maximum (1191 °C) at basicity 3.0 and minimum (1131 °C) at basicity 1.5. The softening-melting range of the burden with sinter of basicity 2.5 is low or narrow. This low or narrow softening-melting range indicates appropriate burden chemistry with iron ore lump used.

**Table 8.3** Characteristics of iron ore lump used for softening and melting tests

Particulars	Values	Standard used					
<b>Physical Characteristics</b>							
Bulk density [t/m <sup>3</sup> ]	2.34	ISO-3852-1988					
Tumbler index [%+6.3mm]	88.30	ISO-3271-1995-11-01					
Abrasion index [%-0.5mm]	8.70	ISO-3271-1995-11-01					
<b>Metallurgical Characteristics</b>							
Reduction Degradation Index [%-2.8mm]	23.78	ISO-4696-2-2007					
Thermal Degradation Index [%-6.3mm]	6.21	IS - 10823 - 1994					
Relative Reducibility [%]	53.94	ISO-7215-2007					
<b>Chemical Analysis</b>							
Contents	Fe [Total]	SiO <sub>2</sub>	Al <sub>2</sub> O <sub>3</sub>	FeO	LOI	S	P
Wt %	68.54	0.86	0.31	0.40	0.54	0.009	0.034

**Table 8.4** Meltdown characteristic of HPS with different basicity

Contents	Basicity					
	0.5	1.0	1.5	2.0	2.5	3.0
70% HPS (g) <sup>#</sup>	196	196	196	196	196	196
30% Iron ore lump (g) <sup>#</sup>	84	84	84	84	84	84
<b>Slag chemistry of the blast furnace burden after softening-melting test</b>						
Al <sub>2</sub> O <sub>3</sub> (wt %)	24.65	18.53	14.83	12.61	10.39	9.20
SiO <sub>2</sub> (wt %)	42.60	33.46	27.31	22.96	20.01	17.91
CaO (wt %)	27.64	39.73	48.35	53.64	57.89	60.19
MgO (wt %)	5.11	8.28	9.51	10.80	11.71	12.70
Weight of slag (g)	16.88	22.25	27.40	32.85	37.99	43.53
Basicity of the slag = $\frac{(CaO + MgO)}{(SiO_2 + Al_2O_3)}$	0.49	0.92	1.37	1.81	2.29	2.69
Non drip material (%) <sup>*</sup>	12.1	13.6	18.6	22.8	27.8	22.1
Liquidus temp of slag (°C) (Calculated)	1608	1464	1611	1628	1514	1398

<sup>#</sup> Crucible capacity = 280 g

<sup>#</sup> 70% of HPS = 280 x 0.70 = 196 g

<sup>#</sup> 30% of iron ore lump = 280 x 0.30 = 84 g

<sup>\*</sup> Left over material in the crucible after the test

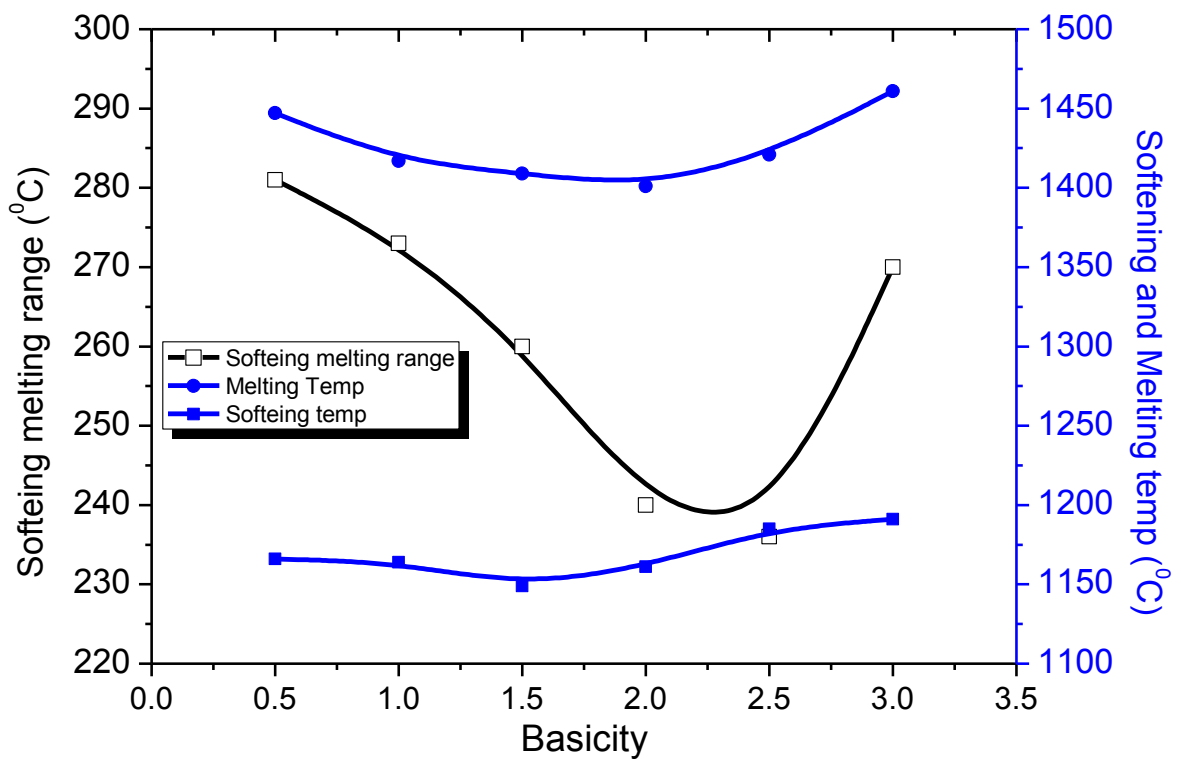


**Fig.8.7** Effect of basicity of sinter on meltdown behavior

The liquidus temperature of slag is affecting softening-melting range of burden (70% HPS Sinter + 30% lump ore). The softening-melting range of the burden with sinter of basicity 0.5 and 3.0 are highest with value of 281°C and 270°C respectively. Their corresponding liquidus temperatures of slag are also high with value of 1608°C and 1398 °C respectively. With iron ore lump from Bailadila deposit-5 and sinter with basicity in the range of 1.5-2.5 have lowest softening melting range (**Fig 8.7**). The lowest melting range signifies narrow cohesive zone in the blast furnace. Narrow cohesive zone is desirable for lower coke rate (**Hino et al., 1999**). In the present study, the basicity of hybrid pellet sinter between 2.0 and 2.5 is appears to be optimum for use with iron ore lump from Bailadila deposit-5 in blast furnace as feedstock. At this burden combination (70% HPS + 30% sized iron ore), the formation of di-calcium silicate in the slag result in narrow melting range, thus more narrower softening-melting range is witnessed as shown in **Fig.8.7**.

## 8.7 Comparison of HPS with blast furnace feed requirement

The HPS prepared with basicity 2.5 was characterized for chemical, physical and metallurgical characteristics and compared with the quality requirement of sinter used as blast furnace feed in **Table 8.5**. It can be observed that the quality of sinter produced from the slime concentrate by adopting hybrid pellet sinter route is meeting the requirement of blast furnace feedstock. The physical properties, like tumbler index and abrasion index of the hybrid pellet sinter are significantly better with values 72.3% and 4.7 % respectively as compared with 65% minimum and 18% maximum of blast furnace requirement. The higher tumbler index indicates generation of lower amount of fines during transportation and handling of sinter during charging of the blast furnace. Lower fines generation will in turn provide better permeability of the charge in the blast furnace. The metallurgical properties of the sinter (basicity 2.5) are observed to be comparatively high with high relative reducibility of 65.7%. The higher reducibility of sinter in turn promotes higher indirect reduction and as a result significant reduction in coke rate can be obtained.

**Table 8.5** Comparison of HPS with blast furnace requirements

S. No	Particulars	Blast furnace requirement	Hybrid pellet sinter produced from concentrate of slime from Bailadila region (Basicity 2.5)
1.	Fe (T)	50% min	55.94 %
2.	SiO <sub>2</sub>	6% max	3.52 %
3.	Al <sub>2</sub> O <sub>3</sub>	3% max	1.88%
4.	Tumbler Index	65% min	72.3%
5.	Abrasion Index	18% max	4.7%
6.	RDI	35% max	29%
7.	Relative Reducibility	55% min	65.7%

## **8.8 Summary:**

Hybrid pellet sinter (HPS) with varying basicity from 0.5 to 3.0 with an increment of 0.5 was prepared from micro-pellets of 3-6 mm size. The physical and metallurgical strength of the hybrid pellet sinter varies with basicity. The strength of sinter at lower basicity ( $\leq 1$ ) and high basicity ( $\geq 2$ ) is high. The sinter with basicity of 1.5 exhibits lowest metallurgical strength under mild reducing condition. Reducibility of hybrid pellet sinter increases with increase of basicity and reaches highest of value 72.1% at basicity 3. High reducibility indicates higher amount of reduction by reducing gases and higher reduction by gases is instrumental in reduction of coke rate in the blast furnace. The feed with 30% iron ore lump from Bailadila deposit-5 and 70% hybrid pellet sinter with basicity 1.5 to 2.5 have lowest softening melting range. Lower softening and melting range is essential for iron making through blast furnace. The physical and metallurgical strength of the hybrid pellet sinter was low at basicity 1.5, hence the range of basicity 2.0 to 2.5 of hybrid pellet sinter is optimum for use in blast furnace as feedstock. The metallurgical properties of the sinter (basicity 2.5) are observed to be comparatively high with high relative reducibility of 65.7%. The higher reducibility of sinter in turn promotes higher indirect reduction and as a result significant reduction in coke rate can be obtained. Overall, the hybrid pellet sinter produced from micro-pellets of 3-6 mm size is meeting feedstock requirement of blast furnace.

### **Calculation of slag rate:**

1.85 ton of HPS will produce 1 ton of hot metal

1 ton of HPS produce  $\frac{1}{1.85}$  ton of hot metal.

In the present study, the capacity of crucible = 280 g =  $280 \times 10^{-6}$  ton

280 g iron bearing material (HPS + iron ore lump) produces  $\frac{1}{1.85} \times 280 \times 10^{-6}$  ton of hot metal

$= 15.14 \times 10^{-5}$  ton hot metal

$15.14 \times 10^{-5}$  ton hot metal generates 43.53 g of slag

1 ton hot metal generate  $\frac{43.53 \times 10^{-6}}{15.14 \times 10^{-5}} = 0.2875$  ton slag /ton of hot metal  
 $= 287.5$  kg slag/ ton of hot metal

Slag rate: 287.5 Kg / ton of hot metal with a charge consisting of 70% HPS with basicity 3 and 30% iron ore lump.

# Chapter 9

## CONCLUSIONS AND FUTURE SCOPE OF WORK

### 7.1 Conclusions

In the present work, iron ore slimes from Bailadila mines located in Chhattisgarh state were selected for the study. The iron ore slimes were subjected to various standard procedures for studying their initial physical and chemical properties. The slimes were also studied microscopically by using optical and scanning electron microscopes to establish the status of liberated minerals. Based on these characterization inputs, gravity, dry magnetic and wet magnetic techniques were used individually to beneficiate the iron ore slimes. As the individual techniques have yielded a limited success, combination of gravity and magnetic techniques were used to obtain beneficiated slime with maximum recovery of iron value. Based on the flow sheet developed at laboratory, a pilot plant was also designed for the beneficiation of iron ore slime on large scale. The laboratory scale results were validated by pilot scale beneficiation facility. The concentrate thus obtained from pilot plant was used for the manufacture of micro-pellets. The resultant micro-pellets were subjected to hybrid pellet sintering using pot grate furnace. The sinter thus produced from micro-pellets was subsequently evaluated for its performance under blast furnace conditions. The performance of the hybrid pellet sinter under blast furnace conditions was meeting requirement of blast furnace feed. The following important conclusions have been derived at various stages of investigations:

#### 7.1.1 Characterization of slime:

- (i) The total iron value (Fe(T)) in the slime is 60.64%. The silica ( $\text{SiO}_2$ ) and alumina ( $\text{Al}_2\text{O}_3$ ) contents in the slime are 7.76% and 3.10% respectively. The total gangue mineral (i.e.  $\text{SiO}_2+\text{Al}_2\text{O}_3$ ) in the slime is 10.86%, which is on higher side to charge in to the blast furnace.
- (ii) Size-wise chemical analysis of slime shows that iron concentration is more in lower size fraction (-105 micron) whereas gangue concentration is high in coarse grains (+105 micron).
- (iii) Specific gravity of slime is 3.66. This lower specific gravity may be due to higher content of gangue minerals.

- (iv) The iron ore slime sample of Bailadila region contains hematite and goethite as primary ore minerals and majority of particles of ore mineral and silica were in liberated state. Quartz is the main source of silica in the slime sample.

#### **7.1.2 Laboratory and pilot scale beneficiation studies with slime:**

- (i) At laboratory scale, all possible gravity, magnetic and flotation separation techniques and combination thereof are considered to obtain slime concentrate meeting the requirement of blast furnace feed with maximum possible recovery. The individual techniques have yielded a limited success.
- (ii) The combined laboratory scale beneficiation studies, i.e. de-sliming using hydrocyclone followed by two stage wet high intensity magnetic separation (WHIMS), reveal that the concentrate assaying 64.74% Fe(T), 2.39 % SiO<sub>2</sub> and 1.82% Al<sub>2</sub>O<sub>3</sub> with a recovery of 85.16% Fe value could be produced. This meets the desired blast furnace feed concentrate specifications.
- (iii) The pilot scale studies reveal further improvement in the grade of the concentrate and the recovery of Fe value. Iron ore concentrate of 65.71 % Fe(T), 2.18% SiO<sub>2</sub> and 1.64% Al<sub>2</sub>O<sub>3</sub> with 87.31 % recovery is generated in pilot scale test.

#### **7.1.3 Micro-pellet making using slime concentrate from pilot plant:**

- (i) The micro-pellets obtained with a blain number of 1610 cm<sup>2</sup>/g possess low drop number and crushing strength, thus they are not suitable. The micro-pellets obtained with a blain number of 1930 cm<sup>2</sup>/g possess higher drop number and crushing strength, but their porosity is low. Further, it also increases the grinding cost. The micro-pellets obtained with a blain number of 1780 cm<sup>2</sup>/g possess optimum values of drop number, crushing strength and porosity. Hence, from these results, it is evident that the micro-pellets with optimum properties can be produced with slime concentrate having a blain number of 1780 cm<sup>2</sup>/g at 0.50 % bentonite and 9.25 % moisture contents.
- (ii) The moisture content and micro-pellet size in the sinter mix has significant impact on permeability of the sinter bed. The sinter bed made of 3-6 mm micro-pellets has exhibited highest permeability. The sinter bed also offers very low resistance to air flow through the bed. High porosity in sinter bed is desirable for high productivity and uniform quality of sinter.

#### **7.1.4 Hybrid pellet sintering studies:**

- (i) Hybrid pellet sinter was successfully obtained using 100% micro-pellets in place of conventional iron ore fines. The sinter produced with micro-pellets was meeting requirement of blast furnace feed stock.
- (ii) The optimized conditions for hybrid pellet sinter making in pot grate furnace with micro-pellets of 3-6mm size are as below:
  - a) Moisture: 6.5%,
  - b) Coke breeze : 5.5%
  - c) Bed height: 350 mm
  - d) Ignition time: 120 s
- (iii) The effect of micro-pellets size on physical and metallurgical characteristics of sinter was established. The hybrid pellet sinter produced with micro-pellets of 3-6 mm size had exhibited high tumbler index (73.18%), highest productivity (1.3182 T/m<sup>2</sup>/Hr), good reducibility and higher physical characteristics and can be considered as good quality of sinter. The results confirm that the micro-pellets of size 3-6 mm can effectively replace iron ore fines in sinter making.

#### **7.1.5 Performance of sinter under blast furnace conditions:**

- i) The metallurgical properties of the sinter (basicity 2.5) are observed to be comparatively high with high relative reducibility of 65.7%. The higher reducibility of sinter in turn promotes higher indirect reduction and as a result significant reduction in coke rate can be obtained.
- ii) The performance of hybrid pellet sinter under blast furnace conditions is better in comparison to conventional sinter with respect to reduction with time and strength at high temperature under reducing condition.
- iii) The hybrid pellet sinter produced from micro-pellets of 3-6 mm size is meeting feedstock requirement of blast furnace.

**On the whole, the iron ore slime from Bailadila (deposit-5) mines is convertible into useful blast furnace feed for iron making, thereby alleviating the problem of space for safe disposal of slime as waste.**

## 7.2 Future scope of work

The present study has helped in developing adequate understanding of the characteristics of slime generated at deposit-5 of Bailadila mines. The flow sheet for beneficiation of slime also developed using gravity and magnetic separation techniques. The concentrate obtained was converted into micro-pellets and these micro-pellets were used in sintering studies. Few areas emerged during the course of the present study, which need further investigations as suggested below:

- (i) In this investigation, finer size of concentrate having less than 100 micron was obtained after beneficiation of slime of Bailadila region. So far no sinter plant is working with 100 % feed of iron ore of size less than 100 microns.
- (ii) An intermediate scale of pilot plant may be designed and constructed before commercialization of the process. The data generated during operation of semi commercial plant (pilot plant) can be used for improvement of design of commercial plant.
- (iii) Attempt can be made to incorporate changes such as intensive mixer and/or disc pelletizer in the design of existing sinter plant for utilization of slime in sintering process.
- (iv) The hybrid pellet sintering process developed for iron ore slime concentrate can be extended and tried with other types of iron ore concentrate, viz. concentrate obtained from magnetite ore or from other sources.
- (v) The reject generated after beneficiation of slime can be successfully used in pavement tiles making. However, its consumption may be limited. Attempt should be made for bulk utilization of reject from slime beneficiation as a main constituent in brick making or additive of cement.

## REFERENCES

- Bai, Yong qiang, Cheng, S. sen, Bai, Yan ming, 2011. Analysis of Vanadium-Bearing Titanomagnetite Sintering Process by Dissection of Sintering Bed. *J. Iron Steel Res. Int.* 18, 8-15,36. [https://doi.org/10.1016/S1006-706X\(11\)60070-8](https://doi.org/10.1016/S1006-706X(11)60070-8)
- Bhagat, R.P., 2007. Fundamentals of Iron Ore Sintering, in: Processing of Iron Ore. pp. 132–149. <https://doi.org/http://eprints.nmlindia.org/5910>
- Clout, J.M.F., Manuel, J.R., 2003. Fundamental investigations of differences in bonding mechanisms in iron ore sinter formed from magnetite concentrates and hematite ores. *Powder Technol.* 130, 393–399. [https://doi.org/10.1016/S0032-5910\(02\)00241-3](https://doi.org/10.1016/S0032-5910(02)00241-3)
- Das, B., Mishra, B.K., Prakash, S., Das, S.K., Reddy, P.S.R., Angadi, S.I., 2010. Magnetic and flotation studies of banded hematite quartzite (BHQ) ore for the production of pellet grade concentrate. *Int. J. Miner. Metall. Mater.* 17, 675–682. <https://doi.org/10.1007/s12613-010-0373-x>
- Dixit, P., Tiwari, R., Mukherjee, A.K., Banerjee, P.K., 2015. Application of response surface methodology for modeling and optimization of spiral separator for processing of iron ore slime. *Powder Technol.* 275, 105–112. <https://doi.org/10.1016/j.powtec.2015.01.068>
- Ennis, B.J., 1996. Agglomeration and size enlargement. *Powder Technol.* 88, 203–225. [https://doi.org/https://doi.org/10.1016/S0032-5910\(96\)03124-5](https://doi.org/https://doi.org/10.1016/S0032-5910(96)03124-5)
- Ernst & Young, 2017. Indian Metals & Mining.
- Fan, J., Qiu, G., Jiang, T., Guo, Y., Hao, H., Yang, Y., 2012. Mechanism of high pressure roll grinding on compression strength of oxidized hematite pellets. *J. Cent. South Univ.* 19, 2611–2619. <https://doi.org/10.1007/s11771-012-1318-5>
- Fan, X., Yang, G., Chen, X., 2015. Evaluation model on the ballability of iron ore concentrates. *Powder Technol.* 280, 219–226. <https://doi.org/10.1016/j.powtec.2015.04.068>
- Forsmo, S.P.E., Apelqvist, A.J., Björkman, B.M.T., Samskog, P.O., 2006. Binding mechanisms in wet iron ore green pellets with a bentonite binder. *Powder Technol.* 197

169, 147–158. <https://doi.org/10.1016/j.powtec.2006.08.008>

Forsmo, S.P.E., Samskog, P.O., Björkman, B.M.T., 2008. A study on plasticity and compression strength in wet iron ore green pellets related to real process variations in raw material fineness. *Powder Technol.* 181, 321–330. <https://doi.org/10.1016/j.powtec.2007.05.023>

Gupta, R., 2015. Theory and Laboratory Experiments in Ferrous Metallurgy. PHI Learning Private Limited, Delhi.

Hamilton, J.D.G., Hoskins, B.F., Mumme, W.G., Borbridge, W.E., Montague, M.A., 1989. The crystal structure and crystal chemistry of Ca<sub>2.3</sub>Mg<sub>0.8</sub>Al<sub>1.5</sub>Si<sub>1.1</sub>Fe<sub>8.3</sub>O<sub>20</sub>(SFCA): solid solution limits and selected phase relationships of SFCA in the SiO<sub>2</sub>-Fe<sub>2</sub>O<sub>3</sub>-CaO(-Al<sub>2</sub>O<sub>3</sub>) system. *Neues Jahrb. fuer Mineral. - Abhandlungen* 161, 1–26.

Henderson, D.K., Machunter, D.M., 2000. A Review of Spiral Technology for Fine Gravity Beneficiation.

Hinkley, J., Waters, A.G., O'Dea, D., Litster, J.D., 1994. Voidage of ferrous sinter beds: new measurement technique and dependence on feed characteristics. *Int. J. Miner. Process.* 41, 53–69. [https://doi.org/10.1016/0301-7516\(94\)90005-1](https://doi.org/10.1016/0301-7516(94)90005-1)

Hino, M., Nagasaka, T., Katsumata, A., Higuchi, K.I., Yamaguchi, K., Kon-No, N., 1999. Simulation of primary-slag melting behavior in the cohesive zone of a blast furnace, considering the effect of Al<sub>2</sub>O<sub>3</sub>, Fe<sub>3</sub>O<sub>4</sub>, and basicity in the sinter ore. *Metall. Mater. Trans. B Process. Metall. Mater. Process. Sci.* 30, 671–683. <https://doi.org/10.1007/s11663-999-0028-3>

IBM, 2008. Iron & Steel Vision 2020.

Indian Bureau of Mines, 2018. Indian Minerals Yearbook 2017 - Iron Ore. p. 23.

Jankovic, A., 2015. Developments in iron ore 8 comminution and classification technologies, in: Lu, L. (Ed.), Iron Ore. Woodhead Publishing Series in Metals and Surface Engineering: Number 66, pp. 251–282.

Kasai, E., Rankin, W.J., Gannon, J.F., 2008. The effect of raw mixture properties on bed

permeability during sintering. *ISIJ Int.* 29, 33–42.

<https://doi.org/10.2355/isijinternational.29.33>

Kawatra, S.K., Halt, J.A., 2011. Binding effects in hematite and magnetite concentrates. *Int. J. Miner. Process.* 99, 39–42. <https://doi.org/10.1016/j.minpro.2011.03.001>

Krishna, S.J.G., Rudrappa, C., Ravi, B.P., Rudramuniyappa, M.V., 2015. Optimization of an Iron Ore Washing Plant. *Procedia Earth Planet. Sci.* 11, 111–114. <https://doi.org/10.1016/j.proeps.2015.06.014>

Loo, C.E., Tame, N., Penny, G.C., 2012. Effect of Iron Ores and Sintering Conditions on Flame Front Properties. *ISIJ Int.* 52, 967–976. <https://doi.org/10.2355/isijinternational.52.967>

Lu, L., 2015. Iron Ore-Mineralogy, Processing and Environmental Sustainability. WOODHEAD Publishing ( Elsevier).

Malysheva, T.Y., Pavlov, R.M., Mansurova, N.R., Detkova, T. V., 2015. Influence of ore formation on the mineral composition and strength of fluxed iron-ore sinter. *Steel Transl.* 45, 190–194. <https://doi.org/10.3103/s0967091215030134>

Malysheva, T.Y., Yusfin, Y.S., Mansurova, N.R., Gibadulin, M.F., Lekin, V.P., 2007. Mechanism of mineral formation and metallurgical properties of sinter of basicity 1.1–3.1 at OAO MMK. *Steel Transl.* 37, 126–130. <https://doi.org/10.3103/s0967091207020118>

Matsui, T., Ishiwata, N., Hara, Y., Takeda, K., 2004. Influence of Gangue Composition on Melting Behavior of Coal-Reduced Iron Mixture 44, 2105–2111.

Meer, F.P. Van Der, 2015. Pellet feed grinding by HPGR. *Miner. Eng.* 73, 21–30. <https://doi.org/10.1016/j.mineng.2014.12.018>

Meyer, K., 1980. Pelletizing of Iron Ore Fines. Springer-Verlag.

Millard, M., 2015. Beneficiation – Concentration, in: Cost Estimation Handbook. pp. 267–294.

Mills, C., 1978. Process design, scale-up and plant design for gravity concentration, in:

Mineral Processing Plant Design. AIMME, New York.

Mishra, A., Kumar, N., and Mukherjee, M., 2017. Iron ore tailing beneficiation via floatation process – A review ., in: Internation Seminar on Mineral Processing Technology.

Mohanty, S., Das, B., 2010. Optimization studies of hydrocyclone for beneficiation of iron ore slimes. Miner. Process. Extr. Metall. Rev. 31, 86–96.

<https://doi.org/10.1080/08827500903397142>

Mos, Y.M., Vermeulen, A.C., Buisman, C.J.N., Weijma, J., 2018. X-Ray Diffraction of Iron Containing Samples: The Importance of a Suitable Configuration. Geomicrobiol. J. 35, 511–517. <https://doi.org/10.1080/01490451.2017.1401183>

Mukherjee, A.K., Thella, J.S., Makhija, D., Patra, A.S., Manna, M., Ghosh, T.K., 2015. Process to recover iron values from high-alumina Indian iron ore slime - A bench-scale study. Miner. Process. Extr. Metall. Rev. 36, 39–44.

<https://doi.org/10.1080/08827508.2013.867854>

Nyembwe, A.M., Cromarty, R.D., Garbers-Craig, A.M., 2017. Relationship Between Iron Ore Granulation Mechanisms, Granule Shapes, and Sinter Bed Permeability. Miner. Process. Extr. Metall. Rev. 38, 388–402.

<https://doi.org/10.1080/08827508.2017.1323750>

Omori, Y., Takahashi, Y., 1977. Test method for evaluating the properties of Iron ore agglomerates at Temperature over 1100C, in: K.V.S.Sastry (Ed.), Second International Symposium on Agglomeration. Atlanta, Ga, p. 287.

Oyama, Nobuyuki, SATO, Hideaki, TAKEDA, Kanji, ARIYAMA, Tatsuro, MASUMOTO, Shinichi, JINNO, Tetsuya, FUJII, Norifumi, OYAMA, N., SATO, H., TAKEDA, K., ARIYAMA, T., MASUMOTO, S., JINNO, T., FUJII, N., 2005. Development of coating granulation process at commercial sintering plant for improving productivity and reducibility. ISIJ Int. 45, 10. <https://doi.org/10.2355/isijinternational.45.817>

Pal, J., Ghorai, S., Das, A., 2015. Development of carbon composite iron ore micropellets

- by using the microfines of iron ore and carbon-bearing materials in iron making. *Int. J. Miner. Metall. Mater.* 22, 132–140. <https://doi.org/10.1007/s12613-015-1053-7>
- Panigrahy, S.C., Verstraeten, P., Dilewijns, J., 1984. The effect of the addition of MgO on mineralogy of iron ore Agglomerates. *Metall. Trans. B* 15, 23–32.  
<https://doi.org/10.1007/BF02661059>
- Pansu, M., Gautheyrou, J., 2006. *Handbook of Soil Analysis*. Springer-Verlag Berlin Heidelberg. <https://doi.org/10.1007/978-3-540-31211-6>
- Panychev, A.A., Nikonova, A.P., 2009. Effect of the composition of the raw materials on the strength of sinter made from Mikhailovskii and Lebedinskii concentrates. *Metallurgist* 53, 713–717. <https://doi.org/10.1007/s11015-010-9237-x>
- Patrick, T.R.C., Pownceby, M.I., 2002. Stability of silico-ferrite of calcium and aluminum (SFCA) in air-solid solution limits between 1240 °C and 1390 °C and phase relationships within the Fe<sub>2</sub>O<sub>3</sub>-CaO-Al<sub>2</sub>O<sub>3</sub>-SiO<sub>2</sub> (FCAS) system. *Metall. Mater. Trans. B* 33, 79–89.
- Pietsch, W., 1997. Size Enlargement by Agglomeration, in: Fayed, M., Otten, L. (Eds.), *Handbook of Powder Science & Technology*. Springer, Boston, MA, pp. 202–377.
- Poveromo, J.J., 2000. Iron Ores, in: *Making Shaping Treating of Steel*. The AISE steel foudation, Pittsburgh, PA, pp. 547–642.
- Reviews, P.-I.I.I.M., 2018. *Yearbook 2017 MINISTRY OF MINES INDIAN BUREAU OF MINES 2017*, 1–5.
- Rocha, L., Canado, R.Z.L., Peres, A.E.C., 2010. Iron ore slimes flotation. *Miner. Eng.* 23, 842–845. <https://doi.org/10.1016/j.mineng.2010.03.009>
- Rumpf, H., 1962. The strength of granules and agglomerates, in: Knepper, W.. (Ed.), *Agglomeration*. pp. 379–418.
- Sahoo, H., Rath, S.S., Rao, D.S., Mishra, B.K., Das, B., 2016a. Role of silica and alumina content in the flotation of iron ores. *Int. J. Miner. Process.* 148, 83–91. <https://doi.org/10.1016/j.minpro.2016.01.021>

Sahoo, H., Rath, S.S., Rao, D.S., Mishra, B.K., Das, B., 2016b. Role of silica and alumina content in the flotation of iron ores. *Int. J. Miner. Process.* 148, 83–91.

Sastry, K.V.S., Fuerstenau, D.W., 1972. Ballability index to quantify agglomerate growth by green pelletization. *AIME Trans.* 254–258.

Scarlett, N.V.Y., Pownceby, M.I., Madsen, I.C., Christensen, A.N., 2004. Reaction sequences in the formation of silico-ferrites of calcium and aluminum in iron ore sinter. *Metall. Mater. Trans. B Process Metall. Mater. Process. Sci.* 35, 929–936. <https://doi.org/10.1007/s11663-004-0087-4>

Seifelnassr, A.A.S., Moslim, E.M., Abouzeid, A.-Z.M., 2013. Concentration of a Sudanese low-grade iron ore. *Int. J. Miner. Process.* 122, 59–62.

<https://doi.org/10.1016/j.minpro.2013.04.001>

Sharma, J., Sharma, T., Mandre, N.R., 2015. Processing of Goethitic Iron Ore Fines. *J. Inst. Eng. Ser. D* 96, 143–149. <https://doi.org/10.1007/s40033-015-0075-7>

Sinnott, R., 2005. *Chemical Engineering Design*. Elsevier Butterworth-Heinemann, Linacre House, Jordan Hill, Oxford OX2 8DP.

Sorby, H., 1858. On the Microscopical, Structure of Crystals, indicating the Origin of Minerals and Rocks. *Q. J. Geol. Soc.* 453–500.

Srb, J., Ruzickova, Z., 1988. Pelletization of fines. *Dev. Miner. Process.* 7.

Srivastava, M.P., Pan, S.K., Prasad, N., Mishra, B.K., 2001. Characterization and processing of iron ore fines of Kiruburu deposit of India. *Int. J. Miner. Process.* 61, 93–107.

[https://doi.org/10.1016/S0301-7516\(00\)00030-2](https://doi.org/10.1016/S0301-7516(00)00030-2)

Srivastava, U., Kawatra, S.K., Eisele, T.C., 2013. Study of organic and inorganic binders on strength of iron oxide pellets. *Metall. Mater. Trans. B Process Metall. Mater. Process. Sci.* 44, 1000–1009. <https://doi.org/10.1007/s11663-013-9838-4>

Steel, Ministry. of, 2017. National Steel Policy 2017. GOI 40–42.

Steinberg, M., Graham, T., Gerards, M., 2015. Recovery of iron ore fines and ultrafines from Tailing by Using Wet High-intensity Magnetic Separator- JINES WHIMS, in: 202

Iron Ore Conference. pp. 191–196.

Thella, J.S., Mukherjee, A.K., Srikakulapu, N.G., 2012. Processing of high alumina iron ore slimes using classification and flotation. *Powder Technol.* 217, 418–426.

<https://doi.org/10.1016/j.powtec.2011.10.058>

Tigerschiöld, M., Ilmoni, P., 1950. Fundamental factors influencing the strength of green and burned pellets made from fine magnetite-ore concentrates, in: *Proc. Blast Furnace, Coke Oven Raw Materials*. pp. 18–45.

Vega-Garcia, D., Brito-Parada, P.R., Cilliers, J.J., 2018. Optimising small hydrocyclone design using 3D printing and CFD simulations. *Chem. Eng. J.* 350, 653–659.

<https://doi.org/10.1016/j.cej.2018.06.016>

Webster, Nathan A S, Pownceby, M.I., Madsen, I.C., 2012. Phase Formation in Iron Ore Sintering. *High Temp. Process. Symp.* 2012 10–12.

Webster, Nathan A.S., Pownceby, M.I., Madsen, I.C., Kimpton, J.A., 2012. Silico-ferrite of calcium and aluminum (SFCA) iron ore sinter bonding phases: New insights into their formation during heating and cooling. *Metall. Mater. Trans. B Process Metall. Mater. Process. Sci.* 43, 1344–1357. <https://doi.org/10.1007/s11663-012-9740-5>

Webster, N.A.S., Pownceby, M.I., Madsen, I.C., Studer, A.J., Manuel, J.R., Kimpton, J.A., 2014. Fundamentals of Silico-Ferrite of Calcium and Aluminum (SFCA) and SFCA-I Iron Ore Sinter Bonding Phase Formation: Effects of CaO:SiO<sub>2</sub> Ratio. *Metall. Mater. Trans. B Process Metall. Mater. Process. Sci.* 45, 2097–2105. <https://doi.org/10.1007/s11663-014-0137-5>

Wills, B.A., 1988a. Gravity Concentration. *Miner. Process. Technol.* 377–419. <https://doi.org/10.1016/B978-0-08-034937-4.50019-3>

Wills, B.A., 1988b. Magnetic and High-Tension Separation. *Miner. Process. Technol.* 596–634. <https://doi.org/10.1016/B978-0-08-034937-4.50022-3>

Wills, B.A., Napier-Munn, T., 2006. *Mineral Processing Technology*, Elsevier Science & Technology Books. <https://doi.org/10.1016/b978-075064450-1/50000-x>

Yang, L.X., 2006. Sintering Fundamentals of Magnetite Alone and Blended with Hematite and Hematite/Goethite Ores. *ISIJ Int.* 45, 469–476.

<https://doi.org/10.2355/isijinternational.45.469>

YANG, L.X., DAVIS, L., 1999. Assimilation and Mineral Formation during Sintering for Blends Containing Magnetite Concentrate and Hematite/Piso Iite Sintering Fines. *ISIJ Int.* 39, 239–245.

Yu, Z., Li, G., Jiang, T., Zhang, Y., Zhou, F., Peng, Z., 2015. Effect of Basicity on Titanomagnetite Concentrate Sintering. *ISIJ Int.* 55, 907–909.

<https://doi.org/10.2355/isijinternational.55.907>

Zhou, M., Zhou, H., O’dea, D.P., Ellis, B.G., Honeyands, T., Guo, X., 2017. Characterization of Granule Structure and Packed Bed Properties of Iron Ore Sinter Feeds that Contain Concentrate. *ISIJ Int.* 57, 1004–1011.  
<https://doi.org/10.2355/isijinternational.isijint-2016-734>

Zhu, D., Pan, J., Lu, L., Holmes, R.J., South, C., 2015. Iron Ore Pelletization, in: Iron Ore. WOODHEAD Publishing ( Elsevier), pp. 435–476.

Zhu, D., Pan, J., Qiu, G., Clout, J., Wang, C., Guo, Y., Hu, C., 2008. Mechano-chemical Activation of Magnetite Concentrate for Improving Its Pelletability by High Pressure Roll Grinding. *ISIJ Int.* 44, 310–315. <https://doi.org/10.2355/isijinternational.44.310>

# List of Publications

## ***Journal Publication***

Vibhuti Roshan, Kamlesh Kumar, Rajan Kumar, G. V. S. Nageswara Rao, *Preparation of Iron Ore Micro-pellets and Their Effect on Sinter Bed Permeability*, Trans Indian Inst Met- Springer (2018) 71: 2157-2164.

## ***Conference presentations:***

1. Vibhuti Roshan, S.K.Sharma and G. V. S. Nageswara Rao, Iron Ore preparation for use in Iron making processes, presented in NMD-ATM 2012 held at Jamshedpur during 16<sup>th</sup> to 19<sup>th</sup> November 2012.
2. Vibhuti Roshan, S.K.Sharma and G. V. S. Nageswara Rao, Study of effect of surface area on micro pellets green properties, Presented at International Conference on Science and Technology of Ironmaking and Steelmaking (STIS-2013), NML, Jamshedpur during 16<sup>th</sup>- 18<sup>th</sup> December 2012.
3. Vibhuti Roshan, S.K.Sharma, Kamlesh Kumar and G. V. S. Nageswara Rao, Impact of suction pressure on the iron ore hybrid sinter properties, presented in NMD-ATM 2013 held at IIT BHU, Varanasi during 12<sup>th</sup> to 15<sup>th</sup> November 2013.
4. Vibhuti Roshan, S.K.Sharma , Kamlesh Kumar and G. V. S. Nageswara Rao, Effect of bed height of properties of hybrid pellet sinter produced from Bialadila slimes, presented in NMD-ATM 2014 held at College of Engineering, Pune during 12<sup>th</sup> to 15<sup>th</sup> November 2014.
5. Vibhuti Roshan, Kamlesh Kumar, Rajan Kumar and G. V. S. Nageswara Rao, Improvement of iron ore sinter bed permeability through addition of micro-pellets, presented in NMD-ATM 2017, held at BITS Goa Campus during 11<sup>th</sup> to 14<sup>th</sup> November 2017.

## Preparation of Iron Ore Micro-pellets and Their Effect on Sinter Bed Permeability

Vibhuti Roshan<sup>1,2</sup> · Kamlesh Kumar<sup>2</sup> · Rajan Kumar<sup>2</sup> · G. V. S. Nageswara Rao<sup>1</sup>

Received: 22 August 2017 / Accepted: 4 June 2018  
© The Indian Institute of Metals - IIM 2018

**Abstract** At present around 6–7% of iron ore slimes, out of total production, are being generated and accumulated at iron ore mine sites of National Mineral Development Corporation Limited, India. The accumulated slimes of finer size and relatively inferior grade should be utilized in an economical way for sustainable mining. These slimes can be agglomerated into micro-pellets for subsequent use in sinter making through hybrid pellet sintering method. However, the micro-pellets of sufficient size and strength are required for hybrid sinter making. The green properties of the micro-pellets depend upon various parameters such as surface area, moisture, binder, etc. In this study, iron ore slimes were beneficiated through gravity, and magnetic separation and concentrate of grade 65% Fe (Total) was obtained. Since the concentrate obtained had low surface area (700–900 cm<sup>2</sup>/grams) rendering it unsuitable for micro-pellet making, it was further subjected to grinding in a ball mill. The requirement of surface area for producing an optimum quality of green micro-pellets was established. The resultant micro-pellets were further used in studying sinter bed properties. The effect of moisture and size of micro-pellets on permeability of sinter bed were examined. The results confirmed that the addition of micro-pellets to the sinter mix improved the permeability of the sinter bed. The sinter bed with highest permeability of JPU 25.25 and void fraction of 36.27% was achieved with micro-pellets of size 3–6 mm at 7% moisture level. Mean granule size of

sinter mix was also studied with respect to moisture content and size of the micro-pellets.

**Keywords** Iron ore slimes · Micro-pellets · Saturation · Sinter bed · Permeability · Void fraction

### 1 Introduction

A huge quantity of iron ore slime is being accumulated during operation of iron ore processing plant of National Mineral Development Corporation (NMDC) Limited, India for last many years. These slimes were stored in tailing dam situated near iron ore mine. Invariably all the mines were located in reserved forest area and acquiring land for construction of another tailing dam is difficult. At present about 20 MT slime is dumped in tailing dams at Bailadila mines and these dams are on the verge of filling. Hence these slimes need to be economically utilized so that additional space can be created for storage of fresh slimes. NMDC Ltd. has taken two prong strategies to deal with slimes; one is to improve the efficiency of the iron ore processing plant. As a result, the present level of slimes generation has reduced to 6–7% against 12–14% a few years back. Second is to explore possible avenues for economical utilization of slime including utilization of slimes in pelletization, smelt reduction process (Hismelt & Romelt), Iron making Technology Mark 3 (ITMK3) process etc. The iron ore fines with less than 10 mm size are usually fed to the sintering process, and only limited fraction (less than 20%) of – 150 micron size of iron ore fines are allowed in the sintering process. The finer sized iron ore may choke the sinter bed and hinder the uniform air suction through the bed. As a result, sinter formation would be affected due to incomplete combustion of coke.

✉ G. V. S. Nageswara Rao  
nr\_gvs@yahoo.com

<sup>1</sup> Metallurgical and Materials Engineering Department,  
National Institute of Technology, Warangal 506 004, India

<sup>2</sup> R&D Centre, National Mineral Development Corporation  
Ltd., Hyderabad 500 076, India

The iron ore slimes can also be utilized in sinter making with or without beneficiation through hybrid pellet sintering.

In hybrid pellet sintering process, iron ore concentrate of relatively finer size is first converted into micro-pellets and these micro-pellets are used in place of iron ore fines. The prerequisite for micro-pellets to be used in hybrid sintering is to have sufficient green strength so that they do not get disintegrated during mixing with other raw materials and during charging on the sinter machine. The works on the preparation of micropellets with sufficient strength containing iron ore fines and coal bearing material for uses in iron making have been reported in the literature [1]. The primary factors influencing the formation of green micro balls and their properties are enumerated as electrostatic forces, Van der Waals forces, surface properties, magnetic forces and individual material characteristics [2–4]. During addition of water for micro-pellets making, the capillary forces also play a significant role in the formation of micro-pellets and thus providing strength to the green micro-pellets [5]. The surface properties can be defined by particle distribution and their size, crystalline structure and particle shape. Similarly, individual material characteristics can be defined as wettability, liquid absorptive capacity due to porous structure, etc. [6].

During sintering, the intimately mixed iron bearing material with other raw materials is fed to the grate and the top layer of bed is ignited by the gas burner. The heat transfer through the sinter bed depends upon the air resistance offered by the bed or ability to permeate air through the bed [7]. Thus, the permeability of the sinter bed is a very important parameter. A good permeability of the sinter bed is desirable to transfer heat from the top layer to the bottom layer in shorter time and to obtain better productivity of the sinter plant [7]. The improvement in permeability and sinter quality has been reported through addition of micro-pellets in the iron ore fines [8]. The air flow through the packed sinter bed is also dependent on void fraction and mean particle diameter [7, 9].

In the present study, iron ore slimes of – 150 micron size were used for making micro-pellets of sufficient size and strength by using disc pelletizer. The requirement of surface area for producing an optimum quality of green micro-pellets with respect to size and strength was established. The effect of moisture content, binder content and specific surface area of iron ore fines on properties of green micro-pellets was studied. These micro-pellets were used as feed stock for preparation of sinter bed in a pot grate furnace. The effect of moisture content and size of micro-pellets on permeability of sinter bed were studied. Mean granule size of sinter mix was also studied with respect to moisture content and size of the micro-pellets.

## 2 Experimental

### 2.1 Materials and Methods

Iron ore slimes from Bailadila-5 (India) mines were used for the present study. The specific surface area (also known as Blain number) of as received slime was  $821 \text{ cm}^2/\text{g}$ . Initially, the slimes were subjected to beneficiation by gravity separation and magnetic separation, followed by wet grinding and filtration to obtain the concentrate. The concentrate was obtained with 87.31% recovery and contained 65.74% Fe, 2.18%  $\text{SiO}_2$  and 1.64%  $\text{Al}_2\text{O}_3$ . Subsequently, the concentrate was subjected to screening using 45 and 90 micron sized sieves. 67.6% concentrate was passed through 45 micron sized sieve and 96.8% concentrate was passed through 90 micron sized sieve. A cyclone was used for analysis of fine tails (– 45 microns) and the results indicated that 18.5% of iron ore fines were below 9.4 micron size. The Fisher's particle size analyzer, utilizing air permeability method, was used for measurement of the surface area of iron ore concentrate obtained after beneficiation followed by close circuit ball mill grinding. The specific surface area and specific gravity of the concentrate were found to be  $1610 \text{ cm}^2/\text{g}$  and  $5.21 \text{ g/cm}^3$  respectively. Finely ground bentonite (– 75 microns) containing 54.0%  $\text{SiO}_2$  and 13.0%  $\text{Al}_2\text{O}_3$  was used as binder for micro-pellet making. The binder was dried in the air oven for overnight at  $105^\circ\text{C}$  before using in micro pelletizing. Prior to use in micro-pellet making, the suitability of the binder was tested by soaking in distilled water for 4 h and the volume increase of binder was found to be 819%, which was more than that required, i.e. 800% [9]. To study the effect of specific surface area on properties of the micro-pellets, the iron ore concentrate was further subjected to grinding in a ball mill for different times to obtain iron ore fines with different Blain numbers. The ball mill details and Blain numbers obtained at different times of grinding operation are presented in Table 1.

### 2.2 Preparation of Micro-pellets

In the pelletizing phase, the preparation and characterization of green micro-pellets was attempted before sintering process. After homogenization of the sample (iron ore concentrate), the first step was to determine chemistry, size analysis, and specific surface area. The need for any additional grinding should become apparent from this information and the required additives or binder could be initially selected. This may require modification during later testing to correct or improve properties of pellets produced. The effect of moisture content, binder content and specific surface area of iron ore fines on properties of

**Table 1** Details of ball mill used for grinding and Blain numbers at different stages

Details of ball mill	Specific surface area/Blain number (cm <sup>2</sup> /g)	
Length: 45 in.	Initial iron ore concentrate	1610
Diameter: 30 in.	After dry grinding for 45 min	1780
Speed of rotation: 12 rpm	After dry grinding for 1 h	1930
Ball size: 20 mm		
Ball weight: 150 kg		

green micro-pellets was studied. For studying the effect of moisture content, the amount of binder content and specific surface area of iron ore fines were fixed at 0.5% and 1610 cm<sup>2</sup>/g respectively and the moisture content was varied between 8 and 9.5%. Similarly for studying the effect of binder content, the specific surface area of iron ore fines was fixed as 1610 cm<sup>2</sup>/g and the binder content was varied between 0 and 1.25%. For studying the effect of specific surface area, the binder and moisture contents were maintained at 0.5 and 9.25% respectively and three different iron ore fines with specific surface area 1610 cm<sup>2</sup>/g, 1780 cm<sup>2</sup>/g and 1930 cm<sup>2</sup>/g were used. The iron ore, moisture, and binder were thoroughly mixed in predetermined proportions in a Muller before feeding to 1 m diameter disc pelletizer. The rotational speed of the pelletizer was maintained at 20 rpm while the disc was inclined at an angle of 45° in all experiments. During pelletizing process, the micro-pellets were continuously withdrawn and screening was done. The micro-pellets of + 3 mm size were collected as feed for sintering and - 3 mm size pellets were again charged into the disc pelletizer. To achieve the correct composition and green properties of micro-pellets, the optimization of green micro-pellet properties were carried out. This was done with the aim of using a minimum amount of bentonite for getting desired green pellet properties at the minimum specific surface area [10]. Green micro-pellets with varying amounts of moisture, binder and specific surface area were produced and characterized.

### 2.3 Characterization of Green Micro-pellets

The micro-pellets obtained were analysed to determine various properties such as green crushing strength, impact strength, porosity, moisture content, absolute density and envelop volume. The crushing strength of green micro-pellets was measured by green crushing strength (GCS) equipment of capacity 50 kg (500 N) with least count of 10 g (0.01 N) [11]. During measurement of GCS, the pressure drop of 10% after reaching the maximum load was taken as breakage point. The impact strength of the green pellet was measured by drop number. The amount of

moisture in the green pellet was determined by drying in the air oven at 105 °C, and weight loss was recorded at an interval of 30 min. The moisture determination was concluded when two successive weight measurement differences was less than 0.02 g. Gas displacement pycnometer (AccuPyc 1330) was used to measure absolute density. The envelope volume of the green pellet was measured in the GeoPyc 1360 instrument by using dry flow material. The porosity of micro-pellets was also measured by using GeoPyc instrument after drying the pellets from the measured absolute density and envelope volume.

### 2.4 Preparation of Sinter Bed and Evaluation of Sinter Bed Properties

The small grate pot unit was used for the measurement of permeability, void fraction and mean granule size of green sinter bed. The sinter mix consisted of micro-pellets, fluxes, coke breeze, and return sinter. For each test, all raw materials including moisture were mixed in drum mixer and the mixed charge was transferred into a pot grate (tube) up to a height of 500 mm bed. 1 mm grate spacing was maintained in the pot to retain finer particles without hearth layer. A venturi equipped with a differential pressure gauge was placed at the top of the pot and sealed properly. Air was passed through the green packed bed to measure permeability. The pressure drop across the bed was measured and reported as Japanese Permeability Unit (JPU). The air flow through the packed bed was manually adjusted with the help of knob to maintain a pressure drop of 1000 mm of water level through green bed. The air flow was measured by venturi. The permeability, expressed in JPU [12], of the packed bed was determined by using the following formula.

$$JPU = \frac{Q}{A} \times \left( \frac{h}{\Delta P} \right)^{0.6} \quad (1)$$

where Q is the air flow rate (m<sup>3</sup>/min), A is the cross sectional area of the bed (m<sup>2</sup>), h is the bed height (mm) and, ΔP is the pressure drop across the bed (mm of water). The void fraction (ε) in the green bed was estimated from the following formula developed by Hinkley [13].

$$\varepsilon = 1 - \frac{\rho_b}{\rho_a} \quad (2)$$

where  $\rho_b$  is the bulk density and  $\rho_a$  is the apparent density. The bulk density was measured by comparing the masses of full and empty 1 l flask and the apparent density was accurately determined by kerosene displacement method [13]. The apparent density was calculated by the equation:

$$\rho_a = \frac{M_{tot} - M_{ker}}{500ml - V_m} \quad (3)$$

where  $M_{tot}$  is the total mass of the flask,  $M_{ker}$  is the mass of the flask filled with 500 ml of kerosene before pouring granules into the flask and  $V_m$  is the volume of kerosene required to fill the flask up to the 1 l mark.

The mean granule size, also known as Sauter mean diameter [14], of the granules was determined from the size distribution of the sinter mix using the equation:

$$d_p = \frac{100}{\sum_i \frac{X_i}{d_{pi}}} \quad (4)$$

where  $d_p$  is the Sauter mean diameter,  $X_i$  is the mass percent (wet basis) of granule's size fraction, and  $d_{pi}$  is the mean granule diameter for size fraction  $i$ .

### 3 Results

#### 3.1 Effect of Moisture Content on the Properties of Green Micro-pellets

For studying the effect of moisture content on the properties of green pellets, the amount of binder is kept constant at 0.5% and the specific area of iron ore fines is fixed at  $1610 \text{ cm}^2/\text{g}$  and moisture content is varied between 8.0 and 9.5%. According to the capillary theory, at  $S$  (Liquid saturation) = 100%, i.e. in the case of 100% water saturation, the situation is called flooding, and the micro-pellet deform either due to its own weight or weight of the pellet placed over it. During further processing, the micro-pellet needs to be dried and while drying the primary binding force changes from capillary forces to the liquid bridge. Literature [2] suggests that after a point of  $S = 30\%$ , the liquid bridge become predominant than capillary forces. After that, the strength of the pellet is provided by liquid bridges. 35% of the total strength of micro-pellets is contributed by fully developed liquid bridges ( $S = 30\%$ ).

$$S = \frac{100F}{100 - F} \cdot \frac{1 - \varepsilon}{\varepsilon} \cdot \frac{\rho_p}{\rho_L} \quad (5)$$

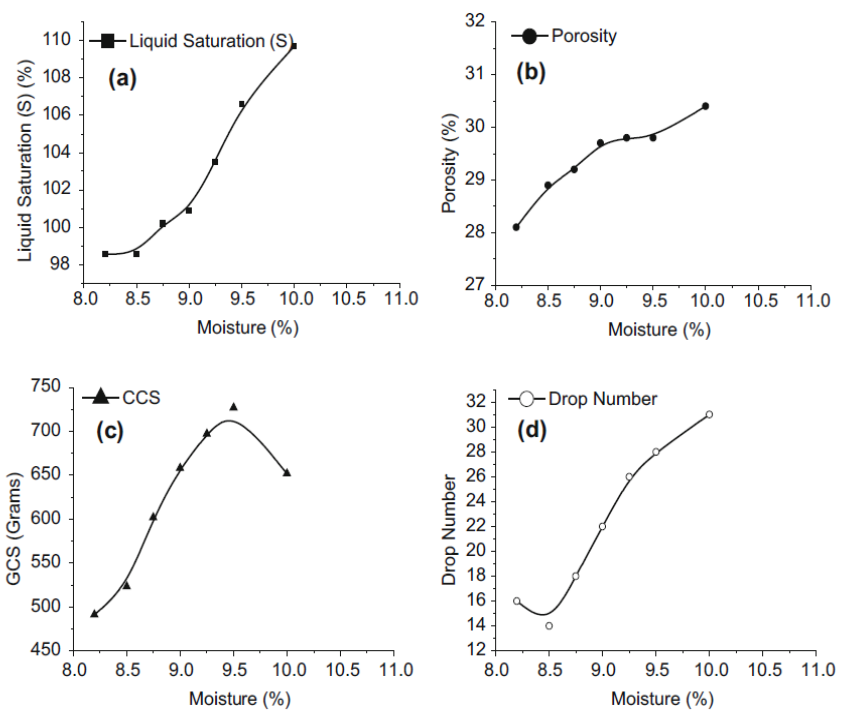
where  $S$  = liquid saturation;  $\varepsilon$  = fractional porosity;  $F$  = moisture content determined through air oven drying;  $\rho_L$ ,  $\rho_p$  = true density for water and particles respectively.

Equation (5) has been used to calculate liquid saturation ( $S$ ), and its variation with moisture content is presented in Fig. 1a. Liquid saturation is increased with increasing moisture content. 100% liquid saturation can be achieved at around 8.75% moisture content. It means that the green micro-pellets can be obtained with 8.75% moisture content in 1 m diameter disc pelletizer. It is observed that once the moisture content crosses 8.75%, the pellet growth can be achieved by spraying more water. The effect of moisture on green porosity of the micro-pellet is shown in Fig. 1b. The porosity increases with moisture content. The variation of physical strength (i.e. GCS) with moisture content is shown in Fig. 1c. The GCS increases with increasing moisture content up to 9.5% and thereafter decreases. The micro-pellets produced with moisture content below 8.75% are under saturated and have lower physical strength (Fig. 1c) with relatively good porosity values (Fig. 1b). During green balling it is observed that once 100% liquid saturation point is crossed, further balling process become self-controlled in such a way that the liquid saturation remains constant. Further addition of moisture has the direct impact on the porosity and physical strength [15]; as explained before, the porosity increases with moisture content and physical strength of pellet increases with moisture content till 9.5% and deteriorates thereafter. The drop number can be measured with varying moisture content, keeping bentonite content constant at 0.5% and specific surface area of iron ore fines at  $1610 \text{ cm}^2/\text{g}$ . Figure 1d shows the variation of drop number with moisture content. The effect of moisture content in the micro-pellet can be seen as an increase in drop number. The drop number increases almost linearly with moisture content (8.5–9.5%). The results are in line with previous work [16]. It is observed that with increase in moisture content in micro-pellet, the plasticity behaviour sets and thus the drop number increases.

#### 3.2 Effect of Bentonite on Green Properties of Micro-pellets

In order to study the effect of bentonite on green properties of micro-pellets, the bentonite content in the feed mixture is varied between 0 and 1.25% keeping specific surface area of iron ore concentrate constant as  $1610 \text{ cm}^2/\text{g}$ . As the bentonite require higher moisture, hence it is difficult to maintain constant moisture in the relatively wider range of bentonite. Considering the moisture requirement of the binder, initial moisture content is found to be 9% in the green micro-pellet with 0% bentonite and gradually increases to 9.5% with 1.25% bentonite. Study on extra moisture requirement at higher bentonite content can be carried out through some additional tests separately. Bentonite addition and its corresponding moisture requirement

**Fig. 1** The variation of a liquid saturation, b porosity, c physical strength (GCS), and d drop number of micro-pellets with moisture content



are determined in the pellet feed. It is evident from the results that during balling, extra water spraying is necessary, though pellet feed contain higher moisture (up to 9.5%) content. In some cases, it is reported that the moisture content is as high as 9.8% in the green micro-pellets. Each test with varying bentonite content can be carried out at least twice and replicate batches of green micro-pellets are produced with each amount of binder. The average value of the GCS obtained from duplicate tests on green micro-pellets as a function of binder content is shown in Fig. 2. The mean value improves the repeatability and confidence level. From Fig. 2, it can be observed that both drop number and green crushing strength (GCS) of micro-pellets increases with increasing bentonite content.

### 3.3 Effect of Specific Surface Area on Properties of Green Micro-pellets

In order to study the effect of specific surface area on the properties of green micro-pellets, the micro-pellets are obtained by using iron ore fines with three specific surface areas viz. 1610, 1780 and 1930  $\text{cm}^2/\text{g}$  keeping constant bentonite (0.5%) and moisture content (9.25%). The properties of green micro-pellet have direct relation with surface area (also known as blain number) and binder content. Higher blain number will impart better green properties and higher bentonite (binder) content will

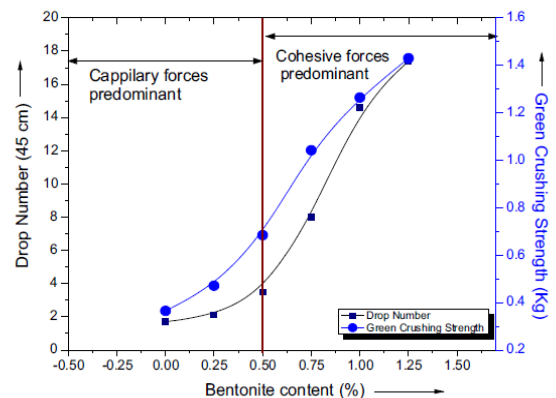


**Fig. 2** Variation of drop number and green crushing strength (GCS) with bentonite

improve overall properties of the green pellets [16]. However, higher blain number leads to increased cost of grinding. Hence it is critical to obtain optimum level of blain number or specific surface area in green micro-pellets. The properties of the green micro-pellets obtained are presented in Fig. 3. The micro-pellets obtained with a blain number of  $1610 \text{ cm}^2/\text{g}$  possesses low drop number and green crushing strength (GCS), thus they are not suitable as the industrially accepted drop number and GCS are 5 and 750 g respectively [9]. Whereas, although the micro-pellets

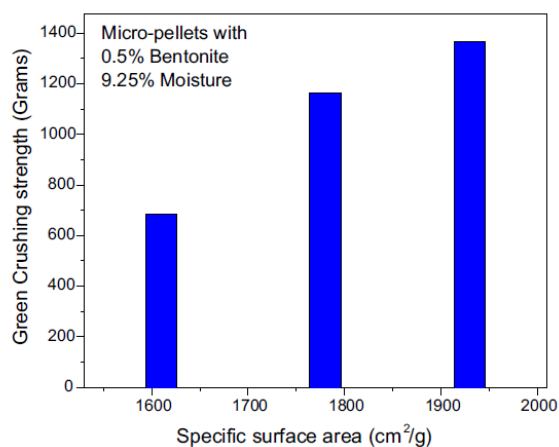


Fig. 3 Green crushing strength versus specific surface area

obtained with a blain number of  $1930 \text{ cm}^2/\text{g}$  possesses higher drop number and GCS, their porosity is low. Further, it also increases the grinding cost. The micro-pellets obtained with a blain number of  $1780 \text{ cm}^2/\text{g}$  possess optimum values of drop number, GCS and porosity. Hence, from these results, it is evident that the micro-pellets with desirable properties can be produced with a blain number of  $1780 \text{ cm}^2/\text{g}$  at 0.50% bentonite and 9.25% moisture contents.

#### 3.4 Effect of Moisture and Micro-pellets Size on Permeability, Void Fraction and Mean Granule Size of Sinter Bed

The effect of moisture on sinter bed permeability, void fraction of the bed and mean granule size of the bed has been evaluated by varying moisture content between 5.5 and 7.5% for different sizes of micro-pellets, viz. 1–3 mm (i.e. +1, –3 mm), 3–6 mm (i.e. +3, –6 mm) and 6–10 mm (i.e. +6, –10 mm) and the experimental results are shown in Fig. 4a–c.

## 4 Discussion

### 4.1 Physical Strength of Micro-pellets

The bentonite addition has positive impact on elastic deformation as shown in Fig. 2. Drop number increases with increase in bentonite content (Fig. 2). Green micro-pellets absorb kinetic energy due to formation of high viscous liquid phase at high shear rates. The elastic deformation of micro-pellet up to a certain extent is desirable to survive during mixing for hybrid sinter production in mixing drum. The physical strength of micro-

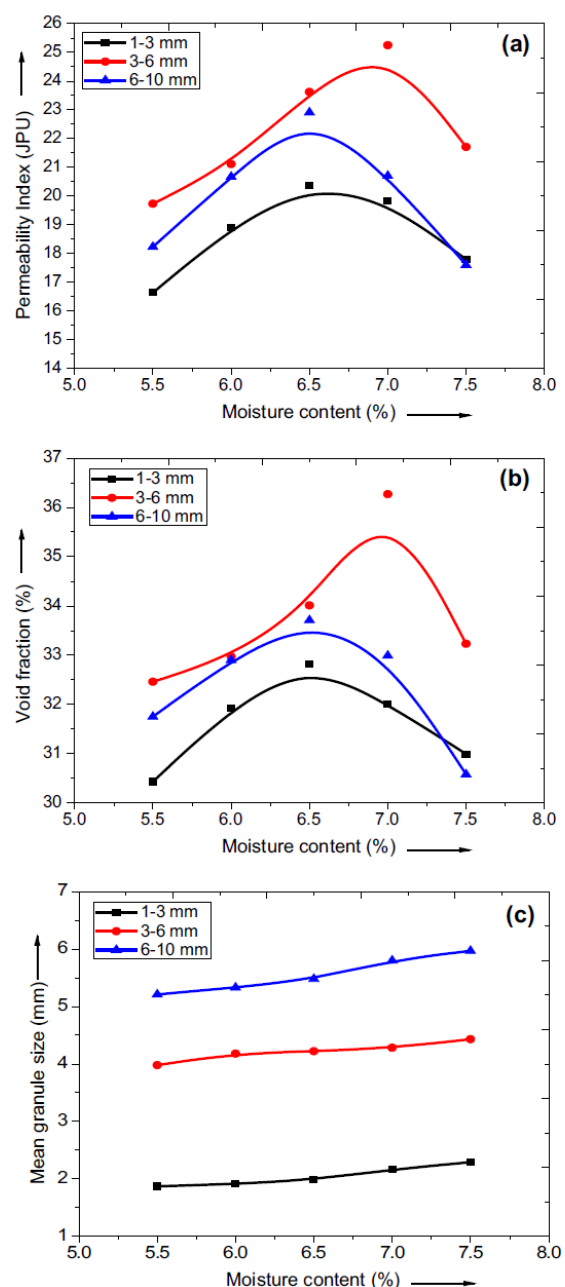


Fig. 4 Effect of moisture content on a permeability, b void fraction, and c mean granule size of sinter bed for different micro-pellet sizes

pellet can be demonstrated through drop number and minimum acceptable drop number (45 cm) is around five [2]. The drop number provide immediate indication of quality of micro-pellets produced; hence drop number is used for controlling the parameter to get optimum quality of micro-pellets. Drop number is mainly dependent on

quantity of bentonite and moisture added during pellet making. It is claimed that drop number is more important parameter than GCS due to its practical uses during micro-pellet making [13].

GCS largely depends upon binder (Bentonite) addition, and however moisture content also has little impact on GCS (Fig. 1). The literature suggests that GCS increases with increase in binder (bentonite) addition [17], the effect of binder (bentonite) addition on GCS can be classified into two segments. The cohesive force (viscous binder) and the capillary force (freely movable liquid) combination act as a main binding force, and it is suggested in literature that individual force contribution depends upon quantity of bentonite addition. At lower quantity of bentonite, the capillary forces predominantly provide strength to the green micro-pellets, however with increase in the quantity of bentonite, cohesive force or viscous binder become main binding force. From results (Fig. 2), it is evident that change over from capillary forces to cohesive force takes place at around 0.5% bentonite. Further addition of binder has significant improvement in the drop number of the green pellets. The improvement in drop number of green pellets indicates increase of elasticity of the green pellets. Therefore at higher amount of bentonite, the cohesive force (viscosity) become major binding forces and also set in high viscous behavior of the green pellets. The increase in adhesion of the particles also increases the wet compressive strength of the micro-pellets. The specific surface area, binder, and moisture requirement are interdependent; for higher content of binder, moisture requirement is higher for green micro-pellet making.

#### 4.2 Effect of Specific Surface Area on Properties of Micro-pellets

During the study, it is established that increase in the specific surface area results in better packing of particles which results in higher consolidation of the micro-pellet. In our micro-balling experiments, the time of formation of agglomerate is kept constant. The porosity of micro-pellets is highly influenced by specific surface area of iron ore and its pattern of consolidation, although the binder is maintained constant. The specific surface area of the feed material and quantity of moisture added in micro-pellets are the controlling factors of porosity of micro-pellets. The porosity of pellet is reduced from 30.3 to 25.8% with increase of specific surface area. This is indication of better consolidation of the particle at higher specific surface area. The improvement in drop number and wet compressive strength with increase of specific surface area is also an indication of better consolidation of particle during micro balling. Porosity is considered as very important parameter and should be more than 28%.

The increase in specific surface area has direct impact on GCS of micro-pellets. The GCS increases significantly with surface area (Fig. 3). The GCS is of utmost importance for micro-pellets to withstand strain and stress during mixing in drum before hybrid pellet sintering. Higher GCS at higher specific surface area may be attributed to better consolidation during green balling stage.

#### 4.3 Effect of Moisture Content and Size of Micro-pellets on Permeability, Void Fraction and Mean Granule Size of Sinter Bed

A high JPU and presence of higher void fraction indicate better permeability in the green sinter bed. It also indicates low resistance to air flow through green bed. The variation of permeability, void fraction and mean granule size with moisture content for different sizes of micro-pellets is shown in Fig. 4a–c respectively. As moisture content increases, the permeability of the bed initially increases and reaches a maximum value and then falls with further increase in moisture content for all sizes of micro-pellets (Fig. 4a). A similar trend can also be observed for void fraction (Fig. 4b). The mean granule size of the sinter bed is slightly increased with moisture content for all sizes of micro-pellets used. However, the size of micro-pellets significantly affect the mean granule size of the sinter bed. The higher the size of micro-pellets, the higher is the mean granule size (Fig. 4c).

The bed made of finer micro-pellets of size 1–3 mm demonstrate lower JPU and void fraction values at all moisture contents (Fig. 4a, b). The permeability Index (JPU) and void fraction of green sinter bed made of 1–3 mm and 6–10 mm sized micro-pellets increases with moisture content up to 6.5% (shows maximum) and further addition of moisture reduce both. However, the sinter bed made of 3–6 mm sized micro-pellets exhibit higher bed permeability and void fraction compared to the bed made of 1–3 and 6–10 mm sized micro-pellets, but at 7% moisture content. At 7.0% moisture level, the JPU value obtained is 25.25 and void fraction is 36.27%. Therefore, the results indicated that the minimum resistance to air flow can be expected for the bed made of 3–6 mm sized micro-pellets with 7% moisture content. High permeability and low resistance to air flow during sinter making are advantageous and desirable for production of good quality of sinter. Permeability index and void fraction for sinter bed of micro-pellets of size 6–10 mm are lower than the sinter bed made of micro-pellets of size 3–6 mm. The permeability of bed depends upon the void fraction present and mean diameter of the raw mix. The sinter bed of micro-pellets of size 6–10 mm has higher mean particle size of around (5.22–5.97 mm). The higher mean particle size creates bigger voids in the bed and smaller particles of

limestone (– 3 mm) and coke (– 3 mm) occupies these voids, which is instrumental in reducing the permeability and void fraction of sinter bed with micro-pellets of size 6–10 mm.

## 5 Conclusions

The micro-pellets with higher specific surface area exhibited better consolidation and as a result higher drop number and higher green crushing strength were achieved. The drop number has a direct correlation with elastic strength and should be sufficiently high to avoid fine generation during mixing of all raw materials for hybrid pellet sinter making. Similarly effect of addition of bentonite as binder on micro-pellets was established. It was evident from the results that the green properties of micro-pellets improved with addition of bentonite. However micro-pellets with sufficient strength were produced at bentonite content of 0.5%. The slime concentrate obtained after beneficiation of Bailadila-5 slimes exhibited excellent physical properties at 0.5% bentonite content and 9.25% moisture at a surface area 1780 cm<sup>2</sup>/gm. Hence this condition was considered optimized for micro-pellet production for hybrid pellet sinter making. The permeability of the sinter bed depended on moisture content and micro-pellet size. Maximum JPU and void fraction of 25.25 and 36.27% respectively were achieved with 3–6 mm micro-pellets at 7% moisture level. The sinter bed prepared with 3–6 mm micro-pellets showed better permeability than desired level. The sinter bed also offered very low resistance to air flow through the bed. These properties of sinter bed were helpful in improving the productivity of sinter.

**Acknowledgements** Authors are thankful to the management of NMDC Ltd., Hyderabad for giving permission to work at R&D Centre, NMDC Ltd. The support and services rendered by colleagues at Agglomeration Department, R&D Centre, NMDC Ltd. are also duly acknowledged.

## References

1. Pal J, Ghorai S, and Das A, *Int J Miner, Metall Mater* 22(2) (2015) 132.
2. Sastry, K V S, and Fuerstenau D W, *AIIME Trans* (1972), 254.
3. Rumpf H, in *Agglomeration*, (ed) Knepper W A (1962), p 379.
4. Forsmo S P E, Apelqvist A J, Björkman B M T, Samskog P-O, *Powder Technol*, 169 (2006) 147.
5. Eisele T C, and Kawatra S K, *Miner Process Extr Metall Rev* 24 (2003) 1.
6. Tigerschiöld M, and Ilmoni P, *Proc Blast Furnace Coke Oven Raw Mater Sess Ore Agglom*, 9 (1950) 18.
7. Poveromo J J, Iron Ores, 11th edition of *Making shaping and treating of steel (MSTS)*, *Iron making volume* (1999).
8. Panigrahy S C, Choudhary A, Rigaud M, and Lien H O, in *Proc of the 5th International symposium on Agglomeration, Institution of Chemical Engineers*, Brighton, UK (1989) p 13.
9. Gupta R C, *Theory and Laboratory Experiments in Ferrous Metallurgy*, PHI Learning Private Limited, Delhi (2015) p 159.
10. Ball D F, Dartnell J, Davison J, Grieve A, and Wild R, *Agglomeration in Iron Ores*, Heinemann Educational Books Ltd., London (1973).
11. Srb J, and Ruzickova Z, *Pelletization of Fines*, Elsevier Science Publishing Company, Inc., New York (1988).
12. Loo C E, and Hutchens M F, *ISIJ Int* 43 (2003) 630.
13. Hinkley J, Waters A G, O'Dea D, Litster J D, *Int J Miner Process* 41 (1994) 53.
14. Coulson J M, and Richardson J F, *Chemical Engineering Volume 2, Fifth Edition, Particle Technology and separation Process*, Butterworth Heinemann Publication (2002) p 13.
15. Newitt D M, Conway-Jones J M, *Trans Inst Chem Eng* 36 (1958) 422.
16. Pietsch W, *Size Enlargement by Agglomeration*, Wiley Chichester (1991).
17. Meyer K, *Pelletizing of Iron Ores*, Springer, Berlin (1980).